2022 Microsystems Annual Research Report

MTL MICROSYSTEMS TECHNOLOGY LABORATORIES
MIT.nano
MASSACHUSETTS INSTITUTE OF TECHNOLOGY

CONTENTS

Foreword

We are thrilled to announce the publication of the 2022 Microsystems Annual Research Report, a joint publication between the Microsystems Technology Laboratories (MTL) and MIT.nano.

The MTL was established in 1984 to promote advanced research in semiconductor materials, technology, devices, circuits, and systems. A state-of-the art semiconductor fabrication facility that was critical to research in these fields was built on site, in Building 39. Over the years, MTL has been a model for interdisciplinary and collaborative research, education, and industrial outreach. MTL has grown to a community of 58 'core' faculty members from 7 departments at MIT, who are engaged in a much wider scope of research including the semiconductor topics the MTL was originally conceived for, but now encompasses much broader areas including biomedical systems, integrated photonics, robotics, quantum and superconducting electronics, and AI, just to name a few.

After more than 30 years of service, the MTL fabrication facility was due for major renovation, and MIT.nano was born. The ultramodern MIT.nano facility was completed in 2018 in Building 12, which was named the Lisa T. Su Building this year. Dr. Su is the current president and CEO of AMD, and her Ph.D. research was carried out in MTL under the guidance of Prof. Dimitri Antoniadis, the first director of MTL. Although MIT.nano is now serving the entire MIT community as an institute facility, and not as a part of MTL, its facilities are still central to many of MTL faculty's research. For this reason, MTL and MIT.nano co-organize and co-host select events and publications. As an example, the Microsystems Annual Research Conference (MARC), the popular student-organized technical conference, was administered and sponsored jointly by MTL and MIT.nano for the first time in 2020, then again in 2021 and 2022. Also, since 2020, the Microsystems Annual Research Report has become a joint publication between MTL and MIT.nano.

As usual, this year's MTL/MIT.nano joint Microsystems Annual Research Report represents a broad cross-section of the MIT community, with 37+ faculty, 118 students, postdoctoral associates, and research staff participating. I hope you will appreciate from this report the tremendous amount of innovations the MTL community and users of MIT.nano's shared facilities bring to the world. It is a true privilege of ours to serve these two remarkable communities as well as to publish their works. On behalf of MTL and MIT.nano, we would like to thank every contributor to this year's Microsystems Annual Research Report, as well as the staff of both organizations who worked tirelessly to produce such an outstanding volume. We hope you are as excited with the 2022 Microsystems Annual Research Report as we are.

Hae-Seung Lee
Director, Microsystems Technology Laboratories

Vladimir Bulović
Director, MIT.nano

August 2022

Acknowledgments

MICROSYSTEMS INDUSTRIAL GROUP

Analog Devices, Inc.
Applied Materials
Draper
Edwards
HARTING
Hitachi High-Tech Corporation
IBM
Lam Research Co.
NEC
TSMC
Texas Instruments

MTL LEADERSHIP TEAM

Hae-Seung Lee, Director
Duane S. Boning, Associate Director, Computation
Vicky Diadiuk, Associate Director, Facilities
Jing Kong, Associate Director,
  Diversity, Equity and Inclusion
Jeffrey H. Lang, Associate Director
Stacy McDaid, Administrative Officer

MTL POLICY BOARD

Vladimir Bulović
Vicky Diadiuk
Hae-Seung Lee
Tomás Palacios
Charles G. Sodini
Carl V. Thompson

MTL TECHNICAL STAFF

Michael J. Hobbs, Systems Administrator
Thomas J. Lohman, Project Leader, Computation
William T. Maloney, Systems Manager
Michael McIlrath, Research Scientist

MTL ADMINISTRATIVE STAFF

Kathleen Brody, Administrative Assistant
Kristin Cook, Financial Officer
Elizabeth Green, Senior Administrative Assistant
Preetha Kingsview, Administrative Assistant
Elizabeth Kubicki, Administrative Assistant
Meghan Melvin, Communications Administrator
Jami L. Mitchell, Administrative Assistant
Jessie-Leigh Thomas, Administrative Assistant

MTL SEMINAR SERIES COMMITTEE

Luis F. Velásquez-García, Chair
Jeffrey H. Lang
Jami L. Mitchell
Vivienne Sze

MARC2022 CONFERENCE ORGANIZERS

STEERING COMMITTEE

Hae-Seung (Harry) Lee, MTL Director
Vladimir Bulović, MIT.nano Director
Stacy McDaid, Administrative Officer
Meghan Melvin, Proceedings / Design
Amanda Stoll, Proceedings / Design
Jami L. Mitchell, Logistics
Shereece Beckford, Logistics
Catherine Bourgeois, Logistics
Jatin Patil, Conference Co-Chair
Kruthika (Kru) Kikkeri, Conference Co-Chair

CORE COMMITTEE

Jaehwan Kim, Website / Proceedings
Rishabh Mittal, Outreach
Nili Persits, MIG/MAP Interview Coordinator
Will Banner, Social / Networking Activities
Maitreyi Ashok, A/V Coordinator
Narumi Wong, Conference Package

SESSION CHAIRS

Sarah Muschinske, Quantum Technologies
Thomas Krause, Power
Kaidong Peng, Electronic Devices
Wei Liao, Medical Devices and Biotechnologies
Jane Lai, Energy-Efficient AI
Isaac Harris, Nanotechnology and Nanomaterials
Ruicong Chen, Integrated Ciruits
Milica Notaros, Optics and Photonics
Abigail Zhien Wang, Materials and Manufacturing

MIT.NANO CONSORTIUM

Analog Devices, Inc.
Draper
Edwards
Fujikura
IBM
Lam Research
NCSOFT
NEC
Oxford Instruments Asylum Research
Raith

MIT.NANO LEADERSHIP TEAM

Vladimir Bulović, Director, MIT.nano
Brian Anthony, Associate Director
Kathleen Boisvert, Administrative Officer
Tom Gearty, Communications and Initiatives Director
Tina Gilman, Assistant Director of Programs
Dennis Grimard, Managing Director
Whitney R. Hess, Assistant Director, Safety Systems and Programs
Nicholas Menounos, Assistant Director of Infrastructure
Anna Osherov, Assistant Director, Characterization.nano
Kris Payer, Assistant Director of Operations
Jorg Scholvin, Assistant Director, Fab.nano

MIT.NANO STAFF

Daniel A. Adams, Research Specialist
Shereece Beckford, Events and Projects Coordinator
Robert J. Bicchieri, Research Specialist
Kurt A. Broderick, Research Associate
David Dunham, EHS DLC Officer
Samantha Farrell, Senior Administrative Assistant
Donal Jamieson, Research Specialist
Ludmila Leoparde, Financial Officer
Gongqin Li, Sponsored Research Technical Staff
Eric Lim, Research Engineer
Paul J. McGrath, Research Specialist
Justin Pellegrine, Technician B Electro-Mechanical
Aubrey Penn, Research Specialist
Scott J. Poesse, Research Specialist
Talis Reks, AR/VR/Gaming/Big Data IT Technologist
Gary Riggott, Research Associate
Amanda Stoll DiCristofaro, Communications and Marketing Administrator
David M. Terry, Sponsored Research Technical Staff
Paul S. Tierney, Research Specialist
Timothy K. Turner, Project Technician Electro - Mechanical
Annie I. Wang, Research Scientist
Dennis J. Ward, Research Specialist

AFFILIATED STAFF FROM OTHER DLCS

Nicole, Bohn, Electron and Surface Microscopy Instrumentation Specialist
Anuradha Murthy Agarwal, Principal Research Scientist
Christopher Borsa, Research Scientist, Dept. of Biology
Edward Brignole, Assistant Director, Dept. of Biology
Jim Daley, Research Specialist, RLE
Rami Dana, Research Specialist, MRL
Vicky Diadiuk, MTL Associate Director
Luis Velasquez-Garcia, Principal Research Scientist, MTL
Thomas Lohman, Senior Software Developer/Systems Manager
Bill Maloney, Systems Manager
Joe Masello, Area Manager, Dept. of Facilities
Mark K. Mondol, Assistant Director, NanoStructures Laboratory
Praneeth Namburi, Research Scientist, Institute for Medical Engineering and Science
Mark Rapoza, Area Manager, Dept. of Facilities
Travis Wanat, Project Manager, Dept. of Facilities
Samantha Young, Administrative Assistant/Mech Eng

MIT.NANO LEADERSHIP COUNCIL

Brian Anthony, MIT.nano
Robert Atkins, Lincoln Laboratory
Karl Berggren, NSL, EECS
Kathy Boisvert, MIT.nano
Vladimir Bulović, MIT.nano
Dennis Grimard, MIT.nano
Pablo Jarillo-Herrero, Physics
James LeBeau, DMSE
Hae-Seung Lee, MTL, EECS
Will Oliver, RLE, Physics
Tomás Palacios, EECS
Katharina Ribbeck, BioEng
Frances Ross, DMSE
Thomas Schwartz, Biology
Carl Thompson, MRL, DMSE
Kripa Varanasi, MechE

MIT.NANO FACULTY ADVOCATES WORKING GROUP - CHARACTERIZATION.NANO

Jim LeBeau, Faculty Lead, DMSE
Anna Osherov, Technical Lead, MIT.nano
Karl Berggren, NSL, EECS
A. John Hart, MechE
Long Ju, Physics
Benedetto Marelli, CEE
Yogesh Surendranath, Chemistry

MIT.NANO FACULTY ADVOCATES WORKING GROUP - FAB.NANO

Tomás Palacios – Faculty Lead, EECS
Jorg Scholvin – Technical Lead, MIT.nano
Vicky Diadiuk – Technical Lead, MTL
Akintunde Ibitayo Akinwande, EECS
Karl Berggren, EECS
Jesus A. del Alamo, EECS
Dirk Englund, EECS
Juejun Hu, MechE
Pablo Jarillo-Herrero, Physics
Jeehwan Kim, MechE/DMSE
Paulo Lozano, AeroAstro
Farnaz Niroui, EECS
Will Oliver, RLE, Physics
Deblina Sarkar, MAS
Caroline Ross, DMSE
Bilge Yildiz, NSE, DMSE

MIT.NANO INTERNAL ADVISORY BOARD

Marc A. Baldo – Director, RLE; EECS
Anantha P. Chandrakasan – Dean, School of Engineering; EECS
John Deutch – Chemistry
Elazer Edelman – Director, IMES
Jeff Grossman – Department Head, DMSE
Paula T. Hammond – Department Head, ChemE
Susan Hockfield – President Emerita and Professor of Neuroscience
Craig Keast – Lincoln Laboratory
Nergis Mavalvala, Dean, School of Science; Physics
Chris Schuh – DMSE
Michael Sipser – Math
Krystyn Van Vliet – Associate Provost, DMSE
Evelyn Wang – Department Head, MechE

Biological, Medical Devices, and Systems

Absolute Blood Pressure Waveform Monitoring Using an Ultrasound Probe

A. Chandrasekhar, A. Aguirre, H.-S. Lee, C. G. Sodini
Sponsorship: MEDRC-Philips, Analog Devices Inc., CICS

Accurate measurement of the absolute blood pressure (ABP) waveform assists clinical decision-making as it helps physicians titrate the cardiovascular therapy for a patient. In an intensive care unit (ICU), physicians use an invasive radial catheter to measure BP, whereas, outside an ICU, one may resort to isolated spot measurement of the BP via a brachial arm cuff device. These cuff devices measure only the systolic and diastolic values of the BP waveform, and unlike an arterial catheter used in an ICU, they do not output the shape of the ABP waveform. Morphology of the ABP waveform is significant as it reflects the hemodynamics of the underlying vasculature, and hence there is a need for a non-invasive and easy-to-use device that can output the ABP waveform. Ultrasound-based devices are a feasible alternative for monitoring the BP waveform as these devices can accurately measure pressure-dependent parameters like the blood flow velocity and arterial diameter waveforms. In this project, we are developing an algorithm (see Figure 1) to convert ultrasound data into an ABP waveform, and in this report, we present the preliminary results on estimating pulse pressure (PP) from the ultrasound data.

Two studies were performed to investigate the proposed PP estimation algorithm (See Algorithm Stage 1 in Fig. 1). In study 1, signals illustrated in Figure 1 were recorded from the carotid artery using a custom-designed ultrasound probe while the subject was supine, whereas, in study 2, the above-mentioned signals were recorded using a Philips ultrasound-transducer (XL-143) while the subject rested supine and in tilted posture. Gold standard PP was measured from the brachial artery using an Omron BP monitor as a reference. The Bland-Altman plot in Figure 2 shows that the estimated PP can track the gold standard PP values.

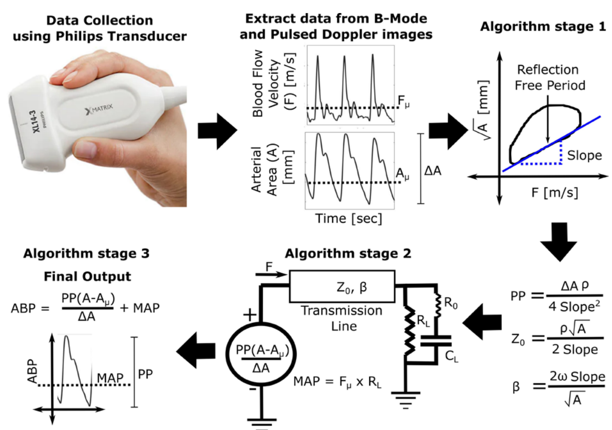

▲ Figure 1: Step by step algorithm to estimate pulse pressure and ABP waveform from ultrasound signals.

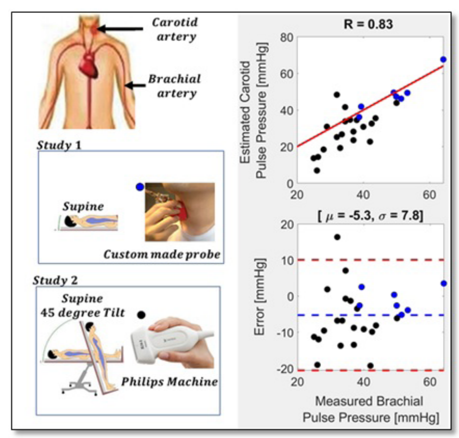

▲ Figure 2: Pulse pressure estimated via ultrasound signals recorded at the carotid artery.

FURTHER READING

- J. Seo, "A Non-invasive Central Arterial Pressure Waveform Estimation System Using Ultrasonography for Real-time Monitoring," Dissertation, Massachusetts Institute of Technology, Cambridge, 2018.

An Implantable Soft Robotic Platform for Enhanced Drug Delivery

D. Goswami, W. Whyte, S. X. Wang, Y. Fan, N. A. Ward, G. P. Duffy, E. B. Dolan, E. T. Roche
Sponsorship: Juvenile Diabetes Research Foundation

Fibrous capsule formation, and its effect on molecular transport, can be detrimental to the long-term efficacy of implantable drug delivery devices, especially when precise spatial and temporal control is necessary for safe and effective therapy delivery. We report an implantable platform which can overcome the diffusional barrier of the fibrous capsule to achieve enhanced transport of small and macromolecular therapy using multiple synergistic soft robotic strategies (Figure 1a, b). Using this platform, small amplitude dynamic actuation (preconditioning) applied to subcutaneous tissue in mice leads to a downstream functional effect: enhanced passive transport of insulin (a model macromolecule) and glycemic control (Figure 1c). Furthermore, rapid actuation of the platform at the time of drug delivery can accelerate transport via convective fluid flow and overcome diffusional limitations caused by the fibrous capsule (Figure 2). This soft actuatable platform has potential clinical utility for mediating and overcoming the host fibrotic response, leading to enhanced delivery of drug therapy for a variety of indications.

The management of type 1 diabetes is one relevant clinical area where our platform could provide synergistic benefit. For example, dynamic actuation could be applied to extend the lifespan of an artificial pancreas, preventing unnecessary fibrous capsule mediated blockages, linked hyperglycemic events, and ultimately simplifying the dosing regimen and patient experience. In synergy, actuation at the time of drug delivery could make rapid insulin adjustments and maintain blood glucose levels in the narrow window necessary to prevent long-term complications. Looking further into the future, application of this platform could enable translation of next-generation bioartificial technologies utilizing human-derived insulin-producing islet cells by modifying the transport-limiting fibrous capsule, which has been a major barrier to the viability of cell-based therapeutics.

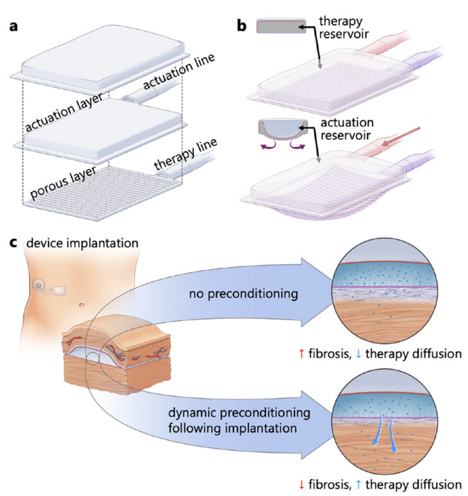

▲Figure 1: a) Exploded view showing the different layers comprising the implantable soft robotic platform. b) Deflection of the actuation and porous layers during actuation. c) Overview of device functionality during dynamic actuation.

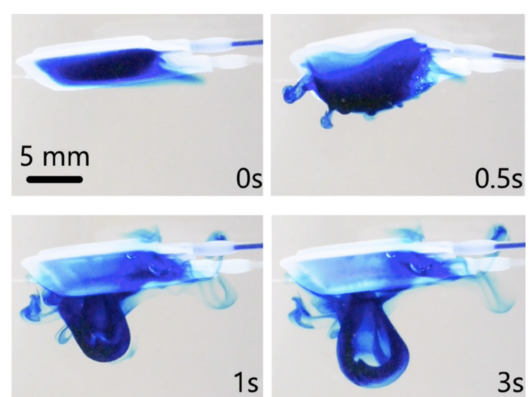

▲Figure 2: Rapid actuation at the time of drug delivery enables convective flow of a model drug, methylene blue, from the therapeutic reservoir of the device.

FURTHER READING

- D. Goswami, D. A. Domingo-Lopez, N. A. Ward, J. R. Millman, G. P. Duffy, E. B. Dolan, and E. T. Roche, “Design Considerations for Macroencapsulation Devices for Stem Cell Derived Islets for the Treatment of Type 1 Diabetes,” *Advanced Science*, vol. 8, no. 16, p. 2100820, Jun. 2021.
- E. B. Dolan, C. E. Varela, K. Mendez, W. Whyte, R. E. Levey, S. T. Robinson, E. Maye, J. O’Dwyer, R. Beatty, A. Rothman, Y. Fan, J. Hochstein, S. E. Rothenbucher, R. Wylie, J. R. Starr, M. Monaghan, P. Dockery, G. P. Duffy, and E. T. Roche, “An Actuatable Soft Reservoir Modulates Host Foreign Body Response,” *Science Robotics*, vol. 4, no. 33, pp. eaax7043, Aug. 2019.

Modeling the Arterial System to Improve Ultrasound Measurements of Hemodynamic Parameters

J. Harabedian, A. Chandrasekhar, C. G. Sodini
Sponsorship: Analog Devices

One of the most crucial parameters for monitoring cardiovascular disease risk is one's arterial blood pressure (ABP). Clinicians use a radial arterial catheter to measure ABP in an intensive care unit (ICU). Although this method is considered the gold standard, its invasive nature makes it undesirable and inaccessible outside an ICU. One solution to this problem is to take advantage of ultrasonic measurements, which are noninvasive and extremely accessible. However, developing an algorithm to convert ultrasound data into a legitimate ABP waveform requires an extensive amount of patient data. The limitation is that this data is difficult to obtain and impossible to fully control.

The solution presented here is to use a flow phantom: a physical, hydraulic system that mimics arterial blood flow. The phantom provides pressure waveforms, which come directly from a catheterized tube, and flow velocity waveforms, from an ultrasonic flow meter, that closely match the morphology of patient data. Developing a physical model of the arterial system allows for control of parameters that are considered uncontrollable in humans (e.g., arterial compliance, cardiac output, critical closing pressure) and enables data collection for a number of parameter combinations that would otherwise be unobtainable.

A flow phantom can be made using a pump, accumulator, compliant tubing, flow control valve, and a reservoir, representing the heart, large arterial compliance, large artery, arteriole resistance, and the ground pressure, respectively. To collect data from the phantom there are two pressure transducers, a flowmeter and the ultrasound device. Figure 1 shows the setup of the entire system. The pressure transducers and the flowmeter can collect control measurements that can be tested against the ultrasound device and the developed ABP estimation algorithm. Figure 2 shows example outputs from these measurement devices.

Experimental validation shows that the flow phantom does in fact mimic the hemodynamic behavior of arterial blood flow. This was confirmed by controlling various parameters of the system (e.g., flow resistance, ground pressure, cardiac output) and comparing its response against known hemodynamic responses.

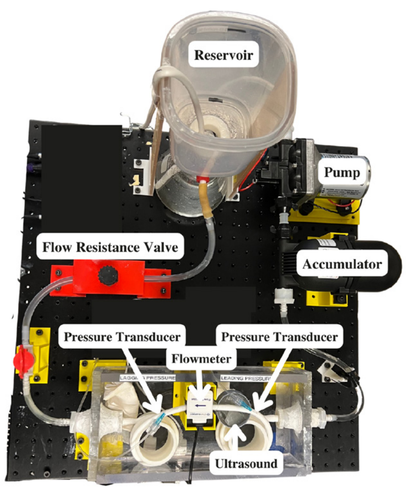

▲ Figure 1: Physical flow phantom system, consisting of the pump, accumulator, compliant tubing, flow control valve and reservoir. There are also the measure-ment devices: two pressure transducers, one flowmeter and in-house ultrasound device.

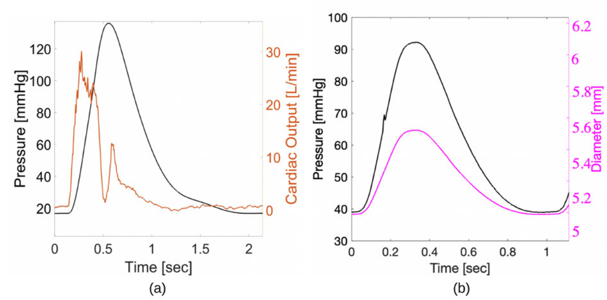

▲ Figure 2: Examples of typical measurements from flow phantom. 2a shows pressure and volumetric flow, with .5 Hz heart beat and pump on for .3 seconds. 2b shows pressure and diameter, with 1 Hz heartbeat and pump on for .2 seconds.

Model-based Noninvasive Intracranial Compliance and Vascular Resistance Estimation

S. M. Imaduddin, C. G. Sodini, T. Heldt
Sponsorship: Analog Devices, Inc. via MIT Medical Electronic Device Realization Center

Existing neuromonitoring methods used for patients with severe head injury tend to be highly invasive and carry a risk of tissue damage and infection. In particular, fluid infusion/withdrawal studies via indwelling catheters are needed to determine intracranial compliance (ICC) – an index of the propensity of rise in intracranial pressure (ICP) in response to changes in cranio-spinal volume. Despite their potential to serve as early indicators of intracranial hypertension, ICC measurements are rarely performed owing to time-consuming, invasive measurement protocols. In addition, measurements of cerebrovascular resistance (CVR) to blood flow are useful in assessing cerebral autoregulation and tracking pathological vascular narrowing such as in moyamoya disease. Like ICC, however, CVR is not regularly obtained at the bedside as the requisite measurements – arterial blood pressure (ABP), cerebral arterial blood flow (CBF), and ICP – are rarely monitored simultaneously.

We previously developed a noninvasive, model-based approach for ICP estimation. Recently, we augmented our approach to additionally estimate ICC and CVR. In particular, subjects' ABP and CBF are related to the ICP, ICC, and CVR via a Windkessel-like model. Measurements of the ABP and CBF are then used to estimate the clinically interpretable model parameters in a noninvasive, patient-specific fashion. Ultrasound-based CBF measurements were made in extracranial (common/internal carotid) arteries. Vessel diameters were estimated with B-mode images and combined with color flow velocity measurements to yield the CBF. Tilt-table studies were carried out to validate the proposed method. We found that our system successfully tracked tilt-induced changes in ICP, ICC, and CVR, paving the way towards convenient and safe neuromonitoring across a wide spectrum of pathologies, patient ages, and disease severities.

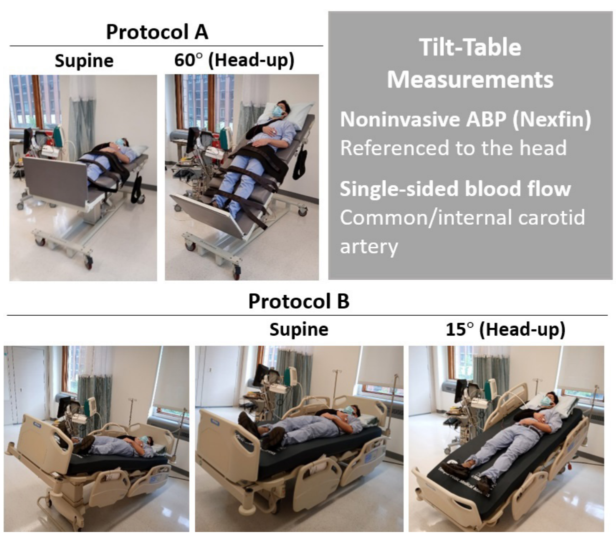

▲Figure 1: Illustration of tilt-table protocols for method validation. Two protocols were established. Protocol A involved transitions from supine to 60° head-up position. Protocol B involved both head-up and head-down transitions of 15°, respectively. Acquired measurements are also listed.Closed electronics box with force and accelerometer analog inputs from the casing and data streaming to a tablet for data collection and display. Bottom: Electronics box components consisting of the DC power source of two series 9V batteries, the force signal amplifier, and the multi-channel analog-to-digital converter.

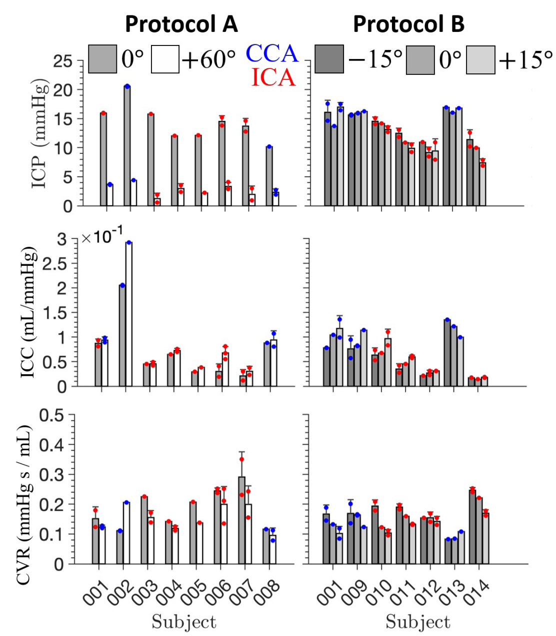

▲Figure 2: Parameter estimation summary. Results obtained with recordings at common carotid (CCA) and internal carotid (ICA) arteries are shown in blue and red, respectively. ICP estimates decreased as subjects progressively moved to head-up positions. ICC estimates increased while CVR estimates decreased on average.

Venous Pressure Waveform Generation with Force-coupled Ultrasound

A. Jaffe, B. Anthony
Sponsorship: Medical Electronic Device Research Center-Philips

Congestive heart failure is diagnosed in 6.2 million people and is on 380,000 death certificates annually in the United States alone. In this syndrome, the heart's pumping ability decreases, causing the circulatory system to compensate by increasing blood volume to make blood easier to pump. Decompensated heart failure occurs when this mechanism is no longer effective, causing a vicious cycle of increasing volume, leading to pulmonary and peripheral edema from high venous pressure, which can lead to death. Currently, accurate venous pressure can be obtained only through invasive catheterization. In our project, we aim to mirror this accuracy in a noninvasive force-coupled ultrasound approach.

In our methodology, we acquire and segment force-coupled ultrasound images of the internal jugular vein (IJV) compression and note how much force is required to completely occlude it–the collapse force. We use the collapse force and IJV area at constant force to inform a 3-D inverse finite element model that produces a venous pressure waveform. We note that the pulsation of the nearby carotid artery compresses the IJV during systole and allows the IJV to expand during diastole. Given we have validated our methodology with the current noninvasive standard at MIT, we now begin a study using the invasive catheterization at Massachusetts General Hospital.

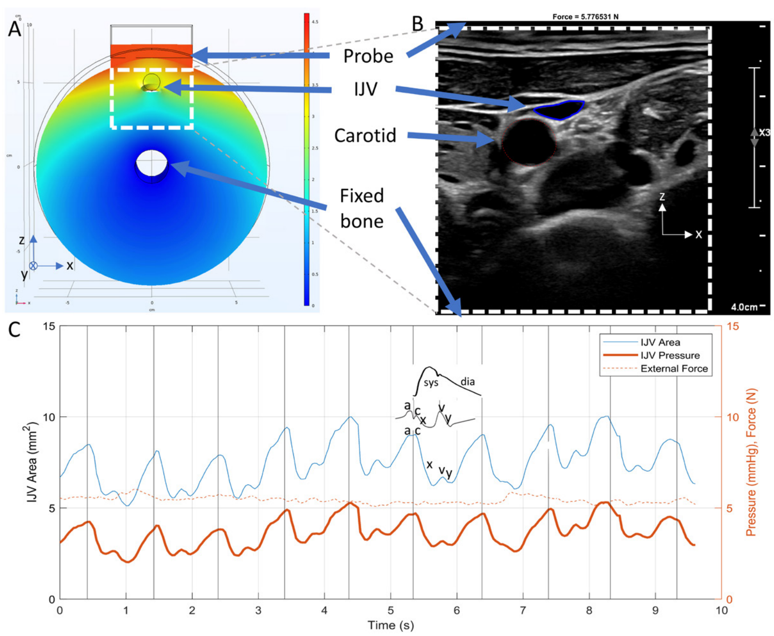

▲Figure 1: (A) Front-view of the 3-D finite element forward model of a force-coupled ultrasound compression of the IJV. (B) Force-coupled ultrasound image of the IJV and carotid short-axis cross-sections at the base of the neck. (C) Inverse finite element model inputs (IJV area and external force) and output (IJV pressure). Components of the venous pressure waveform are labeled (a, c, x, v, and y) and compared to an idealized venous pressure waveform. Vertical lines symbolize end-diastole; an idealized carotid pressure waveform is shown between two vertical lines.

Spiral Inertial Microfluidic System for Membrane-Free Cell Retention with Industrial-scale Cell-density Capacity and Throughput in Biomanufacturing

H. Jeon, T. Kwon, J. Han
Sponsorship: NIIMBL

Therapeutic proteins (e.g., monoclonal antibodies) are secreted from engineered host cells, and their separation from the host cells is essential to harvest purified proteins while the host cells continuously keep producing the therapeutic proteins in a bioreactor. Membrane-based filtration is the most widely used separation method for the biomanufacturing process. Although the method has a great separation efficiency, it has critical issues with membrane fouling and low product recovery due to nonspecific binding to the membrane surface.

To overcome these limitations, we developed and advanced spiral inertial microfluidic system for membrane-free cell retention with the following two key aims: 1) high cell-density capacity and 2) high throughput. For the first aim, elasto-inertial microfluidics was developed to manipulate ultra-high-density cells to achieve stable equilibrium positions in microchannels, aided by the inherent viscoelasticity of high-density cell suspension (Figure 1a, b). Using the cascaded configuration of two spiral devices in series, Chinese hHamster oOvary (CHO) cell retention was demonstrated, from 29.7 PCV% (108.1 million cells/mL) to 8.3 PCV% (33.2 million cells/mL) with overall 72.1% reduction efficiency (Figure 1c). For the second aim, based on channel deformation analysis aided by numerical simulation and confocal imaging, the empirically optimized design of a polydimethylsiloxane (PDMS) device for CHO cell retention was translated to its plastic equivalent. As shown in Figure 1d, the developed plastic device showed great performance on CHO cell retention with a high cell-removal rate (up to 97% at the input CHO cell density of ~12 million cells/mL). Furthermore, withby a simple stacking method, a multiplexed plastic device can be fabricated for high-throughput applications. Using the multiplexed plastic unit, we successfully demonstrated continuous, clogging-free, and ultra-high-throughput (at a processing rate of 1 L/min) cell clarification with a high cell-retention efficiency (Figure 1e, f), which can meet the throughput required for the large-scale industrial biomanufacturing applications.

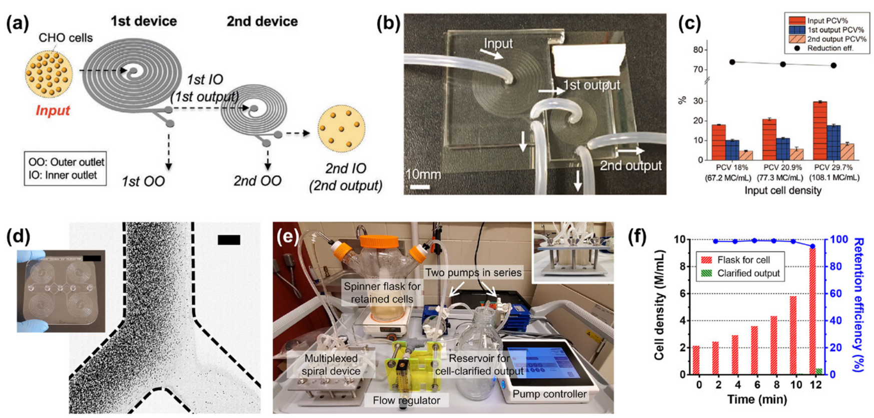

▲ Figure 1: (a) A schematic diagram and (b) an actual photo of two spiral devices in cascaded configuration to process ultra-high cell-density suspension. (c) Density reduction at three different input cell densities using the cascaded configuration. (d) Trajectory of CHO cells at the outlet bifurcation region of the plastic spiral device wiat the flow rate of 40 mL/min (scale bar: 500 μm); the inset represents a photo of the plastic device (scale bar: 20 mm). (e) A photo of the high-throughput cell-clarification platform using a 25-layers-stacked device (inset). (f) Profiles of the cell densities in the flask of the retained CHO cells (red bar), and the cell-clarified output (green bar), and the cell-retention efficiency (blue line) (input volume: ~ 1 L, input flow rate: 1 L/min, flow rate division: 15:1=the inner wall side output: the outer wall side output).

FURTHER READING

- H. Jeon, T. Kwon, J. Yoon, and J. Han, "Engineering a Deformation-free Plastic Spiral Inertial Microfluidic System for CHO Cell Clarification in Biomanufacturing,", *Lab on a Chip*, Vol. 22, no. (2), p. 272, (2022), DOI: 10.1039/D1LC00995H.
- T. Kwon, K. Choi, and J. Han, "Separation of Ultra-High-Density Cell Suspension via Elasto-Inertial Microfluidics,", *Small*, vol. Vol. 17, no. (39), p. 2101880, (2021), DOI: 10.1002/smll.202101880.
- H. Jeon, T. Kwon, J. Yoon, and J. Han, "Biomanufacturing Scale CHO Cell Clarification Using Hard Plastic Spiral Inertial Microfluidic Device,", *presented at MicroTAS 2021*, , In-person & Virtual, Palm Springs, CA, USA (Oct. 10–14, 2021).

Functional Drug Susceptibility Testing Using Single-cell Mass Predicts Treatment Outcome in Patient-derived Cancer Spheroid Models

M. A. Stockslager, S. Malinowski, M. Touat, J. C. Yoon, J. Geduldig, M. Mirza, A. S. Kim, P. Y. Wen, K. H. Chow, K. L. Ligon, S. R. Manalis
Sponsorship: Koch Institute Center for Precision Cancer Medicine, Dana Farber Cancer Institute Center for Patient Derived Models

Functional precision medicine aims to match individual cancer patients to optimal treatment through ex vivo drug susceptibility testing on patient-derived cells. However, few functional diagnostic assays have been validated against patient outcomes at scale because of the limitations of such assays. Here, we describe a high-throughput assay that detects subtle changes in the mass of individual drug-treated cancer cells as a surrogate biomarker for patient treatment response. To validate this approach, we determined ex vivo response to temozolomide in a retrospective cohort of 69 glioblastoma patient-derived neurosphere models with matched patient survival and genomics. Temozolomide-induced changes in cell mass distributions predict patient overall survival similarly to O6-methylguanine-DNA methyltransferase (MGMT) promoter methylation and may aid in predictions in gliomas with mismatch-repair variants of unknown significance, where MGMT is not predictive. Our findings suggest that cell mass is a promising functional biomarker for cancers and drugs that lack genomic biomarkers.

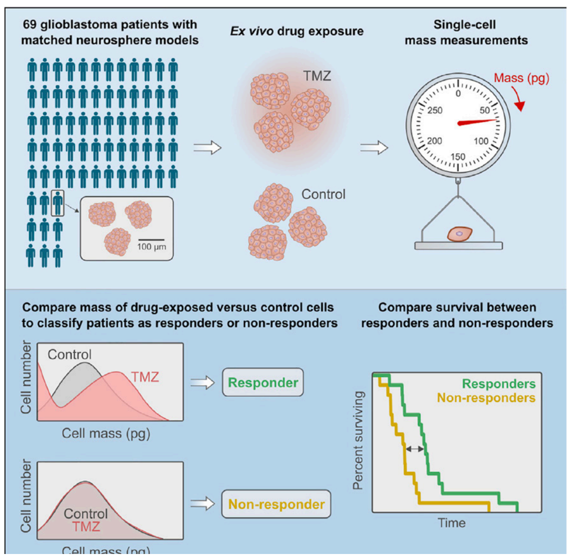

▲Figure 1: In a retrospective study, func-tional drug susceptibility testing predicts the response of patients with glioblastoma to chemotherapy. By detecting subtle changes in tumor cell mass after ex vivo drug exposure, testing can predict treat-ment response with power comparable to the standard-of-care genomic biomarker.

FURTHER READING

- M. A. Stockslager, S. Malinowski, M. Touat, J. C. Yoon, J. Geduldig, M. Mirza, A. S. Kim, P. Y. Wen, K. H. Chow, K. L. Ligon, and S. R. Manalis, "Functional Drug Susceptibility Testing Using Single-cell Mass Predicts Treatment Outcome in Patient-derived cancer Spheroid Models," *Cell Reports*, vol. 37, no. 1, 2021.

Thermally Drawn Piezoelectric Fiber Enables Fabric for Acoustic Healthcare Monitoring

G. Noel, W. Yan, E. Meiklejohn, G. Rui, L. Zhu, Y. Fink
Sponsorship: NSF Graduate Research Fellowship Grant No. 1745302.

Since the invention of the stethoscope, healthcare professionals have used acoustic signals to monitor patient health. Although the stethoscope is widely used, its form factor does not allow continuous monitoring, leaving much of the information from the acoustic signals of the body uncaptured. Here, we present a novel piezoelectric fiber microphone device that can be incorporated into fabrics to effectively detect sound. Using the thermal fiber-drawing technique, multiple viscoelastic materials flow in a laminar regime to produce a device with microscale features that maintain the same cross-sectional geometry as the macroscopic preform. The piezoelectric domain consists of poly(vinylidene fluoride-trifluoroethylene) and barium titanate nanoparticles; during the draw, cavities form between the polymer and the particle on either side of the particle in the direction of the draw, resulting in a novel ferroelectret material with a high piezoelectric coefficient. The fiber's shape and flexibility allow it to be woven into fabrics, and the sensitivity of these "acoustic fabrics" is comparable to that of handheld microphones. In clothing, the fibers reliably detect the heartbeat and breathing rate of the wearer. With further development, arrays of fibers can be used to continuously capture acoustic signals that provide the wearer with insight into their health, making healthcare more accessible outside clinical settings.

Fabrication of Transparent Displays for Wearable Electronic Biomonitors

S. Payra*, S. Ben-David*, C. Gregory*, R. Brenes, R. Ram, F. Niroui
*Contributed equally
Sponsorship: MIT Department of Electrical Engineering and Computer Science, 6.s059 Class

While advances in polymeric materials have enabled the creation of flexible biosensors, there has been limited progress on transparent "electronic skins" that allow wearers to view, monitor, and interact with their biological data. Towards this objective, in this work we present a candidate thin-film organic light-emitting diode (OLED) composition that we utilize to fabricate seven-segment displays upon transparent glass substrates. We compare MEH-PPV and Alq_3 emitting layers and then create, connect, and encapsulate multiple Alq3-based OLED displays using a stackup of {ITO/MoO_3/NPB/Alq_3/LiF/Al}. Spring-loaded pins are used to interface with two devices, and display circuitry is designed with a 9V LED drive level / 3V logic level using a back-to-back n-channel enhancement metal-oxide-semiconductor field-effect transistor (MOSFET) architecture. When interfaced with a microcontroller and temperature sensor, this prototype can display body temperature on the nanofabricated OLED displays. The techniques utilized present a basis upon which to develop wearable biomonitors that measure and display biometric data. Future development will aim at adapting these processes to polymer substrates for the creation of flexible wearable devices that can seamlessly integrate into garments or onto wearers' skin.

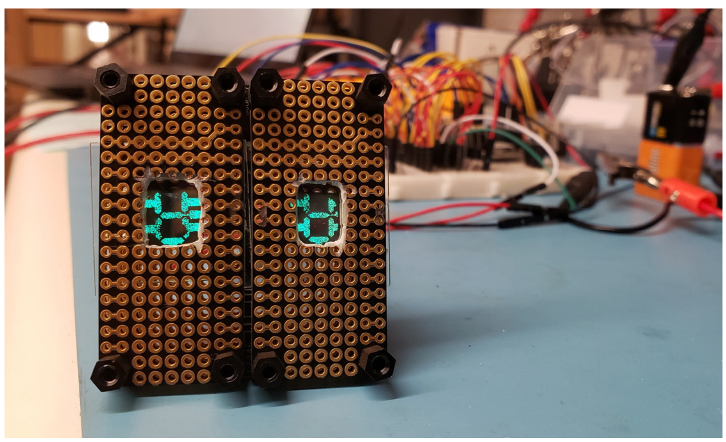

▲ Figure 1: Photograph of the fabricated seven-segment displays connected to a temperature sensor for temperature readout.

Navigational Chemistry for Self-Editing or "Lamarckian" Genomes and Targeted Drug Delivery Using a Bio/Nano TERCOM Approach

J. M. Protz
Sponsorship: Protz Lab Group; BioMolecular Nanodevices, LLC d.b.a. Ariadna

Navigational chemistry has been actively studed by the investigator for two decades. The work described here is focused on developing cells or cell-free reactions that estimate their location by correlating the evolution of their sensed fluid environment (e.g ., temp., salinity, sugar, pH, ion conc., etc.) against an embodied map and then self-edit the content of their genomes in a way that depends on said estimate. Editing the genome shifts the expressed phenotype and the heritable genotype . The laboratory component has been focused on preparing and testing a liposome-encapsulable mixture of oligo-modified ribonucleaic acid (RNA) and nucleases that yields path-dependent doses of therapeutic RNA while en route to a target site. This is the key element of an envisioned self-editing genome reaction chain. In this chain, a read-only "junk DNA" segment of a plasmid would transcribe into RNA strands having a spectrum of coding heads and consumable tails. The tails would be attacked by an exonuclease sensitive to substrate and local environment, causing the tails to function as path-sensitive fuses and the spectrum of the surviving RNA to depend on path. The surviving RNA would be reverse-transcribed into DNA and integrated as expressible genes in a read-write portion of the plasmid, with concurrent random erasures keeping plasmid length roughly constant. By this process, the genetic composition of the read-write region would evolve with changing environmental paths . A related effort led by the investigator explores drug delivery using particles that exhibit path-dependent doses or conformation. Both are related to terrain contour matching (TERCOM), a technique used in air navigation, and both build on prior study by the investigator and his group of nanoparticles that record the trajectory of their environment. Progress might enable new pharmaceuticals or the engineering of organisms that exhibit Lamarckian evolution or gene therapies that confer this ability.

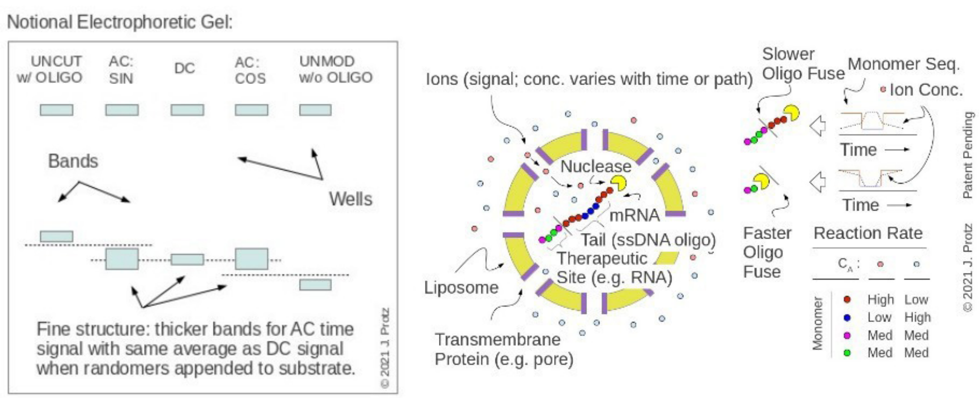

▲Figure 1: (right) Nuclease with environmental and substrate sensitivity consumes tails faster when environmental path and tail sequence are better correlated; (left) if a mix of random tails is used, electrophoretic gel should exhibit fine structure in bands due to varying correlations between tail sequences and environmental paths, causing yielded strand length to vary.

FURTHER READING

- J. Protz, "Self-Editing or "Lamarckian" Genome using Bio/Nano TERCOM Approach," MIT, Cambridge, MA, *MTL Annual Research Report*, p. 13, 2021.
- J. Protz, "Methods and Compositions for Targeted Delivery, Release, and/or Activity," *Int'l. Patent App*. PCT/US2021/016111, 1 Feb 2021. See also Int'l. Patent App. PCT/US2019/031395 (WO/2019/217601), 8 May 2019.
- J. Protz, A. Lee, A. Jain, M. Slowe, E. Vasievich, and T. LaBean, "Bio-Nano TERCOM for Drug Delivery Using Oligos, RNA, and Nuclease," Proc. MIT *MTL Annual Research Conference (MARC 2022)*, S7.05, pp, 25-26, 2022.

Adaptable Engineering of Cellulose-based Vertical Flow Assays for Rapid Diagnostics–The Case of COVID-19

D. M. Y. Tay, S. Kim, E. H. Yee, E. A. Miller, K. J. Sung, Y. Hao, H. D. Sikes
Sponsorship: Deshpande Center for Technological Innovation, NIH Rapid Acceleration of Diagnostics (RADx) program, 3M Company, Quanterix Corporation, Singapore's National Research Foundation

Rapid diagnostic tests (RDTs) are integral to effective disease response and control. To maximize their potential for population-wide epidemiological control, accessibility and widespread use are two key factors. The commonplace lateral flow assays (LFAs) are heavily reliant on nitrocellulose, of which supply can be strained in times of high demand such as during the ongoing COVID-19 pandemic, and also require processing prior to reagent immobilization. These features hamper the necessary large-scale distribution of RDTs. Here, we seek to overcome this limitation by enabling swift and efficient production of cellulose-based paper assays that do not depend on nitrocellulose and require minimal substrate processing. We accomplished this through the engineering of cellulose-binding domain onto binding proteins for rapid immobilization on cellulose. We subsequently demonstrate good clinical and lab-based performance for two orthogonal assay types: serological and antigen rapid tests and their compatibility with roll-to-roll mass manufacturing. Specifically, we were able to detect antibodies present in human serum towards the severe acute respiratory syndrome coronavirus 2 (SARS-CoV-2) nucleocapsid (N) protein, as well as SARS-CoV-2 (N) protein in saliva and swab samples using modified versions of the cellulose-based vertical flow assays (VFAs). Both saliva and swab samples achieve clinically relevant detection ranges appropriate to probe the serological status and viral loads of patients, respectively. We envision that our proposed workflow has the capacity to be implemented in response to immense RDT demands in future pandemics and pave the way to newer and exciting innovations in paper-based assays.

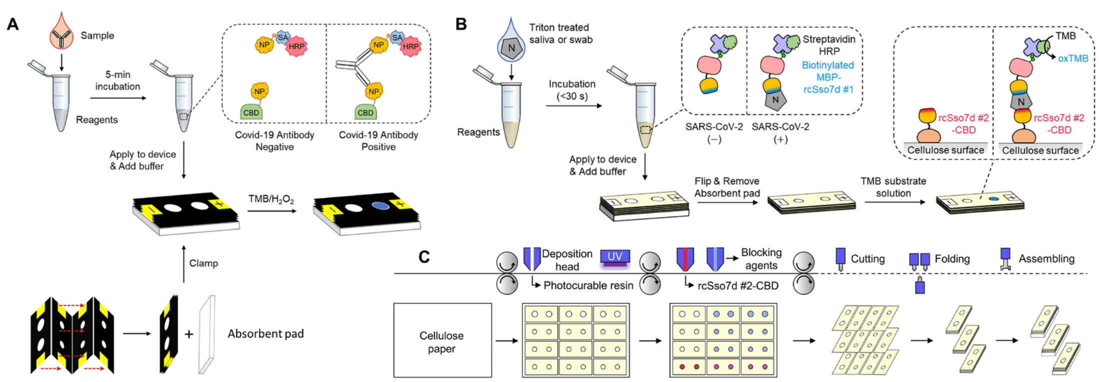

▲ Figure 1: Production and assay workflow of cellulose-based VFAs. (A) Serological assay for SARS-CoV-2 antibodies in human serum. (B) Rapid antigen test for SARS-CoV-2 N protein. (C) Schematic of large-scale manufacture of VFAs.

FURTHER READING

- Kim et al., *ACS Sens.*, vol. 6, p. 1891, 2021.
- Kim et al., *ACS Appl. Mater. Interfaces*, vol. 13, p. 33, 2021.
- Jia et al. *Lab Chip*, vol. 22, no. 7, p. 1321, 2022.

Femtomolar Detection of SARS-CoV-2 via Peptide Beacons Integrated on a Miniaturized TIRF Microscope

S. P. Tripathy, M. Ponnapati, S. Bhat, J. Jacobson, P. Chatterjee
Sponsorship: MIT Media Lab, MIT Center for Bits and Atoms, Jeremy and Joyce Wertheimer

The novel severe acute respiratory syndrome coronavirus 2 (SARS-CoV-2) continues to pose a significant global health threat. Along with vaccines and targeted therapeutics, there is a critical need for rapid diagnostic solutions. The most widely employed diagnostic tests for SARS-CoV-2 are reverse transcription-polymerase chain reaction (RT-PCR)-based methods, though other technologies based on clustered regularly interspaced short palindromic repeats (CRISPR) and loop-mediated amplification have been deployed as well. The best-in-class FDA-authorized diagnostics, such as RT-PCR, have limits of detection (LoD) of 10^2-10^3 ribonucleic acid (RNA) copies/ml, which is about 1-10 attomolar (aM) RNA in the test volume. RT-PCR tests, however, require laborious and expensive nucleic acid isolation, purification, and processing steps, which increases both the turnaround time of detection and the cost of testing. Alternatively, there are Food and Drug Administration- (FDA-)authorized low-sensitivity, inexpensive, and rapid diagnostics. These tests, which often rely on antigen detection, have limit of detection (LoD) of 10^5-10^7 RNA copies/ml, or around 1-100 femtomolar (fM). Recently, there has been a significant effort to detect SARS-CoV-2 via fluorescence-based readouts to allow for specific signal amplification. Such methods largely rely on binding to SARS-CoV-2 RNA or deoxyribonucleic acid (DNA), which requires isolation of nucleic acids, as described above.

In this work, we utilize computational protein modeling tools to suggest molecular beacon architectures that function as conformational switches for high sensitivity detection of the SARS-CoV-2 spike protein receptor-binding domain (S-RBD). Next, adopting the technology of total internal reflection fluorescence (TIRF) microscopy, we fabricate a miniaturized TIRF (mini-TIRF) microscope for seamless detection of peptide beacon activity in response to viral presence, enabling rapid and highly-sensitive detection of SARS-CoV-2. Integrating these beacons on a mini-TIRF microscope, we detect the S-RBD and pseudotyped SARS-CoV-2 with limits of detection in the femtomolar range. We envision that our designed mini-TIRF platform will serve as a robust platform for point-of-care diagnostics for SARS-CoV-2 and future viral threats.

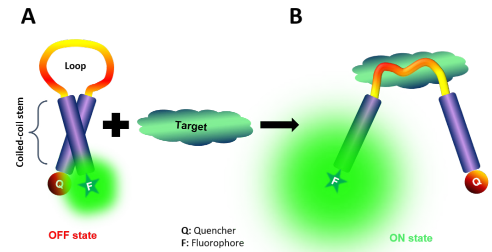

▲Figure 1: Schematic of pep-tide beacon architecture. A) Low-fluorescent state is closed heterodimer state of peptide beacon in absence of S-RBD. B) High-fluorescent state is open-coil state after binding of S-RBD with loop of peptide beacon.

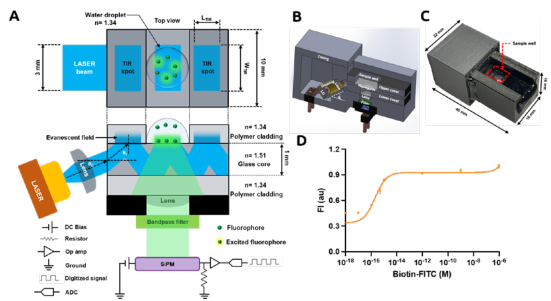

▲Figure 2: Design of mini-TIRF. A) Schematic showing engineering of mini-TIRF device. B) Internal architecture of cartridge shown in sliced solid work model. C) 3D printed cartridge containing laser diode, planar waveguide, collimating lens, optical filter, and SIPM. D) Detection of biotinylated FITC in 1X PBS, pH 7.4 from attomolar to micromolar concentration using mini-TIRF. LoD is defined as signal measured as three times standard deviation of baseline signal.

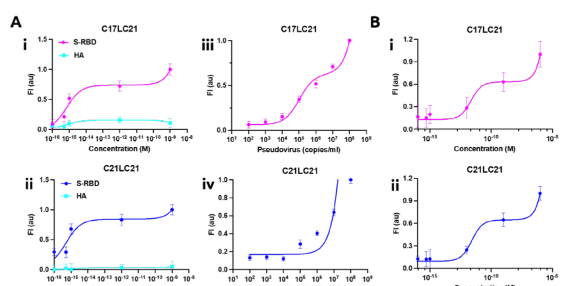

▲Figure 3: Detection of S-RBD and pseudotyped SARS-CoV-2 virus particles on mini-TIRF. A) Detection of recombinant S-RBD and Influenza H3N2 (HA) in 1X PBS by HPLC-purified i) C17LC21 (n=5), ii) C21LC21 (n=5) immobilized on mini-TIRF. Detection of SARS-CoV-2 spike protein bearing pseudovirus by HPLC-purified iii) C17LC21 (n=5), iv) C21LC21 (n=5) immobilized on mini-TIRF. B) Detection of recombinant S-RBD in human saliva sample by HPLC-purified i) C17LC21 (n=3), ii) C21LC21 (n=3) immobilized on mini-TIRF.

FURTHER READING

- C. Mueller and T. N. Grossmann, "Coiled-coil Peptide Beacon: A Tunable Conformational Switch for Protein Detection," *Angewandte Chemie International Edition*, vol. 57, pp. 17079-17083, 2018.
- S. Ramachandran, D. A. Cohen, A. P. Quist, and R. Lal, "High Performance, LED-powered, Waveguide Based Total Internal Reflection Microscopy," *Scientific Reports,* vol. 3, pp. 1–7, 2013.

Highly Tunable, Rapid Manufacturing of Microneedles for Controlled Vaccine Delivery Applications using Multiphoton 3D Printing

D. Varshney, J. Han, J. L. Daristotle, I. Sadeghi, M. Kanelli, R. S. Langer, A. Jaklenec
Sponsorship: Bill and Melinda Gates Foundation (INV-007842)

Rationally designed microneedle drug delivery systems enable precise spatiotemporal control of vaccination. Standard manufacturing processes such as computer numerical controlled (CNC) machining and photolithography are prerequisites for fabricating such delivery devices. However, due to tolerance limitations and lengthy production times, the manufacturing of microneedle patches is inherently restricted by feature size and subject to production inefficiency. In this work, multiphoton 3D printing (MPP) was used to rapidly prototype and develop microneedles varying in size and shape for enhanced vaccination. We report the effect of various printing parameters on feature resolution and printing time. High-resolution MPP enables production scalability and antigen-specific device customizability, where parameters such as needle pitch, patch size, and tip-angle can highly influence vaccine efficacy. Such devices may be critical for rapid response to disease outbreak in future applications.

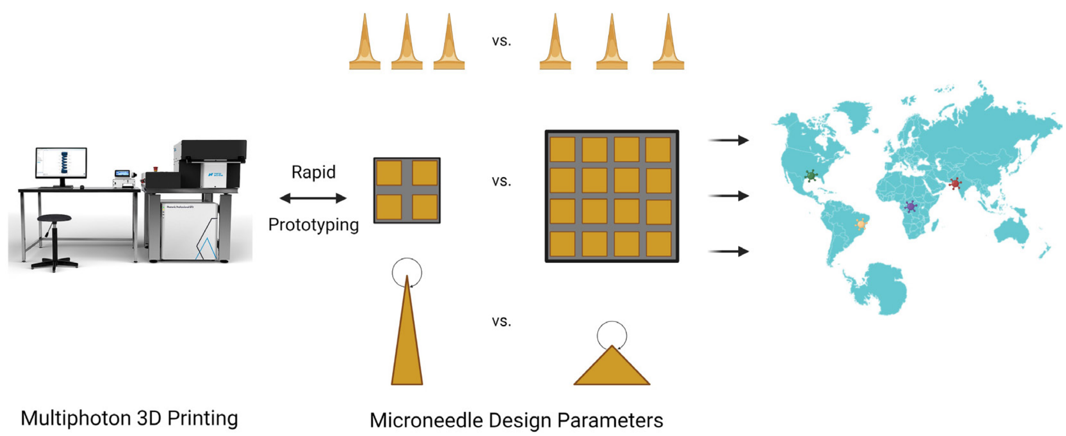

▲ Figure 1: Microneedles manufactured via multiphoton 3D printing enables rapid, customizable, and spatiotemporally controlled vaccination response to global disease outbreak.

Characterization of 3D-printed, Tunable, Lab-grown Plant Materials

A. L. Beckwith, J. Borenstein, L. F. Velásquez-García
Sponsorship: Draper Laboratory

Wood has traditionally been viewed as a low-cost, widespread commodity. However, current practices for wood procurement are unsustainable. Wood supply is increasingly strained, and, in many ways, trees are non-ideal to produce wood: they are affected by climate, seasons, and producing a small fraction of wood from the total mass of the tree.

We recently pioneered an approach to generate plant-based materials in vitro without needing to harvest or process whole plants, making possible the high-density production of plant-based materials unaffected by such constraints. In addition, the process is compatible with additive manufacturing. We now report the first physical, mechanical, and microstructural characterization of plant materials generated with Zinnia elegans cell cultures using such methodology. The results show that the properties of the plant materials vary significantly with adjustments to hormone levels present in growth medium. In addition, the data show that the use of bioprinting and casting enables the production of net-shape objects in forms and scales that do not arise naturally in whole plants (Figure 1). Further work could entail the development of processes for other plant species and/or producing other biopolymers.

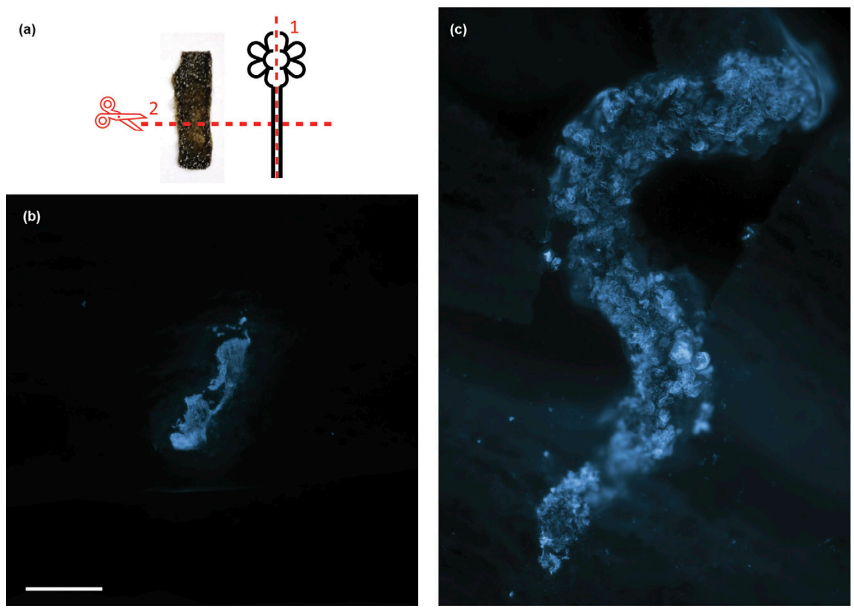

▲Figure 1: (a) Stem samples were halved lengthwise (cut 1) and dried before fixing in wax and sectioning with a microtome along cut 2. (b) Cross-section of a halved and dried Zinnia stem. (c) Cross-section of a grown material sample sliced along the shortest dimension, greatly surpassing the size of the stem, even though they have the same age. Scale bar equals 500 micrometers. From A. Beckwith et al., Materials Today (2022).

FURTHER READING

- A. Beckwith, J. Borenstein, and L. F. Velásquez-García, "Physical, Mechanical, and Micro-structural Characterization of Novel, 3D-printable, Tunable, Lab-grown Plant Materials Generated from Zinnia Elegans Cell Cultures," *Materials Today*, vol. 54, pp. 28 – 41, April 2022. DOI: https://doi.org/10.1016/j.mattod.2022.02.012
- A. L. Beckwith, J. Borenstein, and L. F. Velásquez-García, "Tunable, Plant-based Biomaterials via In Vitro Cell Culture Using a Zinnia Elegans Model," *Journal of Cleaner Production*, vol. 288, p. 125571, Mar. 2021. DOI: https://doi.org/10.1016/j.jclepro.2020.125571
- Z. Sun and L. F. Velásquez-García, "Monolithic, FFF Printed, Biodegradable, Biocompatible, Dielectric–conductive Microsystems," *Journal of Microelectromechanical Systems*, vol. 26, no. 6, pp. 1356 – 1370, Dec. 2017. DOI: https://doi.org/10.1109/JMEMS.2017.2746627

Absolute Blood Pressure Measurement using Machine Learning Algorithms on Ultrasound- based Signals

H. Wang, A. Chandrasekhar, J. Seo, A. Aguirre, S. Han, C. G. Sodini, H.-S. Lee
Sponsorship: MIT J-Clinic, Philips, Analog Devices, MIT-IBM Watson AI Lab, NSF CAREER Award

In an intensive care unit (ICU), physicians can use an invasive arterial catheter to measure the blood pressure (BP) waveform with high resolution. In non-ICU settings, arterial catheters are not used, and clinicians must rely upon isolated spot measurements from a non-invasive arm-cuff device that cannot measure the absolute BP waveform. In this project, we are developing an algorithm to convert data from an ultrasound-based device to absolute BP waveforms. Such a device may offer a quantitative method to perform rapid hemodynamic profiling of patients in an emergency room, step down clinical ward, or outpatient clinic who cannot undergo invasive BP measurements.

We propose a non-invasive way to get BP waveform with blood flow velocity and arterial area obtained from non-invasive ultrasound signals (Figure 1a). One key drawback of the ultrasound-based device is that the output BP waveform has an arbitrary reference, so we have to estimate the mean arterial pressure (MAP) and leverage transmission line model to calculate the absolute BP value. Hence, we propose to use a machine learning model containing transformer encoder layers to regress the MAP accurately. The input features are flow velocity and the shape of BP waveform. Since the number of subjects is limited in the training set, we propose to use contrastive loss to guide the feature extraction and improve generalization. The contrastive loss encourages the features of beats of the same subject to be similar. When we enlarge the contrastive loss , the feature vector will be trained to contain as little subject-specific information as possible. Therefore, the model can generalize better to unseen subjects. On a collected dataset, the proposed method improves the MAP error standard deviation from baseline 10.6 mmHg (only training the MAP regressor) to 9.2 mmHg. Our algorithm has large potential to make affordable BP measurements accessible to everyone.

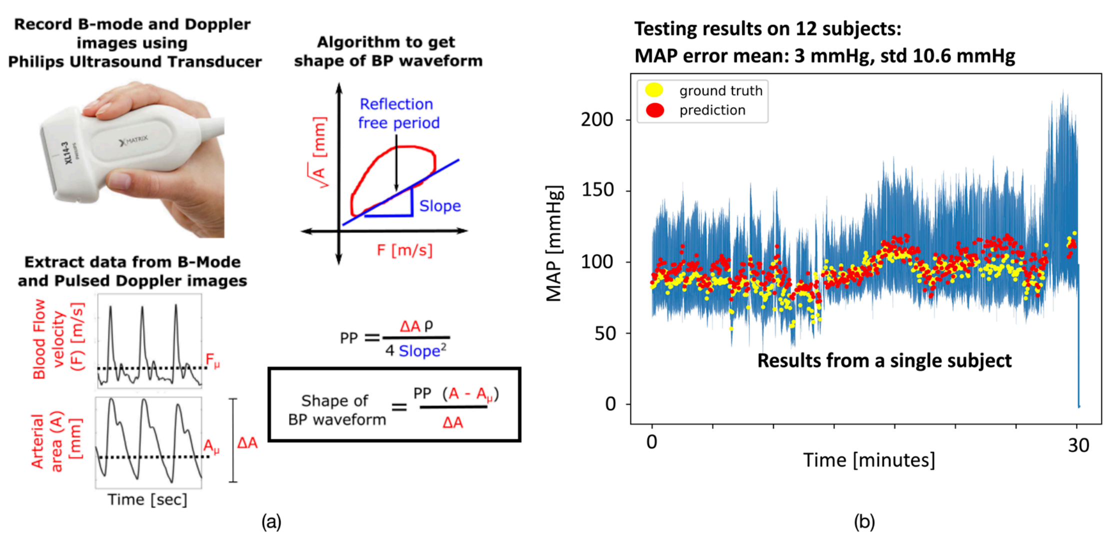

▲ Figure 1: (a) The whole pipeline of using machine learning-based algorithms to get BP waveforms from ultrasound data, and (b) MAP prediction results for a single subject.

FURTHER READING

- V. Novak, and L. Mendez, "Cerebral Vasoregulation in Diabetes" (version 1.0.0), *PhysioNet*, 2020. https://doi.org/10.13026/m40k-4758.

Electrokinetic-based Biomolecule Separation Technology

E. Wynne, J. Prince, C. Long, M. Cui, H. J. Kwon, J. Han
Sponsorship: Federal Drug Administration, SMART CAMP

Contamination of pharmaceutical products by viral and bacterial adventitious agents pose challenges to the safety and cost of a biomanufacturing process. Rapid detection of low abundance contaminants from a large volume requires concentrating the relevant biomolecules into a smaller volume that is compatible with sensitive downstream detection methods.

Electrokinetic (EK) concentration technology uses ion exchange membranes to selectively remove ionic species from a microchannel. When a voltage bias is applied to an EK concentrator, charged biomolecules become trapped by the increased electric field in the ion depletion region.

Recently significant progress has been made in constructing EK concentrators from inexpensive materials that are more compatible with large-scale manufacturing. See figures A and B.

Numerical simulation work is being used to better comprehend the non-linear electroosmotic flow present in these large-scale EK concentrators; an example is seen in Figure (C). Increasingly complex devices have many parameters that can affect performance such as applied voltage, flow rate, and channel dimensions. These simulations could help to find ideal operating parameters.

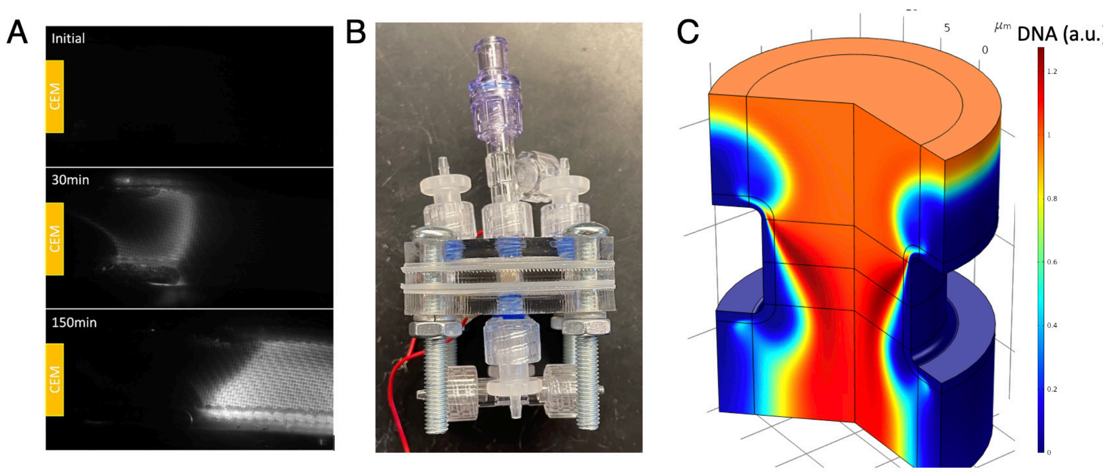

▲ Figure 1: (A) shows accumulation of fluorescently tagged DNA in an EK concentrator constructed using plastic channels and mesh. Additionally, (B) shows a high-throughput device made entirely from plastic that can enrich viruses from several milliliters of solution per hour into a volume as small as 200 microliters. (C) An example of numerical simulation work being used to better comprehend the non-linear electroosmotic flow present in these large-scale EK concentrators.

Minimally Invasive Wireless Stimulation of the Brain

S. Yadav, D. Sarkar
Sponsorship: NIH, Media Lab Consortium

Clinically, neural-stimulation finds application for treatment of neurological diseases like Parkinson's, Alzheimer's, etc. Currently, non-genetic neural stimulation faces challenges that can be classified into two broad categories: (a) tethered but requires invasive surgery (examples include electrodes, multi-electrode arrays, etc.) and (b) untethered but lacks cellular precision (examples include transcranial direct current stimulation, transcranial magnetic stimulation, etc.). Further, modalities that lie in between these two in terms of invasiveness involve implantation of devices inside the brain tissue and can be wirelessly actuated using fields which can be acoustic, magnetic, and electromagnetic, including radio frequency and light. Currently all these technologies are either invasive or cannot achieve spatio-temporally precise stimulation. To solve these challenges, we need to have a technology that qualifies on the following criteria: untethered remotely controlled devices to achieve minimal invasiveness and micron-sized to achieve single cell stimulation with minimal tissue displacement.

To achieve untethered neuron stimulation with single-cell resolution, we have developed photovoltaic arrays that can be wirelessly actuated with light to achieve spatiotemporally precise stimulation with single neuron resolution. These devices are based on organic polymers to operate at selective wavelengths. The chosen device structure is essentially a vertical stack of three components–anode, organic polymer, and cathode–fabricated on a silicon substrate. The choice of electrodes is based on the required built-in electric-field, transparency, and the charge injection capacity. Currently, we are carrying out in-vivo work for wireless stimulation of the brain in rodent models.

An Implantable Piezoelectric Microphone for Cochlear Implants

A. Yeiser, J. Zhang, L. Graf, C. McHugh, K. Broderick, J. Kymissis, E. Olson, H. H. Nakajima, J. H. Lang
Sponsorship: NIH Grant (R01DC016874)

Cochlear implants (CIs) are arguably the most successful sensory implant, with over 700,000 implanted up to 2019. Modern cochlear implants rely on external microphones. While these microphones are quite sensitive, they impose lifestyle restrictions on CI users and cannot replicate the sound localization cues from the shape of the outer ear. The development of a practical implantable microphone is a decades-old problem without good solutions. We think our implantable piezoelectric microphone design makes promising inroads towards this goal.

Our microphone design, shown in Figure 1, is a triangular piezoelectric cantilever about 3 mm long and 3 mm wide at the base. The cantilever consists of two layers of the piezoelectric polymer polyvinylidene difluoride (PVDF) sandwiching a flex printed circuit board, with charge sense electrodes at the layer interface providing a shielded differential output. The tip of the cantilever rests on the umbo—the point of the cone-shaped eardrum and detects audio-frequency displacement as low as 15 picometers when connected to our custom-built differential charge amplifier. When tested in a cadaveric human temporal bone as shown in Figure 2, the cantilever achieved sensitivity comparable to a good hearing aid microphone, with equivalent input noise (EIN) comparison shown in Figure 3.

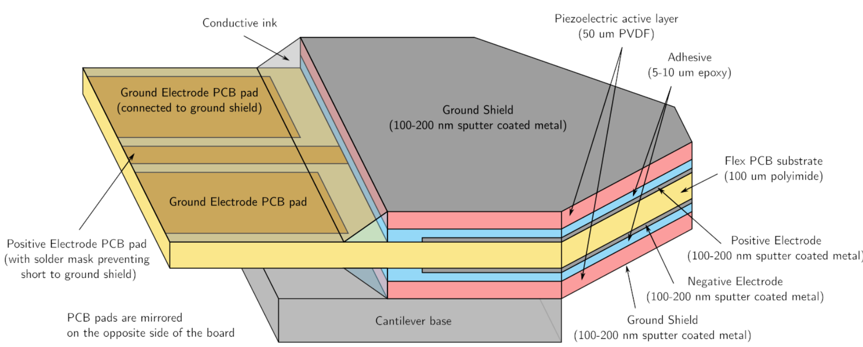

▲ Figure 1: PVDF microphone stackup, showing, showing charge-sense electrodes capacitively coupled to the PVDF through a thin glue layer.

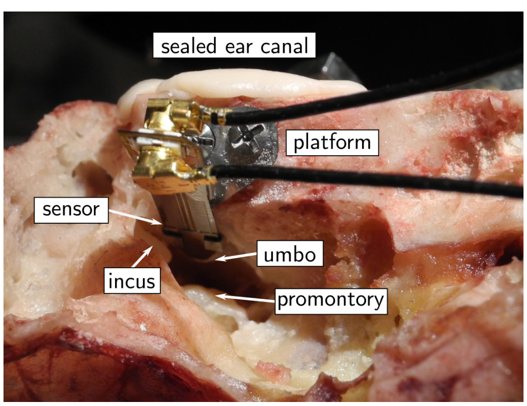

▲ Figure 2: Testing the cantilever-mic in a human temporal bone. The microphone rests on the umbo.

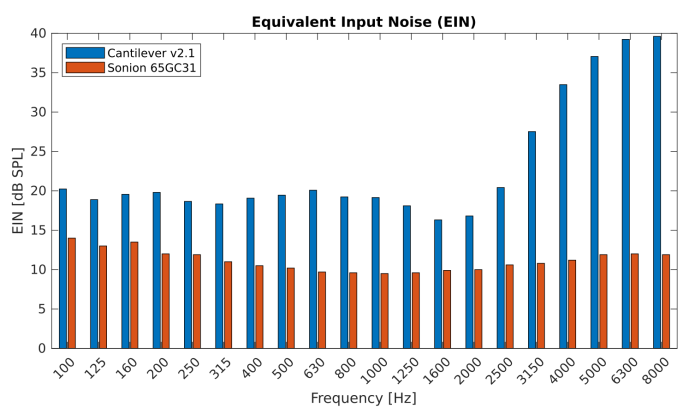

▲ Figure 3: Implanted cantilever EIN vs. a Sonion 65GC31 electret hearing aid microphone.

FURTHER READING

- D. Calero, S. Paul, A. Gesing, F. Alves, and J. A. Cordioli, "A Technical Review and Evaluation of Implantable Sensors for Hearing Devices," *BioMedical Engineering Online*, vol. 17, no. 1, p. 23, Dec. 2018.

Circuits, Systems, and Power Electronics

Randomized Switching Successive Approximation Register (RS-SAR) ADC Protections for Power and Electromagnetic Side Channel Security

M. Ashok, E. V. Levine, A. P. Chandrakasan
Sponsorship: MITRE Innovation Program, NSF Graduate Research Fellowship Program, MathWorks Engineering Fellowship

Analog to digital converters (ADCs) are necessary in most Internet of Things (IoT) devices, to link the physical analog world to digital computation. In many of these applications, the ADC is processing sensitive data such as biomedical signals or private conversations, which should not be accessible to an attacker. Physical side channel attacks (SCAs) have been used to reconstruct information processed within digital integrated circuits in a variety of applications, through power or electromagnetic (EM) traces. These attacks correlate unintentional leakage of information in the current consumption to the operations and data processed by a circuit, allowing for complete reconstruction of private data, as seen in Figure 1a. Specifically, EM SCAs allow fully non-invasive and localized attacks, by simply placing a probe above a packaged chip, eliminating the effectiveness of some global protections.

In this work, we propose the RS-SAR ADC, which decorrelates the data processed by the ADC from the power and EM side channel leakage. In the capacitive DAC, the parallel unit capacitors corresponding to the more significant bits are independently controlled with random bits, as shown in Figure 1b. This controlrandomization leads to variable timing of the binary search conversion, eliminating the attacker's ability to determine which of the digital data bits the various measured current spikes correspond to. When tested on a chip fabricated in TSMC 65-nm complementary metal-oxide-semiconductor (CMOS) (Figure 1c, provided through TSMC University Shuttle), the protected ADC has 82x the attack error of the unprotected ADC for power SCA and 32x the attack error for EM SCA.

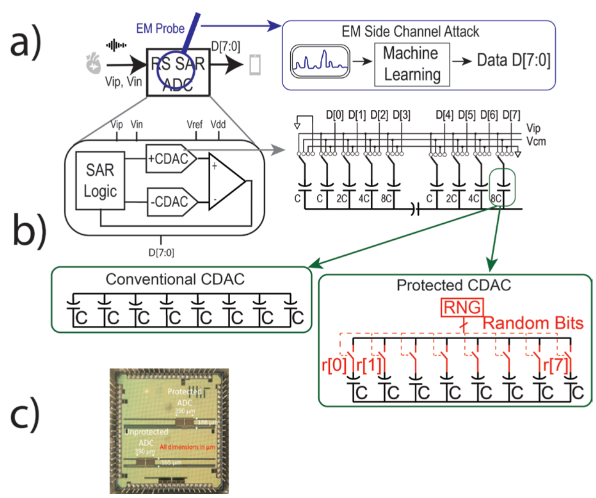

▲Figure 1: (a) Motivation for SAR ADC side channel security, along with (b) proposed RS-SAR architecture and (c) die micrograph. (From first Reading).

FURTHER READING

- M. Ashok, E. V. Levine, and A. P. Chandrakasan, "Randomized Switching SAR (RS-SAR) ADC Protections for Power and Electromagnetic Side Channel Security," presented at *IEEE Custom Integrated Circuits Conference*, Newport Beach, CApp. 1-2, 2022.
- T. Jeong, A. P. Chandrakasan, and H. Lee, "S2ADC: A 12-bit, 1.25MS/s Secure SAR ADC with Power Side-Channel Attack Resistance," *IEEE Custom Integrated Circuits Conference*, pp. 1-4, 2020.

A 140-GHz FMCW TX/RX-Antenna-Sharing Transceiver with Low-Inherent-Loss Duplexing and Adaptive Self-Interference Cancellation

X. Chen, M. I. W. Khan, X. Yi, X. Li, W. Chen, J. Zhu, Y. Yang, K. E. Kolodziej, N. M. Monroe, R. Han

High-resolution integrated radars are crucial in today's automotive, vital sign, and security-sensing applications. Compared to radars operating in the microwave/low-millimeter-wave and optical regimes, the sub-terahertz/terahertz (sub-THz/THz) spectrum shows great opportunities in both high-resolution and all-weather radar imaging capabilities. For isolation between the radar transmitter (TX) and receiver (RX), a bistatic configuration with separate TX and RX antenna positions is commonly adopted. However, in non-MIMO high-angular resolution systems, the radar transceiver should pair with a large lens/reflector for beam collimation. The bistatic arrangement then causes severe misalignment between the peaks of TX and RX beam patterns, as in Figure 1. Radar transceivers with a shared TX and RX antenna interface, or monostatic configuration, are therefore required in this scenario. Prior monostatic radars adopt hybrid/directional couplers for passive TX-RX duplexing, but at the cost of 3dB + 3dB insertion loss inherent to couplers.

As demonstrated in Figure 2, we present a 140-GHz frequency-modulated continuous-wave (FMCW) radar transceiver in 65-nm CMOS, featuring TX/RX antenna sharing that solves the TX/RX beam misalignment problem. A full-duplexing technique based on circular polarization and geometrical symmetry is applied to mitigate that 6dB inherent insertion loss, while maintaining high TX-to-RX isolation. In addition, a self-adaptive self-interference cancellation is implemented to suppress extra leakage due to antenna mismatch from a desired frontside radiation scheme. The TX/RX antenna sharing enables the pairing with a large 3D-printed planar lens and boosts the measured EIRP to 25.2dBm. The measured total radiated power and minimum single-sideband noise figure including antenna and duplexer losses are 6.2dBm and 20.2dB, respectively. The measured total TX-RX isolation is 33.3dB under 14-GHz wide FMCW chirps. Among all reported sub-THz transceivers with TX/RX antenna sharing, our work demonstrates the highest total radiated power and is the only work that has >30dB of TX-RX isolation while mitigating the inherent 6dB coupler loss.

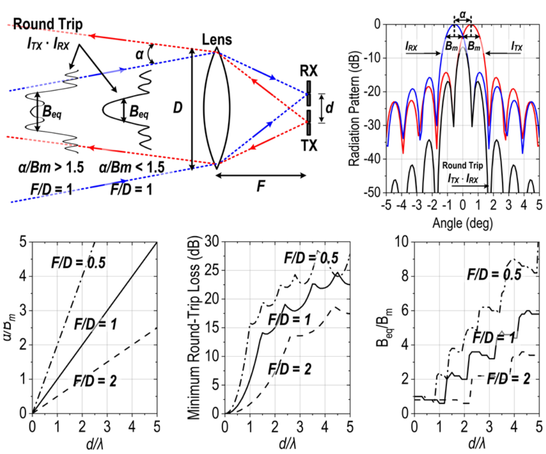

▲ Figure 1: Architecture of cryptographic core and chip micrograph.

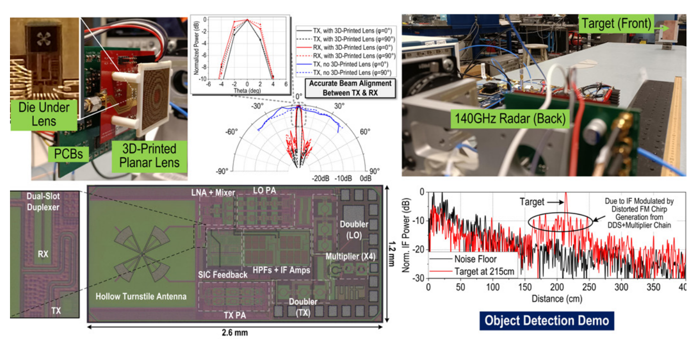

▲ Figure 2: Demo of the 140-GHz FMCW radar transceiver in 65-nm CMOS. The TX/RX antenna sharing enables the pairing with a large 3D-printed planar lens and accurate TX/RX beam alignment.

FURTHER READING

- X. Chen, M. I. W. Khan, X. Yi, X. Li, W. Chen, J. Zhu, Y. Yang, K. E. Kolodziej, N. M. Monroe, and R. Han, "A 140GHz Transceiver with Integrated Antenna, Inherent-Low-Loss Duplexing and Adaptive Self-Interference Cancellation for FMCW Monostatic Radar," *2022 IEEE International Solid- State Circuits Conference (ISSCC)*, pp. 80-82, 2022, doi: 10.1109/ISSCC42614.2022.9731637.
- N. M. Monroe, G. C. Doqiamis, R. Stingel, P. Myers, X. Chen, and R. Han, "Electronic THz Pencil Beam Forming and 2D Steering for High Angular-Resolution Operation: A 98×98-Unit 265GHz CMOS Reflectarray with In-Unit Digital Beam Shaping and Squint Correction," *2022 IEEE International Solid- State Circuits Conference (ISSCC)*, pp. 1-3, 2022, doi: 10.1109/ISSCC42614.2022.9731671.
- X. Yi, C. Wang, X. Chen, J. Wang, J. Grajal, and R. Han, "A 220-to-320-GHz FMCW Radar in 65-nm CMOS Using a Frequency-Comb Architecture," *IEEE Journal of Solid-State Circuits*, vol. 56, no. 2, pp. 327-339, Feb. 2021, doi: 10.1109/JSSC.2020.3020291.

A Bit-level Sparsity-aware SAR ADC with Direct Hybrid Encoding for Signed Expressions Leveraging Algorithm-circuit Co-design

R.-C. Chen, H. -T. Kung, A. P. Chandrakasan, H.-S. Lee
Sponsorship: CICS, DARPA

Machine learning is promising for many applications including image recognition and natural language processing. Machine learning accelerators are needed for these computation-intensive tasks. Analog neural networks are promising for breaking the memory wall for conventional machine learning accelerators. In this work, we propose the first sparsity-aware successive approximation register analog-to-digital converter (SAR ADC) with direct hybrid encoding for signed expressions (HESE) leveraging encoding algorithm-circuit co-design. ADCs are typically a bottleneck of analog neural networks. For a pre-trained convolutional neural network (CNN) inference, ANN with HESE SAR minimizes the non-zero terms and enables a reduction in energy along with the term quantization (TQ). The proposed SAR ADC directly produces the HESE signed-digit representation (SDR) using two thresholds per cycle as a 2-bit look-ahead. A proof-of-concept direct HESE SAR ADC is being fabricated by 65-nm technology. Measurements show that it provides the novel sparsity encoding with a Walden figure-of-merit of 15.2fJ/conv-step at a 45-MHz sampling rate. The core area is 0.072 mm^2. This opens the direction of direct sparsity encoding ADCs.

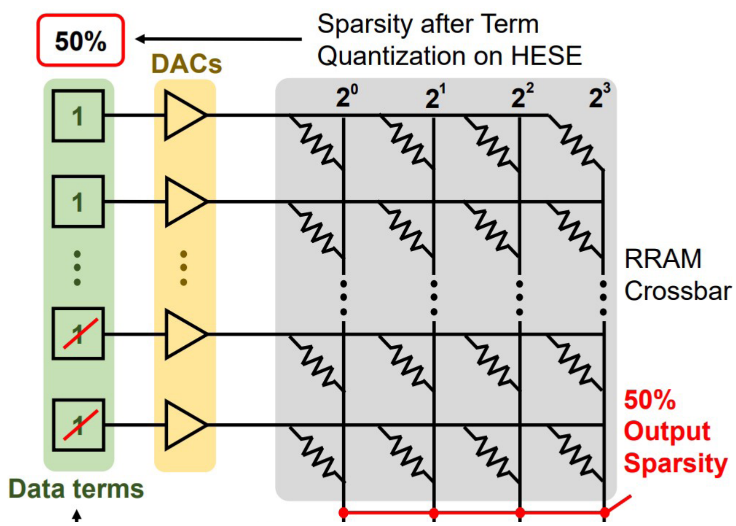

◀ Figure 1: An example crossbar of RRAM with 1-bit RRAM cells and 1-bit input values for computing dot products.

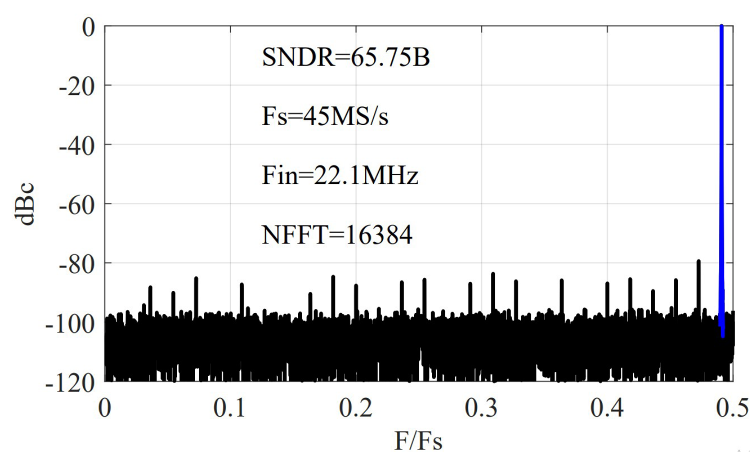

▶ Figure 2: Measured fast Fourier transform spectrum of the proposed direct HESE SAR.

FURTHER READING

- Y. Peng, W. Huaqiang, G. Bin, T. Jianshi, Z. Qingtian, Z. Wenqiang, Y. J. Joshua, and Q. He, "Fully Hardware-implemented Memristor Convolutional Neural Network," Nature, vol. 577, no. 7792, pp. 641–646, 2020.
- H. T. Kung, B. McDanel, and S. Q. Zhang,"Term Revealing: Furthering Quantization at Run Time on Quantized Dnns," arXiv preprint arXiv:2007.06389, 2020.

Physical Tags: Fingerprints and Markers Embedded in Objects for Ubiquitous Sensing and Seamless Interactions

M. D. Dogan, S. Mueller
Sponsorship: NSF, MIT Portugal Initiative, MIT Mechanical Engineering MathWorks Seed Fund Program

Physical tags, i.e., metadata attached to objects for identification, are an essential component of manufactured goods and raw materials. Conventional means of tagging these without electronics involve sticking separate labels (barcodes) to objects. However, such tags do not subtly blend into the objects and are often visually distracting or prone to damage. We propose to replace this synthetic "tagging" process with improved and robust approaches that use unobtrusive physical features of objects and materials as tags.

We focus on two types of unobtrusive tags: natural tags and engineered tags. The former allows us to leverage objects' natural properties as an ID, e.g., their micron-scale surface texture. For SensiCut (ACM UIST' 21), we used laser speckle imaging to sense material sheets in laser cutters without any pre-labeled stickers. Differences in surface structure result in unique speckle patterns for each material, which we use to classify its type with a convolutional neural network. We trained the network with more than 38k images, resulting in an accuracy rate of 97.97%.

Second, engineered tags enable us to define the type of information or pattern we want to embed on an object during the fabrication process. By manipulating a 3D printer's path, we create unique and subtle surface textures for each copy of the same 3D model, which can be distinguished from a single photograph (ACM CHI'20). For this approach, called G-ID, we evaluated how finely these texture-related parameter differences can be differentiated between and built a mobile application that uses image processing techniques to retrieve these parameters from photos. Together, these approaches represent an important first step towards enabling digitally readable tags in objects without disrupting their integrity, look, or feel.

FURTHER READING

- M. D. Dogan, S. V. A. Colon, V. Sinha, K. Akşit, and S. Mueller, "SensiCut: Material-Aware Laser Cutting Using Speckle Sensing and Deep Learning," *Proc. of the 34th Annual ACM Symposium on User Interface Software and Technology*, https://doi.org/10.1145/3472749.3474733, 2021.
- M. D. Dogan, F. Faruqi, A. D. Churchill, K. Friedman, L. Cheng, S. Subramanian, and S. Mueller. "G-ID: Identifying 3D Prints Using Slicing Parameters," *Proc. of the 2020 CHI Conference on Human Factors in Computing Systems* (CHI '20), pp. 1-13, 2020, https://doi.org/10.1145/3313831.3376202.
- M. D. Dogan, A. Taka, M. Lu, Y. Zhu, A. Kumar, A. Gupta, and S. Mueller. 2022. "InfraredTags: Embedding Invisible AR Markers and Barcodes Using Low-Cost, Infrared-Based 3D Printing and Imaging Tools," *Proc. of the 2022 CHI Conference on Human Factors in Computing Systems*, p. 9, 2022, https://doi.org/10.1145/3491102.3501951

A Low-power THz Wakeup Receiver for an Ultra-miniaturized Platform

E. Lee, M. I. Ibrahim, U. Banerjee, R. T. Yazicigil, A. P. Chandrakasan, R. Han
Sponsorship: NSF, Korea Foundation for Advanced Studies

With the increasing demand for wirelessly connected devices, extending the lifetime of the communication nodes has become essential. As wireless communication is often one of the most power-hungry parts of an overall system, it is necessary to use devices with low-power wireless communication capabilities. A wakeup receiver (WuRX) is a circuit block that listens to the predefined token and turns on the node. The WuRX keeps the node in standby mode until a valid request, which helps to reduce unnecessary power consumption and, thus, lengthen the battery lifetime. Among various metrics of WuRXs, sensitivity and power consumption are two major axes that have led the progress of WuRXs in past decades. Several sub gigahertz/gigahertz works have achieved sensitivity-power tradeoff by co-designing off-chip components such as a high-Q antenna. While these have improved sensitivity and power performance, they are not suitable for ultra-miniaturized platforms due to the external components.

Pushing the carrier frequency to terahertz (THz) is key to reducing the form factor near the mm2- scale. Thanks to the small antenna aperture size requirement of the THz electromagnetic waves, antennas can be fabricated on a chip and integrated with the receiver's front-end without any external off-chip components. In this work, we aim at developing a sub-microwatt THz WuRX, operating at 261 GHz. We use an envelope detector first receiver architecture to avoid large power consumption of THz demodulation. To increase the sensitivity of the WuRX, we investigate a method to improve the noise equivalent power of the THz detector. The THz detector output is amplified, filtered, and recovered to the original data. The duty-cycling technique is also applied to reduce power consumption. In addition, we propose a secure wakeup protocol to prevent the battery-drainage attack, which is especially critical to battery size-limited miniaturized platforms. While this project is still in progress, this system will facilitate the use of THz for the ultra-miniaturized platform.

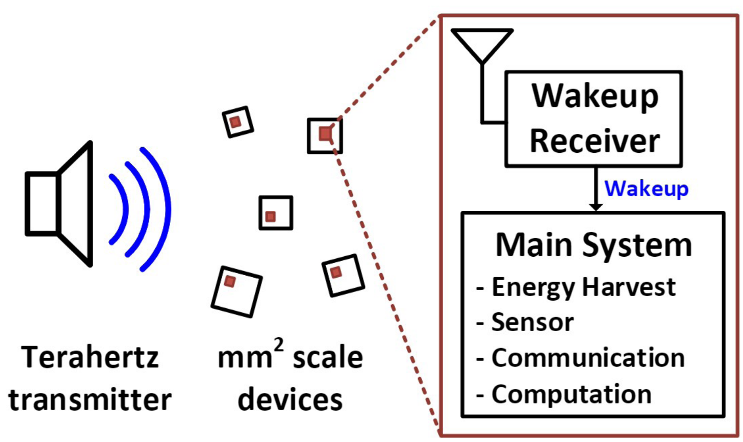

▲ Figure 1: Conceptual application scenario for the THz wakeup receiver.

FURTHER READING

- K. R. Sadagopan et al., "A 365nW −61.5 dBm Sensitivity, 1.875 cm2 2.4 GHz Wake-up Receiver with Rectifier-antenna Co-design for Passive Gain," *2017 IEEE Radio Frequency Integrated Circuits Symposium (RFIC)*, pp. 180-183, 2017.
- H. Jiang et al., "A 22.3-nW, 4.55 cm2 Temperature-Robust Wake-Up Receiver Achieving a Sensitivity of −69.5 dBm at 9 GHz," *IEEE J. Solid-State Circuits,* vol. 55, no. 6, pp. 1530-1541, Jun. 2020.

A Dual-antenna, 263-GHz Energy Harvester in CMOS with 13.6% RF-to-DC Conversion Efficiency at -8dBm Input Power

M. I. W. Khan, E. Lee, N. M. Monroe, A. P. Chandrakasan, R. Han
Sponsorship: NSF (Grant No. SpecEES ECCS-1824360)

Pushing the wave frequency of far-field wireless power transfer (WPT) to the terahertz regime is essential for ultra-miniaturized, battery-less platforms, which currently can only be powered through light or ultra-sound. As an example, the mm²-size THz identification tag (THz-ID) in [1] relies on integrated photo-diodes, and THz WPT will allow embedding the tags into optically-opaque packages of small-size goods (e.g., semiconductor chips). In this work, a 263-GHz energy harvester using Intel's 22nm FinFET process is reported, increasing the highest frequency of CMOS harvester by ~3x. The antenna-integrated harvester is ultra-compact (~0.5mm²) and does not rely on any external component. In Fig.1, a self-biased N-FinFET is simulated with various (v_{gs}, v_{ds}) combinations while keeping input power equal to -8dBm. An ηmax of 25.8% is obtained, when phase difference v_{ds}-v_{gs} is $\Delta\phi_{opt}$=45° and the amplitude ratio $|v_{ds}|/|v_{gs}|$ is A_{opt}=3.75. The schematic meeting these conditions is shown in Fig.2, where the additional phase tuning is provided by TL_7. Lastly, connecting the central AC ground nodes of the patch antennas together enables self-biasing of the transistor without interfering with antenna operations. The same connection is also used to extract DC output power. The measured load line performance of the harvester at 5cm distance, shown in Fig.3a, results in an optimum load of ~1kΩ. Fig. 3b shows that -8dBm input power the measured ηmax is 13.6% and 22µW of DC power is harvested.

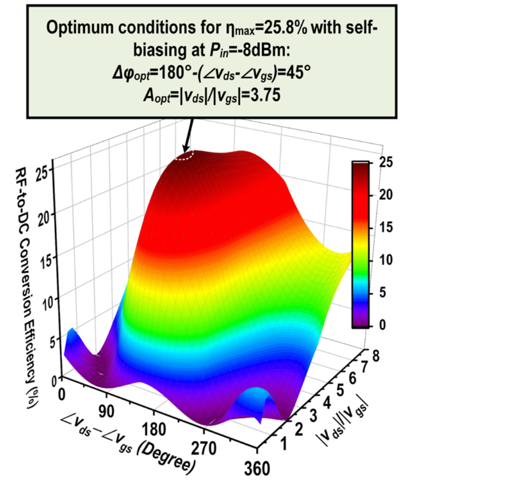

▲ Figure 1 Simulated rectification performance of a N-FinFET at various v_{ds} and v_{gs} ratio and phase difference.

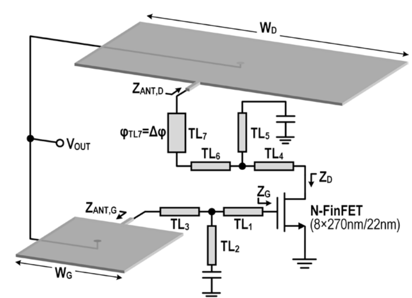

▲ Figure 2 Schematic of the THz energy harvester.

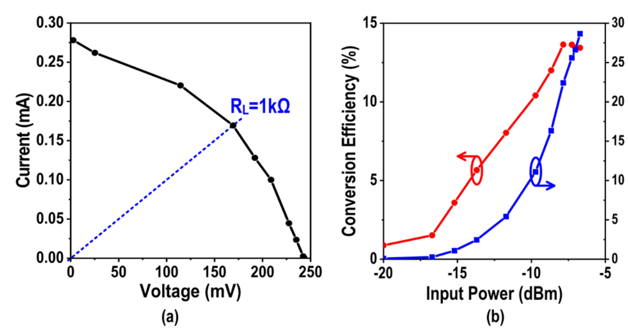

▲ Figure 3 Measured (a) load line, and (b) conversion efficiency and output power with 1kΩ load.

FURTHER READING

- M. I. W. Khan, M. I. Ibrahim, C. S. Juvekar, W. Jung, R. T. Yazicigil, A. P. Chandrakasan, and R. Han, "CMOS THz-ID: A 1.6-mm² Package-Less Identification Tag Using Asymmetric Cryptography and 260-GHz Far-Field Backscatter Communication," *IEEE Journal of Solid-State Circuits*, vol. 56, no. 2, pp. 340–354, 2021.
- M. I. W. Khan, E. Lee, N. M. Monroe, A. Chandrakasan, and R. Han, "A Dual-Antenna, 263-GHz Energy Harvester in CMOS for Ultra-Miniaturized Platforms with 13.6% RF-to-DC Conversion Efficiency at -8dBm Input Power," to be presented at *2022 IEEE Radio Frequency Integrated Circuits Symposium (RFIC)*, Denver, CO, 2022.

Stability Improvement of CMOS Molecular Clocks Using an Auxiliary Loop Based on High-order Detection and Digital Integration

M. Kim, H.-S. Lee, R. Han
Sponsorship: JPL, NSF

An ultra-stable frequency reference is a key element for a wide variety of applications, ranging from sensing to navigation. Recently, chip-scaled molecular clocks (CSMC) have achieved high frequency stability with low power and compact size by using a rotational-mode transition of carbonyl sulfide (OCS) centered around 231.061 GHz as a frequency reference (f0). In the molecular clock, the probing signal generated from the transmitter is frequency-modulated at fm around the center frequency (fc). Since fc is locked to f0 in a feedback loop, the output frequency inherits the excellent stability of the OCS transition frequency. Due to its fully electronic implementation, CSMC provided a solution to significantly reduce the cost of high-stability miniaturized clocks. However, the frequency stability is still limited by a finite loop gain of the frequency locked loop and detection non-idealities coming from baseline variations that are susceptible to environmental disturbance even though an invariant physical constant is used as the frequency reference.

In this work, we propose a new dual loop CSMC architecture based on both fundamental and high-order transition probing as well as digital integration. While the fundamental harmonic detection forms the main loop, the higher-order probing is used in an auxiliary loop. The main loop enables the fast correction of the frequency, and the auxiliary loop responds against long-term frequency variation. As a result, the dual-loop architecture combines the advantages of both fundamental locking and high-order locking: high signal-to-noise ratio (SNR) and robustness against the environmental variations. The proposed CSMC was implemented in 65-nm complementary metal-oxide-semiconductor (CMOS) and achieved 20-ppt Allan Deviation at 104 s averaging time with 71-mW power consumption. This demonstrates the feasibility of miniaturization, as well as the low power and low cost of the clock.

Time Series Anomaly Detection Applied to Switched Reluctance Motor System

C.-Y. Lai, F.-K. Sun, D. S. Boning, J. H. Lang
Sponsorship: Turntide Technologies

We explore methods to enable motor systems to utilize sensor data to assess installation and detect or predict anomalous events before possible breakdown. Here, we use an autoencoder neural network model for unsupervised anomaly detection on an air-handling system driven by a switched-reluctance motor (Figure 1). The motor system consists of a belt-driven blower-motor unit with a 6/10 stator/rotor pole configuration.

Our model (Figure 2) takes the Fourier transform of recorded sensor time signals and trains one autoencoder per feature. The sum of the reconstruction errors is used as an anomaly score for prediction. The autoencoder has been effective on time series datasets in multiple fields. We generate datasets with differences in various parameters (e.g., belt tightness, motor speed, blower output valve condition) and label the data according to the anomalous scenarios. For instance, if a dataset is used for anomaly detection of belt tightness, we label the time series generated with normal belt tightness "normal" and an over tight/loose belt "anomalous." We choose three kinds of sensor data (line current, motor current, vibration) as the time series for anomaly detection. We assume that the system operates normally during training and that sensor data used for training purposes contain few, if any, anomalies.

The base frequencies of motor current and vibration are identical and consistent with the 6:10 pole ratio. Characteristic curves are found in randomly ordered runs for transient sensor data during activation (Figure 3). Results of stable sensor data show 100% area under curve (AUC) / 98% accuracy for anomaly detection of belt tightness, and 95% AUC / 82% accuracy for speed; 52% AUC / 34% accuracy for valve condition indicates that this condition remains difficult to detect. Combining the labels for the three parameters achieves 94% AUC / 87% accuracy. Our model detects anomalies on motor systems for one or several aggregated failure modes.

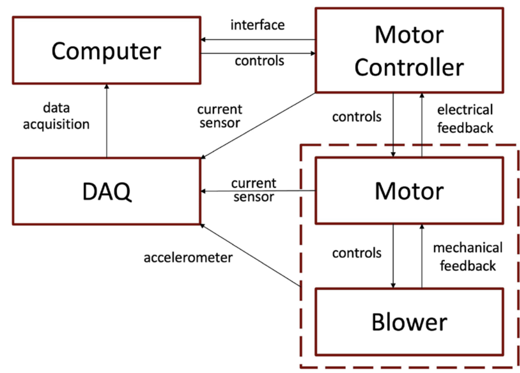

▲ Figure 1: General scheme for motor system.

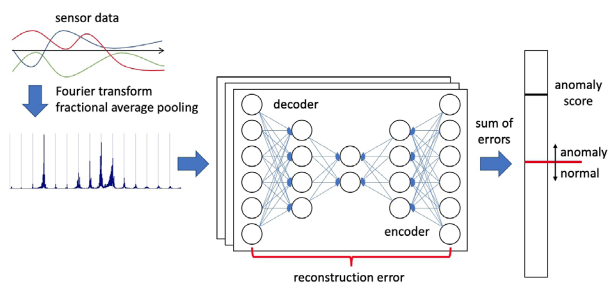

▲ Figure 2: Unsupervised anomaly detection autoencoder model.

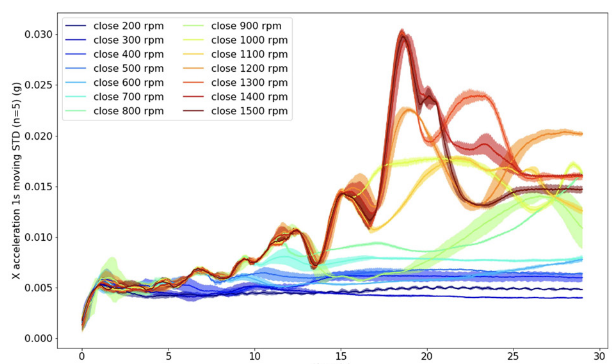

▶ Figure 3: Transient data of acceleration following characteristic curves with valve closed.

FURTHER READING

- F. K. Sun, C. Lang, and D. Boning, "Adjusting for Autocorrelated Errors in Neural Networks for Time Series," *Advances in Neural Information Processing Systems*, vol. 34, 2021.
- C. Desai, M. Krishnamurthy, N. Schofield, and A. Emadi, "Novel Switched Reluctance Machine Configuration with Higher Number of Rotor Poles Than Stator Poles: Concept to Implementation," *IEEE Transactions on Industrial Electronics*, vol. 57, no. 2, pp. 649-659, Feb. 2010.

A Sampling Jitter Tolerant Continuous-time Pipelined ADC in 16-nm FinFET

R. Mittal, H. Shibata, S. Patil, G. Manganaro, A. P. Chandrakasan, H.-S. Lee
Sponsorship: Analog Devices, Inc.

Almost all real-world signals are analog. Yet most of the data is stored and processed digitally due to advances in the integrated circuit technology. Therefore, analog-to-digital converters (ADCs) are an essential part of any electronic system. The advances in modern communication systems including 5G mobile networks and baseband processors require the ADCs to have a large dynamic range and bandwidth. Although there have been steady improvements in the performance of ADCs, the improvements in conversion speed have been less significant because the speed-resolution product is limited by the sampling clock jitter (Figure 1). The effect of sampling clock jitter has been considered fundamental. However, it has been shown that continuous-time delta-sigma modulators may reduce the effect of sampling jitter. But since delta-sigma modulators rely on relatively high oversampling, they are unsuitable for high frequency applications. Therefore, ADCs with low oversampling ratio are desirable for high-speed data conversion.

In conventional Nyquist-rate ADCs, the input is sampled upfront. Any jitter in the sampling clock directly affects the sampled input and degrades the signal-to-noise ratio (SNR). It is well known that for a given root-mean-square (RMS) sampling jitter σt, the maximum achievable SNR is limited to $1/(2\pi fin\sigma t)$, where fin is the input signal frequency. In a silicon-on-chip environment, it is difficult to reduce the RMS jitter below 100 fs. This limits the maximum SNR to just 44 dB for a 10-GHz input signal. Therefore, unless the effect of sampling jitter is reduced, the performance of an ADC would be greatly limited for high-frequency input signals.

We propose a continuous-time pipelined ADC having reduced sensitivity to sampling jitter (Figure 2). The analog input is processed in continuous time in the first stage. The residue is sampled by the backend ADC after amplification and low-pass filtering. This results in a much smaller derivative for the residue signal compared to the analog input. Since the error voltage due to clock jitter is proportional to the derivative of the sampled signal, the effect of sampling jitter is greatly reduced. We are designing this ADC in 16-nm FinFET technology to give a proof-of-concept for improved sensitivity to the sampling clock jitter.

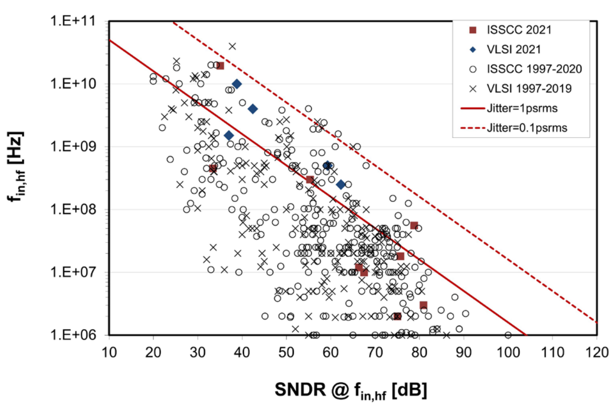

Figure 1: Performance survey for published ADCs (ISSCC 1997-2021 and VLSI 1997-2021).

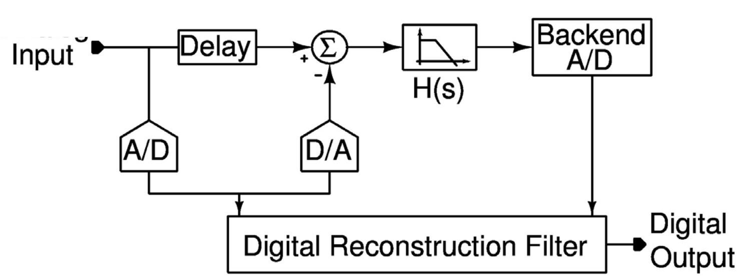

Figure 2: A schematic of the proposed continuous-time pipelined ADC tolerant to sampling jitter.

FURTHER READING

- B. Murmann, "ADC Performance Survey 1997-2021," [Online]. Available: http://web.stanford.edu/~murmann/adcsurvey.html.
- H. Shibata, Hajime, V. Kozlov, Z. Ji, A. Ganesan, H. Zhu, D. Paterson, J. Zhao, S. Patil, and S. Pavan. "A 9-GS/s 1.125-GHz BW Oversampling Continuous-time Pipeline ADC Achieving- 164-dBFS/Hz NSD." *IEEE Journal of Solid-State Circuits* 52, no. 12 (2017): 3219-3234.
- J. D. Boles, E. Ng, J. H. Lang, and D. J. Perreault, "High-efficiency operating Modes for Isolated Piezoelectric-transformer-based DC-DC Converters," *Proc. IEEE Workshop on Control and Modeling for Power Electronics (COMPEL)*, Aalborg, Denmark, Nov. 2020.

Energy-efficient System for Bladder Volume Monitoring with Conformable Ultrasound Patches

V. Mittal, Z. Song, C. Marcus, L. Zhang, S. J. Schoen, V. Kumar, Y. Eldar, C. Dagdeviren, A. E. Samir, H.-S. Lee, A. P. Chandrakasan
Sponsorship: Texas Instruments

Continuous monitoring of bladder volume aids the management of many common conditions such as post-operative urinary retention and benign prostatic hyperplasia. Despite the success of ultrasound technology, there is a lack of wearable ultrasound probes capable of imaging curved body parts with high spatio-temporal resolution and making diagnostic decisions. Current systems are not sufficiently energy-efficient to permit continuous wearable device deployment for more than 1-2 days, as their power budget is several mW. We aim to develop a conformable, energy-efficient, battery-operated, wearable ultrasound patch capable of real-time organ monitoring. The wearable patch will be fully integrated with the transceiver electronics for energy-efficient processing of the ultrasonic signals and an efficient inference engine for bladder volume estimation. This system will incorporate several key innovations, including (1) deep neural network- (DNN) based segmentation algorithms employed to generate accurate bladder volume estimates; (2) low voltage ultrasound transceivers to enable low power, portable integrated system; and (3) signal processing algorithms capable of working with low signal-to-noise ratio (SNR) environments.

We aim to integrate the transducers with the analog front-end and DNN accelerator while ensuring that heat dissipation is within FDA specified limits. The power-efficient patch will operate at low voltage, thus posing the challenge of working with a low SNR signal. The transmitter consists of energy-efficient pulsers, appropriately beam-formed and multiplexed for different sub-apertures of the transducer array. On the receiver end, low-voltage, energy-efficient techniques are used to optimize the active power of the analog front end.

An on-chip DNN will extract the segmented mask from the beamformed image. The network is trained on bladder ultrasound images from MGH. The network is mostly binarized with the remaining operations quantized to minimize the memory requirement and eliminate the need for on-chip floating-point operation support. A DNN accelerator is designed for optimal binary DNN performance but also supports low bit-width computation. Lastly, the bladder volume is extracted from the segmented images and given as the system output using the double area method.

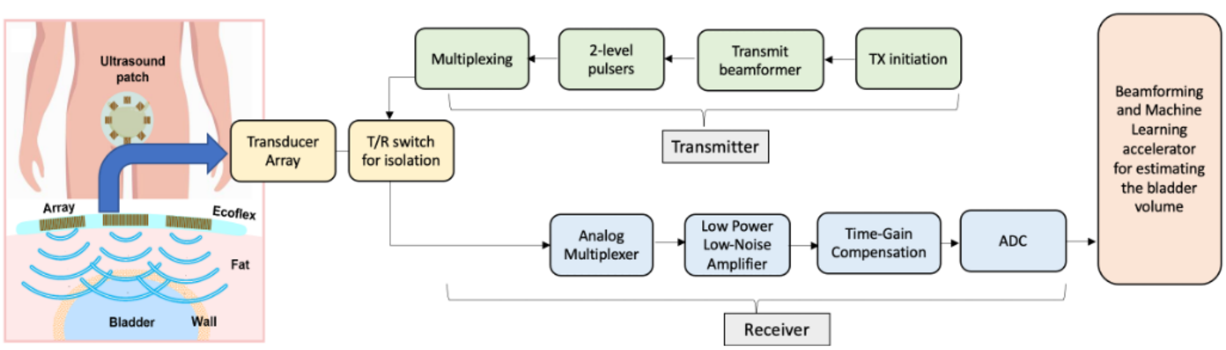

▲ Figure 1: System-level diagram of an ultrasound system.

FURTHER READING

- N. K. Kristiansen, J. C. Djurhuus, H. Nygaard, "Design and Evaluation of an Ultrasound-based Bladder Volume Monitor," *Medical and Biological Engineering and Computing*, vol. 42, pp. 762-769, 2004.
- C. M. W. Daft, "Conformable Transducers for Large-volume, Operator-independent Imaging," *2010 IEEE International Ultrasonics Symposium*, pp. 798-808. 2010.
- M. Dicuio, G. Pomara, F.M. Fabris, V., Ales, C. Dahlstrand, and G. Morelli, "Measurements of Urinary Bladder Volume: Comparison of Five Ultrasound Calculation Methods in Volunteers," *Archivio Italiano Di Urologia e Andrologia*, vol. 77, no. 1, pp. 60–62, 2005.

Hardware Design for Efficient Video Understanding on the Edge

M. Wang, Y. Lin, Z. Zhang, J. Lin, S. Han, A. P. Chandrakasan
Sponsorship: Qualcomm Incorporated

With the rise of various applications including autonomous driving, object tracking for unmanned aerial vehicles, etc., there is an increasing need for accurate and energy-efficient video understanding on the edge. Although there are many deep learning chips designed for images, little work has been done for videos. Video understanding on the edge has three major challenges. First, video understanding requires temporal modeling. For example, it identifies the difference between opening and closing a box, which is distinguishable only with temporal information considered. Second, many applications are delay-critical, such as self-driving cars. Third, high energy efficiency is important for edge devices with a tight power budget. Due to temporal continuity, consecutive frames might share a lot of common information, providing the potential to improve processing efficiency. However, an image-based processing system cannot utilize that since each frame is processed individually.

In this project, we co-design algorithms and hardware for energy-efficient video processing on delay-critical applications. We design architecture to natively support temporal shift module on the backbone of 2D convolutional neural networks for temporal modeling. Moreover, we propose a Real-Time DiffFrame method to utilize temporal redundancy and reduce on-chip energy and dynamic random-access memory (DRAM) traffic for delay critical applications. Compared to an ordinary convolution baseline, our method achieves around 2x reduction in both DRAM and static RAM (SRAM) accesses and 2x improvement in throughput with temporal modeling capability and no accuracy loss. The system has been fabricated in TSMC 28-nm complementary metal-oxide-semiconductor (CMOS) process. Figure 1 shows the chip photograph and specifications. We are evaluating our proposed system and measuring the performance of the chip.

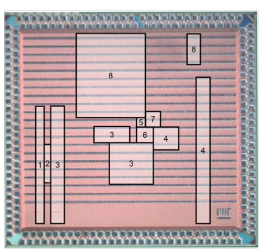

Chip Specifications	
Technology	TSMC 28nm HPC+ 1P10M
Die Size	3000um × 2800um = 8.4mm^2
Core Area	2572um × 2372um = 6.1mm^2
Package	Chip on board
Logic Gates	576.5K (NAND2 equiv.)
On-Chip SRAM	809.984K bits
Number of Multipliers	64
Arithmetic Precision	8-bit WGT & ACT, 22-bit PSUM
Operating voltage	Core: 0.55V~ 0.9V; I/O: 1.8V
Core clock freq.	29.4MHz ~ 90.9MHz

1. Weight buffer (16kB)
2. 8x8 MAC array
3. IA buffer (32kB)
4. OA & RefFrame unit (44kB)
5. DiffFrame generator
6. DiffFrame pruning
7. Kernel map buffer
8. Kernel map generator & Point coordinate buffer

▲ Figure 1: Chip micrograph and specifications.

FURTHER READING

- J. D. Boles, J. J. Piel, and D. J. Perreault, "Enumeration and Analysis of DC-DC Converter Implementations Based on Piezoelectric Resonators," *IEEE Transactions on Power Electronics*, vol. 36, no. 1, pp. 129-145, 2021.
- E. Ng, J. D. Boles, J. H. Lang, and D. J. Perreault, "Non-isolated DC-DC Converter Implementations Based on Piezoelectric Transformers," Proc. *IEEE Energy Conversion Congress and Exposition (ECCE)*, Vancouver, Canada, Oct. 2021.
- J. D. Boles, E. Ng, J. H. Lang, and D. J. Perreault, "High-efficiency Operating Modes for Isolated Piezoelectric-transformer-based DC-DC Converters," *Proc. IEEE Workshop on Control and Modeling for Power Electronics (COMPEL)*, Aalborg, Denmark, Nov. 2020.

Modeling and Design of High-power RF Power Combiners Based on Transmission-lines

H. Zhang, G. Cassidy, A. Jurkov, K. Luu, A. Radomski, D. J. Perreault
Sponsorship: MKS Instruments, Inc.

Industrial plasma generation for semiconductor processing applications are usually characterized by high power levels (e.g., kWs), wide power ranges (e.g., 30dB dynamic range), narrow-frequency-band operations (e.g., 13.56MHz ± <5%), and the need to combine power from multiple sources. Power combiners based on transmission lines are attractive due to their small form factor and high efficiency. However, most existing literature focuses on frequency response, with little consideration regarding losses or co-design with magnetic components. Here we introduce a lumped-element circuit model better suited for this application space and further propose a tuning technique that, by adding two capacitors, minimizes impedance distortion while preserving high efficiency. A 13.56-MHz, 1-kW prototype is designed and built, validating the model and tuning technique with both small-signal measurements and high-power tests. The study would help in realizing radio frequency power generation systems that maintain high efficiency over a very wide power range.

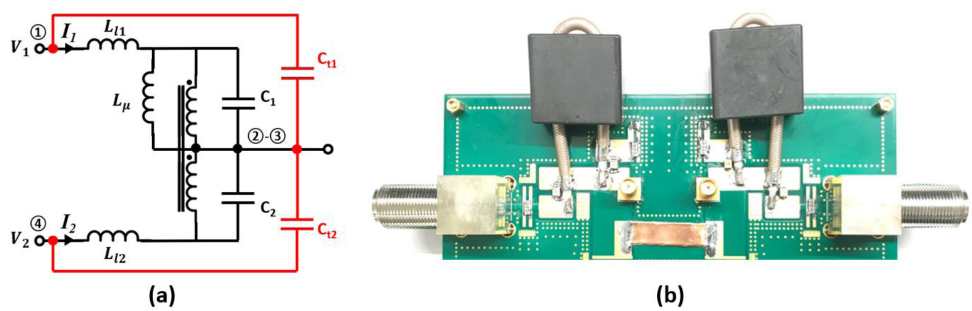

▲Figure 1: (a) Proposed lumped-element circuit model with tuning technique (achieved by adding two capacitors, Ct1 and Ct2), and (b) high-power testbench with 2-combiners connected in a back-to-back fashion.

FURTHER READING

- H. Zhang et. al., “Modeling and Design of High-Power Non-Isolating RF Power Combiners based on Transmission Lines,” *2022 IEEE Applied Power Electronics Conference and Exposition (APEC)*, to be published.
- H. Zhang et. al., “Multi-Inverter Discrete Backoff: A High-Efficiency, Wide-Range RF Power Generation Architecture,” *2020 IEEE 21st Workshop on Control and Modeling for Power Electronics (COMPEL)*, pp. 1-8, 2022, doi: 10.1109/COMPEL49091.2020.9265702.
- A. Al Bastami et. al., "Comparison of Radio-Frequency Power Architectures for Plasma Generation," *2020 IEEE 21st Workshop on Control and Modeling for Power Electronics (COMPEL)*, pp. 1-8, 2020, doi: 10.1109/COMPEL49091.2020.9265700.

Electronic, Magnetic, Superconducting, and Sprintronic Devices

Current-induced Switching of a Ferromagnetic Weyl Semimetal Co_2MnGa

J. Han, B. C. McGoldrick, C.-T. Chou, T. S. Safi, J. T. Hou, L. Liu
Sponsorship: NSF, Semiconductor Research Corporation Program

The introduction of magnetic moments to topological materials provides rich opportunities for studying the interplay among magnetism, electron correlation, and topological orders, which can give rise to exotic magnetoelectric effects and allow one to manipulate the topologically nontrivial band structure via spintronic approaches. Weyl semimetal is a type of novel topological material that exhibits exotic magnetoelectric effects enabled by the Berry curvature around the Weyl nodes of the topological band structure. The valley conservation of Weyl node also provides a potential source of robust tunneling magnetoresistance, which can be utilized to develop energy efficient memory devices.

In this work, current-induced spin orbit torque switching of ferromagnetic Weyl semimetal Co_2MnGa perpendicular magnetic anisotropy (PMA) is demonstrated. X-ray diffraction results confirm that the Co_2MnGa is epitaxially grown and in $L2_1$ phase of the $Fm\bar{3}m$ space group, which has been theoretically predicted and experimentally shown to own topological Weyl states. The strong anomalous Hall effect associated with Weyl states is also observed. The thickness of Co_2MnGa is tuned to have PMA, and current-induced switching of PMA Co_2MnGa is achieved by an adjacent Pt layer through spin-orbit torque. The reversal of the large anomalous Hall signal indicates an effective electrical control of the Berry curvatures and therefore the associated magnetoelectric effects. The efficiency of the spin-orbit torque switching is calibrated to be comparable to that in conventional ferromagnets. Given the compatibility of Co_2MnGa films with various spintronic devices and techniques, our work represents an essential step towards incorporating topological ferromagnetic materials in memory and computing devices.

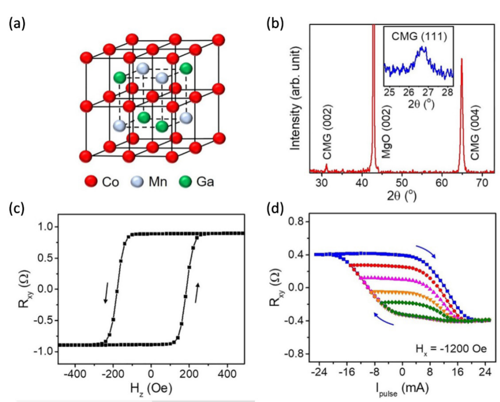

▲Figure 1: (a) Crystal structure of Co_2MnGa (CMG), (b) XRD θ-2θ scan of a 70-nm Co_2MnGa film grown on (001) MgO substrate, (c) Hall resistance as a function of the out-of-plane field Hz, (d) current-induced switching with different minimum writing currents.

FURTHER READING

- J. Han, B. C. McGoldrick, C.-T. Chou, T. S. Safi, J. T. Hou, and L. Liu, “Current-induced Switching of a Ferromagnetic Weyl Semimetal Co2MnGa,” *Appl. Phys. Lett.*, vol. 119, p. 212409, 2021.

3-D Printed Quadrupole Mass Filters for CubeSat Mass Spectrometry

A. Diaz, L. F. Velásquez-García
Sponsorship: MIT Portugal

Mass spectrometry is the gold standard for quantitative chemical analysis. Mass spectrometers employ mass filters that generate electromagnetic fields to sort out in vacuum the ionized constituents of a sample based on their mass-to-charge ratio, making it possible to determine the chemical composition of the sample. However, mass spectrometers are typically large, heavy, and power hungry, restricting their deployability into in-situ, portable, and hand-held scenarios, e.g., CubeSats. Miniaturization of electronics and mass spectrometry hardware has made possible the implementation of compact instruments. Nonetheless, instrument miniaturization has been attained at the expense of great loss in performance, caused in part by fabricating unideal electrode shapes and losing assembly resolution via post-assembly. Via additive manufacturing, it is possible to create monolithically and more precisely electrode shapes, avoiding some or most of the key assembly steps in a traditional mass filter, potentially resulting in hardware that performs better.

In this project we are developing compact, monolithically 3D-printed RF quadrupole mass filters that operate in the MHz range. Figure 1 shows an early-stage prototype of this filter. Moreover, the work includes developing compact, precision electronics for running the quadrupole and reading the current transmitted by the mass filter (Figure 2). We will also explore ideas for improving the performance of the mass filter, e.g., operating the devices in the second stability region.

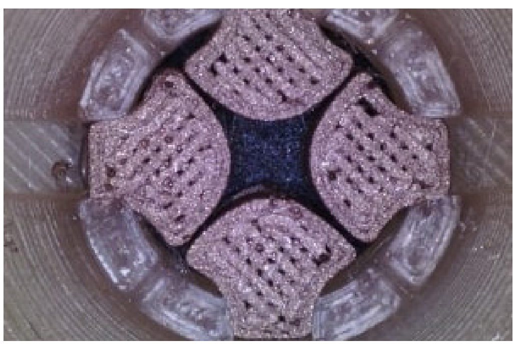

◀ Figure 1: 3-D printed prototype of a quadrupole with conductive electrodes and non-conductive supporting structure.

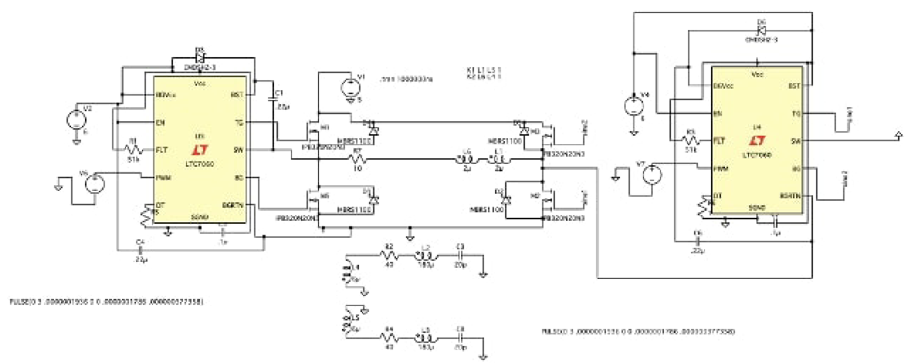

▶ Figure 2: Full bridge class D amplifier setup to maximize power efficiency with a 2.65-MHz driving frequency.

FURTHER READING

- L. F. Velásquez-García, K. Cheung, and A. I. Akinwande, "An Application of 3D MEMS Packaging: Out-Of-Plane Quadrupole Mass Filters," *J. Microelectromech. Syst.*, vol. 16, no. 6, pp. 1430-1438, Dec. 2008.
- K. Cheung, L. F. Velásquez-García, and A. I. Akinwande, "Chip-Scale Quadrupole Mass Filters for Portable Mass Spectrometry," *J. Microelectromech. Syst.*, vol. 19 no. 3, pp. 469-483, June 2010.
- Z. Sun, G. Vladimirov, E. Nikolaev, and L. F. Velásquez-García, "Exploration of Metal 3-D Printing Technologies for the Microfabrication of Freeform, Finely Featured, Mesoscaled Structures," *J. Microelectromech. Sys.*, vol. 27, no. 6, pp. 1171-1185, Dec. 2018.

Compact, Monolithic, Additively Manufactured Quadrupole Mass Filters

C. Eckhoff, L. F. Velásquez-Garcia
Sponsorship: Empiriko Corporation

Mass spectrometry (MS) is the gold standard for identifying matter. Whether quantitative precision is needed to study absolute amounts of target molecules or qualitative resolving power is needed to discriminate isotopes down to a single neutron of difference, MS is often the tool of choice in the biotech and medical fields. However, the emergent focus of medical device industries on point-of-care (POC) testing has not brought with it a POC MS device satisfying the requirements of physicians and clinical regulatory agencies.

Our group seeks to improve POC MS systems by creating novel micro-electromechanical system (MEMS) mass filters, using design techniques permitted exclusively by additive manufacturing. This includes arbitrary electrode shapes, precision electrode alignment, and the efficient use of device space. Our manufacturing approach is to use a digital light processing of glass-ceramic resin to produce monolithically fabricated, pre-aligned hyperbolic electrodes (Figure 1). By integrating parts that are usually separate, monolithic designs reduce the need for fastening, alignment, and mounting hardware. This not only reduces costs but increases assembly precision, improving quadrupole resolution. Furthermore, the hyperbolic geometry of the quadrupole electrode rods eliminates field harmonics that are present on common, commercial circular rods. Plating is used to metallize the electrodes (Figure 2), resulting in thermally stable, electrically conductive electrodes.

Additive manufacturing, mass filter design, and post-print metallization all pose challenges of their own; when these processes are combined, even greater challenges exist. Our research currently focuses on optimizing each of these processes while considering the needs and effects of the other processes. For instance, we have designed a working quadrupole filter that prints well in ceramic while also being easy to metallize. Proof-of-concept data is being collected for the early prototypes, which will guide future refinement and miniaturization of the quadrupole design.

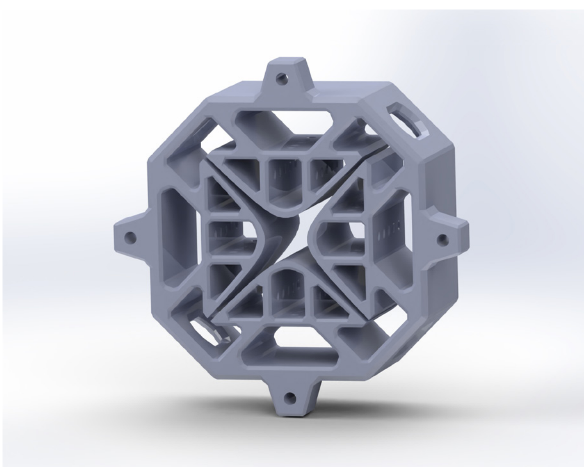

▲Figure 1: CAD model of singular, monolithic quadrupole mass filter.

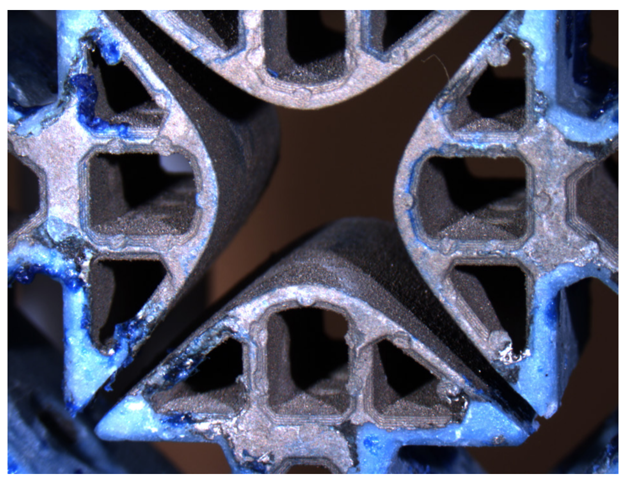

▲Figure 2: Close-up photo of metallized, 3D-printed electrodes.

FURTHER READING

- L. F. Velásquez-García, K. Cheung, and A. I. Akinwande, "An Application of 3D MEMS Packaging: Out-oOf-Plane Quadrupole Mass Filters," *J. Microelectromech. Syst.*, vol. 16, no. 6, pp. 1430- – 1438, Dec. 2008.
- K. Cheung, L. F. Velásquez-García, and A. I. Akinwande, "Chip-Scale Quadrupole Mass Filters for Portable Mass Spectrometry," *J. Microelectromech. Syst.*, vol. 19, no. 3, pp. 469- – 483, June 2010.
- Z. Sun, G. Vladimirov, E. Nikolaev, and L. F. Velásquez-García, "Exploration of Metal 3-D Printing Technologies for the Microfabrication of Freeform, Finely Featured, Mesoscaled Structures," *J. Microelectromech. Sys.*, vol. 27, no. 6, pp. 1171- – 1185, Dec. 2018.

Robust and Scalable Vertical GaN Transistor Technology

J.-H. Hsia, J. Perozek, A. Zubair, R. Molnar, J. Niroula, O. Aktas, V. Odnoblyudov, T. Palacios
Sponsorship: Advanced Research Projects Agency-Energy

Vertical GaN fin field-effect transistors (FinFETs) have attracted significant research interest due to their potential in overcoming the limitations of traditional lateral devices. The unique vertical structure provides area-independent, large breakdown voltages, improved thermal management, and reduced susceptibility to surface states, which make GaN FinFETs excellent candidates for high performance, highly scaled power and radio frequency (RF) devices. However, one of the biggest challenges in this field is the complex, low yield fabrication of these devices. Over last few years, our group has developed a robust process flow for vertical GaN FinFETs, whose basic structure is shown in Figure 1a. One of the key fabrication technologies we use is anisotropic wet etch based on heated tetramethylammonium hydroxide, which smoothens the fin sidewalls and improves channel properties (Figure 1b). The use of this technology produced devices with high yields for both RF and power applications. Furthermore, we have obtained excellent device characteristics for our fully vertical bulk GaN devices (Figure 2). We are currently extending our fabrication technology to build more advanced vertical GaN structures, such as vertical super junction devices.

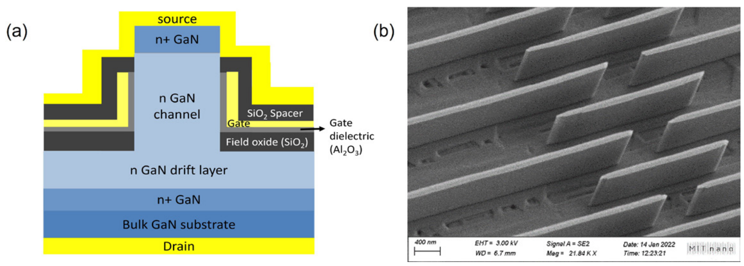

▲ Figure 1: (a) Basic device structure of vertical GaN FinFET. (b) Scanning electron microscope image of GaN fin channels with smooth sidewall.

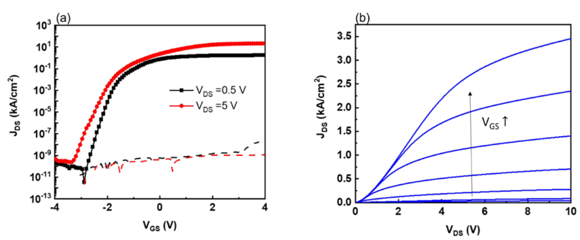

▲ Figure 2: (a) Transfer and (b) Output characteristics of our fully vertical bulk GaN device.

FURTHER READING

- Y. Zhang, M. Sun, J. Perozek, Z. Liu, A. Zubair, D. Piedra, N. Chowdhury, X. Gao, K. Shepard, and T. Palacios, "Large-Area 1.2-kV GaN Vertical Power FinFETs with a Record Switching Figure of Merit," *IEEE Electron Device Letters,* vol. 40, no. 1, pp. 75-78, Jan. 2019, doi: 10.1109/LED.2018.2880306.
- M. Itoh, T. Kinoshita, C. Koike, M. Takeuchi, K. Kawasaki, and Y. Aoyagi, "Straight and Smooth Etching of GaN (1 1 0 0) Plane by Combination of Reactive Ion Etching and KOH Wet Etching Techniques," *Jpn. J. Appl. Phys.*, vol. 45, no. 5A, pp. 3988-3991, May 2006. doi: http://doi.org/10.1143/JJAP.45.3988.

Modeling Defect-level Switching for Highly-Nonlinear and Hysteretic Electronic Devices

J. Dong, R. Jaramillo
Sponsorship: Office of Naval Research MURI (N00014-17-1-2661)

Many semiconductors feature defects with charge state transition levels that can switch due to structure changes following defect ionization: we call this defect-level switching (DLS). For example, DX centers in III-V compounds can switch between deep and shallow donor configurations. This effect is known to produce persistent photoconductivity. We recently demonstrated highly-nonlinear, hysteretic, two-terminal electronic devices using DLS in CdS DLS devices operate in the opposite sense to most resistive switches: they are in a high-conductivity state at equilibrium. Although DLS uses the crystal defects that are responsible for photoconductivity, DLS devices operate without light and can be orders-of-magnitude faster. In this work we use theory and numerical simulation to explore the design space of DLS devices, emphasizing the tradeoff between switching speed and on/off ratio. Our results establish a platform for future numerical optimization of circuits using DLS-based resistive switches.

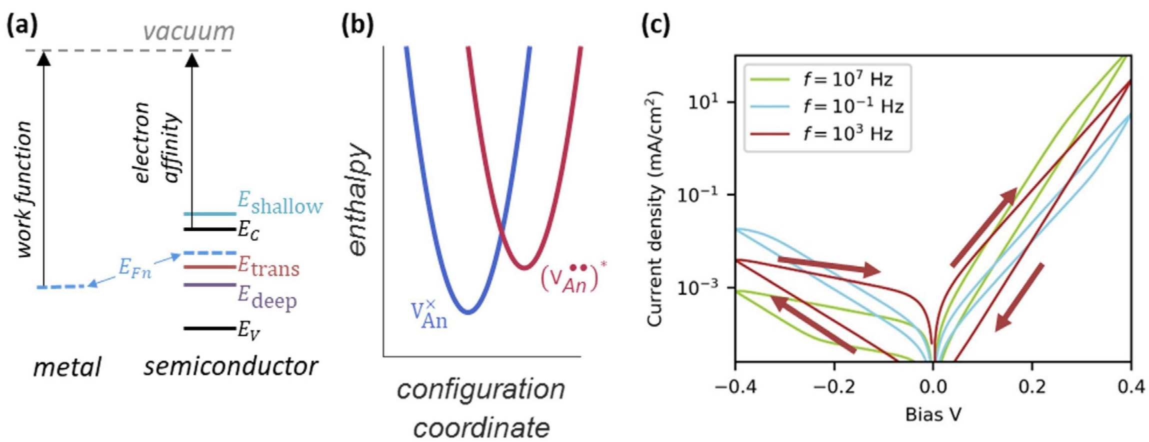

▲ Figure 1: (a) Metal-semiconductor DLS heterojunction device schematic. (b) System enthalpy vs. atomic configuration around the DLS-active defect. (c) Current-voltage characteristics of a DLS device for various drive frequencies.

Impact of Gate Geometry on Threshold Voltage Instability of p-GaN-Gate High-electron-mobility Transistors

E. S. Lee, J. A. del Alamo
Sponsorship: Texas Instruments

Enhancement-mode GaN high-electron-mobility transistors (HEMTs) that incorporate a p-doped GaN layer in the gate stack are attractive for power electronics due to a positive threshold voltage, low resistance, and high voltage capabilities. However, the p-GaN layer brings concerns on instability of the threshold voltage. Experimental studies in this type of devices have revealed the occurrence of threshold voltage shifts, both recoverable and permanent. Furthermore, the p-GaN sidewall has been found responsible for poor reliability and excessive gate leakage. This realization suggests a gate design in which the p-GaN is longer than the Schottky gate contact, resulting in a p-GaN offset, as sketched in Figure 1. Among other considerations, it is important to understand the reliability implications of transistor designs where the p-GaN layer is longer that the metal Schottky barrier.

We have experimentally studied the reliability of industrial pre-competitive p-GaN HEMTs with different gate dimensions. In particular, we have studied the impact of prolonged positive gate bias stress on the electrical characteristics of the devices. Our study reveals a new permanent threshold voltage degradation mechanism that uniquely takes place in the offset region of the gate. This is a concern as it might compromise long-term reliability. Our research thus reveals the existence of a constraint on how long the offset region of p-GaN HEMTs can be.

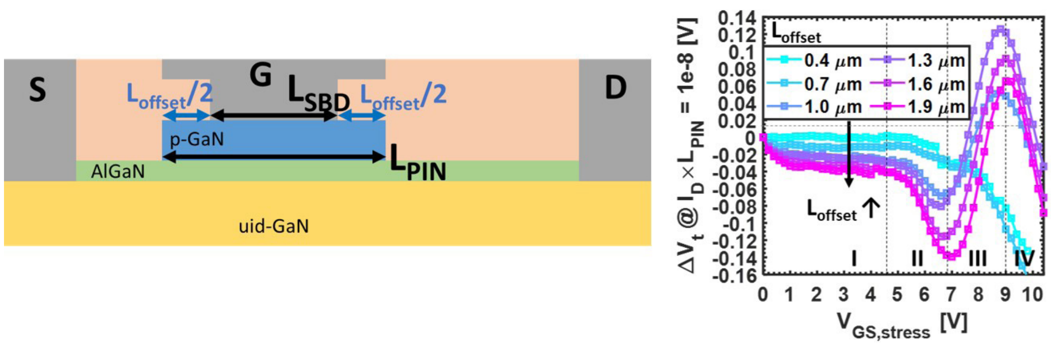

▲ Figure 1: (Left) simplified schematic of p-GaN HEMT. L_{SBD} = 0.7μm is the metal-gate/p-GaN interface length, L_{PIN} is the p-GaN/AlGaN/GaN heterostructure length, and $L_{offset} = L_{PIN} - L_{SBD}$. (Right) changes to V_t as a function of increasing V_{GS} step stress for devices with different L_{offset}. Regime III, associated with a prominent positive V_t shift disappears as L_{offset} is reduced below 0.7 μm.

FURTHER READING

- E. S. Lee, J. Joh, D. S. Lee, and J. A. del Alamo, "Impact of Gate Offset on PBTI of p-GaN Gate HEMTs," *2022 IEEE International Reliability Physics Symposium (IRPS)*, 2022.
- E. S. Lee, J. Joh, D. S. Lee, and J. A. del Alamo, "Gate-geometry Dependence of Dynamic Vt in p-GaN Gate HEMTs," *2022 34th International Symposium on Power Semiconductor Device and Ics (ISPSD)*, 2022.
- E. S. Lee, J. Joh, D. S. Lee, and J. A. del Alamo, "Gate-geometry Dependence of Electrical Characteristics of p-GaN Gate HEMTs," *Appl. Phys. Lett.*, vol. 120, p. 082104, 2022. https://doi.org/10.1063/5.0084123.

In-situ Monitoring of Dynamic Threshold Voltage in GaN Transistors Under Multi-pulse Hard-switching Conditions

A. Massuda, J. A. del Alamo
Sponsorship: Analog Devices

Recently, GaN HEMT technology entered a new generation of development and production. With the prospect of power management applications, a successful technology must meet strict reliability requirements. Since power management applications involve operating the transistors under repeated switching, reliability and robustness under pulsed operation is a concern. In this mode, parameters such as dynamic on-resistance, $R_{DS,ON}$, and threshold voltage, V_{TH}, are subject to the influence of various trapping effects as well as permanent degradation. Since GaN HEMT has relatively low turn-on VTH, it is more susceptible to high di/dt and dv/dt during the dynamic operation.

$R_{DS,ON}$ has been the major focus in switching reliability studies of GaN power transistors. In contrast, the impact of a shift in V_{TH} as an indicator to detect device degradation remains much less studied. This work explores a test system for in-situ monitoring of V_{TH} during sustained double-pulsed switching operation. The circuit diagram is shown in Figure 1a. By using a gate driver design with separate gate resistors for turn-on and -off (Figure 1b.), the user can fine-tune the turn-on speed to optimize the extraction of V_{TH} (Figure 1c,d). This study will contribute to understanding the impact of hard switching on dynamic V_{TH} shifts and dynamic $R_{DS,ON}$ of GaN power transistors.

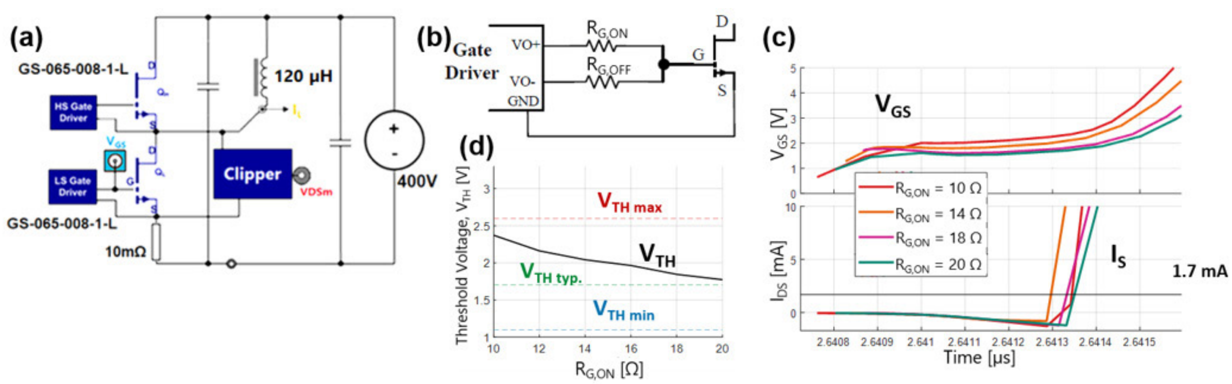

▲ Figure 1: (a) Schematic for the double-pulse test setup. (b) Gate driver design to enable selecting the right gate resistor to tune the turn-on slew rate. (c) Simulation for various R_{GON} in gate driver showing that: (d) extracted V_{TH} is within specs.

FURTHER READING

- H. Wang, J. Wei, R. Xie, C. Liu, G. Tang, and K. J. Chen, "Maximizing the Performance of 650-V p-GaN Gate HEMTs: Dynamic RON Characterization and Circuit Design Considerations," *IEEE Transactions on Power Electronics*, vol. 32, pp. 5539-5549, 2017.
- M. Meneghini, G. Meneghesso, and E. Zanoni, "Analysis of the Reliability of AlGaN/GaN HEMTs Submitted to On-State Stress Based on Electroluminescence Investigation," *IEEE Transactions on Device and Materials Reliability*, vol. 13, pp. 357-361, 2013.

Ising Machine Based on Electrically Coupled Spin Hall Nano-Oscillators

B. C. McGoldrick, J. Z. Sun, L. Liu
Sponsorship: MIT-IBM Watson AI Lab

Combinatorial optimization (CO) problems are ubiquitous in real-world applications, such as computer networking, very large-scale integration (VLSI) circuit design, and operations research. However, most of these problems remain unsolvable on traditional von Neumann computing architectures. These architectures suffer from a "bus bottleneck" whereby the shuffling of data between separate memory and computing units results in high latency. Unconventional computing architectures such as Ising machines have been proposed based on new hardware systems with novel physics that are better-suited for solving CO problems.

The Ising machine is composed of a coupled network of nonlinear oscillators, shown in Figure 1, on which CO problems can be mapped and subsequently solved using the natural phase synchronization dynamics. GHz spin Hall nano-oscillators (SHNOs) are a particularly attractive technology for building fast, energy-efficient, and scalable computing systems; however, due to a lack of general modeling tools, the performance of Ising machines based on electrically coupled SHNOs has not yet been studied in detail.

In this work, we develop a new analytical framework describing SHNO synchronization that is integrated into an efficient device model for scalable circuit-level simulations of the Ising machine. We study the performance of the SHNO-based Ising machine using networks up to hundreds of coupled oscillators. As seen in Figure 2, we predict that the SHNO network can solve CO problems orders of magnitude faster than previous approaches and with ultralow power and a small footprint thanks to the devices' nanoscale size. Our results illuminate important considerations in designing an Ising machine based on SHNOs that can efficiently solve full-scale CO problems with widely useful applications.

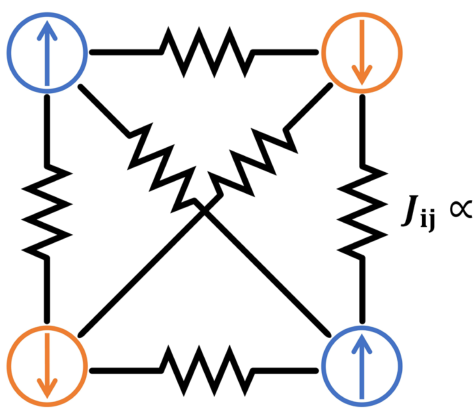

▲ Figure 1: Electrically coupled network of four oscillators that can be used to solve CO problems encoded by coupling weights *Jij*.

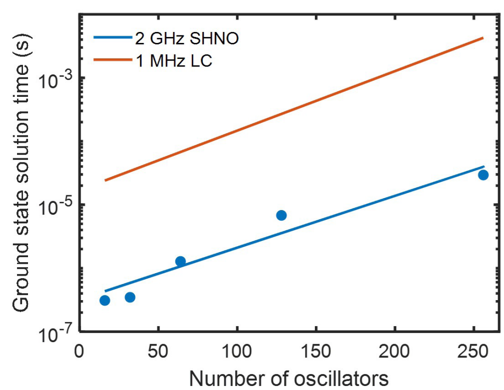

▲ Figure 2: Solution time of SHNO Ising machine (blue) compared to previously proposed LC oscillator Ising machine (orange).

FURTHER READING

- B. C. McGoldrick, J. Z. Sun, and L. Liu, "Ising Machine Based on Electrically Coupled Spin Hall Nano-Oscillators," *Physical Review Applied*, vol. 17, pp. 014006, Jan. 2022.

Nanoscale Protonic Programmable Resistors for Analog Deep Learning

M. Onen, N. Emond, B. Wang, D. Zhang, F. M. Ross, J. Li, B. Yildiz, J. A. del Alamo
Sponsorship: MIT-IBM Watson AI Lab

Interest in engineering the ideal programmable resistor for analog deep learning applications has skyrocketed due to increasing workloads of deep learning problems. Ion intercalation-based programmable resistors have emerged as a potential next-generation technology for analog deep learning applications. While there have been previous successful demonstrations using Li+ and O2- as the working ion, the former is incompatible with Si-integration whereas the latter is too large and heavy to be moved around, limiting the operation speeds and energy efficiency. In this regard, H+ as the lightest ion available and eminently CMOS compatible is an interesting candidate.

Previously, we demonstrated the first back-end CMOS-compatible non-volatile protonic programmable resistor enabled by the integration of phosphosilicate glass (PSG) as the proton solid electrolyte layer. PSG is an outstanding solid electrolyte material that displays both excellent protonic conduction and electronic insulation characteristics. Moreover, it is a well-known material within conventional Si fabrication, which enables precise deposition control and scalability.

In this work, we further optimize the material stack and fabrication process to realize nanoscale devices. The devices show excellent modulation characteristics by means of dynamic range, the number of states, modulation symmetry, retention, endurance, and energy efficiency. Furthermore, we provide a theoretical framework for room temperature ionics, based on electrical characterization under different operation conditions and metrological evidence obtained via TEM. This new device technology presents all-desirable characteristics to realize analog accelerators for deep learning applications and can serve as a platform to further explore ultrafast ionics.

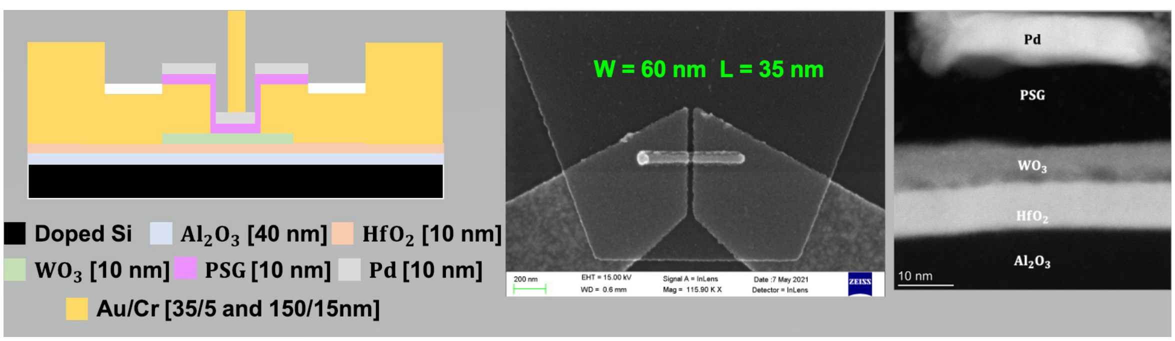

▲Figure 1: Cross section, scanning electron microscopic, and transmission electron microscope images of a nanoscale protonic programmable resistor

FURTHER READING

- M. Onen, N. Emond, J. Li, B. Yildiz, and J. A. del Alamo, "CMOS-compatible Protonic Programmable Resistor Based on Phosphosilicate Glass Electrolyte for Analog Deep Learning," *Nano Letts.*, vol. 21, no. 14, pp. 6111-6116, 2021.

Vertical GaN Superjunction Transistors

J. Perozek, A. Zubair, R. Molnar, T. Palacios
Sponsorship: Advanced Research Projects Agency-Energy Power Nitride Doping Innovation Offers Devices Enabling SWITCHES

Increasing sustainable energy practices have spurred the need for next generation power conversion systems. At their core, these systems, which are essential for solar farms, data centers, and electric vehicles, require small, fast, and affordable power transistors. While gallium nitride (GaN) as a material is uniquely suited for these applications, existing transistors are far from optimized. Their inability to control the electric fields within the device have prevented commercial transistors from achieving the performance promised by theoretical studies.

We aim to use our expertise in fabricating vertical GaN fin field-effect transistors (FinFETs) to push beyond the unipolar limit and create the first GaN superjunction transistors. These transistors use alternating n- and p-type regions to optimize the electric field profile within the transistor to reach the theoretical limits of semiconductor performance. As shown by the red lines in Figure. 1, such devices could outperform existing tech by 50-100× and significantly improve energy conversion efficiency.

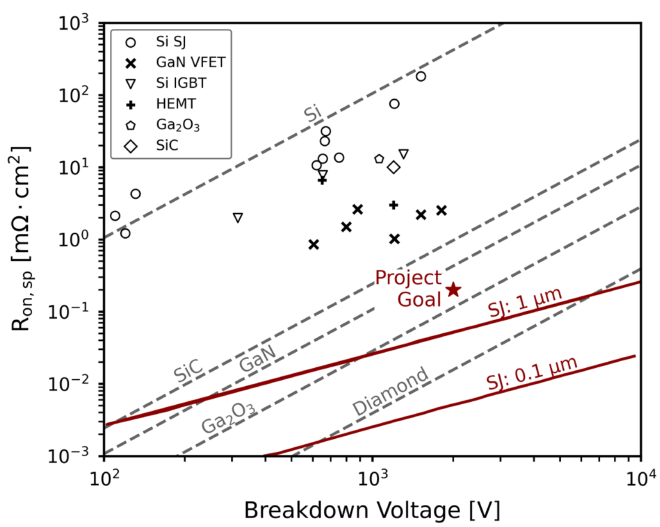

▲ Figure 1: Theoretical limits for the specific on-resistance and breakdown voltages of several material system for both unipolar (gray) and super-junction (red) based devices of varying column widths.

Nanoporous Gadolinium-doped Ceria-based Protonic Solid-state Electrochemical Synapse for CMOS-compatible Neuromorphic Computing

S. Ryu, H. G. Seo, M. Huang, J. A. del Alamo, J. Li, B. Yildiz
Sponsorship: MIT-IBM Watson AI Lab

Artificial neural networks offer great opportunities in artificial intelligence application. However, the hardware structures must overcome the decreasing scaling effectiveness of transistors and the intrinsic inefficiency of employing transistors in von-Neumann computing architectures. Diverse physical neural networks have demonstrated promising implementation of machine learning algorithms. However, currently developed physical processors suffer from poor device-to-device uniformity or high energy dissipation.

To address the issue, we mainly focus on protonic electrochemical artificial synapses. Protons are the smallest ions requiring low energy for transport, and the protonic synapse modulates conductance states via electrochemical proton intercalation. Therefore, the protonic electrochemical memristors can realize low energy computation using shuffling of protons. Also, uniform switching properties can be obtained by controlling a fixed number of protons and electrons into active switching channel materials.

However, most conventional protonic electrochemical artificial synapses are incompatible with complementary metal-oxide-semiconductor (CMOS) fabrication due to polymeric proton electrolytes. Inspired by our former research demonstrating a CMOS-compatible protonic programmable resistor, we developed nanoporous Gd-doped ceria as an inorganic solid proton electrolyte, which provides efficient proton transport at room temperature via physisorbed water channels at the open pores. Controlling microstructures enables higher proton conductivities in the electrolytes and low energy computation based on controlling proton movement. This work provides a path to solution of CMOS-compatible energy efficient computing.

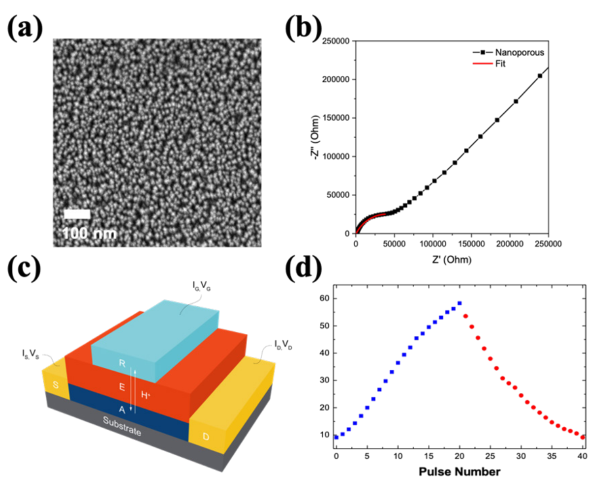

▲Figure 1. (a) Top view scanning electron microscope image of nanoporous Gd:CeO_2 proton electrolytes. (b) Electrochemical impedance spectroscopic analysis of nanoporous Gd:CeO_2 electrolytes. (c) Device schematics of protonic electrochemical random access memory consist of proton reservoir (R), proton electrolytets (E), and active switching channel (A), source and drain (S & D). (d): Representative conductance modulation characteristics of the device.

FURTHER READING

- X. Yao et al., "Protonic Solid-State Electrochemical Synapse for Physical Neural Networks," *Nature Communications*, vol. 11, p. 3134, 2020.
- M. Onen et al., "CMOS-Compatible Protonic Programmable Resistor Based on Phosphosilicate Glass Electrolyte for Analog Deep Learning," *Nano Letters*, vol. 21, no. 14, pp. 6111-6116, 2021.

Sub-10-nm Diameter Vertical Nanowire p-Type GaSb/InAsSb Tunnel FETs

Y. Shao, J. A. del Alamo
Sponsorship: Intel Corporation

Tunnel field-effect transistors (TFETs) have attracted great attention due to their ability to operate with a sub-thermal subthreshold swing (S), which promises significant reduction in supply voltage and static power consumption in logic circuits. III-V materials are of particular interest in designing TFETs, thanks to the flexibility of band engineering and their superior transport properties. To date, III-V n-type TFETs with S < 60 mV/dec and decent drive current have been demonstrated. Nevertheless, for application in logic circuits, a complementary p-type III-V TFET is needed, preferably with similar performance to that of the n-type devices.

In this work, we have fabricated sub-10-nm diameter vertical nanowire (VNW) GaSb/InAsSb broken-band p-type TFETs through a top-down approach. One of our devices demonstrates a peak transconductance of 90 μS/μm at $|V_{ds}|$ = 0.3 V, which improves the state-of-the-art 3-D p-type TFETs by 100%. A linear S_{min} of 225 mV/dec is obtained in the same device, demonstrating a good balance between on-state and subthreshold regime. Clear negative differential resistance is observed at room temperature, a first in any III-V p-type TFETs, with the highest peak-to-valley-current-ratio being 3.1. This work shows the great potential of ultra-scaled III-V VNW TFETs on future complementary logic circuit applications.

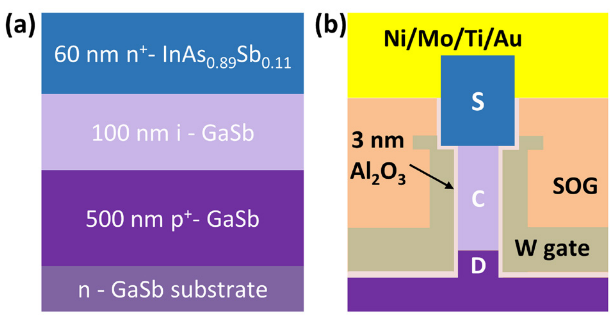

▲ Figure 1: Schematics of (a) starting heterostructure and (b) device cross-sectional view.

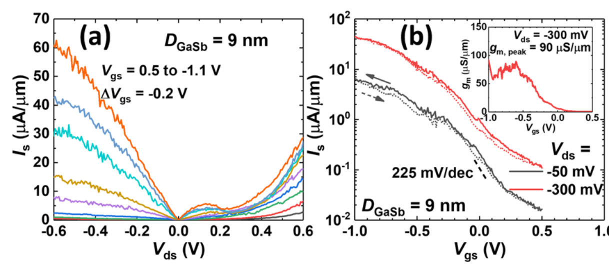

▲ Figure 2: (a) Output and (b) transfer characteristics of a D = 9 nm device. Inset in (b) shows the smoothed transconductance extracted at V_{ds} = -0.3 V.

FURTHER READING

• Y. Shao, and J. A. del Alamo, "Sub-10-nm Diameter Vertical Nanowire p-Type GaSb/InAsSb Tunnel FETs," *IEEE Electron Device Letters*, vol. 43, no. 6, pp. 846-849, Jun. 2022, doi: 10.1109/LED.2022.3166846.

Electronegative Metal Dopants Reduce Switching Variability in Al_2O_3-resistive Switching Devices

V. Somjit, Z. J. Tan, C. Toparli, N. Fang, B. Yildiz

Brain-inspired or neuromorphic hardware holds great promise to reduce energy consumption and accelerate training and inference of deep neural networks. In particular, oxide-based electronics can emulate long- and short-term memory and spiking neurons of the brain by switching the oxide's resistive state via the strength and number of conductive networks. However, high variability of these resistive switching devices is a key drawback hindering reliable training of physical neural networks. In this study, we show that doping an oxide electrolyte, Al_2O_3, with electronegative metals makes resistive switching significantly more reproducible, surpassing the reproducibility requirements for obtaining reliable hardware neuromorphic circuits. Using first principles calculations, we identify that the underlying mechanism is the ease of creating oxygen vacancies in the vicinity of electronegative dopants, due to the capture of the associated electrons by dopant midgap states and the weakening of Al-O bonds. These oxygen vacancies and vacancy clusters also bind significantly to the dopant, thereby serving as preferential sites and building blocks in the formation of conductive oxygen vacancy networks. We validate this theory experimentally by implanting multiple dopants over a range of electronegativities and find superior repeatability with highly electronegative metals, Au, Pt, and Pd. These results establish dopant electronegativity as a descriptor for predicting the ease of oxygen vacancy formation in an insulating oxide, with implications for reducing switching variability.

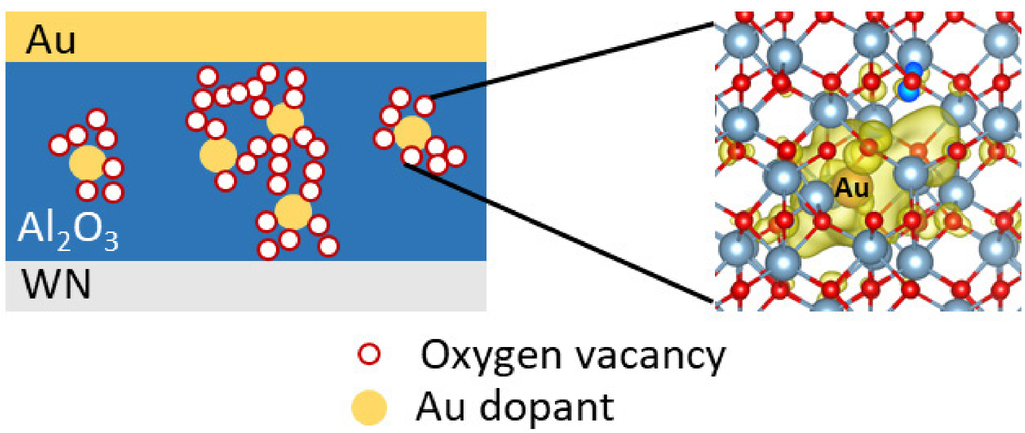

▲ Figure 1: Schematic of proposed switching mechanism in Au-doped Al_2O_3: presence of Au reduces oxygen vacancy formation energy, giving rise to oxygen vacancy clusters preferentially formed around Au, improving switching consistency

Chip-less Wireless Electronic Skins Enabled by Epitaxial Freestanding Compound Semiconductors

Y. Kim, J. M. Suh, Y. Liu, J. Shin, J. Kim
Sponsorship: Amore Pacific

Electronic skin (e-skin) has been developed with a goal to obtain a non-invasive human health monitoring electronic system with its imperceptibility. So far, one of the major shortcomings in this field is the bulky wireless communication system that severely affects its wearability (Figure 1). In this paper, we introduce a single-crystalline non-Si-based e-skin system where fully conformable, ultrathin, piezoelectric, compound semiconductor membranes are incorporated as power-efficient wireless communication modules and extremely high sensitivity sensors without needing bulky chips and batteries. The developed GaN surface acoustic wave (SAW)-based device successfully measured wirelessly three different inputs including strain, ultraviolet light, and ion concentrations (Figure 2). The consistency and accuracy of the measured heart rate and pulse waveforms over a 7-day period, during which the e-skin was re-attached 7 times, strongly demonstrate the reusability and long-term wearability of our device. This study will change the paradigm of e-skins by providing versatile wireless platforms for fully imperceptible e-skins with very high sensitivity and low power consumption.

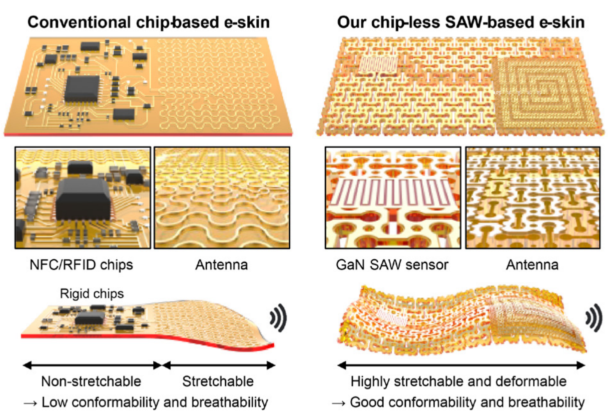

▲Figure 1: Comparison between (left) conventional wireless e-skin based on integrated circuit chips and (right) chip-less wireless e-skin based on SAW devices made of GaN freestanding membranes.

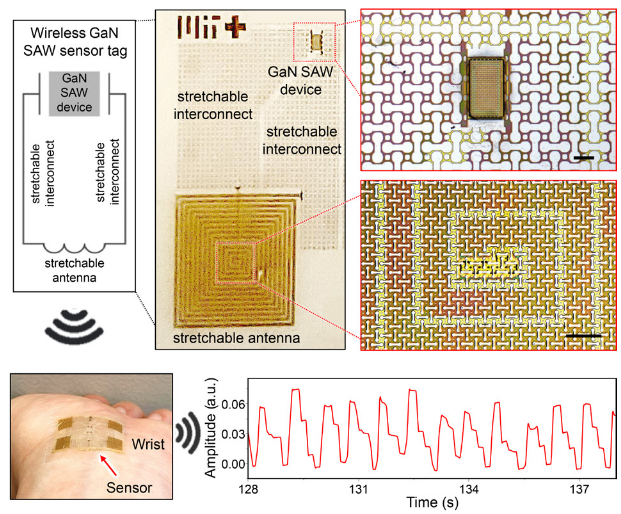

▲Figure 2: Schematic and optical images of our wireless GaN SAW e-skin strain sensor and wireless pulse measurements using GaN SAW e-skin strain sensors. Scale bars indicate 200 μm.

FURTHER READING

- H. Yeon, H. Lee, Y. Kim, D. Lee, Y. Lee, J.-S. Lee, J. Shin, C. Choi, et al., "Long-term Reliable Physical Health Monitoring by Sweat Pore–inspired Perforated Electronic Skins," *Sci. Adv.*, vol. 7, no. 27, eabg.8459, Jun. 2021.
- Y. Kim, S. S. Cruz, K. Lee, B. O. Alawode, C. Choi, Y. Song, J. M. Johnson, C. Heidelberger, et al., "Remote Epitaxy Through Graphene Enables Two-Dimensional Material-based Layer Transfer," *Nature*, vol. 544, pp. 340-343, Apr. 2017.
- H. S. Kum, H. Lee, S. Kim, S. Lindemann, W. Kong, K. Qiao, P. Chen, J. Irwin, et al.,, "Heterogeneous Integration of Single Crystalline Complex-Oxide Membranes," *Nature*, vol. 578, pp. 75-81, Feb. 2020.

Deuterium-terminated Diamond Field-effect Transistor

A. Vardi, M. Geis, B. Zhang, J. A. del Alamo
Sponsorship: DARPA, Bose Fellowship

Due to its extraordinary thermal conductivity, wide bandgap, and large saturation velocity, diamond is a very promising semiconductor for high-power/high-frequency applications. The standard way to form a conducting channel on diamond is by exposing it to hydrogen plasma in a so-called hydrogen termination (D:H) process. This enables the formation of a two-dimensional-hole-gas which can form the basis of a field-effect transistor (FET).

Although the carbon-hydrogen bonds that form on the diamond surface after hydrogenation are stable, it is often observed that during the fabrication process of diamond FETs that there is severe degradation in the channel conductivity and contact resistance. In this work, we explore deuterium termination, diamond:deuterium (D:D), as a way to increase the device stability during the fabrication process. Figure 1 shows the result of the experiment. Initially, D:D gives better results than diamond:hydrogen (D:H), but more significantly, throughout the process, D:H shows a dramatic increase in sheet and contact resistance that persists after the process is completed, while D:D exhibits a lower and stable sheet and contact resistances that are retained well after the process is completed. The figure also compares the transistor characteristics; notably, D:D devices show higher current and deeper depletion-mode characteristics. This all suggests that the available 2D hole concentration in the D:D device is higher and more stable than in the standard D:H device.

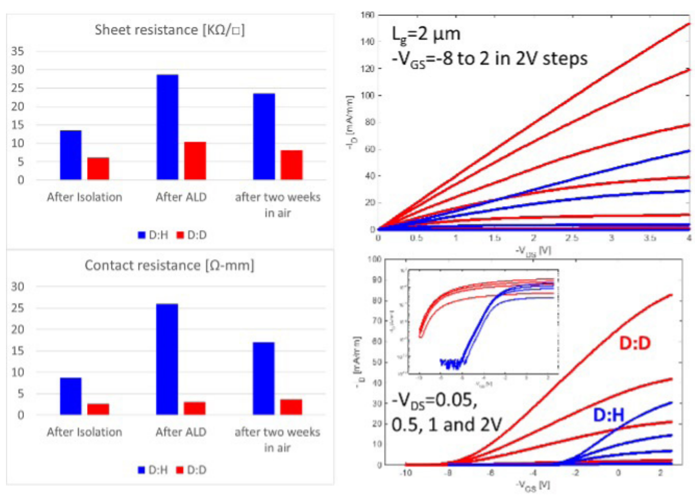

▲ Figure 1: Left: sheet and contact resistance of D:H and D:D throughout and after the process. Right: output, transfer, and sub-threshold (inset) characteristics of D:H and D:D FETs.

FURTHER READING

- A. Vardi, M. Tordjman, J. A. del Alamo, and R. Kalish, "Refractory W-Ohmic Contacts to H-terminated Diamond," *IEEE Transaction on Electrical Devices*, vol. 67, no. 9, pp. 3516-3521, Sept. 2020.
- M. W. Geis, J. O. Varghesea, A. Vardi, J.Kedzierski, J. Daultona, D. Calawaa, M. A. Hollisa, C. H. Wuorioa, G. W. Turnera, S. M. Warnock, T. Osadchy, J. Mallek, A. Melville, J. A. del Alamo, and B. Zhang, " Hydrogen and Deuterium Termination of Diamond for Low Surface Resistance and Surface Step Control," *Diamond and Related Materials*, vol. 118, p. 108518, Oct. 2021.

NbN-Gated GaN Transistor Technology for Applications in Quantum Computing Systems

Q. Xie, N. Chowdhury, A. Zubair, M. S. Lozano, J. Lemettinen, M. Colangelo, O. Medeiros, I. Charaev, K. K. Berggren, T. Palacios
Sponsorship: IBM

High-performance and scalable cryogenic electronics is an essential component of future quantum information systems, which typically operate below 4 K. Superconducting qubits need advanced radio frequency (RF) and pulse-shaping electronics, which typically occupy large instrumentation racks operating at room temperature. Today's approach to the RF control electronics is not scalable to the millions of physical qubits needed in future fault-tolerant quantum systems.

This work explores the use of wide band gap electronics, specifically the AlGaN/GaN high-electron-mobility transistor (HEMT), for cryogenic low-noise applications. These structures take advantage of the polarization-induced two-dimensional electron gas to create a high mobility channel, hence eliminating the heavy doping needed in the other semiconductor technologies. Epitaxially-grown GaN-on-silicon wafers have been demonstrated in large (300 mm) substrates, therefore making the technology an excellent candidate for scalable RF electronics in quantum computing systems.

Furthermore, the use of electrodes using superconducting materials is proposed to significantly reduce the parasitic components and therefore push the RF performance of cryogenic transistors. Short-channel transistors with NbN gates of length 250 nm have been demonstrated with promising performance at 4.2 K.

In the next step, we will study the effect of the superconducting gate on the RF characteristics of the transistors, with the eventual goal of pushing the frequency performance of these transistors to new limits. Improvements to the NbN gate fabrication technology is underway. These transistors will be integrated into low noise amplifier circuits for applications in readout and control electronics at cryogenic temperature. Furthermore, the demonstrated NbN-gated GaN transistor paves the way for the application of high-frequency GaN technology in cryogenic electronics, notably in scalable quantum computing systems, and brings us one step closer to an all-nitride integrated electronics-quantum device platform.

FURTHER READING

- Q. Xie, N. Chowdhury, A. Zubair, M. S. Lozano, J. Lemettinen, M. Colangelo, O. Medeiros, I. Charaev, K. K Berggren, P. Gumann, D. Pfeiffer, and T. Palacios, "NbN-Gated GaN Transistor Technology for Applications in Quantum Computing Systems," *Symposium on VLSI Technology*, Kyoto, Japan, Jun. 2021.
- K. H. Teo, Y. Zhang, N. Chowdhury, S. Rakheja, R. Ma, Q. Xie, E. Yagyu, K. Yamanaka, K. Li, and T. Palacios, "Emerging GaN Technologies for Power, RF, Digital, and Quantum Computing Applications: Recent Advances and Prospects," *J. Appl. Phys.*, vol. 130, no. 16, pp. 160902, Oct. 2021. DOI: 10.1063/5.0061555
- Q. Xie, "Gallium Nitride Electronics for Cryogenic and High Frequency Applications," *S.M. thesis*, Massachusetts Institute of Technology, Cambridge, 2020.

Self-aligned Enhancement-mode GaN p-Channel FinFET with ION > 100 mA/mm and ION/IOFF > 107

N. Chowdhury, Q. Xie, T. Palacios
Sponsorship: Intel Corporation

This work demonstrates self-aligned p-channel fin field-effect transistors (FinFETs) based on a GaN-on-Si wafer. While the self-aligned gate process helps to achieve shortest possible source-to-drain distance to compensate for low hole mobility in GaN (~20 cm2/V·s), the FinFET architecture provides strong electrostatic control over the channel. Our fabricated transistors with 40-nm fin width, LSD=120 nm, and LG=90 nm exhibits an ION≈140 mA/mm, ION/IOFF>107, VTH=1 V, SS=150 mV/dec, gm,max=14 mS/mm, and RON=61 Ω·mm. By precisely controlling the recess depth, enhancement-mode (E-mode) operation was also achieved. Our best E-mode device shows an ION≈125 mA/mm, ION/IOFF>107, VTH=−0.3 V, and RON=69 Ω·mm. In addition, record low subthreshold swing of 80 mV/dec for devices with fin width of 40 nm and LSD=240 nm attests to the strong gate control over the p-channel achieved by the FinFET-architecture.

FURTHER READING

- N. Chowdhury, Q. Xie, and T. Palacios, "Tungsten-Gated GaN/AlGaN p-FET with Imax > 120 mA/mm on GaN-on-Si," *IEEE Electron Device Lett.*, vol. 43, no. 4, pp. 545-548, Apr. 2022. DOI: 10.1109/LED.2022.3149659.
- N. Chowdhury, Q. Xie, and T. Palacios, "Self-Aligned E-Mode GaN p-Channel FinFET with ION > 100 mA/mm and ION/IOFF > 10^7," *IEEE Electron Device Lett.*, vol. 43, no. 3, pp. 358-361, Mar. 2022. DOI: 10.1109/LED.2022.3140281.
- N. Chowdhury, Q. Xie, M. Yuan, K. Cheng, H. W. Then, and T. Palacios, "Regrowth-Free GaN-Based Complementary Logic on a Si Substrate," *IEEE Electron Device Lett.*, vol. 41, no. 6, pp. 820-823, Jun. 2020. DOI: 10.1109/LED.2020.2987003.

Tungsten-gated GaN/AlGaN p-FET with Imax > 120 mA/mm on GaN-on-Si

N. Chowdhury, Q. Xie, T. Palacios
Sponsorship: Intel Corporation

This work demonstrates tungsten (W)-gated p-channel GaN/AlGaN heterostructure field-effect transistors (FETs) on a GaN-on-Si wafer grown by metal organic chemical vapor deposition (MOCVD). The choice of W as the gate metal over the more commonly used Mo induces larger turn-on voltage and lower gate leakage current. An annealing step at 500 ˚C in N2 ambient was introduced to heal the damage introduced during the gate recess step, which resulted in lower channel resistance. Long-channel W-gated p-FETs with LSD=5.5 μm and LG=1.5 μm exhibit an ION≈25 mA/mm and ION/IOFF>103. A scaled transistor of dimensions LSD=1.2 μm and LG=100 nm demonstrates an ION≈125 mA/mm, ION/IOFF≈104, and RON=170 Ω·mm. To the best of the authors' knowledge, the reported device performance represents the state-of-the-art of all planar GaN/AlGaN p-FETs and is comparable with high voltage Si FET on the 65-nm node.

FURTHER READING

- N. Chowdhury, Q. Xie, and T. Palacios, "Tungsten-Gated GaN/AlGaN p-FET with Imax > 120 mA/mm on GaN-on-Si," *IEEE Electron Device Lett.*, vol. 43, no. 4, pp. 545-548, Apr. 2022. DOI: 10.1109/LED.2022.3149659.
- N. Chowdhury, Q. Xie, and T. Palacios, "Self-Aligned E-Mode GaN p-Channel FinFET with ION > 100 mA/mm and ION/IOFF > 10^7," *IEEE Electron Device Lett.*, vol. 43, no. 3, pp. 358-361, Mar. 2022. DOI: 10.1109/LED.2022.3140281.
- N. Chowdhury, Q. Xie, M. Yuan, K. Cheng, H. W. Then, and T. Palacios, "Regrowth-Free GaN-Based Complementary Logic on a Si Substrate," *IEEE Electron Device Lett.*, vol. 41, no. 6, pp. 820-823, Jun. 2020. DOI: 10.1109/LED.2020.2987003.

Efficient Spin-orbit Torques in an Antiferromagnetic Insulator with a Tilted Easy Plane

P. Zhang, C.-T. Chou, H. Yun, B. C. McGoldrick, J. T. Hou, K. A. Mkhoyan, L. Liu
Sponsorship: NSF, U.S. Air Force Office of Scientific Research, Taiwan Semiconductor Manufacturing Company, Semiconductor Research Corporation SMART Center, Mathworks Fellowship

Electrical manipulation of spin textures inside antiferromagnets represents a new opportunity for developing spintronics with superior speed and high device density. Injecting spin currents into antiferromagnets and realizing efficient spin-orbit-torque-induced switching is, however, still challenging due to the complicated interactions from different sublattices. Meanwhile, because of the diminishing magnetic susceptibility, the nature and the magnitude of current-induced magnetic dynamics remain poorly characterized in antiferromagnets, whereas spurious effects further complicate experimental interpretations.

In this work, by growing a thin film antiferromagnetic insulator, α-Fe2O3, along its non-basal plane orientation, we realize a configuration where an injected spin current can robustly rotate the Néel vector within the tilted easy plane, with an efficiency comparable to that of classical ferromagnets. The experimental configuration is illustrated in Figure 1. By measuring the second-harmonic Hall resistance, as shown in Figure 2, we find that the spin-orbit torque effect stands out among competing mechanisms and leads to clear switching dynamics. Thanks to this new mechanism, in contrast to the usually employed orthogonal switching geometry, we achieve bipolar antiferromagnetic switching by applying positive and negative currents along the same channel, a geometry that is more practical for device applications.

By enabling efficient spin-orbit torque control on the antiferromagnetic ordering, the tilted easy plane geometry introduces a new platform for quantitatively understanding switching and oscillation dynamics in antiferromagnets.

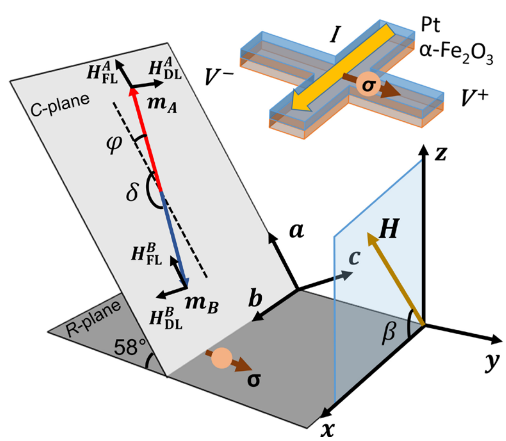

▲Figure 1: 30 nm of α-Fe_2O_3 layer was epitaxially grown on an α-Al_2O_3 R-plane $(01\bar{1}2)$ substrate and further covered by 5 nm of Pt, and patterned into Hall bar devices. Inset: The current channel is parallel to the axis, and the generated spin magnetic moment is parallel to the χ $[\bar{2}110]$ axis and generated spin magnetic moment is parallel to γ axis. The magnetic easy plane of α-Fe_2O_3 is the tilted C-plane (0001).. The external magnetic field is rotated within the xz plane, with the angle defined as β Damping-like torque effective fields $\boldsymbol{H}_{\mathbf{DL}}$ rotate the antiferromagnetic sublattice moments $\boldsymbol{m_A}$ and $\boldsymbol{m_B}$ constructively, while the field-like torque $\boldsymbol{H}_{\mathbf{FL}}$ does not.

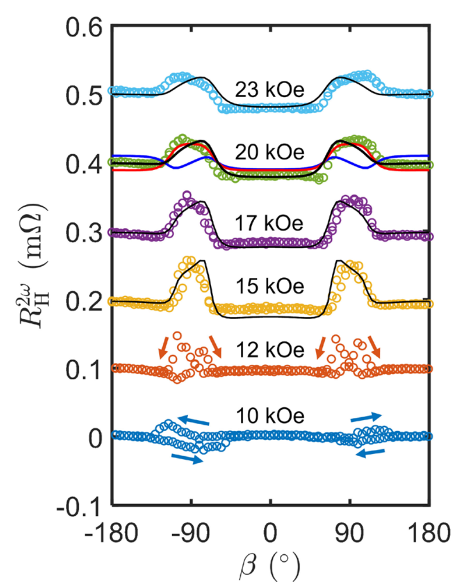

▲Figure 2: The angle-dependent second-harmonic Hall resistance $R_{\mathrm{H}}^{2\omega}$ as a function of β, at different external fields. The current is 4 mA (root mean square value). $H_{\mathbf{DL}}$ (red) and $H_{\mathbf{FL}}$ (blue) contributions to $R_{\mathrm{H}}^{2\omega}$ at $H = 20\ \mathrm{kOe}$ are separately plotted. $H_{\mathbf{DL}}$ corresponds to a damping-like torque efficiency $\xi_{\mathbf{DL}} = 0.015$ comparable to the value of Pt - Ferrimagnetic Insulator bilayers.

FURTHER READING

- P. Zhang, J. Finley, T. Safi, and L. Liu, "Quantitative Study on Current-induced Effect in an Antiferromagnet Insulator/Pt Bilayer Film", *Physical Review Letters*, vol. 123, pp. 247206, Dec. 2019.
- P. Zhang, C.-T. Chou, H. Yun, B. C. McGoldrick, J. T. Hou, K. A. Mkhoyan, and L. Liu, "Efficient Spin-Orbit Torques in an Antiferromagnetic Insulator with Tilted Easy Plane", *arXiv:2201.04732*, Jan. 2022.

Machine Learning, Neurmorphic Computing, and AI

Network Augmentation for Tiny Deep Learning

H. Cai, C. Gan, J. Lin, S. Han
Sponsorship: MIT-IBM Watson AI Lab, NSF, Hyundai, Ford, Intel, Amazon

We introduce Network Augmentation (NetAug), a new training method for improving the performance of tiny neural networks. Existing regularization techniques (e.g., data augmentation, dropout) have shown much success on large neural networks by adding noise to overcome over-fitting. However, we found that these techniques hurt the performance of tiny neural networks. We argue that training tiny models differ from large models: rather than augmenting the data, we should augment the model, since tiny models tend to suffer from under-fitting rather than over-fitting due to limited capacity. To alleviate this issue, NetAug augments the network (reverse dropout) instead of inserting noise into the dataset or the network. NetAug puts the tiny model into larger models and encourages it to work as a sub-model of larger models to get extra supervision, in addition to functioning as an independent model. At test time, only the tiny model is used for inference, incurring zero inference overhead. We demonstrate the effectiveness of NetAug on image classification and object detection. NetAug consistently improves the performance of tiny models, achieving up to 2.2% accuracy improvement on ImageNet. On object detection, achieving the same level of performance, NetAug requires 41% fewer MACs on Pascal VOC and 38% fewer MACs on COCO than the baseline.

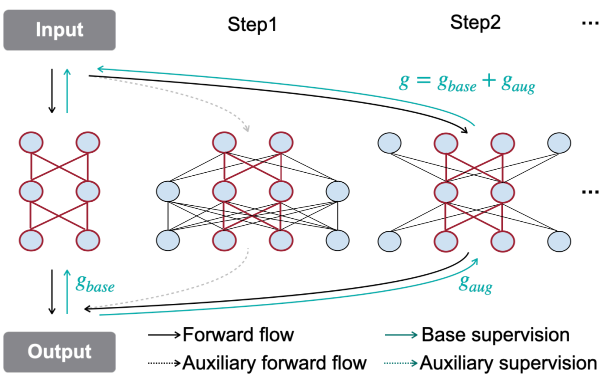

◀ Figure 1: NetAug encourages the target tiny model to work as a sub-model of larger models to get extra supervision.

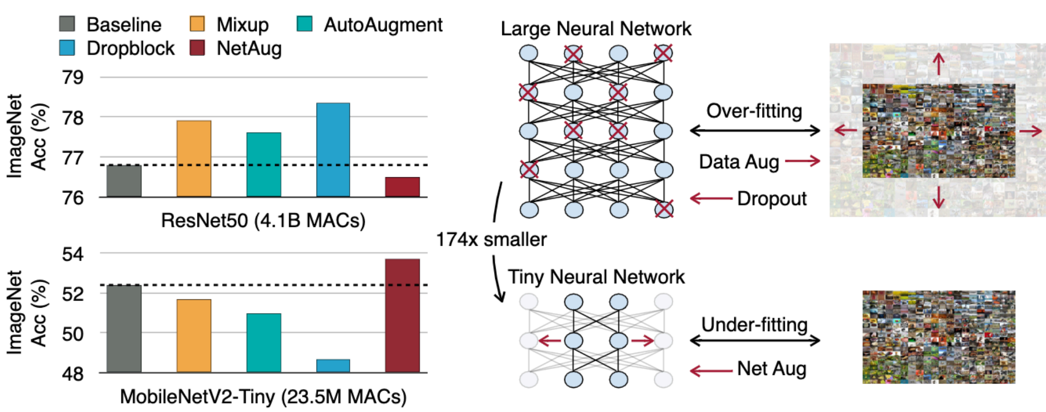

▲ Figure 2: NetAug improves the accuracy of the tiny model while regularization methods hurt its accuracy.

FURTHER READING

- H. Cai, C. Gan, J., Lin, and S. Han, "Network Augmentation for Tiny Deep Learning," *ICLR*, 2022.
- H. Cai, et al. "TinyTL: Reduce Activations, Not Trainable Parameters for Efficient On-Device Learning," *Advances in Neural Information Processing Systems*, vol. 33, p. ?, 2020.
- H. Cai, et al. "Once-for-all: Train One Network and Specialize it for Efficient Deployment," *ICLR*, 2020.

Physics-assisted Generative Adversarial Network for X-Ray Tomography

Z. Guo, J. K. Song, G. Barbastathis, M. E. Glinsky, C. T. Vaughan, K. W. Larson, B. K. Alpert, Z. H. Levine
Sponsorship: Intelligence Advanced Research Projects Activity, Office of the Director of National Intelligence, U.S. Department of Energy's National Nuclear Security Administration, Singapore National Research Foundation

X-ray tomography has applications in biomedical imaging, material study, electronic inspection, and more. The technique is capable of imaging the internal of objects in three dimensions non-invasively but may require prior regularization to obtain satisfactory reconstruction. In this work, we developed a physics-assisted generative adversarial network (PGAN) to determine and apply a learned prior in the reconstruction process. In contrast to previous efforts, our PGAN utilizes the maximum likelihood estimation to regularize the reconstruction with both physical and learned priors. The objects are synthetic integrated-circuits (ICs) from a proposed model dubbed CircuitFaker. Compared with maximum likelihood estimation, our PGAN can dramatically improve the synthetic IC reconstruction quality when the projection angles and photon budgets are limited. The advantages of using learned priors from deep learning in X-ray tomography may further enable its applications in low-photon nanoscale imaging.

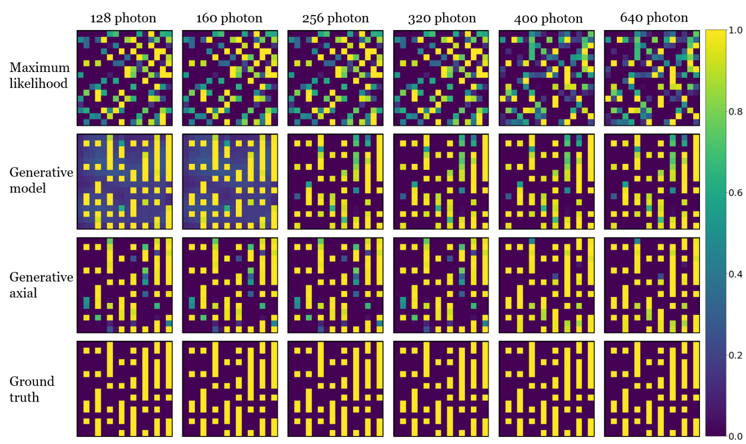

▲Figure 1: Selected examples of IC reconstructions for different methods. Black stands for copper, white stands for silicon.

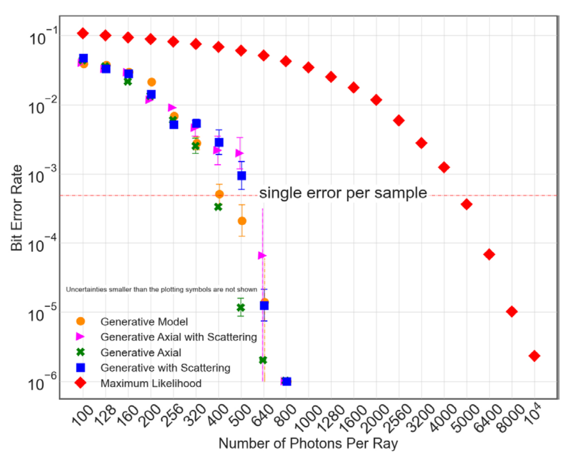

▲Figure 2: Bit-Error-Rate comparison between reconstruction methods at different imaging conditions.

An Equivalent Circuit Model of an Electrochemical Artificial Synapse for Neuromorphic Computing

M. Huang, M. Onen, J. A. del Alamo, J. Li, B. Yildiz
Sponsorship: MIT Quest for Intelligence

Deep learning based on artificial neural networks has achieved outstanding performance in a wide range of artificial intelligence applications. However, such computations are energy intensive to perform on conventional digital computers. A promising energy efficient approach to performing deep learning is to use neuromorphic computing hardware based on analog nonvolatile resistive switching devices in crossbar arrays. Among different resistive switching devices, electrochemical artificial synapses are a promising candidate as they have shown uniform and deterministic switching with low energy consumption. Electrochemical artificial synapses are programmable resistors in a three-terminal configuration where the conductance of a channel is controlled by reversible ion intercalation driven by voltage or current applied to a gate terminal that also serves as ion reservoir. Understanding the physical processes and the behavior of these devices is critical for applying them in brain-inspired computing systems.

In this work, we propose a 1D equivalent circuit model to describe the electrochemical processes of the electrochemical artificial synapse, including ionic transport, charge transfer, and diffusion processes. The model aims to predict the behavior of devices with different geometries and materials properties under various gate voltage or current waveforms. The model provides insight into processes such as the change of channel conductance and its relaxation after electrical pulses are applied to the gate and the interactions between successive pulses. In addition, the model can potentially guide the design of material properties and the optimization of device performance for achieving lower operating voltage, faster operation speed, and improved energy efficiency.

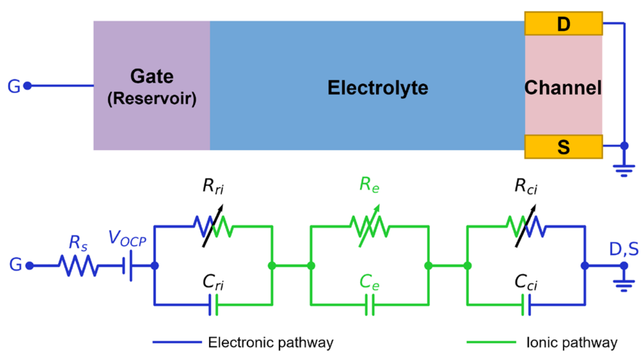

▲Figure 1: Schematic of electrochemical artificial synapses and circuit diagram of the equivalent circuit model.

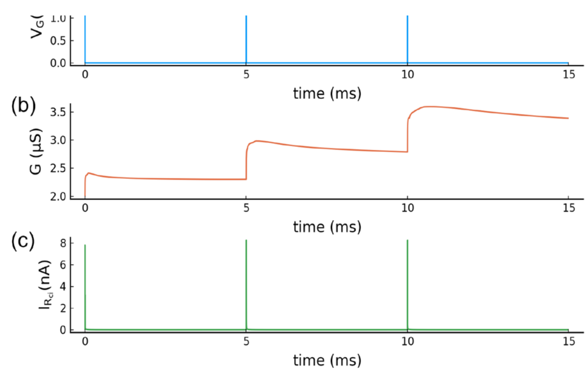

▲Figure 2: Effect of voltage pulse application and post-pulse relaxation showing (a) gate voltage, (b) channel conductance, and (c) Faraday current at the channel electrode as a function of time.

FURTHER READING

- X. Yao, K. Klyukin, W. Lu, M. Onen, S. Ryu, D. Kim, N. Emond, I. Waluyo, A. Hunt, J. A. del Alamo, J. Li, and B. Yildiz, "Protonic Solid-State Electrochemical Synapse for Physical Neural Networks," *Nature Communications*, vol. 11, p. 3134, Jun. 2020.
- M. Onen, N. Emond, J. Li, B. Yildiz, and J. A. del Alamo, "CMOS-Compatible Protonic Programmable Resistor Based on Phosphosilicate Glass Electrolyte for Analog Deep Learning," *Nano Letts.*, vol. 21, pp. 6111–6116, Jul. 2021.

Revisiting Contrastive Learning through the Lens of Neighborhood Component Analysis: An Integrated Framework

C.-Y. Ko, J. Mohapatra, S. Liu, P.-Y. Chen, L. Daniel, T.-W. Weng
Sponsorship: MIT-IBM Watson AI Lab

Contrastive learning has drawn much attention and has become one of the most effective representation learning techniques recently. In essence, contrastive learning aims to leverage pairs of positive and negative samples for representation learning; however, positive/negative pairs are hard to define without the knowledge of downstream tasks. To provide a surrogate of measuring similarity, Current mainstream contrastive learning algorithms build up and optimize over a surrogate of the ideal contrastive loss. Although this formulation seems to put no assumptions on the downstream task classes, we find that there are in fact implicit assumptions on the class probability prior of the downstream tasks

In this project, we formally establish the connection between the neighborhood component analysis (NCA) and the unsupervised contrastive learning. Inspired by this interesting relationship to NCA, we further propose a new contrastive loss (named NaCl) which outperform existing paradigm. Furthermore, by inspecting the robust accuracy of several existing methods (e.g., Figure 1's y-axis, the classification accuracy when inputs are corrupted by crafted perturbations), one can see the insufficiency of existing methods in addressing robustness. Thus, we propose a new integrated contrastive framework (named IntNaCI and IntCl) that accounts for *both* the standard accuracy and adversarial cases: our proposed method's performance remains in the desired upper-right region (circled) as shown in Figure 1. A conceptual illustration of our proposals is given in Figure 2.

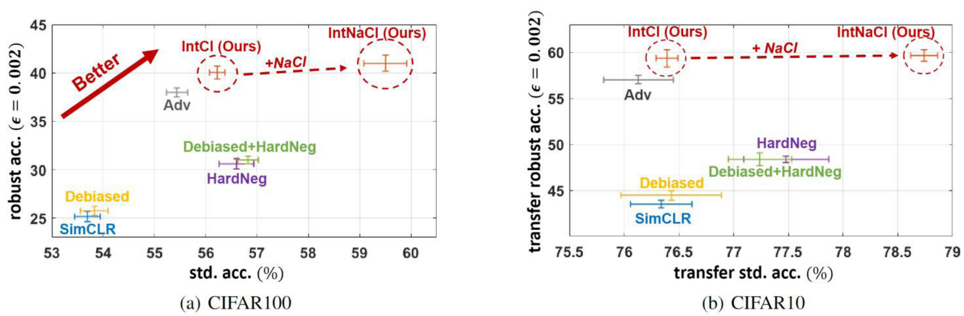

▲ Figure 1. The performance of existing methods and our proposal (IntNaCl & IntCl) in terms of their standard accuracy (x-axis) and robust accuracy under Fast Gradient Sign Method attacks **ε** = 0.002 (y-axis). The transfer performance refers to fine-tuning a linear layer for CIFAR10 with representation networks trained on CIFAR100.

▶ Figure 2. A conceptual illustration of our proposals.

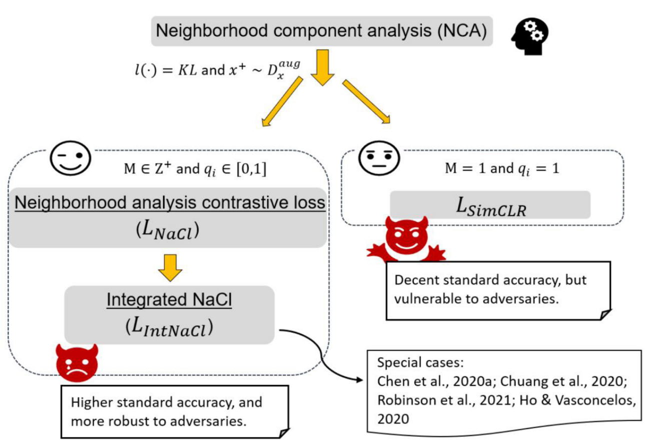

FURTHER READING

- T. Chen, S. Kornblith, M. Norouzi, and G. E. Hinton, "A Simple Framework for Contrastive Learning of Visual Representations," *Proc. of the International Conference on Machine Learning*, pp. 1597-1607, 2020.
- J. Goldberger, G. E. Hinton, S. Roweis, and R. R. Salakhutdinov, "Neighbourhood Components Analysis," *Advances in Neural Information Processing Systems*, pp. 513-520, 2004.

SparseBFA: Attacking Sparse Deep Neural Networks with the Worst-case Bit Flips on Coordinates

K. Lee, A. P. Chandrakasan
Sponsorship: Facebook, Korea Foundation for Advanced Studies

Deep neural networks (DNNs) are shown to be vulnerable to a few carefully chosen bit flips in their parameters, and bit flip attacks (BFAs) exploit such vulnerability to degrade the performance of DNNs. In this work, we show that DNNs with high sparsity that typically result from weight pruning have a unique source of vulnerability to bit flips when their coordinates of nonzero weights are attacked. We propose SparseBFA, an algorithm that searches for a small number of bits among the coordinates of nonzero weights when the parameters of DNNs are stored using sparse matrix formats. Using SparseBFA, we find that the performance of DNNs drops to the random-guess level by flipping less than 0.00005% (1 in 2 million) of the total bits.

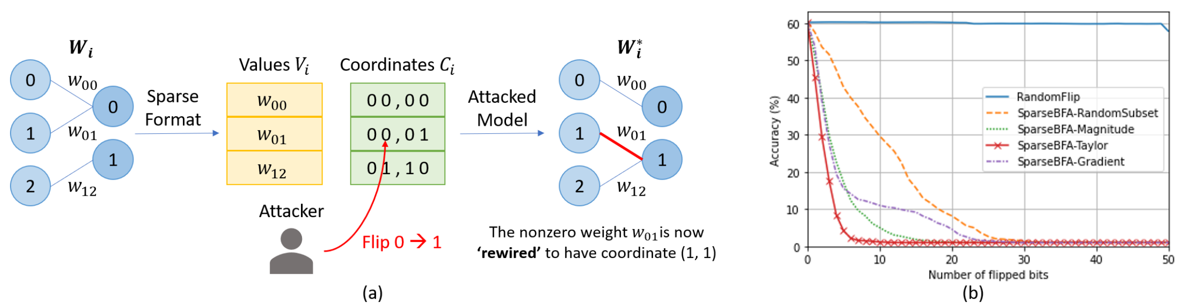

▲ Figure 1: (a) When an attacker flips a bit in the coordinates representing the location of nonzero weights, the connection between neurons is rewired. (b) Accuracy of the ResNet50 model as bits in the coordinate list are flipped using SparseBFA.

Memory-efficient Gaussian Fitting for Depth Images in Real Time

P. Z. X. Li, S. Karaman, V. Sze
Sponsorship: NSF RTML 1937501, NSF CPS 1837212

Energy-constrained microrobots, such as insect-sized flapping wing robots and palm-sized drones, are expected to be deployed for search and rescue missions in dangerous and unknown environments. These robots have very limited battery capacity, which limits the energy available for computation. Since the energy cost of memory access can be significant, algorithms designed for these robots should reduce memory overhead so that most data and variables used during computation can be efficiently stored in and accessed from lower-level caches (KBs in storage) instead of a larger off-chip dynamic random-access memory (DRAM).

Constructing a compact representation for 3D environments is essential for enabling autonomy for tasks such as navigation, localization, and exploration. From a sequence of depth images, many existing algorithms convert each image into a compact Gaussian mixture model (GMM) where each Gaussian models a surface in the environment. Then, GMMs across all images are fused together into a coherent global 3D map (Figure 1). While existing algorithms focus on reducing the size of each GMM, they require significant memory overhead due to the storage of the entire depth image or its intermediate representation in memory for multi-pass processing.

In this work, we present the Single-Pass Gaussian Fitting (SPGF) algorithm that incrementally constructs a GMM one pixel at a time in a single pass through a depth image. Since only one pixel is stored in memory at any time, SPGF achieves orders-of-magnitude lower memory overhead than prior approaches. By processing each depth image row-by-row, SPGF can efficiently and accurately infer surface geometries, which leads to higher precision than prior multi-pass approaches while maintaining the same compactness of the GMM. Using a low-power ARM Cortex-A57 CPU, SPGF operates at 32 fps, requires 43 KB of memory overhead, and consumes only 0.11 J per image. Thus, SPGF enables real-time mapping of large 3D environments on energy-constrained robots.

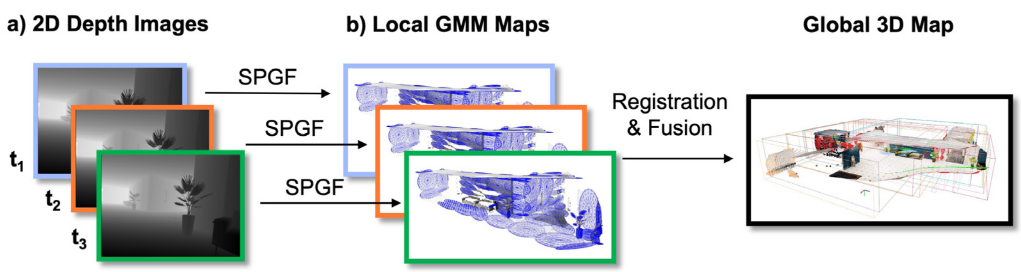

▲ Figure 1: (a) A depth image from a depth camera, and (b) a GMM (blue) generated using the proposed SPGF algorithm with a root-mean-square error of 9 cm, a memory overhead of 43 KB, a throughput of 32 fps, and an energy consumption of 0.11 J per frame using the low-power ARM Cortex-A57 CPU.

FURTHER READING

- P. Z. X. Li, S. Karaman, V. Sze, "Memory-Efficient Gaussian Fitting for Depth Images in Real Time," *IEEE International Conference on Robotics and Automation (ICRA)*, May 2022.

MCUNetV2: Memory-efficient Patch-based Inference for Tiny Deep Learning

J. Lin, W. Chen, H. Cai, C. Gan, S. Han
Sponsorship: MIT-IBM Watson AI Lab, Samsung, Woodside Energy, NSF CAREER Award #1943349

Tiny deep learning on microcontroller units (MCUs) is challenging due to the limited memory size. We find that the memory bottleneck is due to the imbalanced memory distribution in convolutional neural network (CNN) designs: the first several blocks have an order-of-magnitude larger memory usage than the rest of the network. To alleviate this issue, we propose a generic patch-by-patch inference scheduling, which operates only on a small spatial region of the feature map and significantly cuts down the peak memory. However, naive implementation brings overlapping patches and computation overhead. We further propose network redistribution to shift the receptive field and floating-point operations (FLOPs) to the later stage and reduce the computation overhead. Manually redistributing the receptive field is difficult. We automate the process with neural architecture search to jointly optimize the neural architecture and inference scheduling, leading to MCUNetV2. Patch-based inference effectively reduces the peak memory usage of existing networks by 4-8x. Co-designed with neural networks, MCUNetV2 sets a record ImageNet accuracy on MCU (71.8%), and achieves >90% accuracy on the visual wake words dataset under only 32kB static random access memory (SRAM). MCUNetV2 also unblocks object detection on tiny devices, achieving 16.9% higher mean Average Precision (mAP) on Pascal VOC compared to the state-of-the-art result. Our study largely addresses the memory bottleneck in tinyML and paves the way for various vision applications beyond image classification.

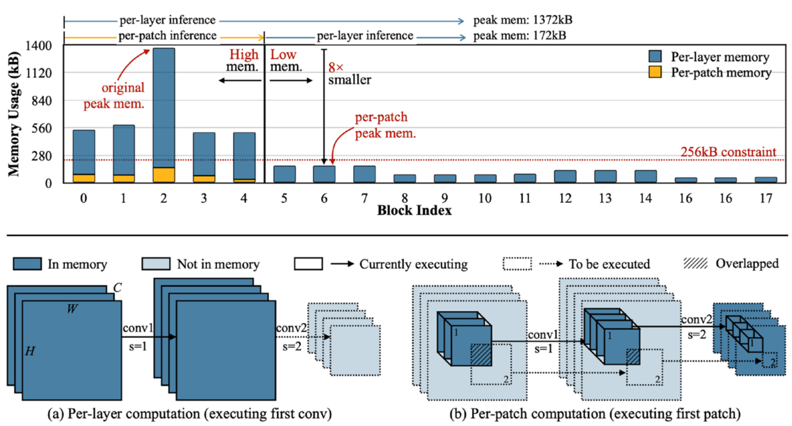

▲ Figure 1: MobileNetV2 has a very imbalanced memory usage distribution: the peak memory is determined by the first 5 blocks with high peak memory, while the later blocks all share a small memory usage. By using per-patch inference, we are able to significantly reduce the peak memory by 8x, fitting MCUs with a 256 kB memory budget.

FURTHER READING

- J. Lin, W. M. Chen, Y. Lin, C. Gan, and S. Han, "MCUNet: Tiny Deep Learning on Iot Devices," *Advances in Neural Information Processing Systems*, vol. 33, pp. 11711-11722, 2020.

PointAcc: Efficient Point Cloud Deep Learning Accelerator

Y. Lin, Z. Zhang, H. Tang, H. Wang, S. Han
Sponsorship: NSF, Hyundai, Qualcomm, MIT-IBM Watson AI Lab

Deep learning on point clouds plays a vital role in a wide range of applications such as autonomous driving and augmented reality (AR) and virtual reality (VR). These applications interact with people in real time on edge devices and thus require low latency and low energy. Compared to projecting the point cloud to 2D space, directly processing 3D point cloud yields higher accuracy and lower number of multiply-accumulations (#MACs). However, the extremely sparse nature of point cloud poses challenges to hardware acceleration. For example, we need to explicitly determine the nonzero outputs and search for the nonzero neighbors (mapping operation), which is unsupported in existing accelerators. Furthermore, explicit gathering and scattering of sparse features are required, resulting in large data movement overhead.

In this work, we comprehensively analyze the performance bottleneck of modern point cloud networks on central processing, graphics processing, and tensor processing units (CPU/GPU/TPU). To address the challenges, we then present PointAcc, a novel point cloud deep learning accelerator. PointAcc maps diverse mapping operations onto one versatile ranking-based kernel, streams the sparse computation with configurable caching, and temporally fuses consecutive dense layers to reduce the memory footprint. Evaluated on 8 point cloud models across 4 applications, PointAcc achieves 3.7× speedup and 22× energy savings over RTX 2080Ti GPU. Co-designed with light-weight neural networks, PointAcc rivals the prior accelerator Mesorasi by 100× speedup with 9.1% higher accuracy running segmentation on the S3DIS dataset. PointAcc paves the way for efficient point cloud recognition.

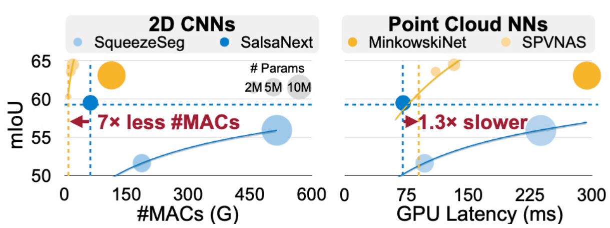

▲ Figure 1: Compared to 2D CNNs, point cloud networks have higher accuracy and lower #MACs, but higher GPU latency due to low utilization brought by sparsity and irregularity.

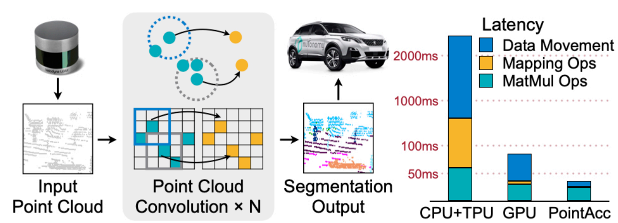

▲ Figure 2: Point cloud deep learning is crucial for real-time AI applications. PointAcc accelerates point cloud computations by resolving sparsity and data movement bottlenecks.

FURTHER READING

- Y. Lin, Z. Zhang, H. Tang, H. Wang, and S. Han, "PointAcc: Efficient Point Cloud Accelerator," *MICRO-54: 54th Annual IEEE/ACM International Symposium on Microarchitecture*, pp. 449-461, Oct. 2021.
- Y. Feng, B. Tian, T. Xu, P. Whatmough, and Y. Zhu, "Mesorasi: Architecture Support for Point Cloud Analytics via Delayed-aggregation," *MICRO-53: 53rd Annual IEEE/ACM International Symposium on Microarchitecture*, pp. 1037-1050, Oct. 2020.

Algorithm-system Co-design for Efficient Calorimetry Clustering

Z. Liu, X. Yang, S. Han
Collaborators: A. Schuy (UW), S-C. Hsu (UW), J. Krupa (MIT), P. Harris (MIT)
Sponsorship: NSF

The content management system (CMS) detector at the Large Hadron Collider (LHC) reconstructs high-energy proton-proton collisions to understand physics beyond the standard model. A key part of the CMS detector is the calorimeter, which reconstructs particle energies by clustering 3D energy deposits from particle showers. The LHC observes ~1 billion collisions per second and must decide within ~1 millisecond which collisions to keep; this imposes a strict throughput/latency requirement. Furthermore, the LHC data flow will increase tenfold by 2027. The corresponding increase in computing requirements using traditional algorithms is beyond our capabilities. Therefore, there is an urgent need to develop accurate algorithms capable of scaling under resource and latency constraints.

3D point cloud neural networks are very suitable for calorimetry clustering. However, they are ten times more computationally expensive than 2D convoluted neural networks (CNNs). Moreover, the sparse and irregular nature of the point cloud makes them less favored by general-purpose hardware (such as CPU, GPU, and TPU). We approach these challenges with algorithm-system co-design.

From the algorithm side, we have developed SPVCNN++, which brings together the best from point-based and voxel-based models. SPVCNN++ is composed of a fine-grained point-based branch that keeps the 3D data in high resolution without large memory footprints and a coarse-grained voxel-based branch that aggregates the neighboring features without many random memory accesses. Compared with the GNN-based approach, our SPVCNN++ achieves a 4% higher panoptic quality on the particle physics benchmark.

From the system side, we have developed TorchSparse, a specialized high-performance GPU computing library for 3D sparse computations. TorchSparse directly optimizes the two bottlenecks of sparse convolution: irregular computation and data movement. As a result, our TorchSparse achieves more than 1.5x measured end-to-end speedup over the state of the art.

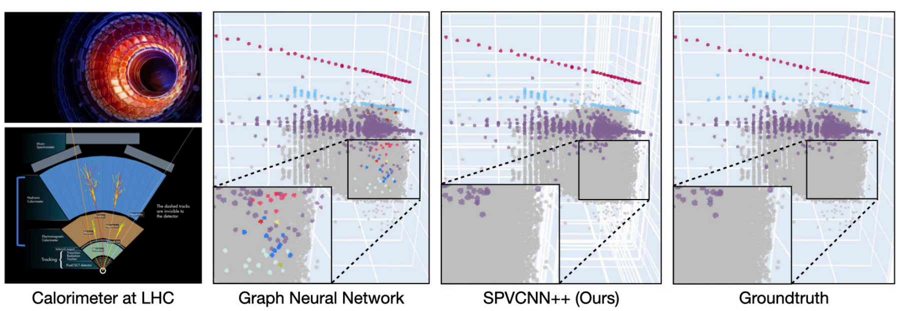

▲ Figure 1: Results of our algorithm-system co-design solution for efficient calorimetry clustering. Compared with conventional GNN-based approach, our SPVCNN++ provides much more accurate clustering results.

FURTHER READING

- H. Tang, Z. Liu, S. Zhao, Y. Lin, J. Lin, H. Wang, and S. Han, "Searching Efficient 3D Architectures with Sparse Point-Voxel Convolution," *European Conference on Computer Vision (ECCV)*, Aug. 2020.
- H. Tang, Z. Liu, X. Li, Y. Lin, and S. Han, "TorchSparse: Efficient Point Cloud Inference Engine," to be presented at *Conference on Machine Learning and Systems (MLSys)*, August 2022.

Fabrication of Electrochemical Artificial Synapses Based on Intercalation of Mg^{2+} Ions

M. Schwacke, J. A. del Alamo, J. Li, B. Yildiz
Sponsorship: SRC, MIT Quest

Deep learning based on neural networks has gained much attention due to its success in a wide range of applications. However, running neural networks on traditional computer systems requires large amounts of power and memory due to the von-Neumann structure which separates the central processing unit (CPU) and memory. Alternatively, crossbar architectures with two-terminal resistive switches can imitate neurons and synapses, allowing for the integration of memory and computation.

Electrochemical artificial synapses (EAS) are a promising, emerging resistive switching mechanism. Ions are shuttled between the reservoir and active layer, changing the ion concentration and thus the conductivity of the channel, which allows for storage of an analog state (Figure 1a). Several studies have demonstrated successful EAS based on the intercalation of protons or Li+ ions. However, Li is incompatible with complementary metal-oxide-semiconductor (CMOS) fabrication, and protons can diffuse out of the channel after insertion, creating problems for the long-term retention of stored states and compromising endurance. This research focuses on EAS that function by the intercalation of Mg2+ ions. Mg was chosen for its abundance, CMOS compatibility, and presence in battery literature.

Current devices based on a radio-frequency sputtered WO3 channel, succinonitrile/Mg(TFSI)2 phase convertible electrolyte (PCE), and Mg metal reservoir show successful modulation in channel conductance with applied current pulses (Figure 1b). However, formation of resistive interfacial phases and electronic conductance through the electrolyte have proven problematic for device performance, in terms of the repeatability, symmetry, and energy consumption. The former problem has been solved by formation of a MgI2 artificial solid-electrolyte interphase (SEI) on the Mg prior to device assembly. To resolve the latter, we are currently developing a thin film, Sodium (Na) Super Ionic Conductor (NASICON)-type electrolyte which has lower electronic conductivity than the PCE and is also compatible with CMOS processing. This could allow these devices to be used as fast, enduring, and energy-efficient computing elements.

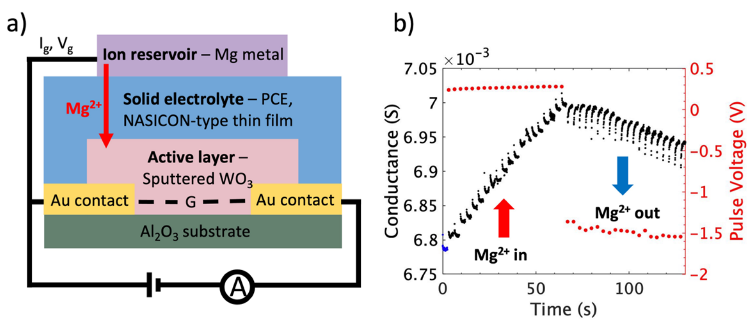

▲Figure 1: (a) Schematic of EAS device based on movement of Mg2+ ions between reservoir and active layer. (b) Modulation of active layer conductance with applied current pulses to gate (15 0.5-s pulses of +20 uA, followed by 15 0.5-s pulses of -60 uA with 2.5-s read between each pulse).

FURTHER READING

- Yao, X., Klyukin, K., Lu, W., Onen, M., Ryu, S., Kim, D., Edmond, N., Waluyo, I. et al. "Protonic Solid-state Electrochemical Synapse for Physical Neural Networks," *Nature Communications*, vol. 11, p. 3134, Jun. 2020.

Uncertainty from Motion for DNN Monocular Depth Estimation

S. Sudhakar, V. Sze, S. Karaman
Sponsorship: NSF Cyber-Physical Systems Program Grant no. 1837212, NSF Real-Time Machine Learning Program Grant no. 1937501, MIT-Accenture Fellowship

Deployment of deep neural networks (DNNs) for monocular depth estimation in safety-critical scenarios on resource-constrained platforms requires well-calibrated and efficient uncertainty estimates. However, uncertainty estimates from state-of-the-art ensembles are computationally expensive, requiring multiple inferences per input. We propose a new algorithm, called Uncertainty from Motion (UfM), that runs only one inference per input by exploiting the temporal redundancy in video inputs to merge incrementally the per-pixel depth prediction and per-pixel uncertainty over a sequence of frames. In a set of experiments using a DenseNet-based autoencoder on a single GPU, UfM offers near ensemble uncertainty quality while consuming on average 5.1 Joules with a latency of 32 ms per frame, which is 8.8x less energy and 6.4x faster than the ensemble. In Figure 1, we compare the results of a DNN that predicts only its data (aleatoric) uncertainty, an ensemble that predicts its overall uncertainty, and a DNN with UfM. We see that UfM retains the uncertainty quality of ensembles at a fraction of the energy and latency, enabling uncertainty estimation for resource-constrained, real-time scenarios.

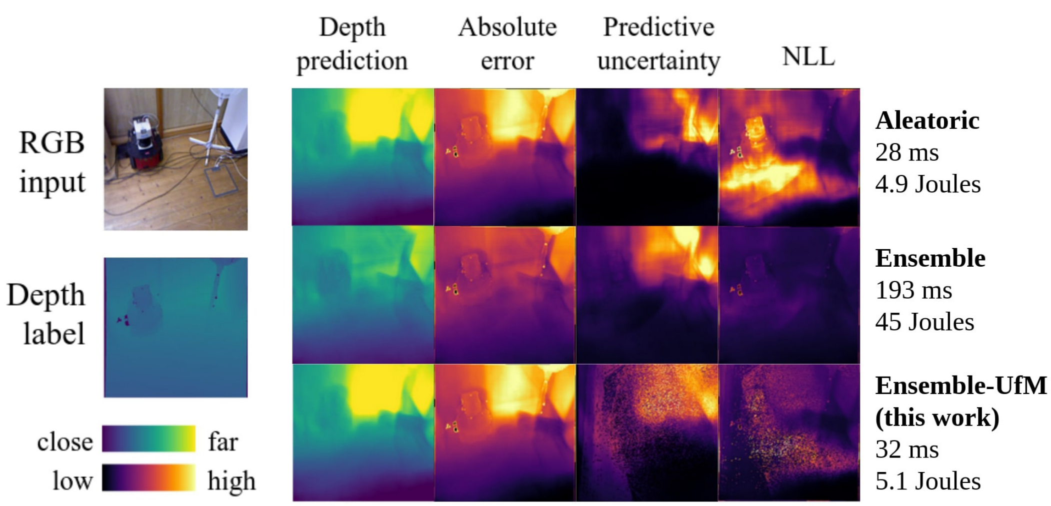

▲ Figure 1: Uncertainty estimation comparison for an aleatoric network, ensemble, and UfM applied to ensembles on an out-of-distribution example from the TUM RGBD dataset. Lower negative log-likelihood (NLL) indicates better uncertainty quality.

FURTHER READING

- S. Sudhakar, S. Karaman, and V. Sze, "Uncertainty from Motion for DNN Monocular Depth Estimation," to be presented at *2022 IEEE International Conference on Robotics and Automation (ICRA)*, IEEE, 2022.

Unsupervised Anomaly Detection on High-frequency Time Series in the Frequency Domain

F.-K. Sun, J. H. Lang, D. S. Boning
Sponsorship: HARTING Technology Group, Lam Research

Unplanned downtime caused by machine faults is costly. By installing sensors and an automated fault detection system, organizations can monitor process and machine sensor data and flag anomalies before problems become serious. However, anomalies are inherently rare, and detecting anomalies typically requires domain expertise.

To address these issues, we formulate the problem as unsupervised anomaly detection on time series. That is, we use only known good data, so our method is applicable even before anomalies are observed. Furthermore, we propose an autoencoder model in combination with several techniques to automatically learn from the data without domain expertise. The autoencoder model is small, so it is suitable when only a small amount of data is available and requires relatively modest computational resources.

The input is the time series representing the sensor values of a manufacturing run. Given the input, we first apply the Fourier Transform to the whole series because frequency domain representation is particularly useful for high-frequency series. Secondly, we propose fractional average pooling to normalize all series to the same number of frequency components. Next, we train the autoencoder on only known good runs, with dropout as data augmentation. Finally, we assign anomaly scores to runs based on the reconstruction error and set two standard deviations as the threshold to classify runs.

We evaluate our method on two vibration datasets about milling machines: one considers worn tools and another considers switching off the cooling system as anomalies. On both datasets, we achieve area-under-curves (AUC) of 99%+ and an average accuracy of 90% on classifying anomaly runs vs. normal runs in the testing set. Our method is applicable to manufacturing industries where high-frequency signals are accessible and has the following advantages: (1) only good run data used, (2) no domain expertise required, and (3) a small and simple model.

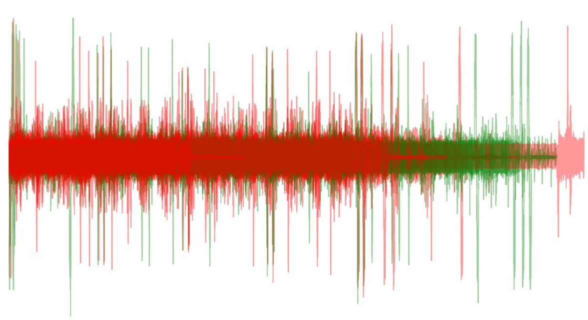

▲ Figure 1: Normal and anomalous series in the time domain are difficult to classify.

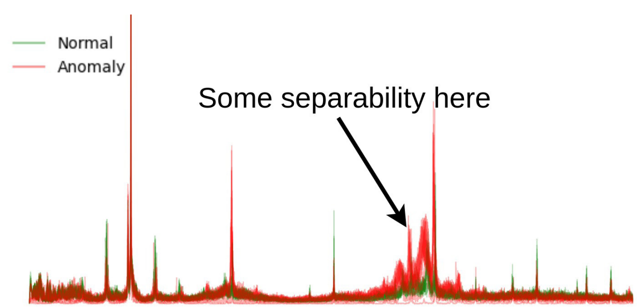

▲ Figure 2: Normal and anomalous series are easier to classify in the frequency domain.

FURTHER READING

• D. W. Martin, "Fault Detection in Manufacturing Equipment Using Unsupervised Deep Learning," *MIT EECS Meng Thesis*, Feb. 2021.

TorchSparse: Efficient Point Cloud Inference Engine

H. Tang, Z. Liu, X. Li, Y. Lin, S. Han
Sponsorship: NSF CAREER Award, Ford, Hyundai, Qualcomm Innovation Fellowship

Deep learning on point clouds has received increased attention thanks to its wide applications in augmented and virtual reality and autonomous driving. These applications require low latency and high accuracy to provide real-time user experience and ensure user safety. Unlike conventional dense workloads, the sparse and irregular nature of point clouds poses severe challenges to running sparse convoluted neural networks efficiently on general-purpose hardware. Furthermore, existing sparse acceleration techniques for 2D images do not translate to 3D point clouds. In this paper, we introduce TorchSparse, a high-performance point cloud inference engine that accelerates sparse convolution computation on graphics processing units. TorchSparse directly optimizes the two bottlenecks of sparse convolution: irregular computation and data movement. It applies adaptive matrix multiplication grouping to trade computation for better regularity, achieving 1.4-1.5x speedup for matrix multiplication. It also optimizes the data movement by adopting vectorized, quantized, and fused locality-aware memory access, reducing the memory movement cost by 2.7x. Evaluated on seven representative models across three benchmark datasets, TorchSparse achieves 1.6x and 1.5x measured end-to-end speedup over the state-of-the-art MinkowskiEngine and SpConv, respectively.

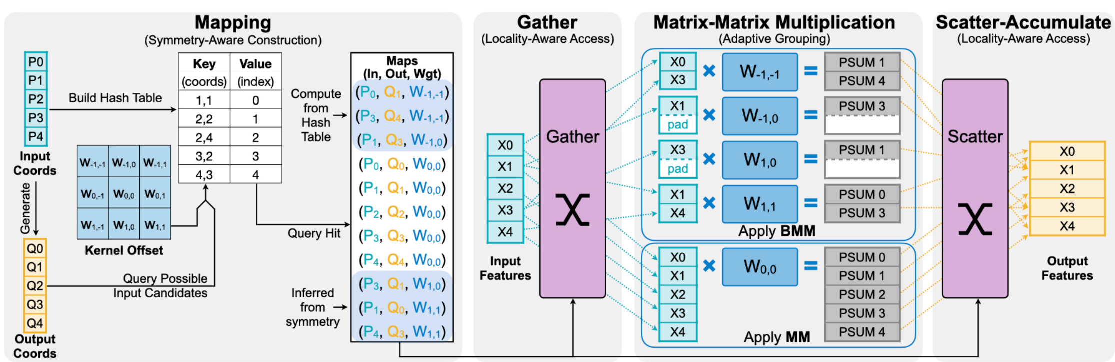

▲ Figure 1: TorchSparse aims at accelerating sparse convolution, which consists of four stages: mapping, gathering, matrix multiplication. and scatter-accumulation. We follow two general principles: (1) memory footprint should be reduced, and (2) computation regularity should be increased to optimize these four components with quantized, vectorized, row-major scatter/gather (Principle 1); adaptively batched MM (Principle 2); and mapping kernel fusion (Principle 1).

FURTHER READING

- H. Tang, Z. Liu, S. Zhao, Y. Lin, J. Lin, H. Wang, and S. Han, "Searching Efficient 3D Architectures with Sparse Point-Voxel Convolution," *European Conference on Computer Vision (ECCV)*, Aug. 2020.
- H. Tang, Z. Liu, X. Li, Y. Lin, and S. Han, "TorchSparse: Efficient Point Cloud Inference Engine," *Conference on Machine Learning and Systems (MLSys)*, Aug. 2022.

QuantumNAS: Noise-Adaptive Search for Robust Quantum Circuits

H. Wang, Y. Ding, J. Gu, Z. Li, Y. Lin, D. Z. Pan, F. T. Chong, S. Han
Sponsorship: MIT-IBM Watson AI Lab, NSF CAREER Award, Qualcomm Innovation Fellowship

Quantum noise is the key challenge in noisy intermediate-scale quantum (NISQ) computers. Previous work on mitigating noise has primarily focused on gate-level or pulse-level noise-adaptive compilation. However, few research efforts have explored a *higher level of optimization* by making the quantum circuits themselves resilient to noise.

We propose QuantumNAS, a comprehensive framework for noise-adaptive co-search of the variational circuit and qubit mapping. Variational quantum circuits are a promising approach for performing quantum machine learning (QML) and simulation. However, finding the best variational circuit and its optimal parameters is challenging due to the large design space and parameter training cost. We propose to decouple the circuit search and parameter training by introducing a novel *SuperCircuit*. The SuperCircuit is constructed with multiple layers of pre-defined parameterized gates and trained by iteratively sampling and updating the parameter subsets (SubCircuits) of it. It provides an accurate estimation of SubCircuits performance trained from scratch. Then we perform an evolutionary co-search of SubCircuit and its qubit mapping. The SubCircuit performance is estimated with parameters inherited from SuperCircuit and simulated with real device noise models. Finally, we perform iterative gate pruning and finetuning to remove redundant gates.

Extensively evaluated with 12 QML and Variational Quantum Eigensolver (VQE) benchmarks on 14 quantum computers, QuantumNAS significantly outperforms baselines. For QML, QuantumNAS is the first to demonstrate over 95% 2-class, 85% 4-class, and 32% 10-class classification accuracy on real quantum machines. It also achieves the lowest eigenvalue for VQE tasks on H_2, H_2O, LiH, CH_4, and BeH_2 compared with UCCSD. We also open-source TorchQuantum (https://github.com/mit-han-lab/torchquantum) for fast training of parameterized quantum circuits to facilitate future research.

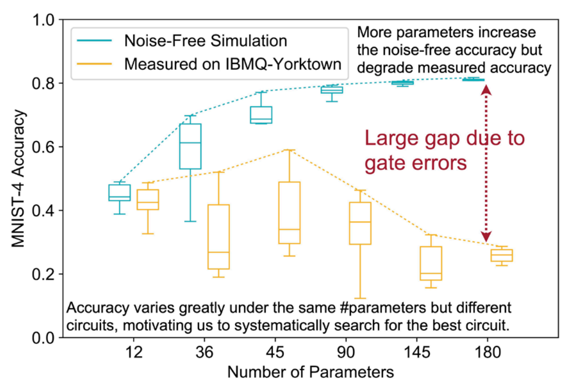

▲Figure 1: MNIST-4 on noise-free simulator / real QC. More parameters increase the noise-free accuracy but degrade measured accuracy due to larger gate errors. Accuracy gap is large.

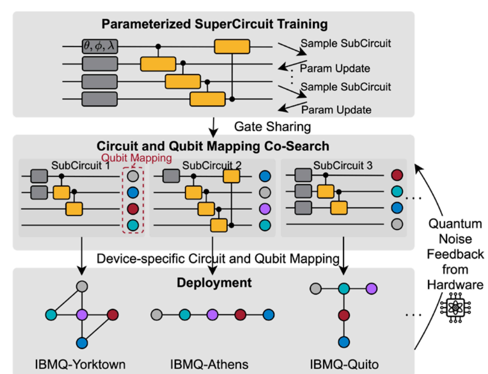

▲Figure 2: Noise-adaptive circuit and qubit mapping co-search improves the robustness on real machines.

FURTHER READING

- H. Wang, Y. Ding, J. Gu, Z. Li, Y. Lin, D. Z. Pan, F. T., Chong, and S. Han, "QuantumNAS: Noise-Adaptive Search for Robust Quantum Circuits," *2022 IEEE International Symposium on High-Performance Computer Architecture (HPCA)*, 2022, pp. 692-708, doi: 10.1109/HPCA53966.2022.00057..
- H. Wang, J. Gu, Y. Ding, Z. Li, F. T. Chong, D. Z. Pan, and S. Han, "QuantumNAT: Quantum Noise-Aware Training with Noise Injection, Quantization and Normalization," *2022 Design Automation Conference*, 2022.
- H. Wang, Z. Li, J. Gu, Y. Ding, D. Z. Pan, & S. Han, "QOC: Quantum On-Chip Training with Parameter Shift and Gradient Pruning," *2022 Design Automation Conference*, 2022.

Sparseloop: An Analytical Approach to Sparse Tensor Accelerator Modeling

Y. N. Wu, P.-A. Tsai, A. Parashar, V. Sze, J. S. Emer
Sponsorship: DARPA (HR0011-18-3-0007), Ericsson

In recent years, a myriad of accelerators has been proposed to efficiently process sparse tensor algebra applications (e.g., neural networks), leading to a large and diverse design space. However, the lack of systematic description and modeling support for these sparse tensor accelerators prevents hardware designers from efficient design space exploration.

To solve the problem, we present Sparseloop, the first fast, accurate, and flexible analytical modeling framework for sparse tensor accelerators. Figure 1 shows Sparseloop's high-level framework. Based on a unified taxonomy to describe the diverse designs, Sparseloop comprehends a wide set of architecture specifications and calculates designs' performance based on stochastic tensor density models. Across a representative set of accelerators and workloads, Sparseloop achieves >600x faster modeling speed than cycle-level simulations, <1% error compared to a custom accelerator model with statistical data modeling, and <8% error compared to simulations with real data.

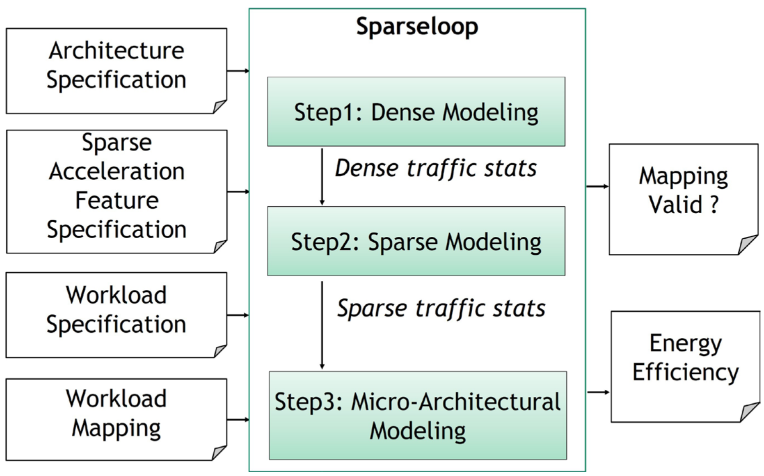

▲ Figure 1: MNIST-4 on noise-free simulator / real QC. More parameters increase the noise-free accuracy but degrade measured accuracy due to larger gate errors. Accuracy gap is large.

FURTHER READING

- Y. N. Wu, P.-A. Tsai, A. Parashar, V. Sze, and J. S. Emer, "Sparseloop: An Analytical, Energy-Focused Design Space Exploration Methodology for Sparse Tensor Accelerators," presented at *2020 IEEE International Symposium on Performance Analysis of Systems and Software (ISPASS)*, Mar., 2021.
- Y. N. Wu, J. S. Emer, and V. Sze, "Accelergy: An Architecture-Level Energy Estimation Methodology for Accelerator Designs," presented at *2019 International Conference on Computer Aided Design (ICCAD)*, Nov. 2019.
- A. Parashar et al., "Timeloop: A Systematic Approach to DNN Accelerator Evaluation," presented at *2019 IEEE International Symposium on Performance Analysis of Systems and Software (ISPASS)*, Mar., 2019.

Fast Convergence of Unstable Reinforcement Learning Problems

W. Zhang

For many of the reinforcement learning applications, the system is assumed inherently stable and with bounded reward, state, and action space. These are key requirements for the optimization convergence of classical reinforcement learning reward function with discount factors. Unfortunately, these assumptions are no longer valid for many real-world problems such as an unstable linear–quadratic regulator (LQR). In this work, we propose new methods to stabilize and speed up the convergence of unstable reinforcement learning problems with the policy gradient methods. We provide theoretical insights on the efficiency of our methods. In practice, we achieve good experimental results over multiple examples where the vanilla method could hardly fail to converge due to system instability.

Latency-tolerant On-device Learning

L. Zhu, S. Han
Sponsorship: MIT-IBM Watson AI Lab, Samsung, Woodside Energy, NSF, Amazon

Much new and sensitive data are generated and collected by intelligent edge devices with rich sensors every day. On-device federated learning is an emerging direction that enables jointly training a model without sharing the data. Since the data is distributed across many edge devices through wireless / long-distance connections, federated learning suffers from inevitable high communication latency. However, the latency issues are undermined in the current literature and existing approaches such as FedAvg become less efficient when the latency increases.

To overcome the problem, we propose delayed gradient averaging (DGA) to address the latency bottleneck. The key idea is to delay the gradient averaging to a future iteration; thus the communication can be pipelined with computation (as shown in Figure 2). By accepting stale average gradients for model updates, DGA allows the communication to execute in parallel with the computation and become scalable even under extreme latency.

We theoretically prove that DGA attains a similar convergence rate as FedAvg and empirically show that our algorithm can tolerate high network latency without compromising accuracy. Specifically, we benchmark the training speed on various vision (CIFAR, ImageNet) and language tasks (Shakespeare), with both independent and identically distributed (IID) and non-IID partitions, and show that DGA can bring 2.55× to 4.07× speedup. Moreover, we built a 16-node Raspberry Pi cluster and show that DGA can consistently speed up real-world federated learning applications

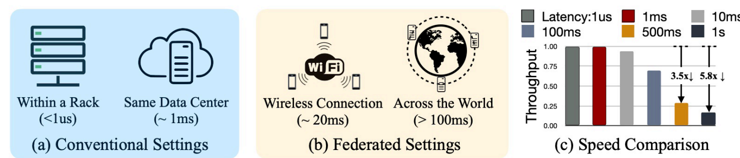

▲Figure 1: Training settings of conventional distributed training and federated learning differ greatly. High latency cost greatly degrades FedAvg's performance, posing a severe challenge to scale up the training.

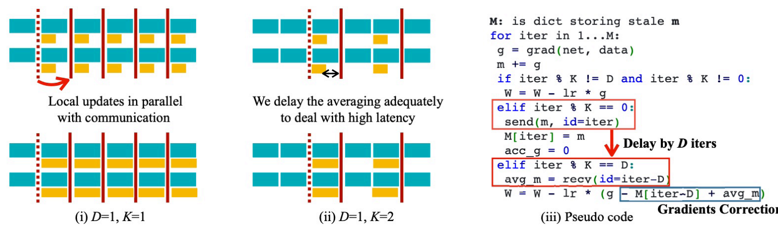

▲Figure 2: Overview of our proposed DGA.

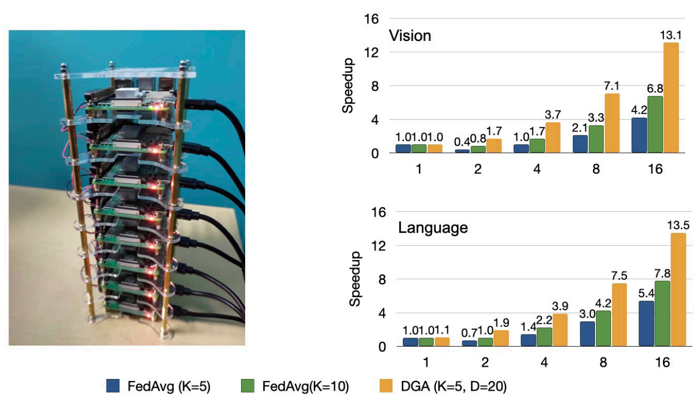

▲Figure 3: Our benchmark Pi Farm setup and speedup comparison.

FURTHER READING

- H. B. McMahan, E. Moore, D. Ramage, S. Hampson, and B. Agüera y Arcas, "Communication-Efficient Learning of Deep Networks from Decentralized Data," *arXiv*, 2016.
- L. Zhu, H. Lin, Y. Lu, Y. Lin, and S. Han, "Delayed Gradient Averaging: Tolerate the Communication Latency for Federated Learning," *NeurIPS* 2021.

MEMS, Field-Emitter, Thermal, Fluidic Devices, and Robotics

Langmuir Probes via Rapid Prototyping for CubeSat and Laboratory Plasma Diagnostics

Z. Bigelow, L. F. Velásquez-García
Sponsorship: MIT Portugal

Langmuir probes (LPs) are widely considered to be the most versatile in-situ plasma sensors due to the simplicity of their design, small cross section, low maintenance requirements, and compatibility with a very broad range of plasma conditions. When operated with compact, low-power electronics, LPs can be installed onboard CubeSats to characterize the space environment surrounding the spacecraft. Moreover, miniaturized LPs can be used to make local plasma measurements. Basic LPs have a single electrode that collects a current while sweeping a bias voltage; from the current–voltage characteristic, plasma parameters such as the electron temperature and number density can be extracted. LPs can also be operated in groups to improve the measurements: for example, double LPs are less sensitive to plasma fluctuations as they are energized by a floating bias voltage. Also, triple LPs conduct faster measurements because they do not need to sweep any voltages during measurement. However, in a multi-probe LP, care must be taken to spatially spread out the probes to avoid cross-talking.

This project focuses on designing, fabricating, and characterizing compact single, double, and triple LPs with integrated, custom electronics (Figure 1) for CubeSat and laboratory plasma applications. The probes will be manufactured via rapid prototyping, exploring the limits of the technology to implement sensors compatible with the coldest, densest plasmas possible, as well as the ionosphere. The circuitry is being designed to enable low-power, autonomous operation. To fabricate the probes, we plan to use metal 3D printing (Figure 2), laser cutting, and plating for creating the electrically conductive parts of the probes and ceramic 3D printing for the dielectric parts of the probe and housing of the electronics. Current research focuses on completing the hardware design, which will be followed by device/driving electronics manufacture and characterization.

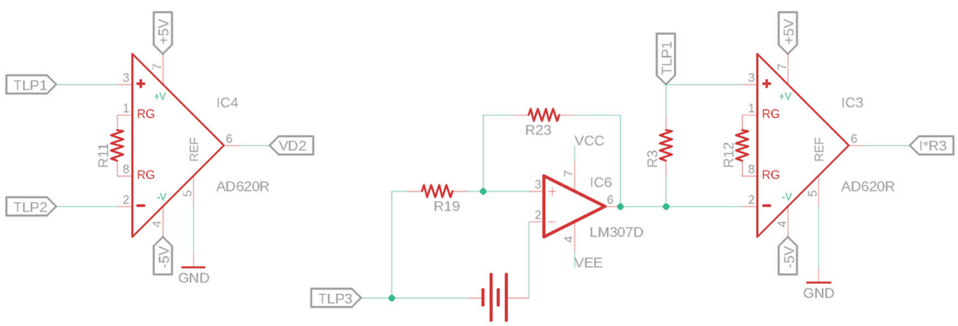

▲ Figure 1: Integrated circuit design for triple LP.

▲ Figure 2: CAD of a 3D-printed, single LP electrode.

FURTHER READING

- L. F. Velasquez-Garcia, J. Izquierdo-Reyes, and H. Kim, "Review of In-Space Plasma Diagnostics for Studying the Earth's Ionosphere," *Journal of Physics D: Applied Physics*, vol. 55, no. 26, p. 263001, 2022
- E. V. Heubel and L. F. Velásquez-García, "Microfabricated Retarding Potential Analyzers with Enforced Aperture Alignment for Improved Ion Energy Measurements in Plasmas," *Journal of Microelectromechanical Systems*, vol. 24, no. 5, pp. 1355-1369, Oct. 2015.
- E. F. C. Chimamkpam, E. S. Field, A. I. Akinwande, and L. F. Velásquez-García, "Resilient Batch-Fabricated Planar Arrays of Miniaturized Langmuir Probes for Real-Time Measurement of Plasma Potential Fluctuations in the HF to Microwave Frequency Range," *Journal of Microelectromechanical Systems*, vol. 23, no. 5, pp. 1131- 1140, Oct. 2014.

Compact, Digitally Manufactured Retarding Potential Analyzers Enabled for CubeSat and Laboratory Plasma Diagnostics

J. Izquierdo-Reyes, Z. Bigelow, N. K. Lubinsky, L. F. Velásquez-García
Sponsorship: MIT Portugal, MIT-Tecnologico de Monterrey Nanotechnology Program

Retarding potential analyzers (RPAs) are multi-gridded sensors that determine a plasma's ion energy distribution (Figure 1). In this project, we are developing novel, digitally manufactured RPAs for CubeSat and laboratory plasma diagnostics. Unlike most RPAs reported in the literature, our devices enforce aperture alignment across the grid stack, maximizing ion transmission. The core of the device is a set of laser-cut electrodes assembled into a 3-D printed Vitrolite® (a glass ceramic) housing (Figure 2). Characterization of the Vitrolite® printing process shows an in-plane, per axis manufacturing accuracy of 60 µm for the as-printed (green) parts and a ~5% shrinkage for the parts annealed at 900 ˚C; higher annealing temperatures cause significant distortion of the printed part due to material reflow, which is problematic for an engineering application. Also, the assembly misalignment between the grids and the housing significantly worsens when using a housing annealed at 900 ˚C. Characterization of the devices via simulations and experiments is consistent with expected performance and the literature. Plasmas with a Debye length as small as 50 µm have been successfully characterized using the reported sensors, matching the performance of state-of-the-art RPAs manufactured via semiconductor micro-fabrication.

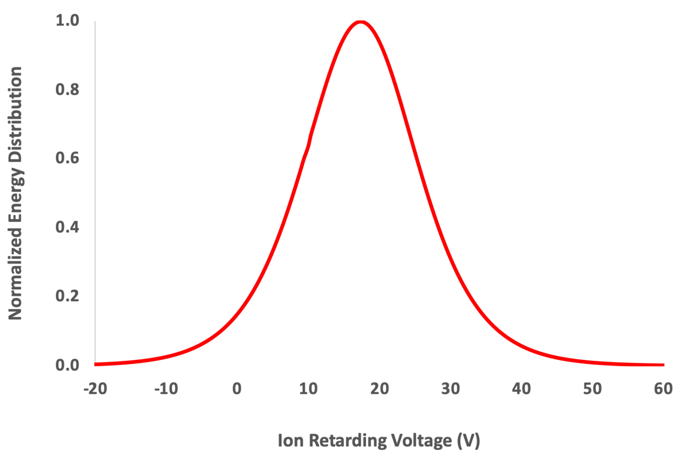

Figure 1: Plasma ion energy distribution measured with a digitally manufactured RPA.

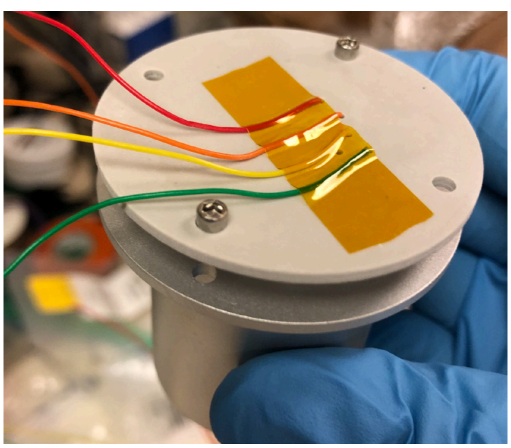

Figure 2: A partially assembled retarding potential analyzer.

FURTHER READING

- E. V. Heubel and L. F. Velásquez-García, "Microfabricated Retarding Potential Analyzers with Enforced Aperture Alignment for Improved Ion Energy Measurements in Plasmas," *J. Microelectromech Syst.*, vol. 24, no. 5, pp.1355-1369, 2015.
- L. F. Velasquez-Garcia, J. Izquierdo-Reyes, and H. Kim, "Review of In-Space Plasma Diagnostics for Studying the Earth's Ionosphere," *Journal of Physics D: Applied Physics*, vol. 55, no. 26, p. 263001, 2022.
- Z. Sun, G. Vladimirov, E. Nikolaev, and L. F. Velásquez-García, "Exploration of Metal 3-D Printing Technologies for the Microfabrication of Freeform, Finely Featured, Mesoscaled Structures," *Journal of Microelectromechanical Systems,* vol. 27, pp. 1171-1185, 2018.

FFF 3D-Printed Inductors for PowerMEMS

J. Cañada, L. F. Velásquez-García
Sponsorship: Empiriko Corporation

Magnetic actuators are among the most essential building blocks of electromechanical systems. In this project, we are exploring ways to manufacture electromagnetic actuators with commodity 3D printers. The 3D printing of electromagnetic actuators can enable fast and inexpensive prototyping and customization in fields like PowerMEMS and robotics, including soft robotics.

Fused filament fabrication (FFF) is a 3D printing method in which a thermoplastic-based material is extruded through a nozzle and deposited layer by layer to construct solid parts. FFF printers equipped with multiple nozzles allow the simultaneous use of several materials, which facilitates the monolithic fabrication of multi-material parts. By using such printers, we intend to monolithically print electromagnetic actuators consisting of permanent magnets, electrically conductive inductors, and rigid or flexible frames.

The 3D printing of magnets has already been demonstrated in previous work, and we are currently working on printing inductors using a copper nanoparticle-doped thermoplastic. The resistivity of this material is three orders of magnitude above that of copper, which raises the challenge of generating useful magnetic fields with only moderately conductive material. A spiral printed with this material is shown in Figure 1.

Figure 2 shows an estimate of the magnetic fields that an inductor built up of stacked spirals like the one shown in Figure 1 can generate. This estimation was computed under two restrictions: (i) the current through the inductor can never exceed the maximum current recommended by the material manufacturer, and (ii) the voltage applied across the inductor cannot exceed 200 V. The results indicate that the maximum achievable magnetic field is on the order of a few Gauss. Upcoming work will explore ways to boost these magnetic fields by adding magnetic cores to the printed inductors.

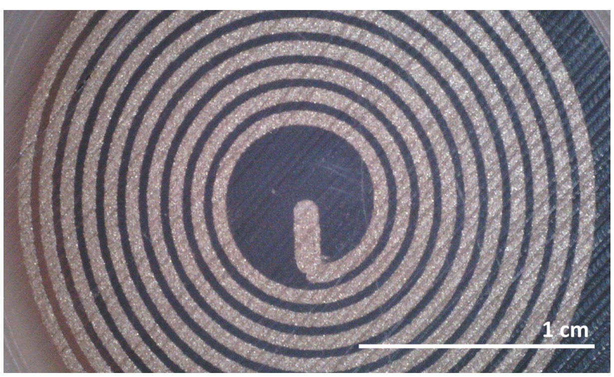

▲ Figure 1: Spiral printed using copper-doped thermoplastic.

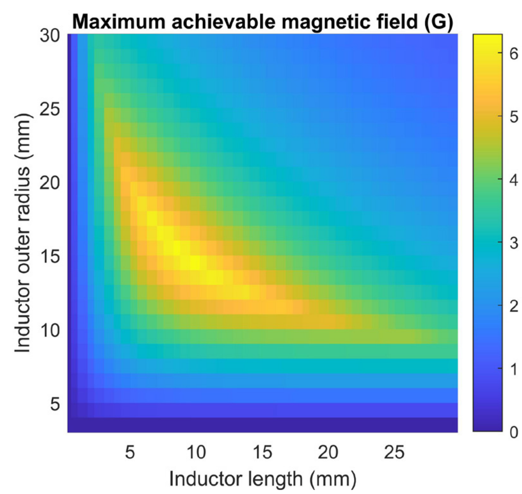

▲ Figure 2: Estimate of maximum achievable magnetic field as a function of inductor size. Outer radius translates to the number of loops in a spiral; length translates to the number of stacked spirals.

FURTHER READING

- A. P. Taylor, C. Vélez Cuervo, D. P. Arnold, L. F. Velásquez-García, "Fully 3D-printed, Monolithic, Mini Magnetic Actuators for Low-cost, Compact Systems," *Journal of Microelectromechanical Systems*, vol. 28, no. 3, pp. 481-493, June 2019, doi: 10.1109/JMEMS.2019.2910215.
- A. P. Taylor, J. Izquierdo-Reyes, L. F. Velásquez-García, "Compact, Magnetically Actuated, Additively Manufactured Pumps for Liquids and Gases," *J. Phys. D: Appl. Phys.*, vol. 53, p. 355002, 2020.
- A. P. Taylor and L. F. Velásquez-García, "Miniaturized Diaphragm Vacuum Pump by Multi-material Additive Manufacturing," *J. Microelectromech. Sys.* vol. 26, no. 6, pp. 1316-1326, Dec. 2017.

Inverse Design of Flexible Tactile Sensor

Z. Liu, M. Cai, S. Hong, J. Shi, S. Xie, G. Li, J. D. Morin, N. Fang, C. Guo
Sponsorship: Southern University of Science and Technology

Tactile sensors with customized performance are desirable for various sensing scenarios. In the case of flexible pressure sensors, designs are mainly empirical and not target-oriented, leading to low efficiency and high cost due to the inevitable long-term trial-and-error. In this project, we explore novel inverse design methodology for dealing with the intractable high-cost problem. With this method, performance targets consist of multiple indicators (sensitivity, sensing range, linearity, etc.) are comprehensively investigated by a machine learning (ML) algorithm, and a hybrid data collection approach is adopted to efficiently shorten the number of iterations. The designs suggested by a well-trained ML model can solve the universal response-saturation problem in a flexible tactile sensor, and further achieve a broad sensing range with steady sensitivity. The finalized configuration can be widely applied to many other material systems. Our proposed configuration and the inverse design methodology build the bridge between mechanical geometries and electrical signals, which is promising to modulate multiple performance indicators and different sensing mechanisms.

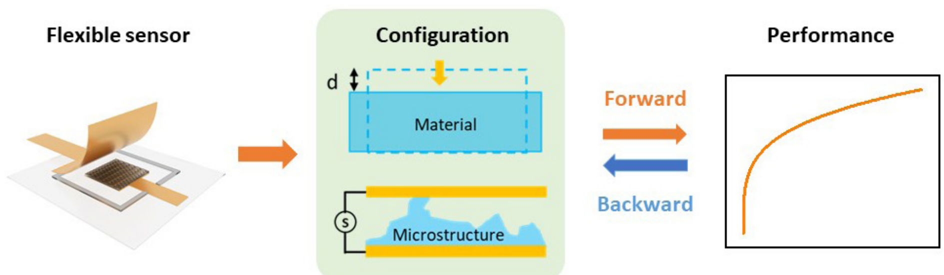

▲ Figure 1: Schematic of forward and inverse design in flexible tactile sensor.

FURTHER READING

- P. Zhu, H. Du, X. Hou, P. Lu, L. Wang, J. Huang, N. Bai, Z. Wu, N. Fang, and C. Guo, "Skin-electrode Iontronic Interface for Mechanosensing," *Nature Communications*, vol. 12, p. 4731, 2021.

Macroscopic Trampoline for Precision Force Sensing

D. S. Fife, V. Sudhir

Silicon nitride nano-trampoline resonators have become established as a platform for low-noise force sensing and optomechanics. These resonators are constructed by patterning a silicon nitride membrane with a central pad suspended by tethers (see Figure 1). Here, a milligram-scale mirror is bonded to the trampoline to couple this resonator with a gravitational potential. Our aim is to perform precision gravity measurements with milligram-scale masses and eventually observe the effect of gravity on massive quantum states.

Macroscopic mechanical oscillators appear to exhibit classical behavior due to the difficulty of isolating them from the ubiquitous thermal environment. However, their thermal noise can be decreased by increasing the quality factor (Q). There are two primary methods being applied to increase Q, dissipation dilution, and phononic bandgap engineering. Dissipation dilution is a phenomenon whereby an external lossless potential is applied to a resonator to stiffen it and reduce energy in lossy modes. The potentials that will be used are the internal stress of the membrane and the radiation pressure from an optical cavity. By engineering phononic crystals into the tether, we confine the phonons compromising the mode to the center of the resonator. This prevents the loss of energy through the clamps to the frame.

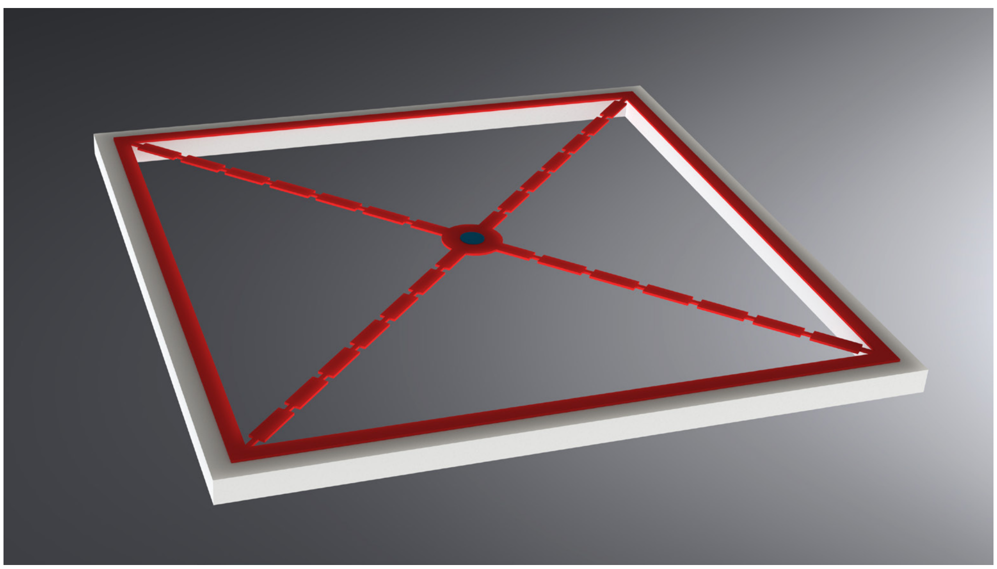

▲ Figure 1: Not-to-scale diagram of a trampoline resonator. Red: silicon nitride. Gray: silicon substrate. Blue: gadolinium gallium garnet mirror.

Knowledge Management System for MEMS Incorporating Heterogeneous Data Sources

J. Gammack, H. Akay, S.-G. Kim
Sponsorship: NSF LEAP-HI

Research at MIT's Microsystems Technology Laboratories (MTL) and micro/nano focused conferences such as Hilton Head Workshop has resulted in decades of micro- and nano-technology innovation. The total information from these contributions is valuable institutional knowledge and is documented meticulously by researchers in the form of theses, published papers, posters, and a wide range of textual and graphical design and process data. Due to the huge scale of this data and the distributed nature of its storage, it can be challenging for newcomers to learn from past achievements of the community. We aim to enable the availability and accessibility of this big data by developing a semantically searchable knowledge management system, so researchers can expedite the process of learning from past design successes and failures.

We applied artificial intelligence-based natural language processing (NLP) models, fine-tuned on technical microsystems research documents, to represent the semantic meaning contained within the text of theses, research papers, and process documents in order to construct a knowledge base from which information can be easily retrieved. By encoding language descriptions of functional information and graphical figures via their captions and referencing sentences, we can represent semantic knowledge from heterogeneous documents to structure and distill vast repositories of unstructured documentation (Figure 1). We developed an interactive question-answering system where users retrieve answers to questions as well as relevant data (Figure 2). Currently, we have encoded 16 years of MTL report abstracts, 4,800 theses, and Hilton Head Transducers Technical Digests from 1984-2021. In the future, this system will be further generalized to extract micro-/nano-specific design knowledge, process sequences, and material choices into an ever-growing knowledge base to benefit MTL researchers.

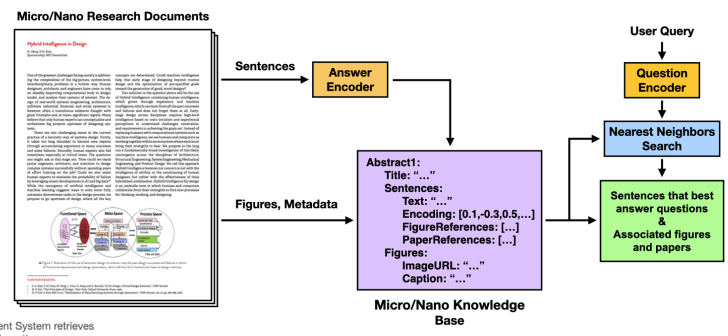

▶ Figure 1: Creation of associative micro/nano knowledge base by automatically crawling MTL reports, theses, and Hilton Head Workshop submissions. To find answers to user queries, we compared queries and encoded sentences in the knowledge base.

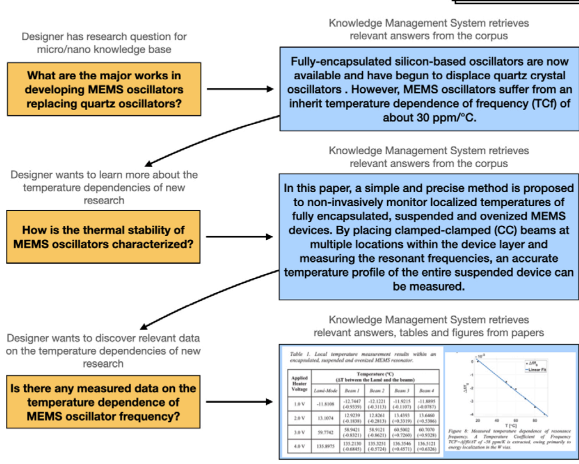

◀ Figure 2: Case study of knowledge retrieval from decades of micro/nano-related research. Answers to questions may be direct textual answers or may include relevant graphical or tabular data that is referenced.

FURTHER READING

- J. Gammack, H. Akay, and S.-G. Kim, "Semantic Knowledge Management System for Design Documentation with Heterogeneous Data Using Machine Learning," *Procedia CIRP*, in press, 2022.
- H. Akay and S.-G. Kim, "Reading Functional Requirements Using Machine Learning-based Language Processing," *CIRP Annals*, vol. 70, no. 1, pp. 139-142, 2021.
- H. Akay, M. Yang, and S.-G. Kim, "Automating Design Requirement Extraction from Text with Deep Learning," *ASME IDETC-CIE Proceedings*, Online, 2021.

Nanowire-Coated Emitter Electrospray Ionizer Coupled to Digital Microfluidics for Liquid Analysis

A. Kachkine, L. F. Velásquez-García
Sponsorship: Empiriko Corporation

Liquid sample processing for mass spectrometry involves the extraction of a target analyte, addition of solvents, and ionization. Solid-state, programmable digital microfluidics have emerged as versatile platforms for sample manipulation, while ionization can be efficiently conducted via electrospray, i.e., the emission of charged molecules from a liquid subjected to a high electric field. Our group previously developed nanowire-coated emitters, which have pure ion emission and are thus of interest to mass spectrometry due to potential noise reduction. We present the first integration of high-efficiency nanowire-coated emitters and digital microfluidics: a single device for sample manipulation and ambient electrospray (Figure 1).

Device fabrication takes ~7 hours and costs ~$5 in materials, with preparation of the digital microfluidic components taking under 10 minutes at a cost of ~$1 with no cleanroom processing. The emitter is made out of steel via binder jetting, and then undergoes electropolishing, seed layer deposition, and zinc oxide nanowire growth in a hydrothermal bath. Digital microfluidic components comprise commercially-fabricated printed circuit boards, laser cut plastics, drop-cast Teflon layers, and a polymeric casing made via digital light processing.

Sample droplets are moved through the device and onto the emitter via a paper conduit. Under comparatively low emitter extraction voltages (2-2.5 kV) our device has two-fold greater electrospray currents than state-of-the-art methods used with digital microfluidics (Figure 2). The electrospray dynamics are time-variant: an initial unstable, short-duration Taylor cone is followed by a secondary, stable electrospray without a visible plume, lasting about 20 seconds while using 5μL of solvent. Ongoing work focuses on characterizing devices interfaced with a mass spectrometer, improving device reliability, and fully characterizing electrospray dynamics. Images are from the first further reading publication below.

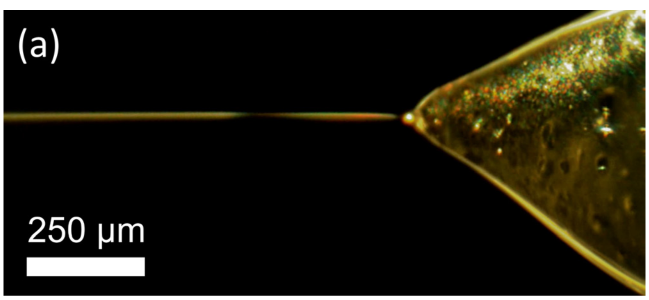

◀Figure 1: (a) Fabricated device with receptor used for externally actuating device functions and (b) labeled exploded view of device, showing key internal components.

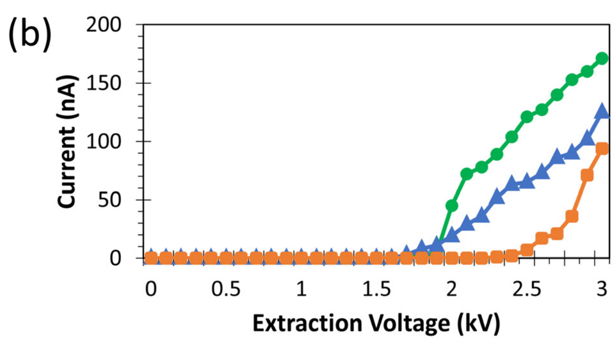

◀Figure 2: (b) Electrospray of isopropanol from nanowire-coated emitter (device casing removed) and (b) plot of average current versus voltage for nanowire-coated emitter (circles), paper emitter (triangles), and coated blade (squares) with isopropanol as solvent.

FURTHER READING

- A. Kachkine and L. F. Velásquez-García, "Nanowire-Coated Emitter Electrospray Ionizer Coupled to Digital Microfluidics for Liquid Analysis," *Proceedings of the IEEE 35th International Conference on Micro Electro Mechanical Systems*, pp. 95-98, 2022.
- D. V. M. Máximo and L. F. Velásquez-García, "Additively Manufactured Electrohydrodynamic Ionic Liquid Pure-ion Sources for Nanosatellite Propulsion," *Additive Manufacturing*, vol. 36, p. 101719, Dec. 2020.
- F. A. Hill, E. V. Heubel, P. J. Ponce de Leon, and L. F. Velásquez-García, "High-throughput Ionic Liquid Ion Sources Using Arrays of Microfabricated Electrospray Emitters with Integrated Extractor Grid and Carbon Nanotube Flow Control Structures," *Journal of Microelectromechanical Systems*, vol. 23, pp. 1237-1248, Oct. 2014.

Internally Fed, Additively Manufactured Electrospray Thrusters for CubeSats

H. Kim, L. F. Velásquez-García
Sponsorship: MIT Portugal

Electrospray engines have one or more emitters that electrohydrodynamically eject high-speed charged particles from liquids to produce thrust. Stable electrospray emission, which can be used in a propulsion application, exists for a limited range of electric fields and flow rates. Whether the thruster emits ions or droplets is determined by the flow rate of the propellant. On the one hand, if the flow rate is below a certain threshold value, the engine emits ions, exerting a high-specific impulse, low force to the spacecraft. On the other hand, if the flow rate is above the threshold value, the engine emits droplets, creating a larger thrust with lower specific impulse. In principle, both kinds of emission are useful for propelling a spacecraft.

The electric field strength needed to activate the electrospray emitters is proportional to the square root of the emitter diameter; therefore, electrospray thrusters benefit from miniaturization, as scaled-down emitters turn-on with less voltage. Miniaturization of electrospray engines has traditionally been accomplished using semiconductor fabrication. However, this manufacturing approach is expensive and time-consuming. Therefore, fabrication approaches that can create complex hardware at a low cost and manufacturing time would greatly help lower the cost of space hardware including CubeSats.

In this project, we are exploring additive manufacturing via digital light processing to create CubeSat electrospray thrusters. We are currently focusing on developing electrospray engines that emit droplets. Before testing multiplexed designs, we are first investigating a single-emitter design to check the essential parameters for electrospray (Figure 1). The high electric field acting on the electrospray emitters is affected by the bias voltage between the propellant and the electrode that extracts droplets, as well as the separation distance between the emitter and the extractor electrode. Therefore, the design needs to be optimized to minimize the start-up voltage. In addition, the upper limit for the flow rate to sustain stable droplet emission needs to be characterized.

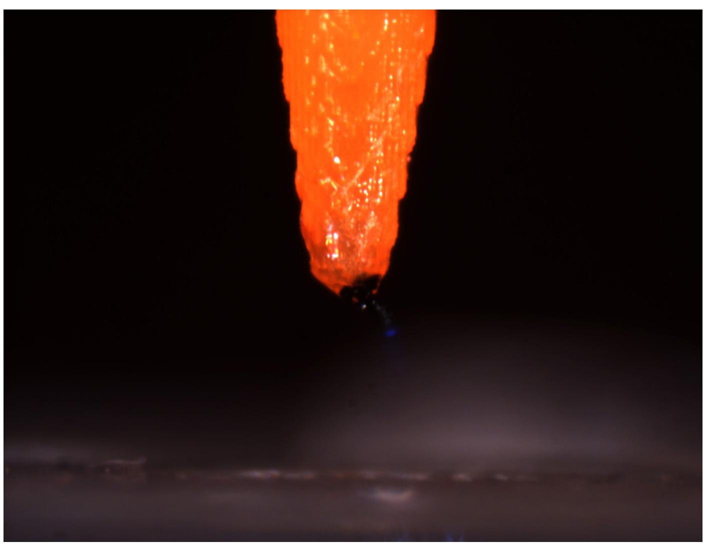

◀ Figure 1: The Taylor cone generated on the additively manufactured emitter.

FURTHER READING

- D. Olvera-Trejo and L. F. Velásquez-García, "Additively Manufactured MEMS Multiplexed Coaxial Electrospray Sources for High-Throughput, Uniform Generation of Core-Shell Microparticles," *Lab on a Chip*, vol. 16, no. 21, pp. 4121-4132, Oct. 2016.
- D. V. Melo Maximo and L. F. Velásquez-García, "Additively Manufactured Electrohydrodynamic Ionic Liquid Pure-Ion Sources for Nanosatellite Propulsion," *Additive Manufacturing*, vol. 36, p. 101719, Dec. 2020.
- E. García-López, D. Olvera-Trejo, and L. F. Velásquez-García, "3-D Printed Multiplexed Electrospinning Sources for Large-Scale Production of Aligned Nanofiber Mats with Small Diameter Spread," *Nanotechnology*, vol. 28, no. 42, p. 425302, Oct. 2017.

FireFly: An Insect-scale Aerial Robot Powered by Electroluminescent Soft Artificial Muscles

S. Kim, K. Chen
Sponsorship: RLE, MIT

Bioluminescence in natural fireflies is an effective and unique feature that enables communication and mating. Inspired by fireflies in nature, we develop a sub-gram (650 mg) aerial robot that emits light during flight (Figure 1). Simultaneous actuation and light emission are achieved by embedding electroluminescent (EL) particles in a dielectric elastomer actuator (DEA) that has highly transparent electrodes. During robot flight, a strong (> 40 V/µm) and high frequency (400 Hz) electric field is generated within the DEA, exciting the EL particles to emit light. Compared to the original DEA, our new design and fabrication methods require small additional weight (2.4%) and actuation power (3.2%) without adding any robotic component. We further evaluate DEAs' mechanical and electrical behaviors with the addition of EL particles, and improve the EL-DEA designs to ensure the robot performance (maximum lift and lifetime) remains unchanged.

Light emission in sub-gram aerial robots enables motion tracking with miniaturized cameras that are receptive to visible light. We develop a fabrication process in which each ELDEA exhibits a different color or pattern (Figure 1). This design makes each ELDEA a unique active marker for visual tracking. We demonstrate controlled hovering flights using a sub-gram robot powered by four ELDEAs (Figure 2). The robot position and attitude are tracked through both a Vicon motion tracking system and a set of three smartphone cameras (Figure 2). Compared to the Vicon system, visual tracking shows a root-mean-square (rms) position and attitude error of 2.55 mm and 2.60 degree, respectively. This result shows the potential of using off-the-shelf microscale cameras for enabling controlled flights. In future studies, we envision light emission can be crucial for enabling communication in coordinated swarm flights of sub-gram aerial robots.

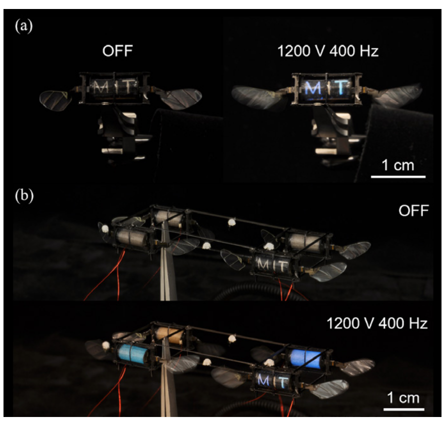

◀ Figure 1: A sub-gram aerial robot powered by ELDEAs. (a) One ELDEA is patterned with three letters, "MIT," and each letter emits a different color when the ELDEA is driven at 1200 V and 400 Hz. (b) Four different colored or patterned ELDEAs are installed in a 650-mg flapping wing robot. The robot emits light when it operates at hovering flight conditions.

▼ Figure 2: Automated tracking and trajectory reconstruction based on the smartphone videos. (a) Automated tracking of the four ELDEAs in the top, side, and front view videos. (b) Camera pose calibration and reconstructed 3D trajectories of each ELDEA. (c) An inset graph of (b) that compares the vision-tracked trajectories with that from the Vicon motion tracking system.

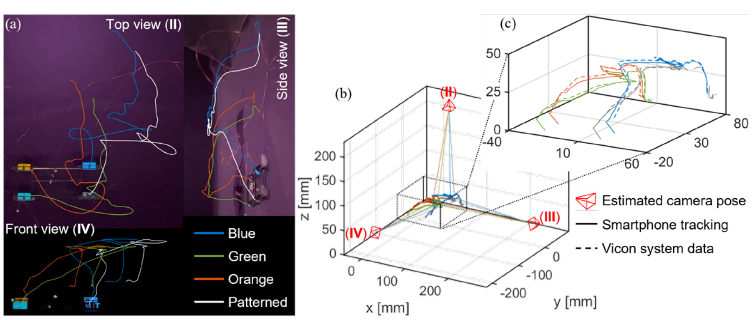

FURTHER READING

- Y. Chen, et al., "Collision Resilient Insect-scale Soft-actuated Aerial Robots with High Agility," *IEEE Transactions on Robotics*, to be published, 2021, DOI: 10.1109/TRO.2021.3053647.
- Y. Chen et al., "Controlled Flight of a Microrobot Powered by Soft Artificial Muscles," *Nature*, vol. 575, no. 7792, pp. 324-329, 2019, DOI: 10.1038/s41586-019-1737-7.
- R. Zhijian, et al. "A High-Lift Micro-Aerial-Robot Powered by Low-Voltage and Long-Endurance Dielectric Elastomer Actuators." *Advanced Materials*, p. 2106757, 2022.

Soft Material Design of Additively Manufactured Actuators to Control Stress Distribution

H. J. Lee, L. F. Velásquez-García
Sponsorship: Empiriko Corporation

Rigid materials are ubiquitous in engineering because their behavior is easy to predict and can support a great amount of weight. However, they are not suitable in unpredictable environments and can be dangerous when used in systems that involve human interaction. Soft and flexible materials, on the other hand, are compliant and can deform to match the shape of any object that comes into contact; this allows the structure to distribute stress and enable safer interaction with the environment. As a result, soft materials are now used in a wide range of applications including flexible electronics, soft robotics, and biological applications. While there are many methods to manufacture structures with soft materials, recent development in additive manufacturing allows fabricating complex designs with geometrical features unmatched by traditional manufacturing methods. Therefore, the structures can be designed to improve many properties for structural or thermal applications.

In this project we are designing and fabricating soft actuator structures to improve the fatigue properties under cyclic compression. Under compression, soft materials tend to fold themselves, which leads to a significant amount of stress concentration. While this might not be a problem for a small number of compressions, the fatigue life becomes an issue when the structure is applied to actual products that require a reasonably long lifespan. In addition to the material properties, structures fabricated through additive manufacturing have anisotropic behavior, where failure is most likely to occur between layers. Figure 1 shows the stress concentration of a flexible ring with a design that distributes the stress to a wider area, reducing the maximum stress within the structure. These designs can easily be fabricated with additive manufacturing, as shown in Figure 2. The sample shown is fabricated with Ninjaflex (a commercial thermoplastic polyurethane printable material) using an extrusion 3D printer.

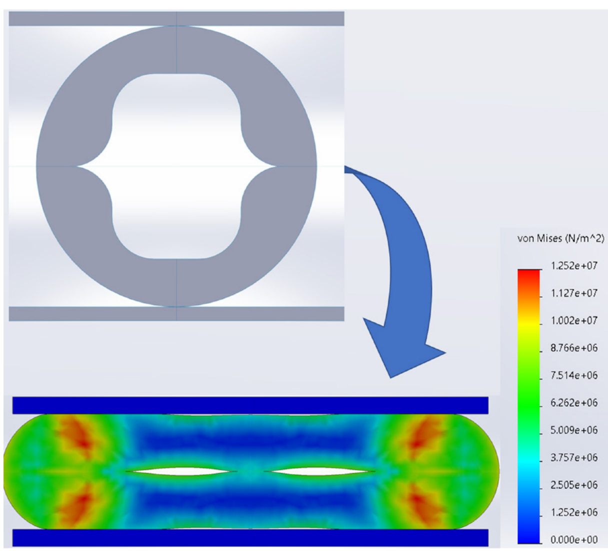

▲ Figure 1: Solidworks was used to simulate the compression of a hyperelastic material. The structure is designed to distribute stress concentration to improve the fatigue property.

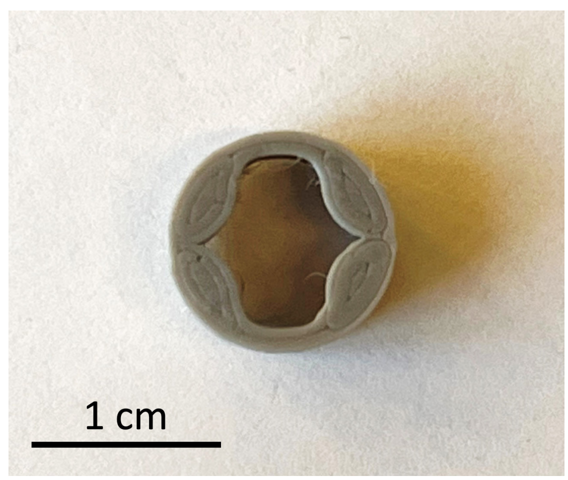

▲ Figure 2: Image shows the structure fabricated through additive manufacturing.

FURTHER READING

- A. P. Taylor, J. Izquierdo Reyes, and L. F. Velásquez-García, "Compact, Magnetically Actuated, Additively Manufactured Pumps for Liquids and Gases," *Journal of Physics D – Applied Physics*, vol. 53, no. 35, p. 355002, Aug. 2020.
- P. Taylor, C. Vélez Cuervo, D. Arnold, and L. F. Velásquez-García, "Fully 3D-printed, Monolithic Magnetic Actuators for Low-cost, Compact Systems," *Journal of Microelectromechanical Systems*, vol. 28, no. 3, pp. 481-493, Jun. 2019.
- A. P. Taylor and L. F. Velásquez-García, "Miniaturized Diaphragm Vacuum Pump by Multi-material Additive Manufacturing," *Journal of Microelectromechanical Systems*, vol. 26, no. 6, pp. 1316-1326, Dec. 2017.

Improving Reliability and Performance of Microhydraulic Electrowetting Actuators

J. Kedzierski, I. Liu, L. Racz, L. F. Velásquez-García
Sponsorship: MIT Lincoln Laboratory

Electrowetting is the phenomenon of altering the surface tension and wetting properties of liquids by applying electric fields. Applying an external voltage to a liquid droplet changes the droplet's shape and contact angle to solid surfaces, thus affecting the attraction and friction between droplets and solid surfaces. Electrowetting can reversibly transport and shape fluids; thus these effects have been used in multiple applications for manipulating small amounts of liquids, such as adjustable fluid optical lenses and droplet display arrays.

Microhydraulic actuators can be made by assembling a rotor and a stator separated by liquid droplets. Applying external electric fields to the droplets modifies the wetting and surface properties, thus actuating the droplets. Microhydraulic actuators offer several benefits over conventional motors. Microhydraulic actuators are lighter, flexible, and scalable to small dimensions. In contrast, conventional motors that rely on wire coils are often limited by coil size and high resistance when scaled down. The small scale of microhydraulic actuators leads to high power density, enabling effective conversion of electrical to mechanical power in compact spaces.

This project is based on prior work at Lincoln Laboratory regarding rotational microhydraulic actuators. The rotor moves relative to the stator by applying external electric fields to the droplets, modifying the wetting and surface properties with electrowetting. The main goal is to improve reliability—currently, the main challenges include lowering friction, stabilizing

rotation, and extending operation time. The project will include experiments to determine the root causes of unreliable operations and incorporate corresponding design changes. The resulting microhydraulic actuators will combine reliable operations with high power density, small size, and precise motion. Thus, the project has vast potential in biomedical and robotics applications.

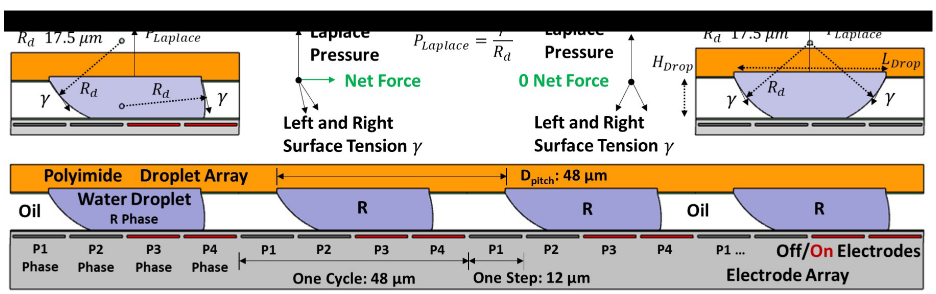

▲ Figure 1: Operating principle of microhydraulic actuators. Water droplets are shifted along by applying sequential electrical phases. From Kedzierski et al., Science Robotics 3, no. 22, eaat5643, 2018.

FURTHER READING

- J. Kedzierski and H. Chea, "Multilayer Microhydraulic Actuators with Speed and Force Configurations," *Microsystems & Nanoengineering* 7, no. 1, pp. 1–10, 2021.
- J. Kedzierski and E. Holihan, "Linear and Rotational Microhydraulic Actuators Driven by Electrowetting," *Science Robotics*, vol. 3, no. 22, p. eaat5643, 2018.

3D-Printed Reflectron for Compact Mass Spectrometry

N. Lubinsky, L. F. Velásquez-García
Sponsorship: Empiriko Corporation

Accurate measurement of blood plasma constituents in the medical clinical setting is incredibly important for drug assays and monitoring of biomarkers. However, the traditional gold standard is a triple quadrupole, an investment requiring a large amount of power, space, and a $10 million budget. Other applications for low false-positive, compact mass spectrometry also face the same economical burdens. Our research group aims to mitigate these with the additive manufacture methods available to 3D printing mass spectrometers for high precision and miniaturization.

We are currently exploring a two-piece reflectron mass spectrometer—a device that measures the time-of-flight (TOF) of ions as they are reflected by the internal electromagnetic fields. The design geometry of a hyperbola (Figure 1) surrounded by a cone creates a potential distribution that is quadratic with distance. Thus, the ions exhibit a repelling force that is independent of the initial energy of the ion; therefore, we can observe a TOF solely dependent on the specific mass-per-charge of the ions.

Methods of operation employed by this reflectron involve the utilization of an entrance gate electrode, with an aperture for ions. Once potential drops to 0 V on the gate, ions flow into the reflectron, ultimately reflecting towards the entrance, to a nearby anode. Ions colliding will draw current; however, the current intensity will vary in time depending on the TOF of the ions. The delay of the gate switching off to the time we register current intensity is completely dependent on the specific charge of the ion, and mass spectrometry can be performed. In our approach, the electrodes are 3D-printed in glass-ceramic via digital light processing (DLP). Post-print, we selectively plate them, forming conductive surfaces. Current research efforts focus on optimizing the hardware and characterizing such hardware in vacuum.

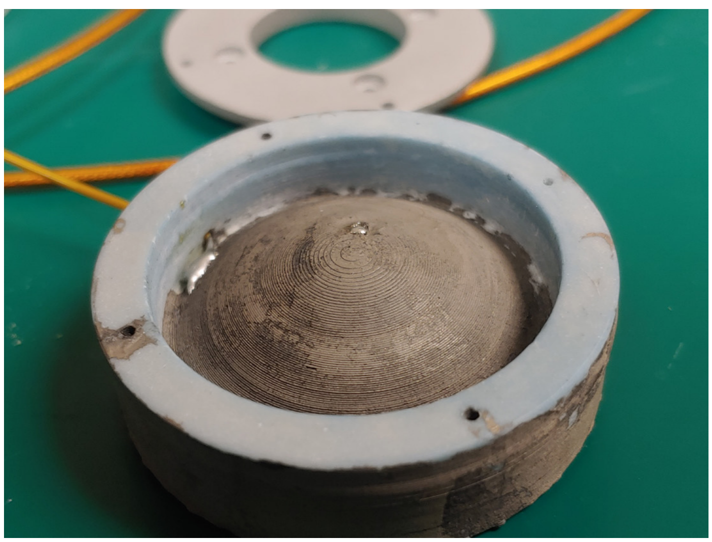

▲ Figure 1: Hyperbolic electrode 3D printed in glass-ceramic via DLP and coated in nickel.

FURTHER READING

- Z. Sun, G. Vladimirov, E. Nikolaev, and L. F. Velásquez-García, "Exploration of Metal 3-D Printing Technologies for the Microfabrication of Freeform, Finely Featured, Mesoscaled Structures," *J. Microelectromech. Sys.*, vol. 27, no. 6, pp. 1171-1185, Dec. 2018
- L. F. Velásquez-García, K. Cheung, and A. I. Akinwande, "An Application of 3D MEMS Packaging: Out-Of-Plane Quadrupole Mass Filters," *J. Microelectromech. Syst.*, vol. 16, no. 6, pp. 1430-1438, Dec. 2008.
- E. Nikolaev, M. Sudakov, G. Vladimirov, L. F. Velásquez-García, P. Borisovets, and A. Fursova, "Multi-Electrode Harmonized Kingdon Traps," *Journal of the American Society for Mass Spectrometry,* vol. 29, no. 11, pp. 2173- – 2181, Nov. 2018.

MEMS Digitalized Igniter or Primer for Solid Propellant Grains and Two-spool Micro Gas Turbine Engine Concept

J. Protz
Sponsorship: Protz Lab Group, microEngine, LLC

Micro-fabricated chemical rocket engines and jet engines have been researched at MIT for over two decades; they are a compelling propulsion option for small air- and space-craft. The investigator's most recent work focuses on microchips as replacements for igniters or primers in model rocket motors and bullets, allowing these to serve as an inexpensive final stage for a miniaturized launch vehicle. As envisioned, a sq. mm -sized micro-electromechanical system (MEMS) chip would combine a complementary metal-oxide-semiconductor (CMOS) guidance computer, MEMS sensors, and a MEMS solid- or liquid- propellant micro rocket motor. The chip would replace the igniter of an otherwise-conventional solid-propellant model rocket motor or the primer of an otherwise-unmodified bullet. By monitoring its evolving state on a waving launch rail and actively timing the firing of the plume of the MEMS rocket into the grain of the solid motor or bullet, the guidance computer would regulate the initial conditions of a ballistic object's trajectory. If the projectile was a satellite, this would regulate its orbital insertion. The advantage of the concept is that it economizes on chip size and, thus, system cost; fine control of initial condition can be an inexpensive alternative to mid-flight control. The effort is in an early stage and focuses on identifying mature technologies that can be joined as a system; if successful, it could enable hobby rocket-sized launch vehicles that utilize concepts already proven by the Japanese at a larger scale. Other recent work by the investigator has focused on mocking up in wood a MEMS-compatible two-spool jet engine configuration that combines a combustor, high-speed turbocharger, and low-speed cold turbine with an integrated electrical generator and mocking up in brass a miniature rocket engine configuration that integrates a steam injector, boiler, decompression chamber, fuel injector, thrust chamber, and battery- powered electric fuel pump.

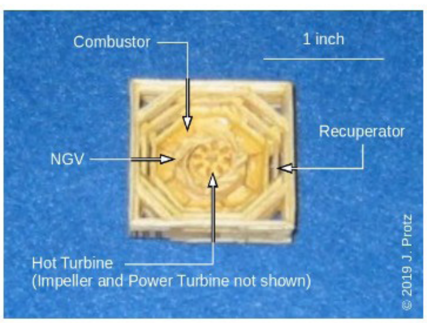

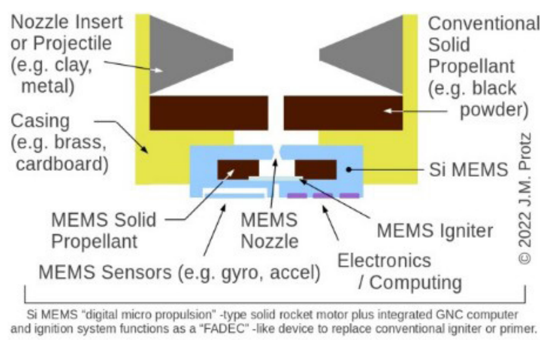

▲ Figure 1: (left) mock-up in wood of a MEMS-compatible micro gas turbine engine with cold turbine; (right) depiction of a MEMS "FADEC" (digitalized igniter or primer) for firing a solid propellant grain.

FURTHER READING

- J. M. Protz, "MEMS Compatible Solid and Liquid Micro Rocket Engines and Micro Gas Turbine Engine," *Proc. MIT MTL Annual Research Conf. (MARC 2022)*, S2.14, 25-26 Jan. 2022.
- J. M. Protz, "Progress Towards an Injector-Pumped Micro Rocket Engine and Vehicle (and Cost of Launch)," *Gas Turbine Laboratory Seminar*, MIT, Cambridge, MA, 7 May, 2019.
- J. M. Protz, "Hybrid and Partially Pressure-Fed Injector-Pumped Micro Rockets," (JANNAF 2019-004BT), presented at the *Joint Army-Navy-NASA-Air Force Joint Meeting of the 13th Modeling and Simulation / 11th Liquid Propulsion / 10th Spacecraft Propulsion Subcommittees and Meeting of the Programmatic and Industrial Base (JANNAF*), Tampa, FL, 2019.

Advanced Electromembrane Process for Portable Desalination Unit

J. Yoon, J. Han
Sponsorship: Abdul Latif Jameel Water and Food Systems Lab (J-WAFS), U.S. Army Combat Capabilities Development Command-Soldier Center

Climate change and human activity are accelerating the water crisis. Seawater desalination plants are a good solution for people in urban areas but are unsuitable for small groups in rural areas and instance demands due to natural disasters. Miniaturized desalination units, known as portable desalination units, have been developed to provide a secure source of drinking water to these groups. Only reverse osmosis-based portable desalination units have been on the market, but they are heavy (> 20 kg) and have power-intensive operation (100~400 W) due to high production rate (> 20 L/h). A need remains for a lightweight and energy-efficient portable desalination unit.

The ion concentration polarization (ICP) process using only cation exchange membrane has been developed to improve energy efficiency and overcome the limitation of electrodialysis (ED). The ICP process has been proposed because a higher diffusivity of anion leads to a thicker diffusion boundary layer next to the cation exchange membrane, which is already known theoretically and experimentally in ED. The ICP process improves ~20 % over current utilization compared to ED when treating seawater. At the same time, dilute and concentrated streams appear in the same spacer, facilitating the removal of suspended solids that ED does not enable.

We present a fully packaged portable desalination unit using an advanced electromembrane process, where the ICP process and ED are serially stacked, forming a multi-stage process. The components, multi-stage module, pumps, customized controller, and battery are assembled in a hard case 42 x 33.5 x 19 cm^3 with a total weight of 9.4 kg. It allows conversion of both brackish water (2.5 ~ 10 g/L) and seawater (30 ~ 45 g/L) into drinking water with the corresponding specific energy consumptions, 0.4 ~ 4 and 15.6 ~ 26.6 Wh/L, respectively. The unit successfully deployed on the beach to make seawater into drinking water.

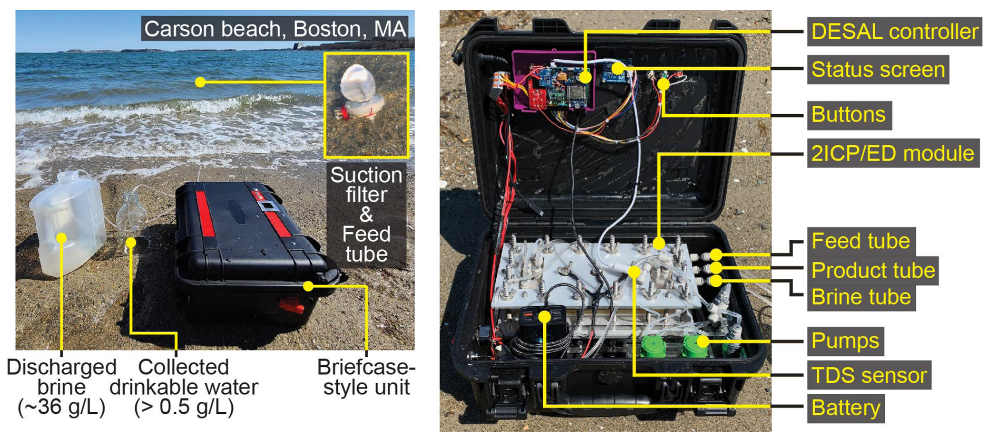

▲Figure 1: Finished, fully integrated portable desalination unit. The photograph of the portable desalination unit deployed on Carson beach and the configuration of the internal parts.

FURTHER READING

- J. Yoon, H. J. Kwon, S. Kang, E. Brack, and J. Han, "Portable Seawater Desalination System for Generating Drinkable Water in Remote Locations," *Environmental Science & Technology*, vol. 56, no. 10, pp. 6733-6743, 2022. https://doi.org/10.1021/acs.est.1c08466.

Nanotechnology, Nanostructures, Nanomaterials

Multifunctional Photonic Janus Particles

Q. He, H. Vijayamohanan, J. Li, T. M. Swager
Sponsorship: Vannevar Bush Faculty Fellowship

Photonic Janus particles with a sphere fused to a cone are created from the phase separation of dendronized brush block copolymers (den-BBCP) and poly(4-vinylpyridine)-*r*-polystyrene (P4VP-*r*-PS) during the solvent evaporation of oil-in-water emulsions. Rapid self-assembly of den-BBCP generates well-ordered lamellar structures stacking along the long axis of the particles, producing structural colors that are dependent on the incident light angle. The colors are tunable over the visible spectrum by varying the molecular weight of den-BBCP. The P4VP-*r*-PS phase can undergo further surface modifications to produce multifunctional photonic Janus particles. Specifically, a real-time magnetic control of the reflected color is achieved by coating the P4VP-*r*-PS phase with citric acid-capped Fe_3O_4 nanoparticles. Charged biomolecules (i.e., antibodies) are electrostatically immobilized to the Fe_3O_4 coating for potential applications in biosensing. As a demonstration, we developed a new photonic sensor for the foodborne pathogen Salmonella with antibody-modified photonic Janus particles, where the angle-dependent structural color plays a key role in the sensing mechanism.

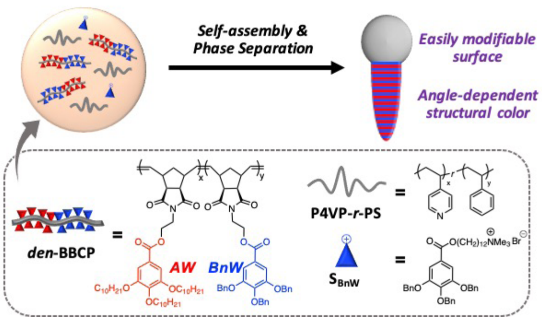

▲Figure 1: Preparation of photonic Janus particles by the phase separation of den-BBCP and P4VP-*r*-PS by the solvent evaporation of dichloromethane emulsions. Self-assembly of den-BBCP produces well-ordered multilayers to produce structural color. The surface of P4VP-*r*-PS phase can undergo further functionalization.

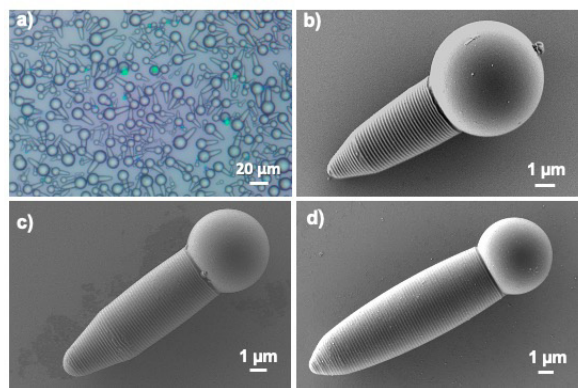

▲Figure 2: Reflected light microscopy and scanning electron microscopy images of photonic Janus particles prepared with different den-$BBCP_{500}$ (M_n = 500 kDa) to P4VP-*r*-PS mass ratios: (a, b) 1:2, (c) 1:1, and (d) 2:1.

FURTHER READING

- Q. He, H. Vijayamohanan, J. Li, and T. M. Swager, "Multifunctional Photonic Janus Particles," *J. Am. Chem. Soc*., vol.144, no. 12, pp. 5661–5667, 2022.

Maskless Fourier Transform Holography Using Structured Light

K. Keskinbora, A. L. Levitan, Y. Yu, R. Comin
Sponsorship: German Research Foundation, Department of Energy

X-ray microscopy emerged as an ideal imaging tool for investigating nanoscale materials and devices with high spatio-temporal resolution. Visualizing the complex textures that underlie the macroscopic behavior of these systems will inform future device design. Advances in the wide availability of powerful graphical processors and high coherence X-ray sources lead to the emergence of new computational coherent imaging methods. However, these coherent imaging methods have many strings attached: some, such as ptychography, are incompatible with ultrafast imaging. Others, such as Fourier transform holography (FTH), which can be used for single-shot ultrafast imaging, are usually limited to preselected regions of interest. This severely limits the applicability of this method to magnetic films with homogeneous textures.

We aimed to develop a new X-ray holographic microscopy method without these limitations for investigating quantum electronic and magnetic solids at the nanoscale. Our technique relies on an X-ray wavefront shaping computer-generated hologram (CGH) to split the incident radiation into reference and sample beams. The reference beam propagates freely while the sample beam traverses the sample and is imprinted with phase information that encodes the sample's internal electronic and magnetic textures, as depicted schematically in Figure 1. A detector then captures the far-field interference pattern from which the sample exit wave is recovered with nanometer spatial resolution. This exit wave reveals the samples' composition, density, and magnetization state. Our approach has several advantages over the conventional FTH: (i) the sample and reference beams are not defined by pre-patterned structures, avoiding the time-consuming sample preparation; (ii) the field of view is not physically anchored to a preselected region, allowing investigation of extended samples; and (iii) the approach is compatible with single-shot, ultra-fast spatiotemporal imaging of dynamics at the nanoscale.

Critically, the method depends on the successful realization of a CGH, synthesized using a double-constraint Gerchberg-Saxton algorithm on MIT's Supercloud cluster. We have utilized a dedicated ion beam lithography tool at MIT.nano to transfer the computer-generated design into a gold-coated silicon nitride membrane with high fidelity to the design file. The resulting diffractive optic (see Figure 2) with a 300-um aperture and 50-nm wide effective outermost zone width was successfully utilized in a recent experiment to demonstrate the first X-ray demonstration of the method. The results of those experiments are currently being analyzed.

Successful further development of the method can have far-reaching applications extending beyond hard condensed matter physics and the study of biological and soft matter through phase-contrast imaging.

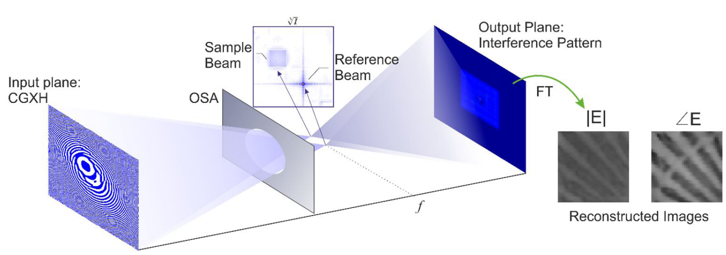

▲ Figure 1: Overview of the experimental setup for a structured illumination X-ray holography experiment. The diffractive optics is the key to the successful realization of the method.

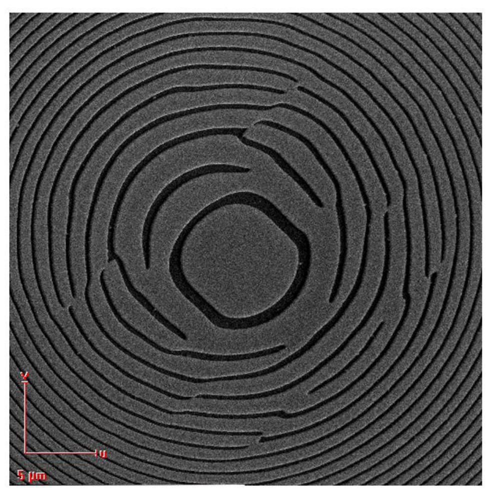

▶ Figure 2: A scanning electron microscope image of the central portion of a computer-generated hologram designed for soft X-rays and fabricated using VELION at MIT.nano.

FURTHER READING

- K. Keskinbora, A. L. Levitan, and R. Comin, "Maskless Fourier Transform Holography," *Opt. Express*, vol. 30, pp. 403-413, 2022.

Impact of 2D-3D Heterointerface on Remote Epitaxial Interaction through Graphene

H. Kim, K. Lu, Y. Liu, H. S. Kum, K. S. Kim, K. Qiao, S. Lee, C. Choi, J. Kim
Sponsorship: DARPA, Department of Energy, U.S. Air Force Research Laboratory

Remote epitaxy has drawn attention as it offers epitaxy of functional materials that can be released from the substrates with atomic precision, thus enabling production and heterointegration of flexible, transferrable, and stackable freestanding single-crystalline membranes. In addition, the remote interaction of atoms and adatoms through two-dimensional (2D) materials in remote epitaxy provides a platform to investigate and utilize electrical/chemical/physical coupling of bulk (3D) materials via 2D materials (3D-2D-3D coupling). Here, we unveil the respective roles and impacts of the substrate material, graphene, substrate-graphene interface, and epitaxial material for electrostatic coupling of these materials, which governs cohesive ordering and can lead to single-crystal epitaxy in the overlying film.

We show that simply coating a graphene layer on wafers does not guarantee successful implementation of remote epitaxy, since atomically precise control of the graphene-coated interface is required, and provide key considerations for maximizing the remote electrostatic interaction between the substrate and adatoms. The experimental study is conducted by exploring various material systems and processing conditions, and we demonstrate that the rules of remote epitaxy vary significantly depending on the ionicity of material systems as well as the graphene-substrate interface and the epitaxy environment. The general rule of thumb discovered provides a cornerstone for expanding 3D material libraries that can be stacked in freestanding form to revolutionize heterogeneous integration.

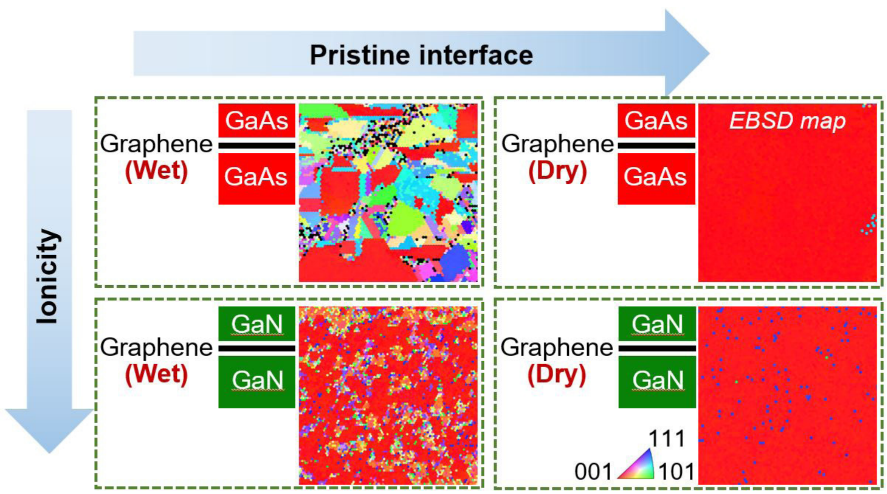

▲ Figure 1: Electron backscatter diffraction (EBSD) maps show better crystal quality in remote epitaxial films when the interface is pristine and the materials have high ionicity.

FURTHER READING

- D. MacNeill, J. T. Hou, D. R. Klein, P. Zhang, P. Jarillo-Herrero, and L. Liu, *Physical Review Letters*, vol. 123, p. 047204, 2019.

Scale Two-dimensional Perovskite with Unity Photoluminescence Quantum Yield

D. Lee, K. Kim, Y. Li, Y. Yu, B. Xu, J. Kim
Sponsorship: Southern University of Science and Technology

Two-dimensional (2D) materials with high photoluminescence quantum yield (PLQY) and broad ranges of bandgap are essential for high performance 2D optoelectronic applications. Even though transition metal dichalcogenides (TMDCs) have been mainstream in 2D material community, their bandgap ranges from 1.5ev to 2eV and cannot cover wide bandgap applications above 2.0eV. In addition, the best PLQY value has been ~95% with chemically doped MoS2, and its lateral dimension has been limited to hundreds of micrometers.

In this regard, 2D organic-inorganic hybrid perovskite (PVSK) has been studied extensively because of its tunable band gap up to 3eV by adjusting organic cations and halide anions. However, achieving high PLQY and isolating bulk 2D PVSK crystal into monolayers in centimeter scale are still challenging.

In this work, we successfully synthesized high-quality single-crystalline 2D PVSK with the world's best PLQY (~99.3%) and isolated them into atomic-scale thickness via a layer-resolved splitting (LRS) process. With the astonishing achievements, the tunable bandgap of 2D PVSK up to 3eV will expand the applications of 2D materials, and device performance would be further improved thanks to its unity PLQY.

Scalable Microfabrication of Microtextured Omniphobic Surface

S. Kim, S.-H. Nam, Y. T. Cho, N. X. Fang
Sponsorship: Ministry of Trade, Industry & Energy (MOTIE, Korea), National Research Foundation (NRF) of Korea

In this joint research between Changwon National University (Korea) and the Fang group at MIT, we explore scalable microfabrication of 2D patterns and 3D shapes–and arrangements of those patterns into different shapes–with potential to control surface wetting and adhesion by tailored microtextures. One of the interesting phenomena is the "rose petal" effect, in which a hydrophilic material macroscopically behaves in a hydrophobic manner if its surface contains the suitable microstructural features. This Rose petal effect produces an effective design for self-cleaning, anti-sticking, oil/water separation, microreactors, and droplet manipulation. As an example, particle aggregation was directionally controlled using contact line dynamics (pinned or slipping) and geometrical gradients on microstructured surfaces by the systematic investigation of the evaporation process on sessile droplets and sprayed microdroplets laden with virus-simulant nanoparticles. We demonstrated the potentials of an engineered microcavity surface to limit the contact transfer of particle aggregates deposited with the evaporation of microdroplets by 93% for hexagonal microwalls and by 96% for inverted pyramidal microwalls. The particle capture potential of the interconnected microstructures was also investigated using biological particles, including adenoviruses and lung-derived extracellular vesicles.

As a continuation of this work, we aim to (1) develop micro-nano surface engineering based on the imprint process and additive manufacturing; (2) fabricate and characterize practical devices for implementing a bio-inspired functional surface (see Figures 1 and 2 from Fang et al.); and (3) employ a prototype in biological, health, energy, and environmental applications. The successful implementation of this work will present effective and practical ways to improve public health and personal hygiene.

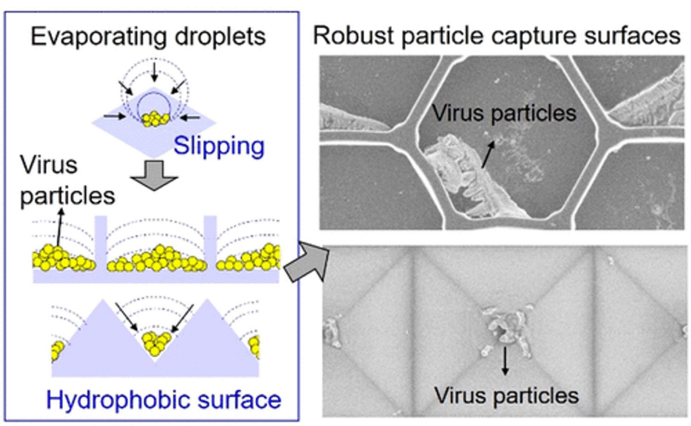

▲Figure 1: Robust particle capture surfaces via ultraviolet imprint.

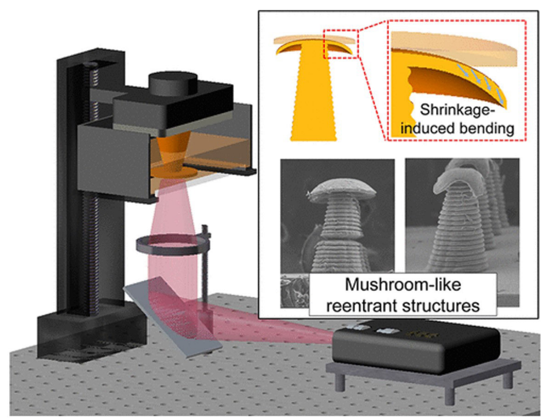

▲Figure 2: 3D printed shape-deformed microstructure exhibits a liquid repellency without perfluorianated coating.

FURTHER READING

- S. Kim, W. Y. Kim, S.-H. Nam, S. Shin, S. H. Choi, D. H. Kim, H. Lee, H. J. Choi, E. Lee, J.-H. Park, I. Jo, N. X. Fang, and Y. T. Cho et al., "Microstructured Surfaces for Reducing Chances of Fomite Transmission via Virus-Containing Respiratory Droplets," *ACS Nano*, vol. 15, no. 9, pp. 14049-14060, August 2021, https://doi.org/10.1021/acsnano.1c01636.
- D. H. Kim, S. Kim, S. R. Park, N. X. Fang, and Y. T. Cho et al., "Shape-Deformed Mushroom-like Reentrant Structures for Robust Liquid-Repellent Surfaces," *ACS Appl. Mater. Interfaces*, vol. 13, pp. 33618-33626, July 2021, https://doi.org/10.1021/acsami.1c06286.

Exciton-phonon Coupling in 2D Silver Phenyl Selenolate Revealed by Impulsive Vibrational Spectroscopy

E. R. Powers*, W. Paritmongkol*, D. C. Yost, W. S. Lee, J. C. Grossman, W. A. Tisdale
*Authors contributed equally
Sponsorship: National Defense Science and Engineering Graduate Fellowship

Semiconductor nanomaterials have the potential to be employed in next-generation optoelectronic devices that exhibit significantly improved performance at reduced cost. Two-dimensional metal-organic chalcogenolates (MOCs) are a newly discovered class of nanomaterials that combine many of the best properties of TMDs transition metal dichalcogenides and 2D perovskites, two more established 2D semiconductor families. Silver phenyl selenolate (AgSePh) is the prototypical example, a hybrid organic-inorganic material comprised of 2D sheets that exhibit a narrow bandwidth 467-nm blue emission and 2D in-plane exciton anisotropy. Additionally, crystalline AgSePh is easy to synthesize and stable under ambient conditions. Owing to these advantages, MOCs may be useful in applications like light-emitting diodes or photodetectors.

While early studies are promising, the underlying physics of AgSePh has not been fully explored. In this work, we employ impulsive vibrational spectroscopy (IVS) to investigate the degree of exciton-phonon coupling in AgSePh. Using this time-domain Raman method, we resolve multiple coherent vibrational signatures, suggesting strong exciton-phonon coupling in this material. Molecular dynamics (MD) and dDensity functional theory simulations are also performed to calculate a phonon density of states for AgSePh. A comparison of experimental and simulation results allows us to visualize the structural displacements that occur as a result of the vibrational modes identified with IVS. From these data, we make conclusions about why certain vibrational modes are electronically coupled while others are not.

These results are also compared to low frequency Raman and temperature-dependent photoluminescence data, corroborating the previous findings and improving our understanding of the vibrational landscape of the AgSePh system. Finally, temperature-dependent IVS studies of the vibrational mode frequencies and lifetimes are performed from 5K to 300K, revealing information about mode anharmonicity and phonon scattering processes.

These results present a convincing picture of strong electronic-vibrational interactions in 2D hybrid AgSePh. Our work provides insight into the underlying structural and electronic properties of AgSePh and other MOCs, which will help to inform future development of new structures and syntheses that can control exciton-phonon coupling and further expand the capabilities and applications of this new material family.

FURTHER READING

- W. Paritmongkol, T. Sakurada, W. S. Lee, R. Wan, P. Muller, and W. A. Tisdale, "Size and Quality Enhancement of 2D Semiconducting Metal-Organic Chalcogenolates by Amine Addition," *Journal of the American Chemical Society*, vol. 143, pp. 20256-20263, Nov. 2021.

Interface Energies of Metallic Nanoislands on Suspended 2D Materials

K. Reidy, J. D. Thomsen, B. Wang, F. M. Ross
Sponsorship: MIT Energy Initiative, Mathworks Engineering

A thorough understanding of the processing and properties of metal deposition on two-dimensional (2D) materials is crucial for tailoring the performance of solid-state devices that incorporate 2D materials. For example, the kinetics of metal deposition on 2D materials, including nucleation, epitaxy, and morphology, strongly influences 2D/3D device properties such as contact resistance, optical response, and high-frequency electrical performance. In particular, the interface energy between the metal and 2D material is an important parameter which determines the nanoislands' shape and resulting catalytic properties, plasmonic behavior, and excitonic coupling of the heterostructure.

Here, we determine the interface energies of single crystalline Au nanoislands with well-defined facetted morphologies grown epitaxially on suspended 2D materials. Focusing initially on Au deposited on MoS_2, we investigate quasi-van der Waals epitaxial growth of compact Au triangles ~20 nm in lateral size, flat topped, and 4-8 nm tall (Figures 1a,b). These nanoisland shapes are consistent with the equilibrium Winterbottom shape of Au on MoS_2, which is bounded by {111}, {110}, and {100} facets. A combination of cross-sectional and plan view transmission electron microscopy (TEM) imaging shown in Figures 1a,b allows us to measure the nanoislands' shape in three dimensions and estimate an interface energy of MoS_2/Au as 0.14-0.18 J/m² through thermodynamic modelling. We then compare these results to Au deposited on graphene, which exhibits more pointed corners due to an Au{111} surface reconstruction (Figure 1c). This leads to a Gr/Au interface energy of ~ 0.07 – 0.14 J/m2, slightly lower than that calculated for the MoS_2/Au system. This difference may be expected due to the difference in strength between Au-C vs. Au-S bonding. The structure and energetics of these quasi-van der Waals interfaces will open opportunities for novel mixed dimensional 2D/3D nanodevices and improve metal integration in current 2D devices.

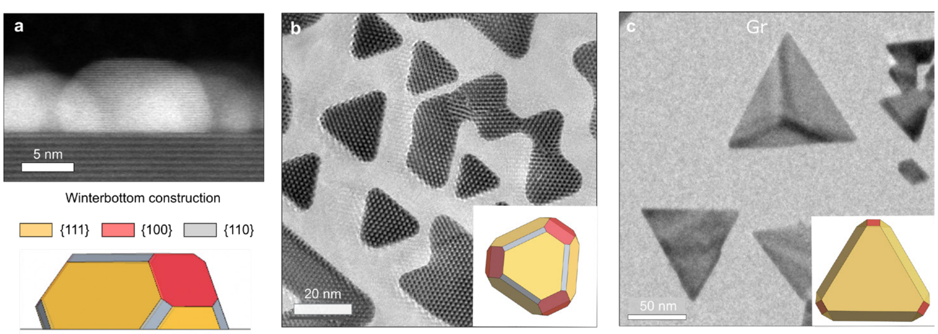

▲ Figure 1: a) Atomic resolution cross-sectional scanning TEM image showing MoS_2/Au island shape (top) and side view of corresponding Winterbottom construction (bottom). b) Plan-view TEM of triangular Au nanoislands on clean suspended MoS_2. Inset show theoretical Winterbottom construction. c) Plan-view TEM of triangular Au nanoislands on clean suspended Gr. Inset show theoretical Winterbottom construction with Au(111) surface energy reduction by 0.15 J/m² to account for surface reconstruction

FURTHER READING

- K. Reidy*, G. Varnavides*, J. D. Thomsen, A. Kumar, T. Pham, A. M. Blackburn, P. Anikeeva, P. Narang, J. M. LeBeau, and F. M. Ross, "Direct Imaging and Electronic Structure Modulation of Moiré Superlattices at the 2D/3D Interface," *Nat Comm*., vol. 12, p. 1290, 2021.
- K. Reidy, J. D. Thomsen, H. Y. Lee, V. Zarubin, Y. Yu, B. Wang, T. Pham, and F. M. Ross, "Quasi-van der Waals Epitaxy of 3D Metallic Nanoislands on Suspended 2D Materials," 2022.

Robotic Synthesis and Testing of Nanocatalysts

Z. Ren, A. Abdelhafiz, Z. Zhang, J. Li
Sponsorship: Honda Research Institute USA

Research solutions aiming to replace existing hydrocarbon fuel technologies with green energy sources have only partially succeeded. Proton-exchange membrane fuel cells (PEMFC) are a very promising candidate for their light weight and high energy density, while catalysts used in the cell electrode limit its performance and durability. Recent studies show that synergistic effects of multiple metals alloyed together yield a material even better than noble metal catalysts. Yet such a very well controlled and precise synthesis of more than tri-metallic nanoparticles is extremely challenging by conventional synthesis techniques at normal/ambient conditions, which thermodynamic rules dictate. Ultrafast Joule heating technique is a promising tool to leverage kinetic rules to form meta-stable high entropy alloys by heating and cooling samples within one second. This extremely fast process makes it practical to make the workflow in a high-throughput manner.

The high throughput system consists of a liquid handler, a carbothermal shock setup, and a robotic testing platform. The liquid handling robot allows us to precisely control the composition of each sample, specifically, the ratio between each metal precursor solution (Figure 1a). Carbothermal shock (Figure 1b) is enabled by conducting a large current (>10 A) to a precursor loaded carbon substrate, which can reach above 2000 K within hundreds of milliseconds. Once the carbon strips are prepared via shocking, a rapid evaluation will be conducted, also in a high-throughput manner. Samples will be cut into pieces and loaded onto testing holders; a robotic arm will load and unload samples to the electrocatalytic testing beaker. Testing software is automated using python scripts, data extraction, and a structured query language (SQL) storage process (Figure 1d). Finally, an active learning step analyzes the dataset using Bayesian optimization to generate the suggestion for the next batch of recipes, based on the surrogate model fitted by the Gaussian process. The newly suggested task will be sent to the liquid handler in Figure 1a, forming a closed-feedback optimization loop. Such a high-throughput and autonomous optimization system will greatly enhance the efficiency of finding new high entropy alloy recipes for electrocatalyst application.

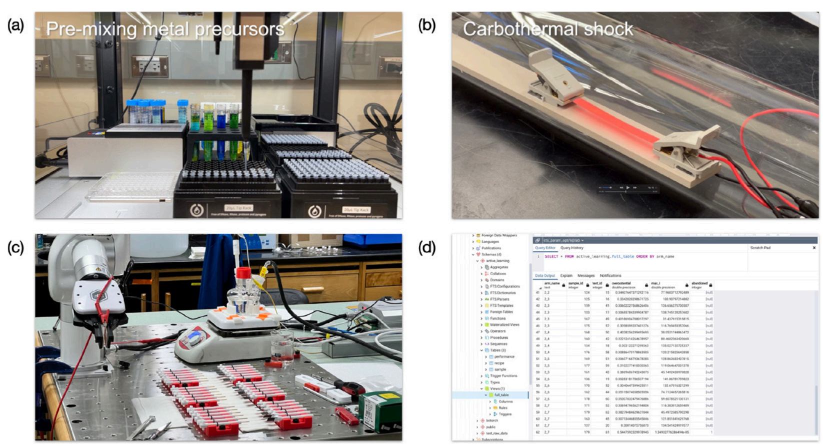

▲ Figure (1a) Liquid handler capable of preparing 72 samples in a batch, (1b) carbothermal shock process that can transform metal precursor to high-entropy alloys within 1 sec, (1c) robotic testing capable of evaluating 36 samples in a batch, (1d) dataset stored on a SQL server that can be read by active learning algorithm.

FURTHER READING

- Z. Ren, "Robotic Synthesis and Testing of Nanocatalysts" [Online]. Available: https://youtu.be/WOQj_EJekoo (Apr. 2022).
- Z. Ren, "Liquid Handling Robot with 3D Printed Pipette Handler," [Online]. Available: https://youtu.be/ScDYSUFRFZ0 (Sept. 2020).
- K. Li, and W. Chen. "Recent Progress in High-entropy Alloys for Catalysts: Synthesis, Applications, and Prospects." *Materials Today Energy*, vol. 20, pp. 100638, Jun. 2021.

Wet-based Digital Etching for High Aspect-ratio GaN Vertical Nanostructures

P.-C. Shih, T. Palacios, in collaboration with G. Rughoobur, A. I. Akinwande
Sponsorship: U.S. Air Force Office of Scientific Research through MURI Empty State Electronics Project

III-Nitrides have been studied and used for high-frequency and power electronics thanks to their excellent material properties. However, there are still challenges for their use in some applications, such as micro-light-emitting diodes, field emitters, and other vertical devices. Traditionally, high-aspect-ratio III-Nitride nanostructures are fabricated by two-step etchings combining (1) plasma dry etching and (b) wet-chemical orientation-dependent etching. Heated tetramethylammonium hydroxide (TMAH) or KOH-based chemicals are usually used for obtaining vertical sidewalls; however, the process yield and variation can be difficult to control due to defects in materials and plasma damage.

GaN vertical sidewalls formed by dry etching have been demonstrated in literature; however, demonstrations of sub-50-nm high-aspect-ratio nanostructures are still limited. In this work, a wet-based digital etching technology is combined with an optimized plasma dry etching for high-aspect-ratio GaN vertical fins and nanowires (NWs). The vertical sidewalls of GaN vertical structures can be obtained by the optimized dry etching, and the width of these vertical structures can be shrunk by the subsequent wet-based digital etching. Vertical fin and NW arrays with sub-40-nm width and a > 10:1 aspect ratio are demonstrated with good uniformity and reproductivity (Figure 1). These developed technologies can be applied for different devices, such as vertical power fin field-effect transistors (FinFETs), NW FETs, micro-LEDs, and lateral FinFETs, with sub-50-nm dimensions and high aspect ratios in the future.

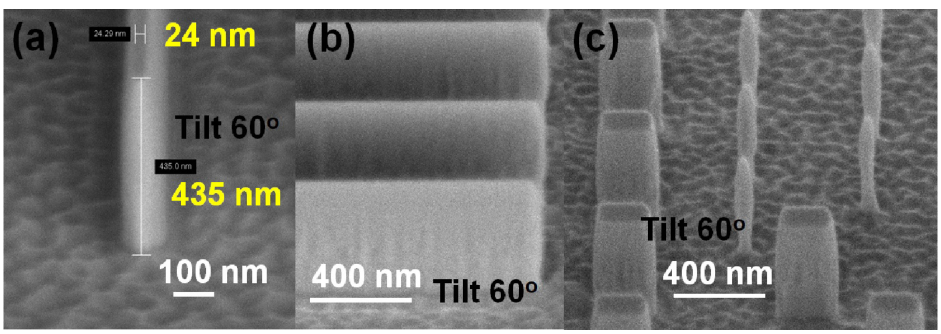

▲ Figure 1: Tilted scanning electron microscope (SEM) images of (a) a GaN vertical fin, (b) fins' sidewalls, and (c) GaN nanowires with >10:1 aspect-ratio after digital etching. The aspect ratio of GaN fin can be close to 20:1 with this approach.

FURTHER READING

- P.-C. Shih, G. Rughoobur, K. Cheng, A. I. Akinwande, and T. Palacios, "Self-Align-Gated GaN Field Emitter Arrays Sharpened by a Digital Etching Process," *IEEE Electron Device Letters*, vol. 42, no. 3, pp. 422-425, Mar. 2021.
- P.-C. Shih, Z. Engel, H. Ahmad, W. A. Doolittle, and T. Palacios, "Wet-based Digital Etching on GaN and AlGaN," *Applied Physics Letters*, vol. 120, p. 022101, 2022.

Chip-less Wireless Electronic Skins Enabled by Epitaxial Freestanding Compound Semiconductors

Y. Kim, J. M. Suh, Y. Liu, J. Shin, J. Kim
Sponsorship: Amore Pacific

Electronic skin (e-skin) has been developed with a goal to obtain a non-invasive human health monitoring electronic system with its imperceptibility. So far, one of the major shortcomings in this field is the bulky wireless communication system that severely affects its wearability (Figure 1). In this paper, we introduce a single-crystalline non-Si-based e-skin system where fully conformable, ultrathin, piezoelectric, compound semiconductor membranes are incorporated as power-efficient wireless communication modules and extremely high sensitivity sensors without needing for bulky chips and batteries. The developed GaN surface acoustic wave-based device successfully measured wirelessly three different inputs including strain, ultraviolet light, and ion concentrations (Figure 2). The consistency and accuracy of the measured heart rate and pulse waveforms over a 7-day period, during which the e-skin was re-attached 7 times, strongly demonstrate the reusability and long-term wearability of our device. This study will change the paradigm of e-skins by providing versatile wireless platforms for fully imperceptible e-skins with very high sensitivity and low power consumption.

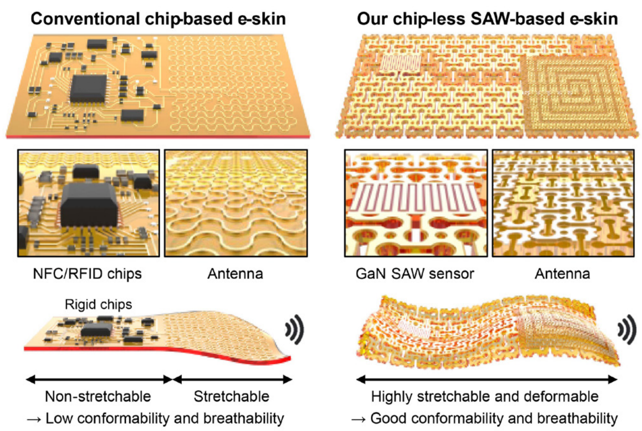

▲ Figure 1: Comparison between (left) conventional wireless e-skin based on integrated circuit chips and (right) our chip-less wireless e-skin based on surface acoustic wave (SAW) devices made of GaN freestanding membranes.

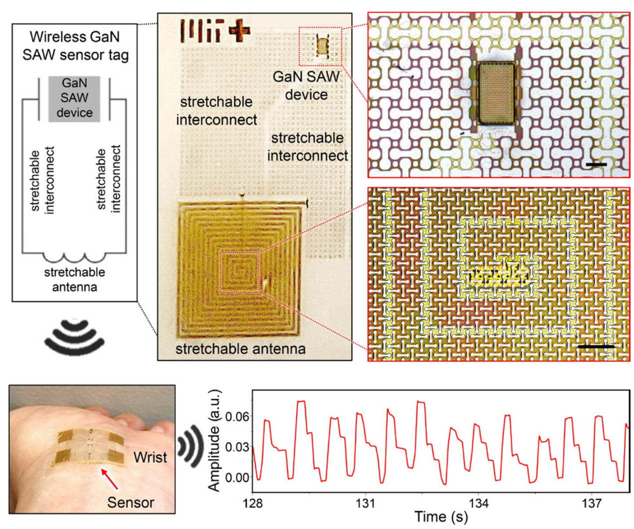

▶ Figure 2: Schematic and optical images of our wireless GaN SAW e-skin strain sensor and wireless pulse measurements using our GaN SAW e-skin strain sensors. Scale bars indicate 200 μm.

FURTHER READING

- H. Yeon, H. Lee, Y. Kim, D. Lee, Y. Lee, J.-S. Lee, J. Shin, C. Choi, et al., "Long-term Reliable Physical Health Monitoring by Sweat Pore–inspired Perforated Electronic Skins," *Sci. Adv.*, vol. 7, no. 27, eabg.8459, Jun. 2021.
- Y. Kim, S. S. Cruz, K. Lee, B. O. Alawode, C. Choi, Y. Song, J. M. Johnson, C. Heidelberger, et al., "Remote Epitaxy Through Graphene Enables Two-Dimensional Material-based Layer Transfer," *Nature*, vol. 544, pp. 340-343, Apr. 2017.
- H. S. Kum, H. Lee, S. Kim, S. Lindemann, W. Kong, K. Qiao, P. Chen, J. Irwin, et al., "Heterogeneous Integration of Single Crystalline Complex-oxide Membranes," *Nature*, vol. 578, pp. 75-81, Feb. 2020.

Fully 3D-Printed Electronics via Multi-Material Microsputtering

Y. S. Kornbluth, L. Parameswaran, R. Mathews, L. M. Racz, L. F. Velásquez-García
Sponsorship: Kansas City National Security Center

Integrated circuits (ICs) are made in multibillion-dollar foundries, involving extreme processing conditions. To attain low per-chip cost, many identical IC chips are batch processed. Lower volume electronics are manufactured at a low cost using printed circuit boards, where premade components, often made in a foundry, are soldered onto a dielectric plate with an arrangement of thin film conductive traces and a set of drilled vias. However, currently, there is no cost-effective approach to make a small batch of ICs, conduct chip-to-chip customization, or rework ICs.

In this project, we are harnessing microsplasma sputtering (i.e., the sputtering of materials at atmospheric pressure using reactors with characteristic length below millimeters) to develop a manufacturing platform for agile manufacturing of ICs. We recently reported the first fully additively manufactured capacitors as a proof-of-concept demonstration of such multi-material microplasma sputtering manufacturing platform. This is also the first demonstration of a cleanroom-quality, multi-material electrical device produced entirely through additive manufacturing. The conductive films are created by sputtering gold in air, attaining near-bulk electrical conductivity. The dielectric films are created by sputtering aluminum in a gas blend of argon and air, resulting in alumina films (Figure 1). The frequency response of the capacitor is described by the universal dielectric response typically found in heterogenous dielectrics and suggests the presence of condensed water in the pores of the alumina film. Future work could entail extending the platform to other transducing materials, e.g., semiconductors.

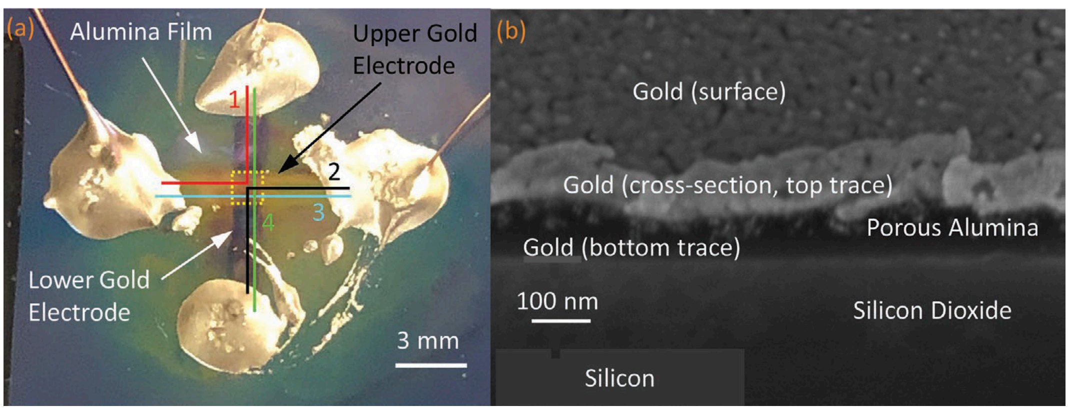

▲ Figure 1: (a) Photograph of a fully microsputtered capacitor composed of two perpendicular gold lines separated by a thin alumina film. (b) SScanning electron Emicroscope (SEM)M cross-section of microplasma-printed capacitor; the gold films are 50 nm thick, while the alumina film is 35 nm thick. From Y. Kornbluth et al., Advanced Materials Technologies (2022).

FURTHER READING

- Y. Kornbluth, R. H. Mathews, L. Parameswaran, L. Racz, and L. F. Velásquez-García, "Fully 3D-printed, Ultrathin Capacitors via Multi-material Microsputtering," *Advanced Materials Technologies*, to be published, 2022.
- Y. Kornbluth, R. H. Mathews, L. Parameswaran, L. Racz, and L. F. Velásquez-García, "Nano-additively Manufactured Gold Thin Films with High Adhesion and Near-bulk Electrical Resistivity via Jet-assisted, Nanoparticle-dominated, Room-temperature Microsputtering," *Additive Manufacturing*, vol. 36, p. 101679, Dec. 2020.
- Y. Kornbluth, R. H. Mathews, L. Parameswaran, L. Racz, and L. F. Velásquez-García, "Room-temperature, Atmospheric-pressure Deposition of Dense, Nanostructured Metal Films via Microsputtering," *Nanotechnology*, vol. 30, no. 28, p. 285602, Jul. 2019.

Implosion Fabrication of Vacant Structures for Nanophotonic Applications

Q. Yang†, G. Yang†, C. Zheng, T. Nambara, Y. Kunai, A. C. Matlock, H. Kusaka, D. Wadduwage, P. T. C. So, E. S. Boyden
†These authors contributed equally to this work.
Sponsorship: Fujikura

Implosion fabrication (ImpFab) is an emerging nanofabrication strategy that allows complex free-form 3D architectures to be crafted with nanometer precision while being compatible with a wide range of organic and inorganic materials. In ImpFab, a hydrogel is photopatterned with a multiphoton laser, chemicals, and nanoparticles attached to the photopatterned sites; the sample is then shrunk to yield nanoprecise features. Such a method presents a strong potential for applications in nanophotonics, where the refractive index (RI) difference between a structure and its environment is critical. Volumetric deposition of high RI nanoparticles is a promising direction; conversely, volumetric ablation/removal to generate RI differences between the hydrogel matrix and inner vacant structures is another possible way.

We have achieved high-resolution vacant structures appears in Figure 1a. The fabrication procedure begins with soaking the hydrogel scaffold matrix in dye solution, followed by the two-photon patterning and shrinking process, to generate high-density and high-resolution vacant structures in the scaffold. The "C-type" vacant structure array in Figure 1b demonstrates the capability of ImpFab to achieve complex architectures for potential nanophotonic application. The RI difference is essential; measurement results by holotomography microscopy appear in Figure 1c. RI difference between the scaffold and the $CaCl_2$ solution is ~ 0.03.

One promising photonic application of the proposed technology is an optical computing device. Such a device can achieve all-optical inference/prediction, which is considered much faster than traditional electron-based computing. To prove the concept, our first design appears in Figure 2a. The fluorescent image of the structure appears in Figure 2b. Tuning the thickness of each vacant structure can control the phase change. Figure 2c shows a grating structure with vacant structures at a thickness of ~ 4.4 µm, which presents a 0.3 π phase change when measured.

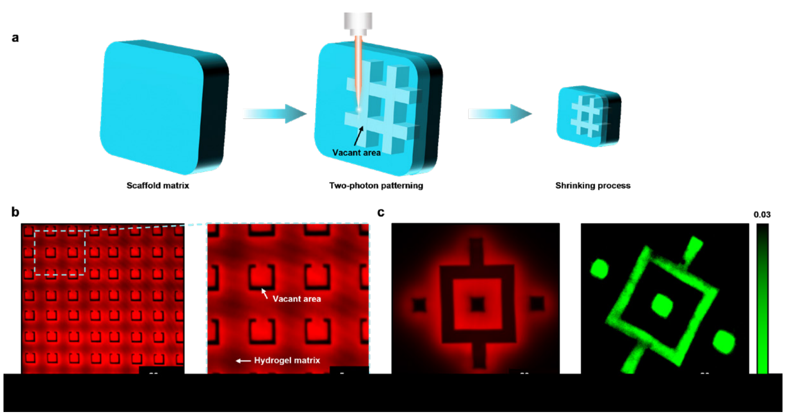

◀Figure 1: 3D vacant structures by ImpFab. a) ImpFab constructs vacant structures. b) Complex vacant structure array with nine-fold shrinkage. c) Holotomography microscopic measurement of the RI difference.

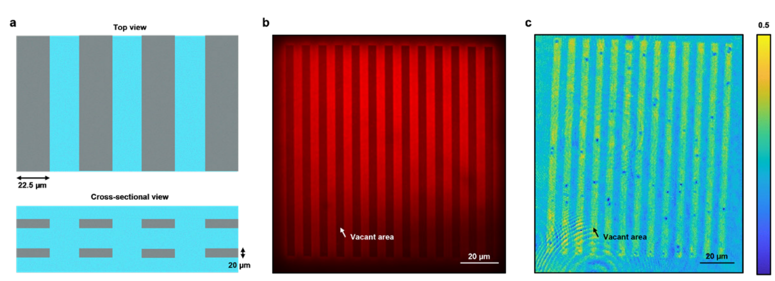

◀Figure 2: Grating structures for optical computing devices. a) Top and cross-sectional views of grating designs. b) A fluorescent image of the grating pattern. c) Phase difference measurement presents ~ 0.3 π change between the vacant structure and the scaffold.

FURTHER READING

- D. Oran, S. G. Rodriqus, R. Gao, S. Asano, M. A. Skylar-Scott, F. Chen, P. W. Tillberg, A. H. Marblestone, and E. S. Boyden, "3D Nanofabrication by Volumetric Deposition and Controlled Shrinkage of Patterned Scaffolds," *Science*, vol. 362, pp. 1281-1285, Dec. 2018.

3D Nanofabrication of Multi-materials by Diversified Fluorescent Microprinting and Volumetric Deposition

G. Yang, Q. Yang, C. Zheng, D. Oran, E. S. Boyden
Sponsorship: Fujikura and International Relations and Security Network (ISN-5-PPA-02)

Multi-material (MM) 3D printing, which enables production of highly functional structures by integrating MMs, has attracted attention, and a variety of fabrication methods have been developed. Most 3D printing approaches so far, however, require complex equipment, and the printed structures are limited in accuracy and resolution. Unlike the conventional approaches, we developed an advanced MM 3D patterning method for high-speed and high-accuracy construction of nanoscale structures. By utilizing photo-activatable chromophores and varied multiphoton laser powers, we combine different chromophores into a polyacrylate hydrogel in predetermined locations and combinations. After selective deposition of different materials to the patterned chromophore regions, the hydrogel is lineally shrunk to generate an MM 3D nanostructure.

As Figure 1 shows, increasing laser intensity achieves three chromophores with different fluorescent profiles, making it feasible to selectively activate one chromophore at a time. After that, a 3D multi-pattern was generated, in the absence of a complex microfluidic system or mechanical control. Moreover, this method could keep the sample static in the whole process and thus lead to high printing accuracy. Figure 2 demonstrates fabrication of an MM structure in a step-by-step manner. After the multi-patterning process, different molecules or nanoparticles were selectively deposited one by one. In this nanoscale "MIT" logo, each single letter was patterned with one chromophore and deposited with different materials: the letter "M" was filled with silver and gold, "I" with cadmium telluride, and "T" with carbon nanotubes. Next, we plan to fabricate 3D metastructures and electrical components in nanoscale (shown in Figure 3), which might be used for optical or optoelectronic devices.

With regard to applications, we expect our new nanofabrication of MMs with complex, non-self-supporting 3D geometries to substantially broaden the applicability of nanoscale photonic devices, nanoelectronics, biosensors, diffractive optical elements, holograms, and multi-functional lenses.

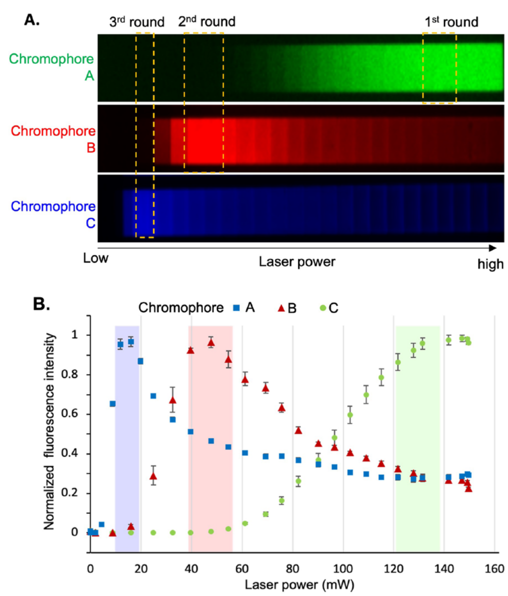

▲Figure 1: A) Fluorescent images of linear gradient patterns of chromophores generated by varied two-photon laser power. B) Corresponding fluorescent intensity of patterned chromophores activated by varied laser power.

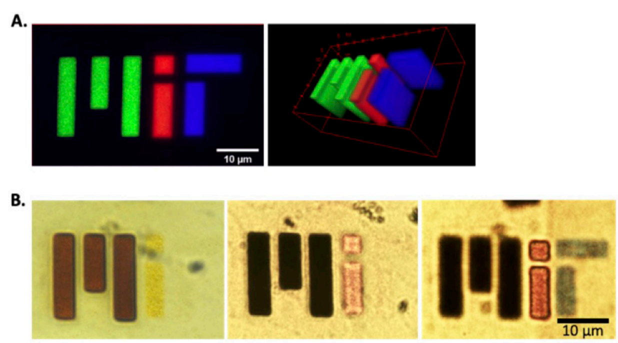

▲Figure 2: A) Fluorescent images of multi-patterned MIT logo; B) Bright field images of selective deposition of different materials in each step.

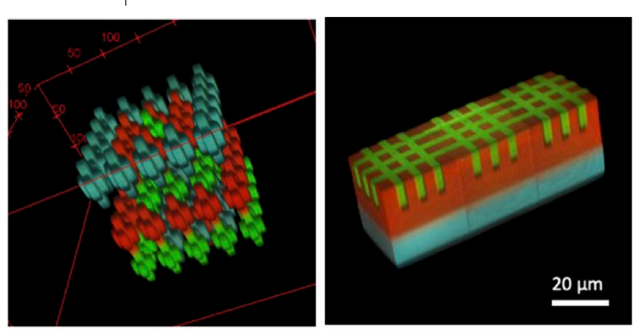

▲Figure 3: Fluorescent images of 3D demos of metastructure (left) and electrical components (right).

FURTHER READING

- D. Oran, S. G. Rodriqus, R. Gao, S. Asano, M. A. Skylar-Scott, F. Chen, P. W. Tillberg, A. H. Marblestone, and E. S. Boyden, "3D Nanofabrication by Volumetric Deposition and Controlled Shrinkage of Patterned Scaffolds," *Science*, vol. 362, pp. 1281-1285, Dec. 2018.

Controlled Synthesis of Large 2D Ultrathin SnSe Crystals with In-plane Ferroelectricity

T. Zhang, M. Chiu, N. Mao, X. Ji, J. Kong
Sponsorship: Army Research Office MURI (W911NF-18-1-0432), NSF Science and Technology Center for Integrated Quantum Materials (DMR-1231319)

Tin selenide (SnSe) is an emerging member of two-dimensional (2D) layered materials with many intriguing properties, such as excellent thermoelectric performance, purely in-plane ferroelectricity, large piezoelectric coefficients, and strong non-linear optical responses. Moreover, as a semiconducting material that is structurally analogous to layered black phosphorus, a rising star for next-generation nanoelectronics, 2D SnSe is anticipated to possess attractive electronic and optoelectronic properties, such as thickness-dependent bandgap and high photoresponse. In this context, to facilitate the exploration of functional properties and applications of 2D SnSe, it is crucial to develop controllable synthesis routes that yield large-area, ultrathin, and high-quality SnSe crystals.

In this work, we demonstrate the growth of 2D SnSe crystals on mica via a low-pressure physical vapor deposition (PVD) method (Figure 1); the crystals display in-plane ferroelectricity that is confirmed using polarization-dependent reflectivity spectroscopy. Effects of substrate pre-annealing, temperature, pressure, and growth time on the lateral size and thickness of as-grown SnSe are further systematically studied, enabling us to rationally optimize the growth parameters to obtain large ultrathin SnSe. Growth temperature and pressure are identified as crucial factors for tuning the ultimate size and thickness of SnSe crystals because they can largely affect the precursor evaporation, diffusion, and deposition processes. Besides, we find that air-annealing of mica at 400 oC before the growth process can lead to SnSe crystals with increased lateral sizes. Under optimized growth conditions, 2D SnSe crystals with lateral size up to ~23.0 μm and controllable thicknesses down to ~2.0 nm (3-4 layers) are achieved. Our work takes a significant step forward on the large-scale controllable synthesis of 2D SnSe, facilitating the investigation of its thickness-dependent properties and related applications.

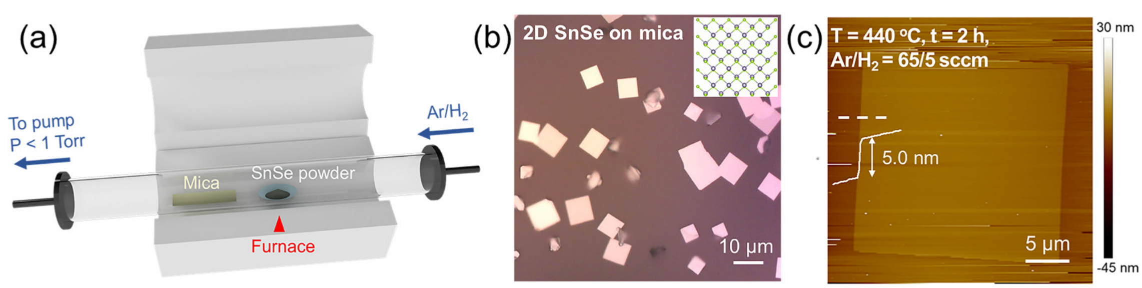

▲ Figure 1: Controlled synthesis of 2D SnSe crystals. (a) Schematic illustration of low-pressure PVD setup for SnSe synthesis. (b) Typical optical microscopy image of as-synthesized SnSe crystals on mica. (Inset: top view of the crystal structure of orthorhombic SnSe). (c) Optimized growth conditions for synthesizing large-sized ultrathin SnSe crystals (5.0 nm thin with a lateral size of 23.0 μm) and a corresponding atomic force microscopy image.

Low-temperature Synthesis of Monolayer MoS_2 on 200-mm Silicon Platform

J. Zhu, J.-H. Park, M. Mohamed, T. Zhang, M. Xue, J. Kong, T. Palacios
Sponsorship: Ericsson, Semiconductor Research Corporation (SRC)

The emerging 2D materials have attracted great attention in the past decade and are being considered as promising candidates for the next-generation heterogeneous electronic and photonic systems. There have also been many demonstrations of wafer-scale synthesis, e.g., 2-inch or 4-inch, of monolayer MoS2. However, these chemical vapor deposition (CVD) or metal-organic chemical vapor deposition (MOCVD) methods require high growth temperature (> 600°C), which is not compatible with silicon back-end-of-line (BEOL) integration unless an additional wafer-scale transfer process is used. This makes the heterogenous integration of 2D materials and silicon very difficult.

In this work, we demonstrate, for the first time, 8-inch MoS2 monolayer thin film grown at 250°C by the MOCVD method. The short growth time (40-70 mins), in combination with the low thermal budget, allows direct silicon BEOL- compatible integration without any transfer process. The synthesized MoS2 demonstrates good wafer-level uniformity (Figure 1) and does not degrade the silicon transistors underneath (Figure 2). This novel low-temperature synthesis method paves the way for heterogenous integration of 2D materials with silicon circuits, allowing the higher-density integration needed in the next-generation of electronics, e.g., Internet-of-Things applications.

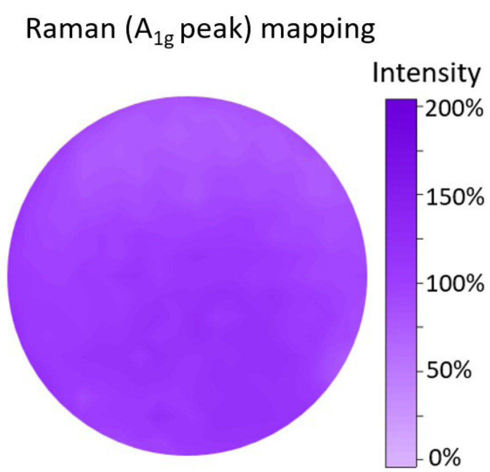

▲Figure 1: Measured Raman mapping (A1g peak) over the 8-inch wafer. Excellent material uniformity can be observed.

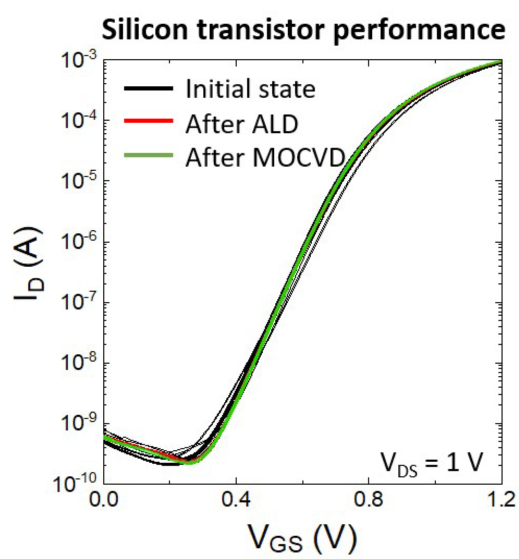

▲Figure 2: Measured transfer characteristics of: (black lines) 10 as-fabricated silicon transistors, (red line) 1 silicon transistor after depositing 20-nm Al2O3 by using a commercial ALD (250°C, 57 min.) and (green line) 1 silicon transistor after depositing monolayer MoS2 thin film using our new MOCVD growth process (250°C, 60 min.).

FURTHER READING

- H. Wang, L. Yu, Y.-H. Lee, Y. Shi, A. Hsu, M. L. Chin, L.-J. Li, M. Dubey, J. Kong, and T. Palacios, “Integrated Circuits Based on Bilayer MoS2 Transistors,” *Nano Letters*, vol. 12, pp. 4674-4680, 2012.
- L. Yu, D, El-Damak, U. Radhakrishna, X. Ling, A. Zubair, Y. Lin, Y. Zhang, M.-H. Chuang, Y.-H. Lee, D. Antoniadis, J. Kong, A. Chandrakasan, and T. Palacios, “Design, Modeling, and Fabrication of Chemical Vapor Deposition Grown MoS2 Circuits with E-Mode FETs for Large-Area Electronics,” *Nano Letters*, vol. 16, pp. 6349-6356, 2016.
- M.-Y. Li, S.-K. Su, H.-S. P. Wong, and L.-J. Li, “How 2D Semiconductors Could Extend Moore’s Law,” *Nature*, vol. 567, pp. 169-170, 2019.

Carbon Nanotube Nano-contacts for MoS_2 Transistors

J. Zhu, Y. Guo, E. Shi, J.-H. Park, J. Kong, T. Palacios
Sponsorship: Institute of Soldier Nanotechnologies (ISN)

With the scaling of electronic devices, the contact length is also shrinking rapidly and is about 20 nm in the most advanced silicon technology nodes. Further scaling of contact length will be difficult as the electron scattering from the grain boundaries and sidewalls of the metal contacts will be more and more significant, increasing the resistance of the metal contacts and also degrading the contact quality. Carbon nanotubes (CNTs), however, possess smooth surfaces and nanometer-scale diameter and avoid grain boundary scattering thanks to their long aspect ratio. All these properties make CNTs promising candidates for future nanoscale contacts.

In this work, we demonstrate, for the first time, MoS_2 transistors with CNT bundles as the source/drain contacts. By using super-aligned CNT bundles, we fabricated a high-density 8x8 array of MoS_2 transistors with single device area of ~ 0.06 µm2 (Figure 1). The clean van der Waals interface between CNTs and MoS_2 allows the CNT bundles to demonstrate a very low contact resistance ~2.0 kΩ·µm (the lowest being 1.6 kΩ·µm), which is comparable to the one in graphene contacts and even better than most of the conventional metal contacts, e.g., Au or Ni. This low contact resistance allows the device to show excellent electrical performance, which makes them ideal for highly scaled electronics.

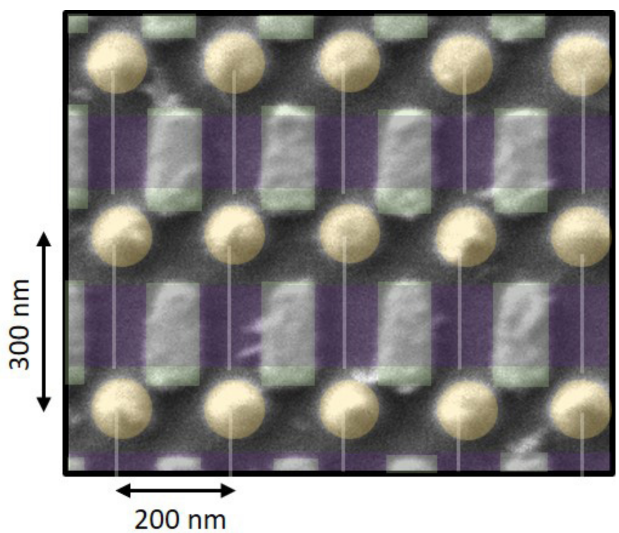

▲Figure 1: False color scanning electron microscope image of eight local top-gate transistors in a 2D MoS_2 transistor array with single device area of 0.06 µm^2. Green rectangles are the local top gates. Dark yellow/orange circles are the vertical metal-filled via in contact with the CNT bundles (white lines). Purple rectangles are monolayer MoS_2 channels. 10-nm Al_2O_3 is used as the top-gate dielectric. (Guo 2022).

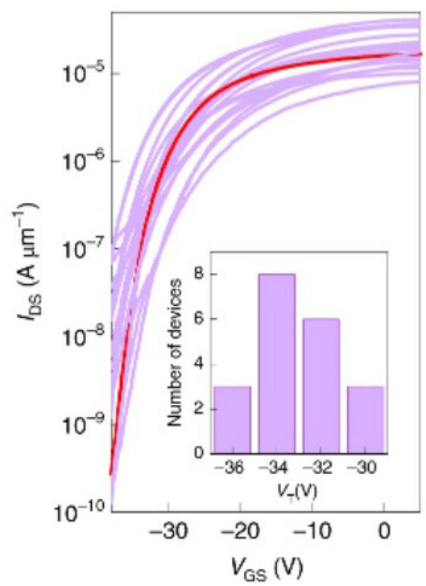

▲Figure 2: Measured transfer characteristics of 20 MoS_2 transistors with CNT bundle contacts at room temperature and V_{DS} = 1V. The red line demonstrates the representative performance among the 20 devices; inset, threshold voltage (V_T) distribution of the 20 devices. (Guo 2022).

FURTHER READING

- Y. Guo†, E. Shi†, J. Zhu†, P.-C. Shen, J. Wang, Y. Lin, Y. Mao, S. Deng, B. Li, J.-H. Park, A.-Y. Lu, S. Zhang, Q. Ji, Z. Li, C. Qiu, S. Qiu, Q. Li, L. Dou, Y. Wu, J. Zhang, T. Palacios, A. Cao, and J. Kong, "Soft-lock Drawing of Super-aligned Carbon Nanotube Bundles for Nanometer Electrical Contacts," *Nature Nanotechnology*, vol. 17, pp.. 278-284, 2022.
- H. Wang, L. Yu, Y.-H. Lee, Y. Shi, A. Hsu, M. L. Chin, L.-J. Li, M. Dubey, J. Kong, and T. Palacios, "Integrated Circuits Based on Bilayer MoS2 Transistors," *Nano Letts*. vol. 12, pp. 4674-4680, 2012.
- L. Yu, D El-Damak, U. Radhakrishna, X. Ling, A. Zubair, Y. Lin, Y. Zhang, M.-H. Chuang, Y.-H. Lee, D. Antoniadis, J. Kong, A. Chandrakasan, and T. Palacios, "Design, Modeling, and Fabrication of Chemical Vapor Deposition Grown MoS2 Circuits with E-Mode FETs for Large-Area Electronics," *Nano Letts*. vol. 16, pp. 6349-6356, 2016.

Photonics and Optoelectronics

On-demand Directional Photon Emission Using Waveguide Quantum Electrodynamics

B. Kannan, A. Almanakly, Y. Sung, A. Di Paolo, D. A. Rower, J. Braumuller, A. Melville, B. M. Niedzielski, A. Karamlou, K. Serniak, A. Vepsalainen, M. E. Schwartz, J. L. Yoder, R. Winik, J. I-Jan Wang, T. P. Orlando, S. Gustavsson, J. A. Grover, W. D. Oliver

Sponsorship: AWS Center for Quantum Computing, Department of Defense, US Army Research Office, Department of Energy Office of Science - National Quantum Information Science

Routing quantum information between non-local computational nodes is a foundation for extensible networks of quantum processors. Quantum information can be transferred between arbitrary nodes by photons that propagate between them or by resonantly coupling nearby nodes. Notably, conventional approaches involving propagating photons have limited fidelity due to photon loss and are often unidirectional, whereas architectures that use direct resonant coupling are bidirectional in principle but can generally accommodate only a few local nodes. Here, we demonstrate high-fidelity, on-demand, bidirectional photon emission using an artificial molecule comprising two superconducting qubits strongly coupled to a waveguide. Quantum interference between the photon emission pathways from the molecule generate single photons that selectively propagate in a chosen direction. This architecture is capable of both photon emission and capture and can be tiled in series to form an extensible network of quantum processors with all-to-all connectivity.

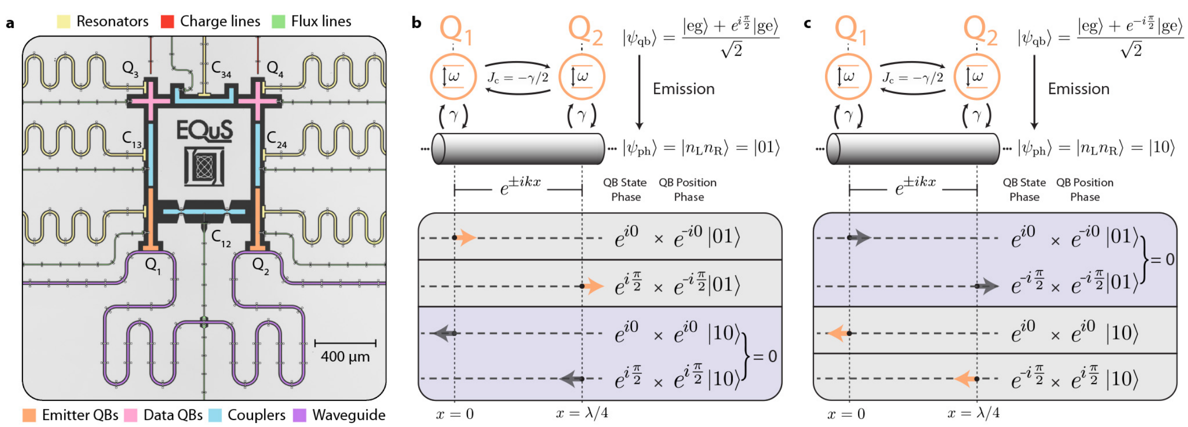

▲Figure 1: a) A false-colored optical micrograph of the device. b) Schematic outlining the quantum interference effect that enables the emission of a rightward-propagating photon in the waveguide. c) Same as b) but for a leftward-propagating photon.

FURTHER READING:

- B. Kannan, A. Almanakly, Y. Sung, A. Di Paolo, D. A. Rower, J. Braumuller, A. Melville, B. M. Niedzielski, A. Karamlou, K. Serniak, A. Vepsalainen, M. E. Schwartz, J. L. Yoder, R. Winik, J. I.-J. Wang, T. P. Orlando, S. Gustavsson, J. A. Grover, and W. D. Oliver, "On-demand Directional Photon Emission Using Waveguide Quantum Electrodynamics," *arXiv:2203.01430*, 2022.
- N. Gheeraert, S. Kono, and Y. Nakamura, "Programmable Directional Emitter and Receiver of Itinerant Microwave Photons in a Waveguide," *Phys. Rev. A*, vol. 102, p. 053720, 2020.

Programmable Organic Light-emitting Diode (OLED) Matrix

S. Cheung*, B. John*, S. Moezzi*, M. Saravanapavananantham, R. Ram, F. Niroui
*Contributed equally
Sponsorship: MIT EECS, 6.S059 class

Organic light-emitting diodes (OLEDs) have reached commercial prominence in recent decades for their improved image quality, durability, and lower power consumption. Future developments in OLED performance can engender the next generation of electronics, including flexible transparent devices. Either a passive-matrix (PMOLED) or active-matrix (AMOLED) control scheme can drive the OLED display. Although PMOLEDs use a simpler, less efficient single pixel control scheme, they are optimal for small displays due to their lack of thin film transistors (TFTs) and resulting low manufacturing cost. Here, we demonstrate a programmable PMOLED matrix with the ability to control individual pixels. Using a device architecture verified from Zou et al., w e fabricated an 8x8 OLED display and designed a printed circuit board (PCB) to control the OLED through custom driver software. The simple and inexpensive manufacturing process highlights the potential for ubiquitous PMOLED displays in everyday consumer lifestyles.

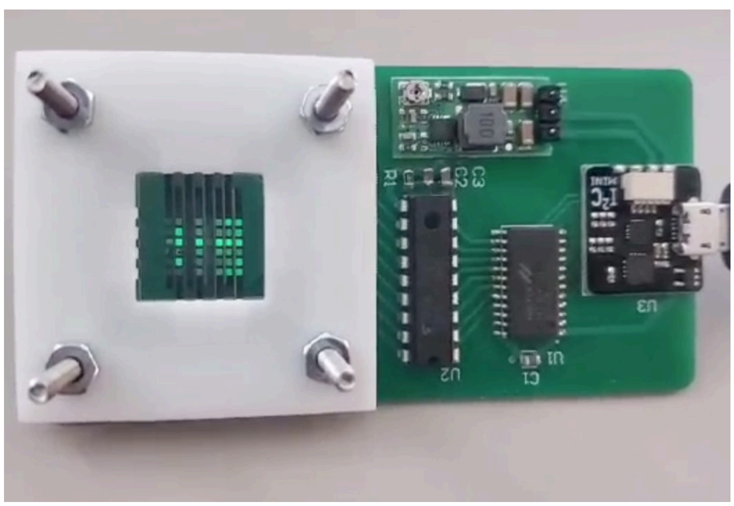

▲ Figure 1: Photograph of the OLED matrix display held by a 3D printed substrate holder, alongside the custom-designed PCB.

Silicon Photonics for Chip-Based 3D Printing

S. Corsetti, M. Notaros, T. Sneh, A. Stafford, Z. Page, J. Notaros
Sponsorship: MIT Rolf G. Locher Endowed Fellowship

3D printing has contributed to diverse scientific advancements in fields ranging from personal healthcare to soft robotics. To maximize build speed while minimizing material strain, modern laser-based 3D printers rely on intricate mechanical systems. The cost and upkeep of these systems, in addition to the UV-wavelength laser printing standard, have historically presented a barrier for the implementation of 3D printing in low-cost and sensitive-material applications, such as live-cell hydrogel printing.

To address these cost and material constraints, in this work, we combine the fields of silicon photonics and polymer chemistry to develop an on-chip integrated photonic system that enables dynamic non-mechanical control of visible light and controllably cure a custom visible-light-curable liquid resin. This research takes the first step towards a system that will allow for non-mechanical, volumetric 3D printing with interference patterns generated by a single chip. The complete development of this technology would allow for a highly-compact, portable, low-cost, high-speed solution for the next generation of 3D printers.

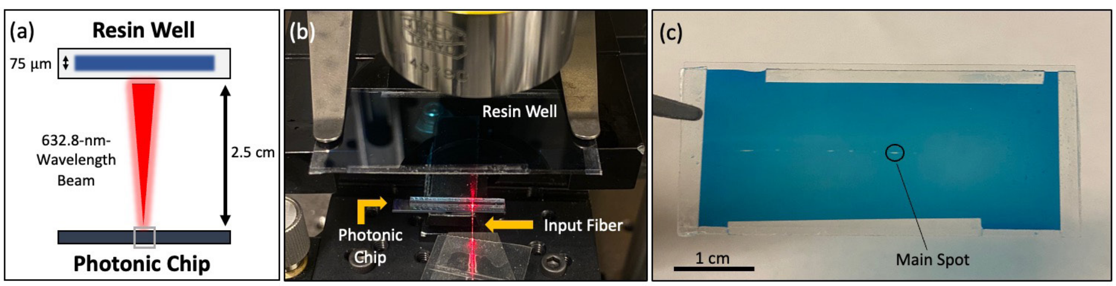

▲ Figure 1: (a) Conceptual diagram (not to scale) of the system with a photonic chip emitting red light into a glass resin well. (b) Photograph of the experimental setup, in which an input fiber couples 632.8-nm-wavelength light onto the photonic chip that projects a beam upwards into a prototype resin well. (c) Photograph of resin regions selectively cured using the chip, with the curing resulting from the main lobe labeled.

FURTHER READING

- S. Corsetti, M. Notaros, T. Sneh, A. Stafford, Z. A. Page, and J. Notaros, "Visible-Light Integrated Optical Phased Arrays for Chip-Based 3D Printing," under review in *Proceedings of Integrated Photonics Research (IPR)*, 2022.
- M. Notaros, T. Dyer, M. Raval, C. Baiocco, J. Notaros, and M. R. Watts, "Integrated Visible-light Liquid-crystal-based Phase Modulators," *Opt. Express*, vol. 30, pp. 13790-13801, 2022.
- D. Ahn, L. M. Stevens, K. Zhou, and Z. A. Page, "Rapid High-Resolution Visible Light 3D Printing," *ACS Central Science*, vol. 6, no. 9, pp. 1555-1563, 2020.

Photo-Enhanced Ionic Conductivity across Grain Boundaries in Polycrystalline Ceramics

T. Defferriere, D. Klotz, J. C. Gonzalez-Rosillo, J. L. M. Rupp, H. L. Tuller
Sponsorship: DoE, Japan Society for The Promotion Of Science, Kakenhi Grant-In-Aid, Swiss National Science Foundation, Equinor

Oxide based ionic conductors are critical for energy conversion and storage devices such as fuel cells or batteries, or for nano-electronic memory and gas sensing devices. However, cost-effective fabrication methods for both bulk and thin films samples often result in polycrystalline microstructures whose grain boundaries block ion migration. This has been explained by space-charge potential barriers, featuring depletion zones and band bending, forming between adjacent grains, which typically limits the overall material conductivity, particularly as one approaches ambient temperatures. Above bandgap light is known to reduce band bending at interfaces in photovoltaic and photoelectrochemical systems by providing photogenerated charge carriers that screen potential barriers. We demonstrate here that the same principle (Figure a and b) applies to a solid-state oxygen ion conductor and that we can decrease its grain boundary resistance by optical illumination. We further demonstrated that this effect is not caused by heat or electronic conductivity. Our conclusions are based on electrochemical impedance spectroscopy (Figure c) and intensity-modulated photocurrent spectroscopy (IMPS) measurements, performed on polycrystalline and epitaxial samples, and backed by theoretical considerations of grain boundary potential heights and distributions. This discovered effect has the potential to lead to improved electrochemical storage and conversion efficiencies and reduced temperature operation as well as offering contactless diagnosis of ionic conduction in polycrystalline solids.

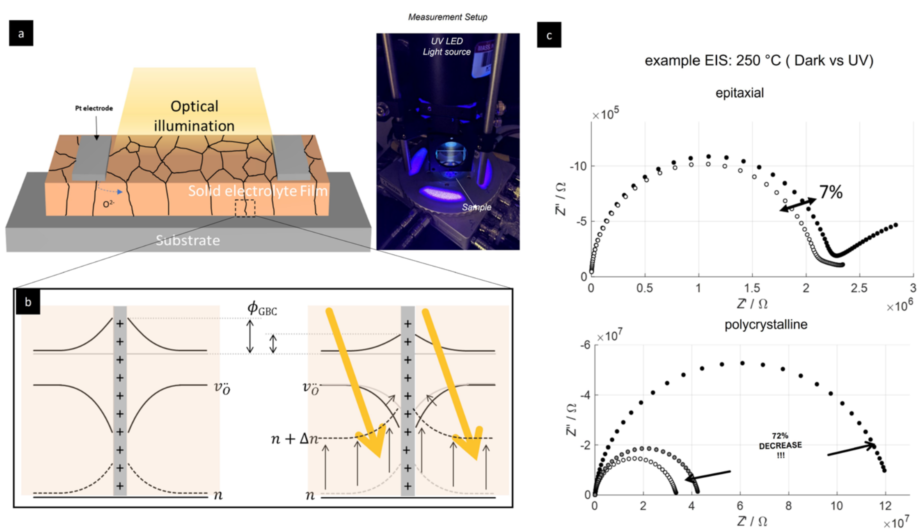

▲ Figure 1: (a) Schematic of polycrystalline oxide-based oxygen solid electrolyte thin film and the optical setup used to characterize sample conductivity under illumination, (b) Simplified diagram of grain boundary space charge potential modulation by above band gap optical illumination and the induced change in band bending. (c) Electrochemical impedance spectroscopy (EIS) results obtained at 250°C in the dark (black circle) and under UV illumination (brighter circles) for epitaxial and polycrystalline sample's demonstrating large resistance decrease only in the polycrystalline sample.

FURTHER READING

- T. Defferriere, D. Klotz, J. C. Gonzalez-Rosillo, J. L. M. Rupp & H. L. Tuller "Photo-enhanced Ionic Conductivity Across Grain Boundaries in Polycrystalline Ceramics." *Nat. Mater*. 21, 438-444 (2022).

Automatic Design of a Broadband Directional Coupler via Bayesian Optimization

Z. Gao, Z. Zhang, D. S. Boning

Integrated silicon photonics has emerged as an attractive technology that brings breakthroughs in data communications, super-computing, etc. Directional couplers (DCs) are an important device in integrated silicon photonics, due to their capability to realize complicated functionalities. During the past few decades, a DC operating in broadband is of high interest to researchers, and various design methods have been proposed. However, all of these methods rely on the knowledge of design experts and manual adjustment of design parameters (e.g., the height of the rib or the width of the waveguide).

In this work, we propose a fully automatic design method to synthesize a broadband DC via Bayesian optimization. Bayesian optimization is a gradient-free black-box global optimization technique, made up of two steps in combination: (i) building a surrogate model and (ii) optimizing a user-defined acquisition function. These two steps will be repeatedly performed until the maximum number of iterations is reached. As demonstrated in Figure 1, our simulation results show that within 120 simulations, an initial trivial DC design can be evolved into an attractive broadband one, with an excess loss around 0.27 dB and a maximum imbalance around 16%. The proposed Bayesian optimization method could largely reduce the human effort in designing a broadband DC and shorten the design time.

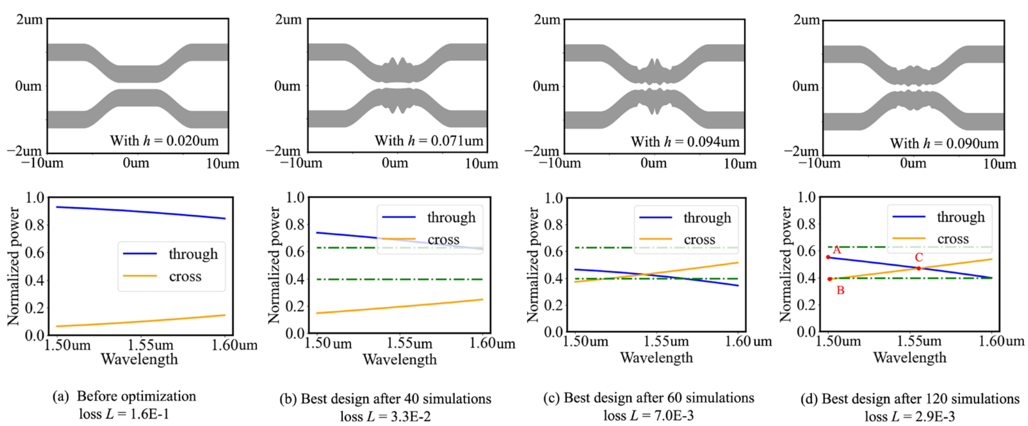

▲ Figure 1: Minimizing loss L defined on a directional coupler via Bayesian optimization. In (d), points A, B, and C have coordinates (1.50, 0.55), (1.50, 0.39), and (1.56, 0.47), respectively.

FURTHER READING

- B. Shahriari, K. Swersky, Z. Wang, R. P. Adams, and N. de Freitas, "Taking the Human Out of the Loop: A Review of Bayesian Optimization," *Proc. of the IEEE*, vol. 104, no. 1, pp. 148-175, Jan. 2016.
- Z. Gao, Z. Zheng, and D. S. Boning, "Automatic Design of a Broadband Directional Coupler via Bayesian Optimization," *2022 Conference on Lasers and Electro-Optics (CLEO)*, pp. 1-2, 2022.

Scalable Quantum Information Processing Architecture Using a Programmable Array of Spin-photon Interfaces

L. Li, L. D. Santis, I. Harris, K. C. Chen, Y. Song, I. Christen, M. Trusheim, C. E. Herranz, R. Han, D. R. Englund
Sponsorship: MITRE, Center for Integrated Quantum Materials, NSF

A central challenge in quantum information processing is to generate a large-scale entanglement of quantum systems. A leading hardware platform consists of qubits in the form of spin states of color centers in diamond. However, it is estimated that for general-purpose quantum information processors, millions of qubits will be required, motivating the need for hardware architectures that are highly scalable using modern semiconductor integration systems.

Here, we demonstrate a scalable quantum information processing architecture in a proof of concept consisting of a 2D array of tin-vacancy centers, addressable and tunable across thousands of diamond cavities hybrid integrated on a control chip based on the foundry process. We demonstrate core capabilities including tuning of the color center emission wavelength, spin initialization, and single-shot spin readout. The above works together are a proof of concept for a freely scalable architecture capable of hosting thousands toward millions of qubits.

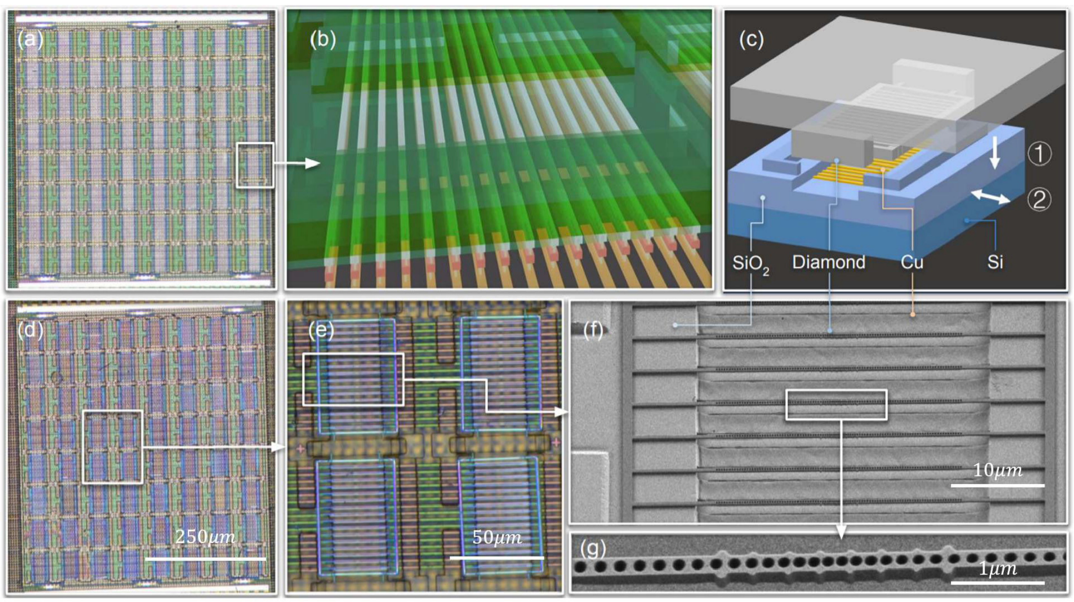

▲Figure 1: (a) The complementary metal-oxide-semiconductor (CMOS) chip after surface post-processing. (b) CMOS chip region marked by the white box in (a) with chiplet locking structure and metal routing. (c) The scalable hybrid integration illustration. (d) The 1024 diamond cavities hybrid integrated on CMOS control chip. (e) The zoom-in optical microscope image. (f) The diamond chiplet scanning electron microscopy (SEM) image. (g) The SEM image of the perturbative cavity design optimized for free space collection.

FURTHER READING:

- L. Li, L. D. Santis, I. Harris, K. C. Chen, Y. Song, I. Christen, M. Trusheim, C. E. Herranz, R. Han, and D. Englund. "Scalable Quantum Information Processing Architecture Using a Programmable Array of Spin-photon Interfaces," *CLEO: QELS_Fundamental Science*. Optical Society of America, 2022.

Integrated-Photonics-Based Visible-Light Holographic Augmented-Reality Display

M. Notaros, T. Dyer, M. Raval, C. Baiocco, E. P. Ippen, M. R. Watts, J. Notaros
Sponsorship: DARPA Visible Integrated Photonics Enhanced Reality (VIPER) program (Grant No. FA8650-17-1-7713), NSF Graduate Research Fellowship (Grant No. 1122374)

Augmented-reality head-mounted displays (HMDs) that display information in the user's field of view have many wide-reaching applications in defense, medicine, gaming, etc. However, current commercial HMDs are bulky, heavy, and indiscreet. Moreover, current displays are incapable of producing holographic images with full depth cues; this lack of depth information results in eyestrain and headaches that limit long-term and wide-spread use of these displays (also known as the vergence-accommodation conflict).

In this work, recent advances in the development of a novel integrated-photonics-based holographic display are reviewed. The display consists of a single transparent chip that sits directly in front of the user's eye and projects 3D holograms that only the user can see using amplitude- and phase-encoded liquid-crystal-based integrated optical phased arrays. The display presents a highly discreet and fully holographic solution for the next generation of augmented-reality displays.

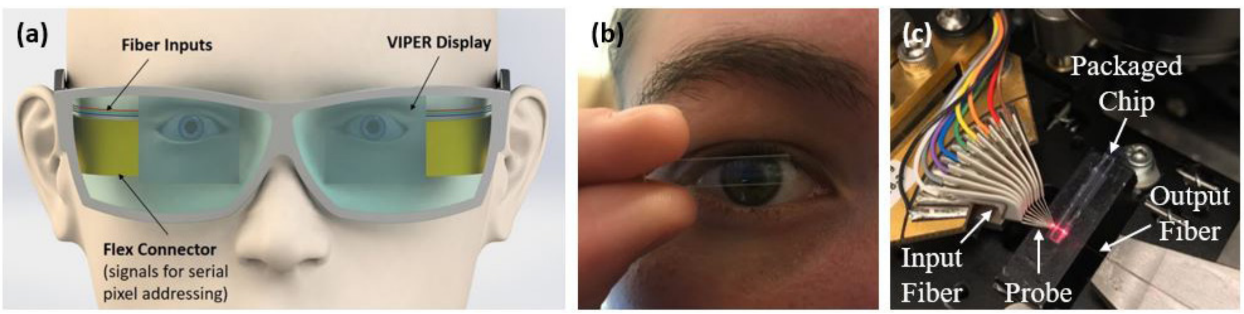

▲ Figure 1: (a) Diagram of the chip-based direct-view near-eye head-mounted display. (b) Photograph of a transparent photonic chip held in front of an eye. (c) Photograph of a photonic chip packaged with liquid crystal on an experimental setup.

FURTHER READING

- M. Notaros, T. Dyer, M. Raval, C. Baiocco, J. Notaros, and M. R. Watts, "Integrated Visible-Light Liquid-Crystal-Based Phase Modulators," *Optics Express*, vol. 30, no. 8, pp. 13790-13801, Apr. 2022.
- M. Notaros, J. Notaros, M. Raval, and M. R. Watts, "Integrated Visible-Light Liquid-Crystal Variable-Tap Amplitude Modulator," in *Proceedings of Integrated Photonics Research, Silicon, and Nanophotonics (IPR)*, paper ITh2C.6, 2019.
- J. Notaros, M. Raval, M. Notaros, and M. R. Watts, "Integrated-Phased-Array-Based Visible-Light Near-Eye Holographic Projector," in *Proceedings of Conference on Lasers and Electro-Optics (CLEO)*, paper STu3O.4, 2019.

3D Printed Micro-reflectors for Broadband, Low-loss and High-density Fiber-to-chip Coupling

L. Ranno, S. Yu, Q. Du, S. Serna, C. McDonough, N. Fahrenkopf, T. Gu, J. Hu
Sponsorship: Advanced Research Projects Agency – Energy (Department of Energy) under the ENLITENED Program (Award Number: DE-AR0000847)

Packaging constitutes a notable fraction of the cost of photonic integrated circuits, mainly due to the challenges related to fiber-to-chip optical coupling, such as the large modal mismatch between fiber and waveguide modes and the resulting tight alignment tolerances. Conventional packaging methods utilizing edge or grating coupling suffer have major limitations such as high insertion losses, low bandwidth density, limited alignment tolerances, or strong wavelength and polarization dependance. We propose a novel coupling scheme that capitalizes on the high resolution and design freedom offered by two-photon polymerization to address the challenges described above. The coupling scheme makes use of free-form reflective micro-optics that are directly printed onto the exposed facet of a waveguide and allow both redirecting the incoming light and expanding the waveguide mode size, improving the coupling efficiency with an optical fiber. We employ Fermat's principle to vastly simplify the free-form shape optimization process from a brute force local optimization of each point, requiring a large number of simulations, down to two single finite difference time domain (FDTD) simulations. The fabrication of the micro-reflectors can be easily included as a backend process in standard photonics foundry runs without any custom requirements. Simulations and experimental results show that the reflectors can reach the record-low insertion loss for surface-normal coupling of 0.5 dB and broadband operation with 1 dB bandwidth exceeding 300 nm, while also exhibiting alignment tolerances over 2 µm, commensurate with the mode profile of the optical fiber being used and compatible with passive alignment schemes. The micro-reflectors also boast high bandwidth densities and solder reflow compatibility, making them a promising coupling solution for applications ranging from wavelength division multiplexing telecommunications to non-linear optics or broadband sensing.

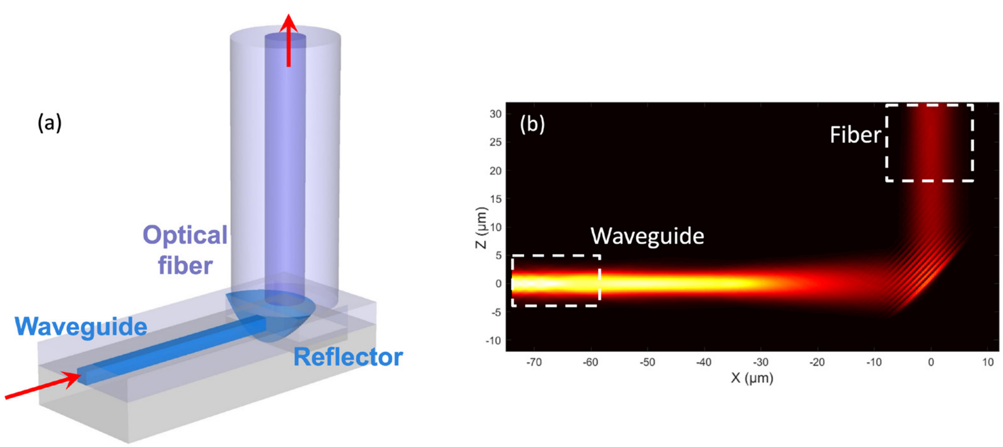

▲ Figure 1: (a) Schematic showing the structure described in the main text, where a TPP reflector is printed directly on a waveguide facet. (b) FDTD simulation of light coupling from a silicon nitride waveguide into an SMF-28 fiber mediated by an optimized micro-reflector.

FURTHER READING

- S. Yu, L. Ranno, Q. Du, S. Serna, C. McDonough, N. Fahrenkopf, T. Gu, and J. Hu. "Free-form Micro-optics Enabling Ultra-broadband Low-loss Fiber-to-chip Coupling," *arXiv:2112.14357*, 2021.
- S. Yu, H. Zuo, X. Sun, J. Liu, T. Gu, and J. Hu. "Optical Free-Form Couplers for High-density Integrated Photonics (OFFCHIP): A Universal Optical Interface," J. *Light. Technol.*, vol. 38, pp. 3358-3365, 2020.
- S. Yu, J. Lu, V. Ginis, S. Kheifets, S. W. D. Lim, M. Qiu, T. Gu, J. Hu, and F. Capasso. "On-chip Optical Tweezers Based on Freeform Optics," *Optica.* vol. 8, pp. 409-414, 2021.

CMOS-Compatible Focusing Optical Phased Arrays for Steerable Chip-Based Optical Trapping

T. Sneh, S. Corsetti, M. Notaros, J. Notaros
Sponsorship: MIT Frederick R. (1953) and Barbara Cronin Fellowship

Silicon photonics has in recent years seen success in translating complex and expensive bulk optical systems to the chip scale for applications such as LiDAR and holographic displays, with facile manufacturing enabled by existing complementary-metal-oxide-semiconductor technology. Optical traps, which have attracted significant interest for their utility in force measurements, cell measurement, and biophysics research, typically require large optical setups. Existing efforts to bring this tool to the chip scale have been limited to trapping within 100 microns, too short for practical integration with existing research.

In this work, we use integrated optical phased arrays, which enable dynamic spatial control of light, to generate focused light 5 mm above the chip surface and demonstrate trapping of microspheres. This system represents an easy-to-use optical trapping apparatus, with the potential to broaden the availability of optical-trapping technology and act as a force multiplier for biophysics and related research fields.

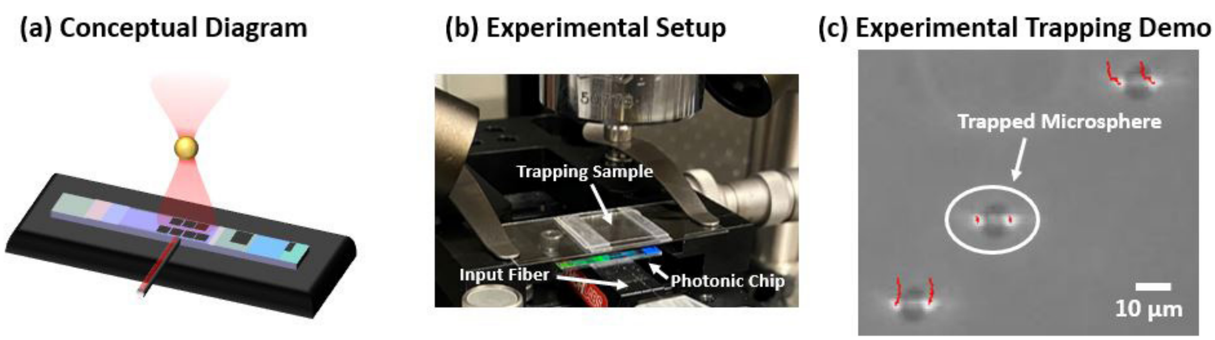

▲Figure 1: (a) Conceptual diagram (not to scale) of the chip-based optical-trapping system showing a photonic chip emitting a focused beam and trapping a microsphere. (b) Photograph of the experimental setup showing the input optical fiber, photonic chip, and microsphere sample stage. (c) Microscope image of the microspheres in the sample stage with superimposed tracks showing their motion over time (red lines); the motion of the microsphere located at the focal spot of the OPA (circled in white) is significantly reduced compared to its neighbors, indicating successful trapping.

FURTHER READING

- T. Sneh, S. Corsetti, M. Notaros, and J. Notaros, "Focusing Integrated Optical Phased Arrays for Chip-Based Optical Trapping," *Proc. Conference on Lasers and Electro-Optics (CLEO)*, paper STh4G.4, 2022.
- J. Notaros, M. Raval, M. Notaros, and M. R. Watts, "Integrated-Phased-Array-Based Visible-Light Near-Eye Holographic Projector," *Proc. Conference on Lasers and Electro-Optics (CLEO)*, paper STu3O.4, 2019. (Chair's Pick Award)
- J. Notaros, C. V. Poulton, M. Raval, and M. R. Watts, "Near-field-focusing Integrated Optical Phased Arrays," *Journal of Lightwave Technology*, vol. 36, no. 24, pp. 5912-5920, 2018.

Exsolution Synthesis of Nanocomposite Perovskites with Tunable Electrical and Magnetic Properties

J. Wang, K. Syed, S. Ning, I. Waluyo, A. Hunt, E. J. Crumlin, A. K. Opitz, C. A. Ross, W. J. Bowman, B. Yildiz
Sponsorship: Exelon Corporation, MIT Energy Initiative Seed Fund Program

Nanostructured functional oxides play an important role in clean energy technologies (such as solid oxide fuel cells) and novel memory devices. Here, we present a novel method in fabricating self-assembled nanostructures in a process termed "exsolution." Exsolution is a partial decomposition process in which oxides precipitate nano-scale secondary phases under extreme reducing conditions. Using thin-film perovskites as a model system, we successfully fabricated nanocomposite oxides with exsolution. Moreover, the exsolved nanocomposite is redox-active even at moderate temperatures. Such redox capabilities can enable dynamic control of the nanocomposite functionality by tailoring the oxygen non-stoichiometry. We demonstrate this concept with a continuous modulation of magnetization between 0 and 110 emu/cm3. These findings point out that exsolution may serve as a platform for scalable fabrication of complex metal oxide nanocomposites for electrochemical and electronic applications.

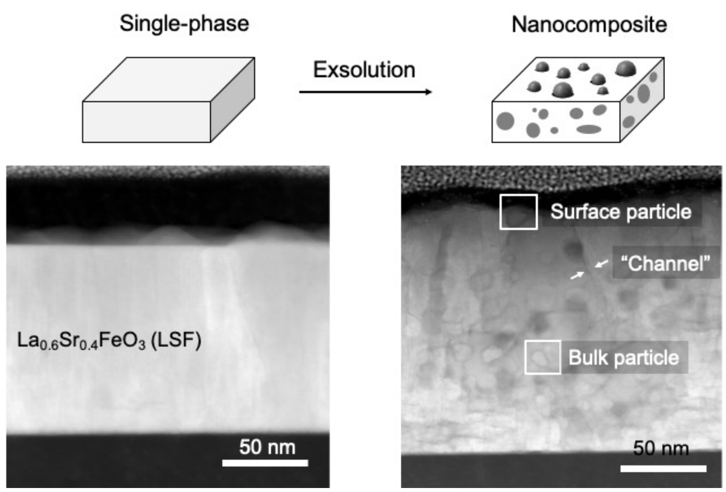

▲ Figure 1: Schematics of fabricating self-assembled nanocomposite functional oxides with exsolution.

FURTHER READING

• *Adv. Funct. Mater.* 2022, 32, 2108005

Non-mechanical Reconfigurable Zoom Metalenses

F. Yang†, H. Lin†, M. Y. Shalaginov†, K. Stoll, S. An, C. Rivero-Baleine, M. Kang, A. Agarwal, K. Richardson, H. Zhang, J. Hu, T. Gu
†These authors contributed equally to the work
Sponsorships: DARPA Defense Sciences Office Program: EXTREME Optics and Imaging (EXTREME) under agreement no. HR00111720029, MIT Skoltech Seed Fund Program.

Zoom lenses with variable focal lengths and magnification ratios are essential for many optical imaging applications. Conventional zoom lenses are composed of multiple refractive optics; optical zoom is attained via translational motion of one or more lens elements, which adds to module size, complexity, and cost. Here, we present a zoom lens design based on multi-functional optical metasurfaces which achieves large step zoom ratios, minimal distortion and diffraction-limited optical quality without requiring mechanical moving parts. Two embodiments of the concept were experimentally demonstrated based on polarization-multiplexing in the visible and phase change materials in the mid-infrared, both yielding 10x parfocal zoom in accordance with our design.

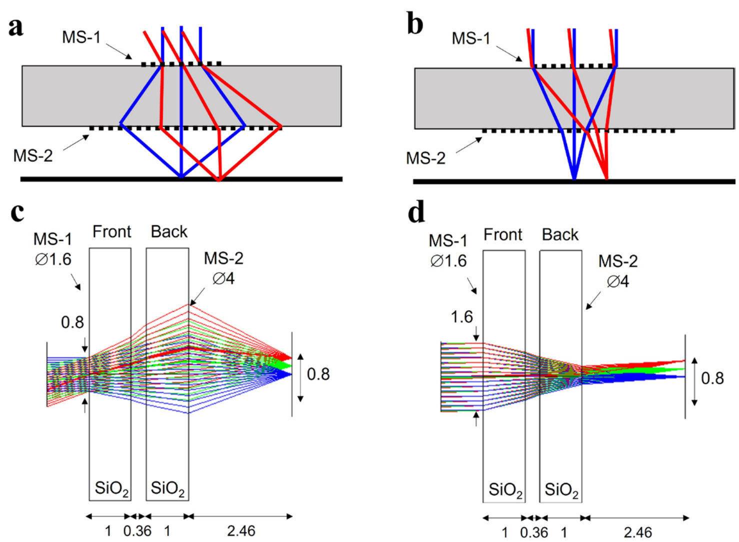

▲ Figure 1: (a)-(b) Schematic illustration of the doublet zoom metalens configuration in the (a) wide-angle mode and (b) telephoto mode. MS-1 and MS-2 label the front and back metasurfaces, respectively. Note that the optical aperture sizes differ in the two imaging modes. (c)-(d) Ray trace simulation of the optimized polarization-multiplexed zoom metalens in the (c) wide-angle mode and (d) telephoto mode. All the units are in mm.

Generative Modeling of Random Process Variation in Silicon Photonics

Z. Zhang, S. I. El-Henawy, D. S. Boning

Silicon photonics, where photons instead of electrons are manipulated, shows promise for higher data rates, lower energy communication and information processing, biomedical sensing, and novel optically based functionality applications such as wavefront engineering and beam steering of light. In silicon photonics, both electrical and optical components can be integrated on the same chip, using a shared silicon integrated circuit (IC) technology base. However, silicon photonics does not yet have mature process, device, and circuit variation models for the existing IC and photonic process steps; this lack presents a key challenge for design in this emerging industry.

Our goal is to develop key elements of a robust design for manufacturability (DFM) methodology for silicon photonics. In particular, generative compact models based on statistics are needed for random process variation analysis to achieve high-yield manufacturing.

In this work, we present two approaches for generative modeling: decomposed S-parameter representation and variational autoencoders (VAE), which ameliorate the issue of non-physical generation due to non-linear behavior of the response. We apply our proposed approaches on Y-splitters with imposed line edge roughness (LER) variations and show their improvement compared to the naïve linear principal component analysis approach. While the decomposed S-parameter representation provides simple generative models for each specific group of LER parameters, the VAE is capable of building a sophisticated model that captures changes from LER parameters and correlation among S-parameters. The method can be extended to other photonic components and circuits with other process variations, providing fast and accurate compact models to help designers predict and optimize photonic component performance, and facilitates the design of high-yield silicon photonic circuits in the future.

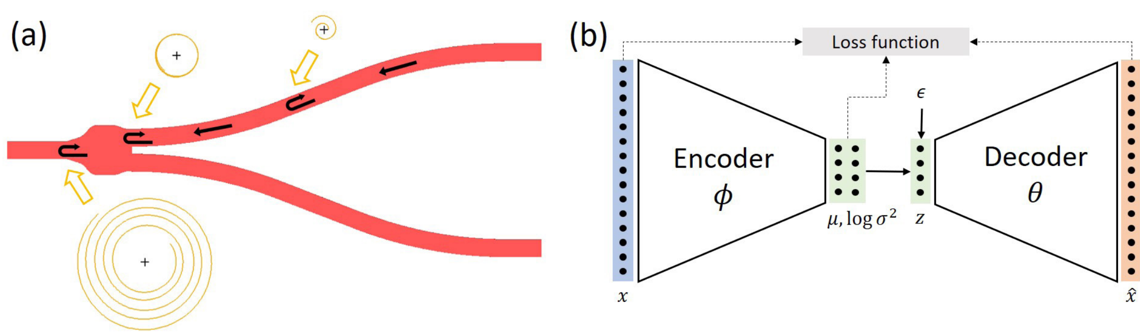

▲ Figure 1: (a) Physics behind the decomposed representation, (b) the architecture of the variational autoencoder.

FURTHER READING

- L. Chrostowski and M. Hochberg, "Silicon Photonics Design: from Devices to Systems," Cambridge: *Cambridge University Press*, 2015.
- Z. Zhang, S. I. El-Henawy, R. Miller, and D. S. Boning. "Decomposed Representation of S-parameters for Silicon Photonic Variation Analysis," *Optical Modeling and Performance Predictions XI*, vol. 11484, pp. 29-41, SPIE, 2020.

Research Centers

Center for Integrated Circuits and Systems

Professor Hae-Seung Lee, Director

The Center for Integrated Circuits and Systems (CICS) at MIT, established in 1998, is an industrial consortium created to promote new research initiatives in circuits and systems design, as well as to promote a tighter technical relationship between MIT's research and relevant industry. Eight faculty members participate in the CICS: Director Hae-Seung (Harry) Lee, Anantha Chandrakasan, Ruonan Han, Song Han, David Perreault, Negar Reiskarimian, Charles Sodini, and Vivienne Sze.

CICS investigates a wide range of circuits and systems, including wireless and wireline communication, high-speed, THz, and RF circuits, microsensor/actuator systems, imagers, digital and analog signal processing circuits, biomedical circuits, deep learning systems, hardware security, emerging technologies, and power conversion circuits, among others.

We strongly believe in the synergistic relationship between industry and academia, especially in practical research areas of integrated circuits and systems. CICS is designed to be the conduit for such synergy.

CICS's research portfolio includes all research projects that the eight participating faculty members conduct, regardless of source(s) of funding, with a few exceptions.

Technical interaction between industry and MIT researchers occurs on both a broad and individual level. Since its inception, CICS recognized the importance of holding technical meetings to facilitate communication among MIT faculty, students, and industry. We hold two informal technical meetings per year open to CICS faculty, students, and representatives from participating companies. Throughout each full-day meeting, faculty and students present their research, often presenting early concepts, designs, and results that have not been published yet. The participants then offer valuable technical feedback, as well as suggestions for future research. The meeting also serves as a valuable networking event for both participants and students. Closer technical interaction between MIT researchers and industry takes place during work on projects of particular interest to participating companies. Companies may invite students to give on-site presentations, or they may offer students summer employment. Additionally, companies may send visiting scholars to MIT or enter into a separate research contract for more focused research for their particular interest. The result is truly synergistic, and it will have a lasting impact on the field of integrated circuits and systems.

MIT/MTL Center for Graphene Devices and 2-D Systems

Professor Tomás Palacios, Director

The MIT/MTL Center for Graphene Devices and 2-D Systems (MIT-CG) brings together MIT researchers and industrial partners to advance the science and engineering of graphene and other two-dimensional (2-D) materials.

Two-dimensional materials are revolutionizing electronics, mechanical and chemical engineering, physics and many other disciplines thanks to their extreme properties. These materials are the lightest, thinnest, strongest materials we know of. At the same time that they have extremely rich electronic and chemical properties. MIT has been leading research on the science and engineering of 2-D materials for more than 40 years. Since 2011, the MIT/MTL Center for Graphene Devices and 2-D Systems (MIT-CG) has played a key role in coordinating most of the work going on at MIT on these new materials, and in bringing together MIT faculty and students, with leading companies and government agencies interested in taking these materials from a science wonder to an engineering reality.

Specifically, the Center explores advanced technologies and strategies that enable 2-D materials, devices, and systems to provide discriminating or breakthrough capabilities for a variety of system applications ranging from energy generation/storage and smart fabrics and materials to optoelectronics, RF communications, and sensing. In all these applications, the MIT-CG supports the development of the science, technology, tools, and analysis for the creation of a vision for the future of new systems enabled by 2-D materials.

Some of the many benefits of the Center's membership include complimentary attendance to meetings, industry focus days, and live webcasting of seminars related to the main research directions of the Center. Our industrial members also gain access to a resume book that connects students with potential employers, as well as access to timely white papers on key issues regarding the challenges and opportunities of these new technologies. There are also numerous opportunities to collaborate with leading researchers on projects that address some of today's challenges for these materials, devices, and systems.

The MIT Medical Electronic Device Realization Center

Professor Charles Sodini, Director

The vision of the MIT Medical Electronic Device Realization Center (MEDRC) is to revolutionize medical diagnostics and treatments by bringing health care directly to the individual and to create enabling technology for the future information-driven healthcare system. This vision will, in turn, transform the medical electronic device industry. Specific areas that show promise are wearable or minimally invasive monitoring devices, medical imaging, portable laboratory instrumentation, and the data communication from these devices and instruments to healthcare providers and caregivers.

Rapid innovation in miniaturization, mobility, and connectivity will revolutionize medical diagnostics and treatments, bringing health care directly to the individual. Continuous monitoring of physiological markers will place capability for the early detection and prevention of disease in the hands of the consumer, shifting to a paradigm of maintaining wellness rather than treating sickness. Just as the personal computer revolution has brought computation to the individual, this revolution in personalized medicine will bring the hospital lab and the physician to the home, to emerging countries, and to emergency situations. From at-home cholesterol monitors that can adjust treatment plans, to cell phone-enabled blood labs, these system solutions containing state-of-the-art sensors, electronics, and computation will radically change our approach to health care. This new generation of medical systems holds the promise of delivering better quality health care while reducing medical costs.

The revolution in personalized medicine is rooted in fundamental research in microelectronics from materials to sensors, to circuit and system design. This knowledge has already fueled the semiconductor industry to transform society over the last four decades. It provided the key technologies to continuously increase performance while constantly lowering cost for computation, communication, and consumer electronics. The processing power of current smart phones, for example, allows for sophisticated signal processing to extract information from this sensor data. Data analytics can combine this information with other patient data and medical records to produce actionable information customized to the patient's needs. The aging population, soaring healthcare costs, and the need for improved healthcare in developing nations are the driving force for the next semiconductor industry's societal transformation, Medical Electronic Devices.

The successful realization of such a vision also demands innovations in the usability and productivity of medical devices, and new technologies and approaches to manufacturing devices. Information technology is a critical component of the intelligence that will enhance the usability of devices; real-time image and signal processing combined with intelligent computer systems will enhance the practitioners' diagnostic intuition. Our research is at the intersection of Design, Healthcare, and Information Technology innovation. We perform fundamental and applied research in the design, manufacture, and use of medical electronic devices and create enabling technology for the future information-driven healthcare system.

The MEDRC has established a partnership between microelectronics companies, medical device companies, medical professionals, and MIT to collaboratively achieve needed radical changes in medical device architectures, enabling continuous monitoring of physiological parameters such as cardiac vital signs, intracranial pressure, and cerebral blood flow velocity. MEDRC has 4 sponsoring companies, 8 faculty members, 12 active projects, and approximately 15 students. A visiting scientist from a project's sponsoring company is present at MIT. Ultimately this individual is the champion that helps translate the technology back to the company for commercialization and provide the industrial viewpoint in the realization of the technology. MEDRC projects have the advantage of insight from the technology arena, the medical arena, and the business arena, thus significantly increasing the chances that the devices will fulfill a real and broad healthcare need as well as be profitable for companies supplying the solutions. With a new trend toward increased healthcare quality, disease prevention, and cost-effectiveness, such a comprehensive perspective is crucial.

In addition to the strong relationship with MTL, MEDRC is associated with MIT's Institute for Medical Engineering and Science (IMES) that has been charged to serve as a focal point for researchers with medical interest across MIT. MEDRC has been able to create strong connections with the medical device and microelectronics industry, venture-funded startups, and the Boston medical community. With the support of MTL and IMES, MEDRC will serve as the catalyst for the deployment of medical devices that will reduce the cost of healthcare in both the developed and developing world.

Faculty Profiles

Anuradha M. Agarwal

Principal Research Scientist, Materials Research Laboratory
Leader, Lab for Education and Application Prototypes (LEAP), AIM Photonics Academy
Director, Electronic-Photonic Packaging Consortium

Planar, integrated, Si-CMOS-compatible microphotonics platform for on-chip MIR hyperspectral imaging and chem-bio sensing applications; radiation effects on silicon microphotonics; non-linear materials and devices; chalcogenide glasses; aerosol detection; lead chalcogenide detectors, optoelectronic packaging.

Rm. 13-4126 | **617-253-5302** | **anu @ mit . edu**

VISITING/SUMMER STUDENTS/UROP

Abhishek Agrahari
Kenan Cicek, Fulbright Scholar
Anastacia De Gorostiza, MICRO Student
Elena Su, EECS UROP
Juan Jose Arango Uribe
Francesco Zanetto, Progetto Rocca Scholar

GRADUATE STUDENTS

Eveline Postelnicu, DMSE
Katherine Stoll, DMSE
Drew Weninger, DMSE

SELECTED PUBLICATIONS

P. Su, K. E. Stoll, S. Agarwal, O. Maksimov, P. Bhattacharya, H. B. Bhandari, K. Wada, L. C. Kimerling, and A. M. Agarwal, "Impacts of oxygen sensitization methods on the deposition and microstructure of ternary lead chalcogenide alloys," *Current Applied Physics*, 36, 71-75, 2022.

P. Xing, G. F-R. Chen, H. Gao, A. M. Agarwal, L. C. Kimerling, and D. T.-H. Tan, "Microresonator Frequency Comb Based High-Speed Transmission of Intensity Modulated Direct Detection Data," *arXiv preprint:2111.07874*, 2021.

E. Guglielmi, P. Su, F. Zanetto, K. Stoll, S. Serna, G. Ferrari, M. Sampietro, K. Wada, L. C. Kimerling, and A. M. Agarwal, "1/f Noise Characteristics of Waveguide-Integrated PbTe MIR Detectors and Impact on Limit of Detection," *J. of Lightwave Technology*, 39 (22), 7326-7333, 2021.

H. Lin, C. S. Kim, L. Li, M. Kim, W. W. Bewley, C. D. Merritt, C. L. Canedy, I. Vurgaftman, A. M. Agarwal, and K. Richardson, "Monolithic chalcogenide glass waveguide integrated interband cascaded laser," *Optical Materials Express,* 11 (9) 2869-2876, 2021.

J. W. Choi, E. Sahin, B.-U. Sohn, G. F-.R. Chen, D. K.-T. Ng, A. M. Agarwal, L. C. Kimerling, and D. T.-H. Tan, "High spectro-temporal compression on a nonlinear CMOS-chip," *Light: Science & Applications*, 10 (1), 2021.

O. Maksimov, P. Su, P. Bhattacharya, K. E. Stoll, K. Wada, L. C. Kimerling, A. M. Agarwal, and H. B. Bhandari, "High detectivity PbSxSe1-x films for mid-wavelength infrared detectors," *Thin Solid Films*, 731, 138749, 2021.

P. Su, M. Shalaginov, T. Gu, S. An, D. Li, L. Li, H. Jiang, S. Joo, L. C. Kimerling, and H. Zhang, "Large-area optical metasurface fabrication using nanostencil lithography" *Optics Letters* 46 (10) 2324-2327, 2021.

S. An, B. Zheng, M. Y. Shalaginov, H. Tang, H. Li, L. Zhou, Y. Dong, M. Haerinia, A. M. Agarwal, and C. Rivero Baleine, "Deep convolutional neural networks to predict mutual coupling effects in metasurfaces," *Advanced Optical Materials*, 10 (3), 2102113, 2022.

Duane S. Boning

Clarence J. LeBel Professor of Electrical Engineering
Professor of Electrical Engineering & Computer Science
Department of Electrical Engineering & Computer Science

Design for manufacturability of processes, devices, and circuits. Understanding and reduction of variation in semiconductor, photonics and MEMS manufacturing, emphasizing statistical, machine learning, and physical modeling of spatial and operating variation in circuits, devices, and CMP, electroplating, spin coating, etch, and embossing processes.

Rm. 39-415a | 617-253-0931 | boning @ mtl . mit . edu

GRADUATE STUDENTS

Christian Allinson, EECS and Sloan
Uttara Chakraborty, EECS
Sally El-Henawy, EECS
Farri Gaba, EECS and TPP
Zhengqi Gao, EECS
Andrew Lai, EECS
Christopher Lang, EECS
Colin Poler, EECS and Sloan
Tareq Saqr, SDM
Fan-Keng Sun, EECS
Andrew Tindall, EECS and Sloan
Peter Tran, EECS
Zhengxing Zhang, EECS

SUPPORT STAFF

Jami L. Mitchell, Administrative Assistant

SELECTED PUBLICATIONS

C. Lang, A. Jansen, S. Didari, P. Kothnur, and D. S. Boning, "Modeling and Optimizing the Impact of Process and Equipment Parameters in Sputtering Deposition Systems Using a Gaussian Process Machine Learning Framework," *IEEE Transactions on Semiconductor Manufacturing*, vol. 35, no. 2, pp. 229-240, May 2022.

Z. Gao, Z. Zhang, and D. Boning, "Automatic Design of a Broadband Directional Coupler via Bayesian Optimization," *CLEO 2022*, San Jose, CA, May 2022.

Z. Zhang, S. I. El-Henawy, C. Rios, and D. S. Boning, "Inference of Process Variations in Silicon Photonics from Characterization Measurements," *CLEO 2022*, Jan Jose, CA, May 2022.

C. I. Lang, F.-K. Sun, R. Veerasignam, J. Yamartino, and D. S. Boning, "Understanding and Improving Virtual Metrology Systems Using Bayesian Methods," IEEE Transactions on Semiconductor Manufacturing, Apr. 2022.

D. S. Boning, S. I. El-Henawy, and Z. Zhang, "Variation-Aware Methods and Models for Silicon Photonic Design-for-Manufacturability," *J. of Lightwave Technology*, vol. 40, no. 6, pp. 1776-1783, Mar. 2022.

F.-K. Sun, C. I. Lang, and D. S. Boning, "Adjusting for Autocorrelated Errors in Neural Networks for Time Series Regression and Forecasting," *Advances in Neural Information Processing Systems (NeurIPS)*, Dec. 2021.

C. Lang, D. Boning, R. Sprenkle, E. Wilson, and A. Samolov, "Machine Learning-Based Optimization of Dose Uniformity for Ion Implantation Systems," *AEC/APC Symposium Asia 2021*, Nov. 2021.

D. S. Boning, S. I. El-Henawy, and Z. Zhang, "Process Variation-Aware Photonic Design," paper Tu5B.1, 2021 *Optical Fiber Communications Conference and Exhibition (OFC)*, Jun. 2021.

Edward S. Boyden

Y. Eva Tan Professor in Neurotechnology at MIT
Co-Director, Center for Neurobiological Engineering, K Lisa Yang Center for Bionics, Departments of Brain and Cognitive Sciences, Media Arts and Sciences, Biological Engineering, McGovern Institute and HHMI

Developing tools that enable the mapping of the molecules and wiring of the brain, the recording and control of its neural dynamics, and the repair of its dysfunction. Systematically analyzing and repairing normal and pathological-brain computations.

Rm. 46-2171C | 617-324-3085 | edboyden @ mit . edu

RESEARCH SCIENTISTS AND STAFF

Bobae An, McGovern
Debarati Ghosh, McGovern
Burcu Guner-Ataman, McGovern
Konstantinos Kagias, McGovern
Youngmi Lee, McGovern
Kylie Leung, McGovern
Jack Lovell, McGovern
Demian Park, McGovern
Brett Pryor, McGovern
Marat Vasilenko, McGovern
Doug Weston, McGovern
Aimei Yang, McGovern
Jian-Ping Zhao, McGovern

POSTDOCTORAL ASSOCIATES

Shahar Bracha, McGovern
Jaebin Choi, McGovern
Jinyoung Kang, McGovern
Changyang Linghu, McGovern
Yangning Lu, McGovern
Yong Qian, McGovern
Nava Shmoel David, McGovern
Sapna Sinha, McGovern
Panagiotis (Panos) Symvoulidis, McGovern
Giovanni Talei Franzesi, McGovern
Hao Wang, McGovern
Gaojie Yang, McGovern
Quansan Yang, McGovern
Chi Zhang, McGovern

GRADUATE STUDENTS

Jenna Lauren Aronson, BCS
Nick Barry, MAS
Cristina Torres Caban, BE
Alexi Georges Choueiri, BCS
Danielle Orozco Cosio, BCS
Amauche Emenari, BCS
Kettner Griswold, MAS
Nathan Han, EECS
Jordan Harrod, HST
Siddharth Iyer, Biology
Brennan Jackson, HST
Shannon Johnson, MAS
Daniel Leible, BCS
Yixi Liu, EECS
Camille Mitchell, BCS
Mitchell Murdock, BCS
Verna Peng, BCS
Cipriano Romero, EECS
Catherine Marin Della Santina, BE
Margaret Elizabeth Schroeder, BCS
Tay Won Shin, MAS
Anubhav Sinha, HST
Michael Skuhersky, BCS
Corban Swain, BE
Shiwei Wang, Chem
Zeguan Wang, MAS
Caroline Zhang, MAS
Ruihan Zhang, MAS

SUPPORT STAFF

Macey Lavoie, Administrative Assistant
Lisa Lieberson, Senior Administrative Assistant
Fira Zainal, Administrative Assistant

SELECTED PUBLICATIONS

R. Gao, C. J. Yu, L. Gao, K. D. Piatkevich, R. L. Neve, J. B. Munro, S. Upadhyayula, and E. S. Boyden, "A Highly Homo- geneous Polymer Composed of Tetrahedron-like Mono- mers for High-isotropy Expansion Microscopy," *Nature Nanotechnology*, doi: 10.1038/s41565-021-00875-7. Online ahead of print, 2021.

S. Alon, D. R. Goodwin, A. Sinha, A. T. Wassie, F. Chen, E. R. Daugharthy, Y. Bando, A. Kajita, A. G. Xue, K. Marrett, R. Prior, Y. Cui, A. C. Payne, C. C. Yao, H. J. Suk, R. Wang, C. J. Yu, P. Tillberg, P. Reginato, N. Pak, S. Liu, S. Punthambaker, E. P. R. Iyer, R. E. Kohman, J. A. Miller, E. S. Lein, A. Lako, N. Cullen, S. Rodig, K. Helvie, D. L. Abravanel, N. Wagle, B. E. Johnson, J. Klughammer, M. Slyper, J. Waldman, J. Jané-Valbuena, O. Rozenblatt-Rosen, A. Regev; IMAXT Consortium, G. M. Church, A. H. Marblestone, and E. S. Boyden, "Expansion Sequencing: Spatially Precise In Situ Transcriptomics in Intact Biological Systems," *Science* 371(6528):eaax2656, 2021.

A. C. Payne, Z. D. Chiang, P. L. Reginato, S. M. Mangiameli, E. M. Murray, C. C. Yao, S. Markoulaki, A. S. Earl, A. S. Labade, R. Jaenisch, G. M. Church, E. S. Boyden, J. D. Buenrostro, F. Chen, "In Situ Genome Sequencing Resolves DNA Sequence and Structure in Intact Biological Sam- ples," *Science*, doi:10.1126/science.aay3446. Online ahead of print, 2020.

C. Linghu, S. L. Johnson, P. A. Valdes, O. A. Shemesh, W. M. Park, D. Park, K. D. Piatkevich, A. T. Wassie, Y. Liu, B. An, S. A. Barnes, O. T. Celiker, C.-C. Yao, C.-C. (Jay) Yu, R. Wang, K. P. Adamala, M. F. Bear, A. E. Keating, and E. S. Boyden, "Spatial Multiplexing of Fluorescent

Vladimir Bulović

MIT.nano Director
Fariborz Maseeh (1990) Professor of Emerging Technology
Department of Electrical Engineering and Computer Science

Physical properties of nanostructured materials and composite structures and their use in development of electronic, excitonic, optical, and nano-mechanical devices. Applications of nanostructures in large-scale technologies.

Rm. 13-3138 | **617-253-7012** | **bulovic @ mit . edu**

RESEARCH SCIENTISTS

Jeremiah Mwaura, RLE
Annie Wang, RLE

POSTDOCTORAL ASSOCIATES

Dane deQuilettes, RLE
Benjia Dak Dou, RLE
Jinchi Han, EECS
Richard Swartout, EECS

GRADUATE STUDENTS

Roberto Brenes, EECS, NSF Fellow
Matthew Ruiyan Chua, EECS, A*STAR Fellow
Jamie Geng, EECS
Tamar Kadosh, DMSE
Madeliene Laitz, EECS, NSF Fellow
Brendan Motes, EECS
Mayuran Saravanapavanantham, EECS, NSF Fellow
Melany Sponseller, EECS
Ella Wassweiler, EECS, NSF Fellow

SUPPORT STAFF

Samantha Farrell, Sr. Administrative Assistant

SELECTED PUBLICATIONS

R. Swartwout, R. Patidir, E. Belliveau, B. Dou, D. Beynon, P. Greenwood, N. Moody, D. deQuilettes, M. Bawendi, T. M. Watson, and V. Bulović, "Predicting Low Toxicity and Scalable Solvent Systems for High Speed Roll-to-Roll Perovskite Manufacturing," *Solar RRL* 6, 2100567 (2022).

J. Han, J. Lang, and V. Bulovic, "An Ultra-Thin Flexible Loudspeaker Based on a Piezoelectric Micro-Dome Array," I*EEE Transactions on Industrial Electronics* (2022).

C. Yang, *at al.*, "Consensus statement: Standardized reporting of power-producing luminescent solar concentrator performance," *Joule* 6 (1), 8-15 (2022).

D. W. deQuilettes, R. Brenes, M. Laitz, B. T. Motes, M. M. Glazov, and V. Bulović, "Impact of Photon Recycling, Grain Boundaries, and Nonlinear Recombination on Energy Transport in Semiconductors," *ACS Photonics* 9, 110–122 (2021).

J. Shi, F. Y. Gao, Z. Zhang, H. Utzat, U. Barotov, A. Farahvash, J. Han, J. Deschamps, C.-W. Baik, K. S. Cho, V. Bulović, A. P. Willard, E. Baldini, N. Gedik, M. G. Bawendi, and K. A. Nelson, "Terahertz Field-Induced Reemergence of Quenched Photoluminescence in Quantum Dots," arXiv:2112.08533 (2021).

J. Han, Z. Nelson, M. R. Chua, T. M. Swager, F. Niroui, J. H. Lang, and V. Bulović, "Molecular Platform for Fast Low-Voltage Nanoelectromechanical Switching," *Nano Letts.* 21 (24), 10244-10251 (2021).

F. Niroui, M. Saravanapavanantham, J. Han, J. J. Patil, T. M. Swager, J. H. Lang, and V. Bulović, "Hybrid Approach to Fabricate Uniform and Active Molecular Junctions," *Nano Letts.* 21, 1606-1612 (2021).

J. J. Yoo, G. Seo, M. R. Chua, T. G. Park, Y. Lu, F. Rotermund, Y. K. Kim, C. S. Moon, N. J. Jeon, J.-P. Correa-Baena, V. Bulović, S. S. Shin, M. G. Bawendi, and J. Seo, "Efficient perovskite solar cells via improved carrier management," *Nature* 590, 587-593 (2021).

T. Sannicolo, W. H. Chae, J. Mwaura, V. Bulović, and J. C. Grossman, "Silver Nanowire Back Electrode Stabilized with Graphene Oxide Encapsulation for Inverted Semitransparent Organic Solar Cells with Longer Lifetime," *ACS Applied Energy Materials* 4, 1431-1441 (2021).

M. Wu, T. A. Lin, J. O. Tiepelt, V. Bulović, and M. A. Baldo, "Nanocrystal-Sensitized Infrared-to-Visible Upconversion in a Microcavity under Subsolar Flux," *Nano Letts.* 21, 1011-1016 (2021).

M. M. Tavakoli, J. H. Park, J. Mwaura, M. Saravanapavanantham, V. Bulović, and J. Kong, "Monolayer Hexagonal Boron Nitride: An Efficient Electron Blocking Layer in Organic Photovoltaics," *Advanced Functional Materials*, 2101238 (2021).

S. S. Peled, M. Perez, D. Meron, A. Osherov, V. Bulović, E. A. Katz, and Y. Golan, "Morphology control of perovskite films:a two-step, all solution process for conversion of lead selenide into methylammonium lead iodide," *Materials Chemistry Frontiers* 5, 1410-1417 (2021).

Jacopo Buongiorno

TEPCO Professor, Department of Nuclear Science and Engineering
MacVicar Faculty Fellow
Director, Center for Advanced Nuclear Energy Systems (CANES),
Director of Science and Technology, Nuclear Reactor Laboratory (NRL)

Innovations in nuclear technology; boiling heat transfer; nuclear reactor design and safety; offshore floating nuclear power plant; nanofluids for nuclear applications.

Rm. 24-206 | 617-253-7316 | jacopo @ mit . edu

GRADUATE STUDENTS

Santiago Andrade Aparicio, Sloan
Isabel Naranjo De Candido, NSE
Edward James Garcia, NSE
Carmen Sleight, MechE

UNDERGRADUATE STUDENT

Lucy M. Nester, NSE
Beau Walsh

SUPPORT STAFF

Carolyn Carrington, Administrative Assistant

SELECTED PUBLICATIONS

J. Buongiorno, B. Carmichael, B. Dunkin, J. Parsons, D. Smit, "Can Nuclear Batteries Be Economically Competitive in Large Markets?," *Energies*, 14, 4385, 2021.

J. Buongiorno, R. Freda, S. Aumeier, K. Chilton, "A Strategy to Unlock the Potential of Nuclear Energy for a New and Resilient Global Energy-Industrial Paradigm," *The Bridge*, 51, 2, Jun. 2021.

E. Lizarraga-Garcia, J. Buongiorno, E. Al-Safran, "Computational Fluid Dynamics (CFD) Simulations of Taylor Bubbles in Vertical and Inclined Pipes with Upward and Downward Liquid Flow," *SPE J.*, 26(06), 3832–3847, 2021.

J. Buongiorno, and M. Bucci, "The not-so-subtle flaws of the force balance approach to predict the departure of bubbles in boiling heat transfer," *Physics of Fluids,* Vol. 33, Issue 1, 2021.

S. Faucher, D. J. Lundberg, X. A. Liang, X. C. Jin, D. Parviz, J. Buongiorno, M. Strano, "A Virucidal Face Mask Based on the Reverse-flow Reactor Concept for Thermal Inactivation of SARS-CoV-2," *AIChE J.*, 2021. DOI: 10.1002/aic.17250

P. Eash-Gates, M. M. Klemun, G. Kavlak, J. McNerney, J. Buongiorno, J. E. Trancik, "Sources of cost overrun in nuclear power plant construction call for a new approach to engineering design," *Joule*, 4, 2348-2373, Nov. 2020.

K. Dawson, M. Corradini, J. Parsons, J. Buongiorno, "Deep Decarbonization of the Power Sector: the Need for a Low-Carbon, Dispatchable, Scalable and Widely Available Energy Source," *The Bridge*, 50, 3, Sep. 2020.

A. Kossolapov, F. Chavagnat, R. Nop, N. Dorville, B. Phillips, J. Buongiorno, M. Bucci, "The boiling crisis of water under exponentially escalating heat inputs in subcooled flow boiling at atmospheric pressure," *Int. J. Heat Mass Transfer*, 160, 120137, 2020.

J. Conway, N. Todreas, J. Halsema, C. Guryan, A. Birch, T. Isdanavich, J. Florek, J. Buongiorno, M. Golay, "Physical Security Analysis and Simulation of the Multi-Layer Security System for the Offshore Nuclear Plant (ONP)," *Nuc. Eng. Design*, 352, 2019.

G. Su, F.P. D'Aleo, B. Phillips, R. Streich, E. Al-Safran, J. Buongiorno, H.M. Prasser, "On the oscillatory nature of heat transfer in steady annular flow," *International Communications in Heat and Mass Transfer*, 108, 104328, 2019.

J. Buongiorno, M. Corradini, J. Parsons, and D. Petti, "The Future of Nuclear Energy in a Carbon-constrained World," *IEEE Power and Energy Magazine*, Mar. 2019.

J. Parsons, J. Buongiorno, M. Corradini, and D. Petti, "A Fresh Look at Nuclear Energy," *Science*, vol. 363, issue 6423, p. 105, 11 Jan. 2019.

S. Afkhami, J. Buongiorno, A. Guion, S. Popinet, R. Scardovelli, and S. Zaleski, "Transition in a Numerical Model of Contact Line Dynamics and Forced Dewetting," *J. Computational Physics*, 374, pp. 1061–1093, 2018.

A. Richenderfer, A. Kossolapov, J. H. Seong, G. Saccone, E. Demarly, R. Kommajosyula, E. Baglietto, J. Buongiorno, and M. Bucci, "Investigation of Subcooled Flow Boiling and CHF using High-resolution Diagnostics Experimental Thermal and Fluid Science," *Experimental Thermal and Fluid Science*, 99, pp. 35-58, 2018.

J. L. Moran, A. L. Cottrill, J. D. Benck, P. Liu, Z. Yuan, M. S. Strano, and J. Buongiorno, "Noble-Gas-Infused Neoprene Closed-cell Foams Achieving Ultra-low Thermal Conductivity Fabrics," *RSC Advances*, 8, pp. 21389-21398, 2018.

M. Trojer, R. Azizian, J. Paras, T. McKrell, K. Atkhen, M. Bucci, and J. Buongiorno, "A Margin Missed: the Effect of Surface Oxidation on CHF Enhancement in IVR Accident Scenarios," *Nucl. Eng. Design*, 335, pp. 140-150, 2018.

Anantha P. Chandrakasan

Dean of Engineering, Vannevar Bush Professor of Electrical Engineering & Computer Science
Department of Electrical Engineering and Computer Science

Design of digital integrated circuits and systems. Energy efficient implementation of signal processing, communication and medical systems. Circuit design with emerging technologies.

Rm. 38-107 | **617-258-7619** | **anantha @ mit . edu**

POSTDOCTORAL ASSOCIATE

Yeseul Jeon, RLE

GRADUATE STUDENTS

Aya Amer, EECS
Maitreyi Ashok, EECS
Ruicong Chen, EECS (co-supervised with H. Lee)
Adam Gierlach, EECS (co-supervised with G. Traverso)
Alex Ji, EECS
Jaeyoung Jung, EECS
Dimple Kochar, EECS
Eunseok Lee, EECS (co-supervised with R. Han)
Kyungmi Lee, EECS
Saurav Maji, EECS
Vipasha Mittal, EECS (co-supervised with H-S. Lee)
Rishabh Mittal, EECS (co-supervised with H-S. Lee)
Zoey Song, EECS
Miaorong Wang, EECS
Jongchan Woo, EECS (co-supervised with Rabia T. Yazicigil)
So-Yoon Yang, EECS (co-supervised with G. Traverso)
Deniz Yildirim, EECS

VISITING SCHOLARS

Rabia Tugce Yazicigil, Boston University

SUPPORT STAFF

Jessie-Leigh Thomas, Administrative Assistant

SELECTED PUBLICATIONS

A. Maitreyi, M. J. Turner, R. L Walsworth, E. V. Levine, and A. P. Chandrakasan, “Hardware Trojan Detection Using Unsupervised Deep Learning on Quantum Diamond Microscope Magnetic Field Images,” *ACM J. on Emerging Technologies in Computing Systems*, Apr. 2022.

A. Maitreyi, E. Levine, and A. P. Chandrakasan, “Randomized Switching SAR (RS-SAR) ADC Pro-tections for Power and Electromagnetic Side Channel Security,” I*EEE Custom Integrated Circuits Conference (CICC)*, Apr. 2022.

G. Preet, V. Schaffer, B. Haroun, S. Ramaswamy, J. Wieser, J. Lang, and A. P. Chandrraksan, “A Duty-Cycled Integrated-Fluxgate Magnetometer for Current Sensing,” *IEEE J. of Solid-State Circuits*, Mar. 2022.

S. Maji S., U. Benerjee, S. H. Fuller, and A. P. Chandrakasan, “A Threshold-Implementation-Based Neural-Network Accelerator Securing Model Parameters and Inputs Against Power Side-Channel Attacks,” *IEEE International Solid-State Circuits Conference (ISSCC)*, Feb. 2022.

M. I. W. Khan, J. Woo, X. Yi, M. I. Ibrahim, R. T. Yazicigil, A. P. Chandrakasan, and R. Han, “A 0.31-THz Orbital-Angular-Momentum (OAM) Wave Transceiver in CMOS With Bits-to-OAM Mode Mapping,” *IEEE J. of Solid-State Circuits*, pp.1-1, Jan. 2022.

K. Lee, and A. P. Chandrakasan, “Understanding the Energy vs. Adversarial Robustness Trade-Off in Deep Neural Networks,” *IEEE Workshop on Signal Processing Systems (SiPS)*, Oct. 2021.

M. I. W. Khan, J. Woo, X. Yi, M. I. Ibrahim, R. T. Yazicigil, A. P. Chandrakasan, and R. Han, “A 0.31THz CMOS Uniform Circular Antenna Array Enabling Generation/Detection of Waves with Orbital-Angular Momentum,” *IEEE Radio-Frequency Integrated Circuit Symposium (RFIC)*, Jun. 2021.

X. Yi, C. Wang, Z. Hu, J. W. Holloway, M. I. W. Khan, M. I. Ibrahim, M. Kim, G. C. Do-giamis, B. Perkins, M. Kaynak, R. T. Yazicigil, A. P. Chandrakasan, R. Han, “Emerging Terahertz Integrated Systems in Silicon,” *IEEE Transactions on Circuits and Systems I: Regular Papers*, pp.1-14, Jun. 2021.

T. Jeong, A. P. Chandrakasan, and H.-S. Lee, “S2ADC: A 12-bit, 1.25MS/s Secure SAR ADC with Power Side-Channel Attack Resistance,” *IEEE J. of Solid-State Circuits*, vol. 56, no. 3, pp.844-854, Mar. 2021.

Yufeng (Kevin) Chen

Assistant Professor of Electrical Engineering Department of Electrical Engineering & Computer Science

Biomimetic Robotics, Insect-scale robots, intermediate Reynolds number fluid dynamics, unsteady aerodynamics, soft artificial muscles, electroactive polymer actuators

Rm. 10-140H | 617-253-7351 | yufengc @ mit . edu

POSTDOCTORAL RESEARCHER

Younghoon Lee, EECS

GRADUATE STUDENTS

Yi-Husan Hsiao, EECS
Suhan Kim,EECS
Zhijian Ren, EECS

UNDERGRADUATE STUDENT

Cathleen Arase, MechE
Kyle Heinz, EECS

SUPPORT STAFF

Catherine Bourgeois, Administrative Assistant

SELECTED PUBLICATIONS

Z. Ren, S. Kim, X. Ji, W. Zhu, F. Niroui, J. Kong, and Y. Chen, “A High-Lift Micro-Aerial-Robot Powered by Low-Voltage and Long-Endurance Dielectric Elastomer Actuators,” *Advanced Materials*, 2106757, 2022.

Y. Chen, S. Xu, Z. Ren, and P. Chirarattananon, “Collision Resilient Insect-Scale Soft-Actuated Aerial Robotswith High Agility,” *IEEE Transaction on Robotics*. vol. 37, no. 5, pp. 1752-1764, Oct. 2021.

Y. Chen, N. Doshi, and R. J. Wood, “Inverted and Inclined Climbing Using Capillary Adhesion in a Quadrupedal Insect-Scale Robot,” *IEEE Robotics and Automation Letts*. 5(3), 4820-4827, 2020.

K. Becker, Y. Chen, and R. J. Wood, “Mechanically Programmable Dip Molding of High Aspect Ratio Soft Actuator Arrays,” *Advanced Functional Materials*. 1908919, 2020.

Y. Chen, H. Zhao, J. Mao, P. Chirarattananon, E. H. Helbling, N.-s. P. Hyun, R. D. Clarke, and R. J. Wood, “Controlled Flight of a Microrobot Powered by Soft Artificial Muscles,” *Nature*. 575(7782), 324-329, 2019.

Y. Chen, N. Doshi, N. Goldberg, H. Wang, and R. J. Wood, “Controllable Water Surface to Underwater Transition Through Electrowetting in a Hybrid Terrestrial-aquatic Microrobot,” *Nature Communications*. 9(1), pp 2495, 2018.

Y. Chen, H. Wang, E. F. Helbling, N. T. Jafferis, R. Zufferey, A. Ong, K. Ma, N. Gravish, P. Chirarattananon, M. Kovac, and R. J. Wood, “A Biologically Inspired, Flapping-wing, Hybrid Aerial-aquatic Microrobot,” *Science Robotics*. 2(11), eaao5619, 2017.

Y. Wang*, X. Yang*, Y. Chen*, D. K. Wainwright, C. P. Kenaley, Z. Gong, Z. Liu, H. Liu, J. Guan, T. Wang, J. C. Weaver, R. J. Wood, and L. Wen, “A Biorobotic Adhesive Disc for Underwater Hitchhiking Inspired by the Remora Suckerfish,” *Science Robotics*. 2(10), eaan8072, 2017. (*equal contribution).

Luca Daniel

Professor
Department of Electrical Engineering & Computer Science

Development of numerical techniques: parameterized model order reduction, uncertainty quantification, inverse problems and robust optimization for high dimension parameter spaces. Current applications: magnetic resonance imaging; electrical power distribution networks; robustness & stability of deep neural networks.

Rm. 36-849 | **617-253-2631** | **luca @ mit . edu**

POSTDOCTORAL ASSOCIATE

Praneeth Namburi, IMES

GRADUATE STUDENTS

Ching-Yun (Irene) Ko, EECS
Jose E. C. Serralles, EECS
Jeet Mohapatra, EECS (co-advisor Tommi Jaakkola)
Adina Bechhofer, EECS (co-advisor Karl Berggren)
Marco Turchetti, EECS (co-advisor Karl Berggren)
Quang P. Kieu, EECS (co-advisor Martha Gray)
Zachary Gromko, EECS (Cadence co-supervisor Shirin Farrahi)
Sam Chevalier, MechE
Wang Zhang, MechE
Lydia Thurman, LGO-EECS
Anjali Krishnamachar, LGO-EECS
Elizabeth Hau, LGO-EECS
Taylor Facen, LGO-EECS
Andrew Mighty, LGO-EECS
Lauren Heintz, LGO-EECS
Mercer Borris, LGO-EECS

UNDERGRADUATE STUDENTS

Marina Zhang, EECS
Tuomas Oikarinen, EECS
Victor Rong, EECS
Alexander Gu, EECS
Ishan Pakuwal, EECS
Pawan Goyal, EECS

SUPPORT STAFF

Chadwick Collins, Administrative Assistant

SELECTED PUBLICATIONS

I. Giannakopoulos, J. E. C. Serralles, L. Daniel, D. K. Sodickson, A. G. Polimeridis, J. K. White, and R. Lattanzi, "Magnetic-resonance-based electrical property mapping using Global Maxwell Tomography with an 8-channel head coil at 7 Tesla: a simulation study," *IEEE Transactions on Biomedical Engineering*, vol. 68, no. 1, pp. 236-246, Jan. 2021. doi: 10.1109/TBME.2020.2991399

Z. Zhang, S. I. El-Henawy, A. Sadun, R. Miller, L. Daniel, J. K. White, and D. S. Boning, "Enabling Wavelength-Dependent Adjoint-Based Methods for Process Variation Sensitivity Analysis in Silicon Photonics," *J. of Lightwave Technology* (Volume: 39, Issue: 6, Mar. 15, 2021). doi: 10.1109/JLT.2020.3041186

T. Bradde, S. Chevalier, M. De Stefano, S. Grivet-Talocia, and L. Daniel, "Handling Initial Conditions in Vector Fitting for Real Time Modeling of Power System Dynamics," *Energies Journal*, vol. 14, no. 14, Apr. 2021, doi: 10.3390/en14092471.

I. I. Giannakopoulos, G .D. Guryev, J. E. C. Serralles, I. P. Georgakis, L. Daniel, J. K. White, and R. Lattanzi, "Compression of volume-surface integral equation matrices via Tucker decomposition for magnetic resonance applications," *IEEE Transactions on Antennas and Propagation*, Jun. 2021. doi: 10.1109/TAP.2021.3090835

S. Chevalier, F. M. Ibanez, K. Cavanagh, K. Turitsyn, L. Daniel, and P. Vorobev, "Network Topology Invariant Stability Certificates for DC Microgrids with Arbitrary Load Dynamics," *IEEE Transactions on Power Systems*, Sep. 2021, doi:10.1109/TPWRS.2021.3110803.

S. Chevalier, L. Schenato, and L. Daniel, "Accelerated Probabilistic Power Flow in Electrical Distribution Networks via Model Order Reduction and Neumann Series Expansion," *IEEE Transactions on Power Systems*, Oct. 2021, doi: 10.1109/TPWRS.2021.3120911.

J. Mohapatra, C.-Y. Ko, T.-W. Weng, P.-Y. Chen, S. Liu, and L. Daniel, "Hidden Cost of Randomized Smoothing," *Proceedings of The 24th International Conference on Artificial Intelligence and Statistics*, PMLR 130:4033-4041, 2021.

T. Oikarinen, W. Zhang, A. Megretski, L. Daniel, and T.-W. Weng, "Robust Deep Reinforcement Learning through Adversarial Loss," *NeurIPS*, 2021.

A. Boopathy, T.-W. Weng, S. Liu, P.-Y. Chen, G. Zhang, and L. Daniel, "Fast Training of Provably Robust Neural Networks by SingleProp," in *Proceedings of the 35th AAAI Conference on Artificial Intelligence 2021*: 6803-6811

C.-Y. Ko, J. Mohapatra, P.-Y. Chen, S. Liu, L. Daniel, and T.-W. Weng, "Revisiting Contrastive Learning through the Lens of Neighborhood Component Analysis: an Integrated Framework," *NeurIPS*, 2021.

M. Turchetti, Y. Yang, M. R. Bionta, A. Nardi, L. Daniel, K. K. Berggren, and P. D. Keathley, "Emission Behavior of Planar Nano-Vacuum Field Emitters," *34th International Vacuum Nanoelectronics Conference (IVNC)*, IEEE, 2021.

Jesús A. del Alamo

Donner Professor
Professor of Electrical Engineering
Department of Electrical Engineering & Computer Science

Nanometer-scale III-V compound semiconductor transistors for future digital, power, RF, microwave and millimeter wave applications. Reliability of compound semiconductor transistors. Diamond transistors. Ionic non-volatile programmable AI synapses.

Rm. 38-246 | 617-253-4764 | alamo @ mit . edu

RESEARCH SCIENTIST

Alon Vardi, MTL

GRADUATE STUDENTS

Taekyong Kim, EECS
Ethan Lee, EECS
Aviram Massuda, EECS
Murat Onen, EECS
Yanjie Shao, EECS
Difei Zhang, EECS

VISITING SCIENTIST

Jongwook Kim, SK hynix

SUPPORT STAFF

Elizabeth Kubicki, Administrative Assistant

SELECTED PUBLICATIONS

E. S. Lee, J. Joh, D. S. Lee, and J. A. del Alamo, "Gate-geometry dependence of dynamic Vt in p-GaN gate HEMTs," To be presented at *2022 International Symposium on Power Semiconductor Devices and ICs*, Vancouver, Canada, May 22-26, 2022.

Y. Shao, M. Pala, D. Esseni, and J. A. del Alamo, "Scaling of GaSb/InAs Vertical Nanowire Esaki Diodes Down to Sub-10 nm Diameter," *IEEE Transactions on Electron Devices,* Vol. 69, No. 4, pp. 2188-2196, Apr. 2022.

E. S. Lee, J. Joh, D. S. Lee, and J. A. del Alamo, "Impact of Gate Offset on PBTI of p-GaN Gate HEMTs," *2022 IEEE International Reliability Physics Symposium*, Dallas, TX, Mar. 27-31, 2022.

E. S. Lee, J. Joh, D. S. Lee, and J. A. del Alamo, "Gate-Geometry Dependence of Electrical Characteristics of p-GaN Gate HEMTs," *Applied Physics Letts.*, Vol. 120, 082104, Feb. 23, 2022.

D. Antoniadis, T. Kim and, J. A. del Alamo, "Nucleation-Limited Switching Dynamics Model for Efficient Ferroelectrics Circuit Simulation," *IEEE Transactions on Electron Devices*, Vol. 69, No. 1, pp. 395-399, Jan. 2022.

Y. Shao, M. G. Pala, D. Esseni, and J. A. del Alamo, "Sub-10-nm Diameter GaSb/InAs Vertical Nanowire Esaki Diodes with Ideal Scaling Behavior: Experiments and Simulations," *2021 IEEE International Electron Devices Meeting*, San Francisco, CA, Dec. 11-15, 2021.

J. A. del Alamo, B. Yildiz, T. Palacios, A. Vardy, K. Klyukin, J. Wang, J. Niroula, M. Geis, M. Hollis, J. Varghese, J. Daulton, D. Calawa, J. Kedzierski, S. Warnock, G. Turner, and B. Zhang, "Progress Toward High Performance Diamond Surface FETs," *Electronics Resurgence Initiative Summit and MTO Symposium*. Online, Oct. 19-21, 2021.

J. A. del Alamo, Invited Paper, "Nanoscale InGaAs Electronics: Lessons towards transistor innovation in new material systems," *40th Electronic Materials Symposium*. Online, Oct. 11-13, 2021.

D. Choi, A. Vardi, and J. A. del Alamo, "Analysis of Mo Sidewall Ohmic Contacts to InGaAs Fins," *IEEE Transactions on Electron Devices*, Vol. 68, No. 10, pp. 4847-4853, Oct. 2021.

M. W. Geis, J. O. Varghese, Alon Vardi, J. Kedzierski, J. Daulton, D. Calawa, M. A. Hollis, C. H. Wuorio, G. W. Turner, S. M. Warnock, T. Osadchy, J. Mallek, A. Melville, J. A. del Alamo, and B. Zhang, "Hydrogen and deuterium termination of diamond for low surface resistance and surface step control," *Diamond and Related Materials,* Vol. 118, article 108518, Jul. 2021.

J. A. del Alamo, "Nanoscale InGaAs Electronics: Lessons towards transistor innovation in new material systems," *32nd European Symposium on Reliability of Electron Devices*, Failure Physics and Analysis, Oct. 4-8, 2021, Invited Keynote

J. A. del Alamo, X. Cai, X. Zhao, A. Vardi, and J. Grajal, Invited Paper, "Nanoscale InGaAs FinFETs: Band-to-Band Tunneling and Ballistic Transport," *51st European Solid-State Device Research Conference*, Online, Sep. 2021.

J. A. del Alamo, "Microchip Manufacturing in the U.S. and the Drive to Reassert Leadership in Microelectronics," *2nd USA/Mexico Energy Corridor Symposium*. Online, Sep. 23-24, 2021, Invited Paper.

M. Onen, N. Emond, J. Li, B. Yildiz, and J. A. del Alamo, "CMOS-compatible Protonic Programmable Resistor based on Phosphosilicate Glass Electrolyte for Analog Deep Learning," *Nano Letts.*, Vol. 21, pp. 6111-6116, 2021.

Y. Shao and J. A. del Alamo, "Sub-10 nm Diameter Vertical Nanowire p-Type GaSb/InAsSb Tunnel FETs," *IEEE Electron Device Letts.*, Vol. 43, No. 6, pp. 846-849, June 2022.

Dirk R. Englund

Associate Professor
Department of Electrical Engineering & Computer Science

Quantum Communications, Quantum Computing, and Quantum Sensing: Devices and systems.

Rm. 36-351 | 617-324-7014 | englund @ mit . edu

RESEARCH SCIENTISTS

Ryan Hamerly, RLE
Matthew Trusheim, ISN
Stefan Krastanov, RLE
Franco Wong, RLE

POSTDOCTORAL ASSOCIATES

Carlos Errando Herranz, RLE
Hyeongrak Choi, RLE
Laura Kim, RLE
Adrian Menssen, RLE
Sivan Trajtenberg-Mills, RLE
Bevin Huang, RLE
Artur Hermans, RLE
Mohamed ElKabbash, RLE
Jawaher Almutlaq, RLE
Sri Krishna Vadlamani, RLE
Valeria Saggio, RLE
Ethan Arnault, RLE
Yong Hu, RLE
Chao Li, RLE
Avinash Kumar, RLE

GRADUATE STUDENTS

Eric Bersin, NSF Graduate Fellowship
Mihika Prabhu, NSF Graduate Fellowship
Ian Christen, NDSEG Graduate Fellowship
Kevin C. Chen, NSF Graduate Fellowship
Isaac B. Harris, EECS
Liane Bernstein, EECS
Ronald Davis, EECS
Alex Sludds, NSF Graduate Fellowship
Hugo Larocque, EECS
Saumil Bandyopadhyay, NSF Graduate Fellowship
Linsen Li, RLE
Yuqin (Sophia) Duan, EECS
Hana Azzouz, EECS
Marc Davis, DOE Graduate fellowship
Hamza Raniwala, NSF graduate fellowship
Hanfeng Wang, EECS
Thomas Propson, NSF graduate fellowship
Reggie Wilcox, RLE
Connor Gerlach, EECS
Cole Brabec, NSF graduate fellowship

UNDERGRADUATE STUDENTS

Pedro Sales, EECS
Sophie S. Zhang, EECS
Agnes Villanyi, EECS
Tareq A. El Dandachi, EECS
Abhijatmedhi Chotrattanapituk
Jiahui Du, Physics
Quynh The Nguyen, Physics

LABORATORY STAFF

Andrew Birkel, Lab Operations Manager

SUPPORT STAFF

Janice Balzer, Administrative Assistant

SELECTED PUBLICATIONS

L. De Santis, M. Trusheim, K. Chen, and D. Englund, "Investigation of the Stark Effect on a Centrosymmetric Quantum Emitter in Diamond," *Phys. Rev. Lett.* 127, 147402 (2021).

S. Bandyopadhyay, R. Hamerly, D. Englund, "Hardware Error Correction for Programmable Photonics," *Optica* Vol. 8, Issue 10, pp. 1247-1255 (2021).

M. Dong, G. Clark, A. J. Leenheer, M. Zimmermann, D. Dominguez, A. J. Menssen, D. Heim, G. Gilbert, D. Englund, and M. Eichenfield, "High-speed programmable photonic circuits in a cryogenically compatible, visible-NIR 200 mm CMOS architecture," *Nature Photonics* (2021).

R. Debroux, C. P. Michaels, C. M. Purser, N. Wan, M. E. Trusheim, J. A. Martínez, R. A. Parker, A. M. Stramma, K. C. Chen, L. de Santis, E. M. Alexeev, A. C. Ferrari, D. Englund, D. A. Gangloff, and M. Atatüre, "Quantum control of the tin-vacancy spin qubit in diamond," *Phys. Rev. X* 11, 041041 (2021).

K. C. Chen, W. Dai, C. Errando-Herranz, S. Lloyd, and D.Englund, "Scalable and High-Fidelity Quantum Random Access Memory in Spin-Photon Networks," *PRX Quantum* 2, 030319 (2021).

E. R. Eisenach, J. F. Barry, M. F. O'Keeffe, J. M. Schloss, M. H. Steinecker, D. R. Englund, D. A. Braje, "Cavity quantum electrodynamic readout of a solid-state spin sensor," *Nature Communications* 12, Article number: 1357 (2021).

E. D. Walsh, W. Jung, G.-H. Lee, D. K. Efetov, B.-I. Wu, K.-F. Huang, T. A. Ohki, T. Taniguchi, K. Watanabe, P. Kim, D. Englund, and K. C. Fong, "Josephson-junction Infrared Single-photon Detector," *Science* (2021).

N. H. Wan, T.-J. Lu, K. C. Chen, M. P. Walsh, M. E. Trusheim, L. De Santis, E. Bersin, I. Christen, I. B. Harris, S. L. Mouradian, E. S. Bielejec, and D. Englund, "Large-scale inte-

Jongyoon Han

Professor

Department of Electrical Engineering & Computer Science Department of Biological Engineering

Nanofluidic / Microfluidic technologies for advanced biomolecule analysis and sample preparation: cell and molecular sorting, novel nanofluidic phenomena, biomolecule separation and pre-concentration, seawater desalination and water purification.

Rm. 36-841 | 617-253-2290 | jyhan @ mit . edu

POSTDOCTORAL ASSOCIATES

Hyungkook Jeon, RLE
Hyukjin Kwon, RLE
Taehong Kwon, RLE
Yaoping Liu, SMART
Center Ishita Shrivastava, RLE
Dahou Yang, SMART Center
Cong Wang, SMART Center
Mingyang Cui, RLE
Daniel Roxby, NTU/SMART Center
Tan Dai Nguyen, SMART Center

RESEARCH SCIENTISTS

Kerwin Keck, SMART Center
Junghyo Yoon, RLE

GRADUATE STUDENTS

Kyungyong Choi, EECS
Matthew Flavin, EECS
Zhumei Sun Rohskopf, ME
Eric Wynne, EECS
Alexander Bevacqua, BE
Itay Fayer, BE
Jerome Tan, NTU/SMART Center

VISITORS

Eric Brack, Army Natick Research Center
Yejin Park, Dongguk University, Korea

SUPPORT STAFF

Cindy Higgins, Administrative Assistant

SELECTED PUBLICATIONS

H. Jeon, C. Cremers, D. Le, J. Abell, and J. Han, "Multi-dimensional-double-spiral (MDDS) inertial microfluidic platform for sperm isolation directly from the raw semen sample," *Scientific Reports*, 12, 4212 (2022).

H. Jeon, T. Kwon, J. Yoon, and J. Han, "Engineering deformation-free plastic spiral inertial microfluidic system for CHO cell clarification in biomanufacturing," *Lab on a Chip*, 22, 272 – 285 (2022).

X. Huang, H. Jeon, J. Liu, J. Yao, M. Wei, W. Han, J. Chen, L. Sun, and J. Han, "Deep-Learning Based Label-Free Classification of Activated and Inactivated Neutrophils for Rapid Immune State Monitoring," *Sensors*, 21, 8360 (2021).

A. C. Barksdale, J. Yoon, H. J. Kwon, and J. Han, "Refinement of brine for lithium extraction using ion concentration polarization," *Separation and Purification Technology*, 282,B, 120055 (2021).

A. Xiong, S. Kausahl, I. J. Tay, B. P. Engelward, J. Han, and P. R. Preiser, "MalariaCometChip for high-throughput quantification of DNA damage in Plasmodium falciparum," *Protocol*, 2(3), 100797 (2021).

T. Kwon, K. Choi, and J. Han, "Separation of Ultra-High Density Cell Suspension via Elasto-Inertial Microfluidics," *Small*, 17(39), 2101880, (2021).

H. Jeon, D.-H. Lee, B. Juni, M. Pinilla-Vera, R. M. Baron, B. D. Levy, J. Voldman, and J. Han, "Fully Automated, Sample-to-Answer Leukocyte Functional Assessment Platform for Continuous Sepsis Monitoring via Microliters of Blood," *ACS Sensors*, 6, 2747 (2021).

B. Juni, D.-H. Lee, H. Jeon, M. G. Duvall, J. Nijmeh, R.-E. E. Abdunour, M. Pinilla-Vera, R. M. Baron, J. Han, J. Voldman, and B. D. Levy, "Inflammation resolution circuits are uncoupled in acute sepsis and correlate with clinical severity," *JCI Insight*, 6(15),e148866, (2021).

Z. Liu, R. Screven, D. Yu, L. Boxer, M. Meyers, J. Han, and L. Devireddy, "Microfluidic separation of canine adipose-derived mesenchymal Stromal cells," *Tissue Engineering Part C: Methods*, 27(8), 10.1089/ten.tec.2021.0082 (2021).

J. Yoon, M. T. Flavin, and J. Han, "Current efficiency and selectivity reduction caused by co-ion leakage in electromembrane processes," *Water Research*, 201, 117351, (2021).

I. Shrivastava, E. Eric Adams, B. Al-Anzi, A. C. Chow, and J. Han, "Confined plunging liquid jets for dilution of brine from desalination plants," *Processes*, 9(5), 856, (2021).

K. K. Zeming, R. Lu, K. L. Woo, G. Sun, K. Y. Quek, L. F. Chow, C.-H. Chen, J. Han, and S. L. Lim, "Multiplexed Single-Cell Leukocyte Enzymatic Secretion Profiling from Whole Blood Reveals Patient-Specific Immune Signature," *Analytical Chemistry*, 93, 10, 4374-4382, (2021).

Ruonan Han

Associate Professor
Department of Electrical Engineering & Computer Science

Integrated circuits and systems operating from RF to THz frequencies for sensing and communication applications. Electromagnetism, Chip-scale wave-matter interactions for miniature spectroscopy and frequency metrology.

Rm. 39-527A | 617-324-5281 | ruonan @ mit.edu

GRADUATE STUDENTS

Xibi Chen, EECS
Mohamed Elsheikh, EECS
Mohamed I. Ibrahim, EECS
Muhammad I. Khan, EECS
Mina Kim, EECS (Co-supervised with Hae-Seung Lee)
Eunseok Lee (Co-supervised with Anantha Chandrakasan)
Nathan Monroe, EECS
Jinchen Wang, EECS
Alec Yen, EECS

UNDERGRADUATE STUDENTS

Reed Foster, EECS
Shiqi Chen, EECS

SUPPORT STAFF

Kathleen Brody, Administrative Assistant

SELECTED PUBLICATIONS

M. I. W. Khan, E. Lee, N. Monroe, A. Chandrakasan, and R. Han, "A Dual-Antenna, 263GHz Energy Harvester in CMOS for Ultra-Miniaturized Platforms with 13.6% RF-to-DC Conversion Efficiency at -8dBm Input Power," *IEEE Radio-Frequency Integrated Circuit Symposium (RFIC)*, Denver, CO, Jun. 2022.

M. Kim, C. Wang, L. Yi, H. Lee, and R. Han, "A Sub-THz CMOS Molecular Clock with 20 ppt Stability at 10,000 s Based on A Dual-Loop Spectroscopic Detection and Digital Frequency Error Integration," *IEEE Radio-Frequency Integrated Circuit Symposium (RFIC)*, Denver, CO, Jun. 2022.

Q. Yu, G. Kim, J. Garrett, D. Thomson, G. Dogiamis, N. M. Monroe, R. Han, Y. Ma, J. Waldemer, Y. S. Nam, G. Beltran, V. Neeli, S. Ravikumar, S. Rami, C. Pelto, and E. Karl, "Low-Loss On-Chip Passive Circuits Using C4 Layer for RF, mmWave and sub-THz Applications," *IEEE International Microwave Symposium (IMS)*, Denver, CO, Jun. 2022.

M. I. W. Khan, J. Woo, X. Yi, M. I. Ibrahim, R. T. Yazicigil, A. P. Chandrakasan, and R. Han, "A 0.31-THz Orbital-Angular-Momentum (OAM) Wave Transceiver in CMOS With Bits-to-OAM Mode Mapping," *IEEE J. of Solid-State Circuits, RFIC Special Issue*, 2022. (Invited)

X. Li, W. Chen, S. Li, Y. Wang, F. Huang, X. Yi, R. Han, and Z. Feng, "A High-Efficiency 142-182 GHz SiGe BiCMOS Power Amplifier With Broadband Slotline-Based Power Combining Technique," *IEEE J. of Solid-State Circuits*, 2022.

N. M. Monroe, G. C. Dogiamis, R. Stingel, P. Myers, X. Chen, and R. Han, "Electronic THz Pencil Beam Forming and 2D Steering for High Angular-Resolution Operation: A 98×98 Unit, 265GHz CMOS Reflectarray with In-Unit Digital Beam Shaping and Squint Correction," *IEEE International Solid-State Circuit Conf. (ISSCC)*, San Francisco, CA, Feb. 2022.

X. Chen, M. I. Wasiq Khan, X. Yi, X. Li, W. Chen, J. Zhu, Y. Yang, K. E. Kolodziej, N. M. Monroe, and R. Han, "A 140GHz Transceiver with Integrated Antenna, Inherent-Low-Loss Duplexing and Adaptive Self-Interference Cancellation for FMCW Monostatic Radar," *IEEE International Solid-State Circuit Conf. (ISSCC)*, San Francisco, CA, Feb. 2022.

X. Li, W. Chen, S. Li, H. Wu, X. Yi, R. Han, and Z. Feng, "A 110-to-130GHz SiGe BiCMOS Doherty Power Amplifier with Slotline-Based Power Combining Technique Achieving >22dBm Saturated Output Power and >10% Power Back-Off Efficiency," *IEEE International Solid-State Circuit Conf. (ISSCC)*, San Francisco, CA, Feb. 2022.

X. Yi, C. Wang, Z. Hu, J. Holloway, M. I. Khan, M. Ibrahim, M. Kim, G. Dogiamis, B. Perkins, M. Kaynak, R. Yazicigil, A. Chandrakasan, and R. Han, "Emerging Terahertz Integrated Systems in Silicon," *IEEE Transactions on Circuits and Systems-I*, vol. 68, no. 9, Sept. 2021. (Invited)

M. I. W. Khan, J. Woo, X. Yi, M. Ibrahim, R. Yazicigil, A. Chandrakasan, and R. Han, "A 0.31THz CMOS Uniform Circular Antenna Array Enabling Gen- eration/Detection of Waves with Orbital-Angular Momentum," *IEEE Radio-Frequency Integrated Circuit Symp. (RFIC)*, Atlanta, GA, Jun. 2021. (Best Student Paper Award).

L. Yi, H. Javadi, W. Zhang, J. Mckelvy, M. Kim, A. Yen, and R. Han, "Sub-Terahertz Heterodyne Spectroscopy of Carbonyl Sulfide," *IEEE International Frequency Control Symposium (IFCS)*, Jul. 2021.

Song Han
Associate Professor
Department of Electrical Engineering & Computer Science

Machine learning, artificial intelligence, model compression, hardware accelerator, domain-specific architecture.

Rm. 38-344 | 617-253-0086 | songhan @ mit . edu

POSTDOCTORAL ASSOCIATES
Wei-Ming Chen, EECS
Wei-Chen Wang, EECS

GRADUATE STUDENTS
Han Cai, EECS
Ji Lin, EECS
Yujun Lin, EECS
Zhijian Liu, EECS
Haotian Tang, EECS
Hanrui Wang, EECS
Zhekai Zhang, EECS
Ligeng Zhu, EECS

UNDERGRADUATE STUDENTS
Kevin Shao, EECS

SUPPORT STAFF
Jami L. Mitchell, Administrative Assistant

SELECTED PUBLICATIONS

J. Lin, W. Chen, H. Cai, C. Gan, and S. Han, "MCUNet-v2: Memory-Efficient Inference for Tiny Deep Learning," *Neural Information Processing System(NeurIPS)*, 2021.

L. Zhu, H. Lin, Y. Lu, Y. Lin, and S. Han, "Delayed Gradient Averaging: Tolerate the Communication Latency for Federated Learning," *Neural Information Processing System(NeurIPS)*, 2021.

Y. Lin, Z. Zhang, H. Tang, H. Wang, and S. Han, "PointAcc: Efficient Point Cloud Accelerator," *International Symposium on Microarchitecture (MICRO)*, 2021.

Y. Lin, M. Yang, and S. Han, "NAAS: Neural Accelerator Architecture Search," *Design Automation Conference (DAC)*, 2021.

Y. Ding, L. Zhu, Z. Jia, G. Pekhimenko, and S. Han, "IOS: Inter-Operator Scheduler For CNN Acceleration,"*Conference on Machine Learning and Systems (MLSys)*, 2021.

J. Lin, W.-M. Chen, Y. Lin, J. Cohn, C. Gan, and S. Han, "MCUNet: Tiny Deep Learning on IoT Devices," *Neural Information Processing System(NeurIPS)*, spotlight presentation, 2020.

H. Cai, C. Gan, L. Zhu, and S. Han, "Tiny Transfer Learning: Reduce Activations, not Trainable Parameters for Efficient On-Device Learning," *Neural Information Processing System (NeurIPS)*, 2020.

S. Zhao, Z. Liu, J. Lin, J. Zhu, and S. Han, "Differentiable Augmentation for Data-Efficient GAN Training," *Neural Information Processing System (NeurIPS)*, 2020.

H. Cai, C. Gan, T. Wang, Z. Zhang, and S. Han, "Once For All: Train One Network and Specialize It for Efficient Deployment," *International Conference on Learning Representations (ICLR)*, 2020.

H. Wang, K. Wang, J. Yang, L. Shen, N. Sun, H.-S. Lee, and S. Han, "Transferable Transistor Sizing with Graph Neural Networks and Reinforcement Learning," *Design Automation Conference (DAC)*, 2020.

Z. Zhang, H. Wang, S. Han, and B. Dally, "SpArch: Efficient Architecture for Sparse Matrix Multiplication," *International Symposium on High-Performance Computer Architecture (HPCA)*, 2020.

Z. Liu, H. Tang, Y. Lin, and S. Han, "Point Voxel CNN for Efficient 3D Deep Learning," *Neural Information Processing System (NeurIPS)*, Spotlight presentation.2019.

L. Zhu, Z. Liu, and S. Han, "Deep Leakage from Gradients," *Neural Information Processing System (NeurIPS)*, 2019.

J. Lin, C. Gan, and S. Han, "TSM: Temporal Shift Module for Efficient Video Understanding," *International Conference on Computer Vision (ICCV)*, 2019.

H. Cai, L. Zhu, and S. Han, "ProxylessNAS: Direct Neural Architecture Search on Target Task and Hardware," *International Conference on Learning Representations (ICLR)*, 2019.

Juejun (JJ) Hu

Associate Professor
Department of Materials Science & Engineering

Integrated photonics, optical thin films, glass and amorphous materials, siliconphotonics, light management in photovoltaics, magneto-optical isolation,integration on unconventional substrates (polymers, optical crystals, 2-D materials, etc.), infrared imaging, spectroscopy, metasurface.

Rm. 13-4054 | 302-766-3083 | hujuejun @ mit . edu

RESEARCH SCIENTIST

Tian Gu, MRL

POSTDOCTORAL ASSOCIATES

Sensong An, DMSE
Diana Mojahed, DMSE
Mikhail Shalaginov, DMSE
Hung-I Lin, DMSE
Louis Martin, DMSE

GRADUATE STUDENTS

Cosmin Constantin Popescu, DMSE
Tushar Karnik, DMSE
Gillian Micale, DMSE
Luigi Ranno, DMSE
Fan Yang, DMSE
Khoi Phuong Dao, DMSE
Brian Mills, DMSE
Maarten Peters, DMSE

VISITOR

Samuel Serna, Bridgewater State University

SUPPORT STAFF

Sandra Crawford, Administrative Assistant

SELECTED PUBLICATIONS

Y. Zhang, C. Fowler, J. Liang, B. Azhar, M. Shalaginov, S. Deckoff-Jones, S. An, J. Chou, C. Roberts, V. Liberman, M. Kang, C. Ríos, K. Richardson, C. Rivero-Baleine, T. Gu, H. Zhang, and J. Hu, "Electrically Reconfigurable Nonvolatile Metasurface Using Low-Loss Optical Phase Change Material," *Nat. Nanotechnol.* vol. 16, pp. 661-666, 2021.

S. Yu, J. Lu, V. Ginis, S. Kheifets, S. Lim, M. Qiu, T. Gu, J. Hu, and F. Capasso, "On-chip optical tweezers based on freeform optics, "On-chip optical tweezers based on freeform optics," *Optica*, vol. 8, pp. 409-414, 2021.

M. Shalaginov, S. An, Y. Zhang, F. Yang, P. Su, V. Liberman, J. Chou, C. Roberts, M. Kang, C. Ríos, Q. Du, C. Fowler, A. Agarwal, K. Richardson, C. Rivero-Baleine, H. Zhang, J. Hu, and T. Gu, "Reconfigurable all-dielectric metalens with diffraction limited performance," *Nat. Commun.*, vol. 12, pp. 1225, 2021.

M. Shalaginov, S. An, F. Yang, P. Su, D. Lyzwa, A. Agarwal, H. Zhang, J. Hu, and T. Gu, "Single-Element Diffraction-Limited Fisheye Metalens," *Nano Lett.*, vol. 20, pp. 7429-7437, 2020.

Y. Zhang, J. Chou, J. Li, H. Li, Q. Du, A. Yadav, S. Zhou, M. Shalaginov, Z. Fang, H. Zhong, C. Roberts, P. Robinson, B. Bohlin, C. Rios, H. Lin, M. Kang, T. Gu, J. Warner, V. Liberman, K. Richardson, and J. Hu, "Broadband Transparent Optical Phase Change Materials for High-Performance Nonvolatile Photonics," *Nat. Commun.*, Vol. 10, pp. 4279, 2019.

Y. Zhang, Q. Du, C. Wang, T. Fakhrul, S. Liu, L. Deng, D. Huang, P. Pintus, J. Bowers, C. A. Ross, J. Hu, and L. Bi, "Monolithic Integration of Broadband Optical Isolators for Polarization-diverse Silicon Photonics," *Optica*, vol. 6, pp. 473-478, 2019.

D. Kita, B. Miranda, D. Favela, D. Bono, J. Michon, H. Lin, T. Gu, and J. Hu, "High-performance and Scalable On-chip Digital Fourier Transform Spectroscopy," *Nat. Commun.*, vol. 9, pp. 4405, 2018.

D. Kita, J. Michon, S. G. Johnson, and J. Hu, "Are Slot and Sub-wavelength Grating Waveguides Better than Strip Waveguides for Sensing?" *Optica*, vol. 5, pp. 1046-1054, 2018.

L. Zhang, J. Ding, H. Zheng, S. An, H. Lin, B. Zheng, Q. Du, G. Yin, J. Michon, Y. Zhang, Z. Fang, M. Shalaginov, L. Deng, T. Gu, H. Zhang, and J. Hu, "Ultra-thin, High-efficiency mid-Infrared Transmissive Huygens Meta-optics," *Nat. Commun.*, vol. 9, pp. 1481, 2018.

L. Li, H. Lin, Y. Huang, R. Shiue, A. Yadav, J. Li, J. Michon, D. Englund, K. Richardson, T. Gu, and J. Hu, "High-performance Flexible Waveguide-integrated Photodetectors," *Optica*, vol. 5, pp. 44-51, 2018.

L. Li, H. Lin, S. Qiao, Y. Huang, J. Li, J. Michon, T. Gu, C. Ramos, L. Vivien, A. Yadav, K. Richardson, N. Lu, and J. Hu, "Monolithically Integrated Stretchable Photonics," *Light Sci. Appl.*, vol. 7, e17138, 2018.

H. Lin, Y. Song, Y. Huang, D. Kita, S. Deckoff-Jones, K. Wang, L. Li, J. Li, H. Zheng, Z. Luo, H. Wang, S. Novak, A.Yadav, C. Huang, R. Shiue, D. Englund, T. Gu, D. Hewak, K. Richardson, J. Kong, and J. Hu, "Chalcogenide Glass-on-Graphene Photonics," *Nat. Photonics*, vol. 11, pp. 798-805, 2017.

Qing Hu

Professor

Department of Electrical Engineering & Computer Science

Physics and applications of millimeter-wave, terahertz, and infrared devices.

Rm. 36-465 | 617-253-1573 | qhu @ mit . edu

COLLABORATORS

Jianrong Gao, Delft University
John L. Reno, Sandia National Lab.
Zbig Wasilewski, University of Waterloo
Gerard Wysocki, Princeton University
Kevin Lascola, Thorlabs

POSTDOCTORAL ASSOCIATES

Ali Khalatpour, RLE

GRADUATE STUDENTS

Theodore Letsou, EECS
Andrew Paulsen, EECS
Tianyi Zeng, EECS

SUPPORT STAFF

Shayne Fernandes, Administrative Assistant

SELECTED PUBLICATIONS

A. Khalatpour, A. K. Paulsen, C. Deimert, Z. R. Wasilewski, and Qing Hu, "High power portable terahertz laser systems," *Nat. Phot.* 15, 16-20, 2021.

B. Mirzaei, Y. Gan, M. Finkel, C. Groppi, A. Young, C. Walker, A. Khalatpour, Q. Hu, and J. R. Gao, "4.7 THz asymmetric beam multiplexer for GUSTO," *Opt. Ex.* 29, 24434 (2021).

Q. Hu, "High power portable THz laser systems," *International Symposium on Terahertz Frontier Progress 2021*, Shanghai, China, Jan. 5-6, 2021. (Invited)

Q. Hu, "Development of high-temperature THz QCLs ," *2021 CLEO*, San Jose, May 9-14, 2021. (Invited)

Rafael Jaramillo

Thomas Lord Associate Professor of Materials Science and Engineering
Department of Material Science and Engineering

Developing compound semiconductors for application to photonics, electronics, and energy conversion. Emphasis on lesser-studied materials, chalcogenide thin film processing including molecular beam epitaxy (MBE), and advanced characterization.

Rm. 13-5025 | 617-324-6871 | rjaramil @ mit . edu

POSTDOCTORAL ASSOCIATES

Wouter Mortelmans, DMSE
Ida Sadeghi, MRL

GRADUATE STUDENTS

Jiahao Dong, DMSE
Yifei Li, DMSE
Jack van Sambeek, DMSE
Kevin Ye, DMSE

SELECTED PUBLICATIONS

S. S. Jo, C. Wu, L. Zhu, L. Yang, M. Li, and R. Jaramillo, "Photonic Platforms Using In-Plane Optical Anisotropy of Tin (II) Selenide and Black Phosphorus," *Advanced Photonics Research* 2, 2100176 (2021).

Y. Li, Y. Wu, H. Yu, I. Takeuchi, and R. Jaramillo, "Deep Learning for Rapid Analysis of Spectroscopic Ellipsometry Data," *Advanced Photonics Research* 2, 2100147 (2021).

I. Sadeghi, K. Ye, M. Xu, Y. Li, J. M. LeBeau, and R. Jaramillo, "Making $BaZrS_3$ Chalcogenide Perovskite Thin Films by Molecular Beam Epitaxy," *Advanced Functional Materials* 31, 2105563 (2021).

H. Yin, A. Kumar, J. M. LeBeau, R. Jaramillo, "Defect-Level Switching for Highly Nonlinear and Hysteretic Electronic Devices," *Phys. Rev. Applied* 15, 014014 (2021).

S. S. Jo, A. Singh, L. Yang, S. C. Tiwari, S. Hong, A. Krishnamoorthy, M. G. Sales, S. M. Oliver, J. Fox, R. L. Cavalero, D. W. Snyder, P. M. Vora, S. J. McDonnell, P. Vashishta, R. K. Kalia, A. Nakano, and R. Jaramillo, "Growth Kinetics and Atomistic Mechanisms of Native Oxidation of ZrS_xSe_{2-x} and MoS_2 Crystals," *Nano Letts.* 20, 8592–8599 (2020).

A. Singh, S. S. Jo, Y. Li, C. Wu, M. Li, and R. Jaramillo, "Refractive Uses of Layered and Two-Dimensional Materials for Integrated Photonics," *ACS Photonics* 7, 3270–3285 (2020).

S. Filippone, B. Zhao, S. Niu, N. Z. Koocher, D. Silevitch, I. Fina, J. M. Rondinelli, J. Ravichandran, and R. Jaramillo, "Discovery of highly polarizable semiconductors $BaZrS_3$ and $Ba_3Zr_2S_7$. *Phys. Rev. Materials* 4, 091601 (2020).

Long Ju

Assistant Professor of Physics
Department of Physics

Two-dimensional materials, optical spectroscopy, optoelectronics.

Rm. 13-2005 | 617-253-4828 | longju @ mit . edu

POSTDOCTORAL ASSOCIATES

Tianyi Han, MRL
Varun Kamboj, Physics
Zhengguang Lu, Physics
Fangzhou Xia, Physics

GRADUATE STUDENTS

Tonghang Han, Physics
Junseok Seo, Physics
Jixiang Yang, Physics

UNDERGRADUATE STUDENT

Christopher Tong, Physics
Yuqing Xie, Physics

SUPPORT STAFF

Gerry Miller, Administrative Assistant

SELECTED PUBLICATIONS

J. Yang, G. Chen, T. Han, Q. Zhang, Y.-H. Zhang, L. Jiang, B. Lyu et al, "Spectroscopy signatures of electron correlations in a trilayer graphene/hBN moiré superlattice," *Science* 375, no. 6586 (2022): 1295-1299.

Z. Lu, P. Hollister, M. Ozerov, S. Moon, E. D. Bauer, F. Ronning, D. Smirnov, L. Ju, and B. J. Ramshaw, "Weyl Fermion magneto-electrodynamics and ultralow field quantum limit in TaAs," *Science Advances* 8, no. 2 (2022): eabj1076.

T. Han, J. Yang, Q. Zhang, L. Wang, K. Watanabe, T. Taniguchi, P. L. McEuen, L. Ju "Accurate measurement of the gap of graphene/hBN moiré superlattice through photocurrent spectroscopy," *Physical Review Letts.*, 2021.

L. Ju, L. Wang, X. Li, F. Zhang, S. Moon, Z. Lu, K. Watanabe, T. Taniguchi, D. Smirnov, F. Rana, and P. L. McEuen, "Unconventional valley-dependent optical selection rules and Landau level mixing in bilayer graphene," *Nature Communications*, 2020.

L. Ju, L. Wang, T. Cao, T. Taniguchi, K. Watanabe, S. G. Louie, F. Rana, et al. "Tunable excitons in bilayer graphene," *Science* 358, no. 6365 (2017): 907-910.

L. Jiang, Z. Shi, B. Zeng, S. Wang, J.-H. Kang, T. Joshi, C. Jin et al, "Soliton-dependent plasmon reflection at bilayer graphene domain walls," *Nature Materials* 15, no. 8 (2016): 840-844.

J. Velasco Jr., L. Ju, D. Wong, S. Kahn, J. Lee, H.-Z. Tsai, C. Germany et al., "Nanoscale control of rewriteable doping patterns in pristine graphene/boron nitride heterostructuresm," *Nano Letts.* 16, no. 3 (2016): 1620-1625.

D. Wong, J. Velasco Jr., L. Ju, J. Lee, S. Kahn, H.-Z. Tsai, C. Germany et al., "Characterization and manipulation of individual defects in insulating hexagonal boron nitride using scanning tunnelling microscopy," *Nature Nanotechnology* 10, no. 11 (2015): 949.

L. Ju, Z. Shi, N. Nair, Y. Lv, C. Jin, J. Velasco Jr., C. Ojeda-Aristizabal et al. "Topological valley transport at bilayer graphene domain walls," *Nature* 520, no. 7549 (2015): 650-655.

Y.-Q. Bie, J. Horng, Z. Shi, L. Ju, Q. Zhou, A. Zettl, D. Yu, and F. Wang, "Vibrational spectroscopy at electrolyte/electrode interfaces with graphene gratings," *Nature Communications* 6, no. 1 (2015): 1-6.

L. Ju, J. Velasco Jr., E. Huang, S. Kahn, C. Nosiglia, H.-Z. Tsai, W. Yang et al., "Photoinduced doping in heterostructures of graphene and boron nitride," *Nature Nanotechnology* 9, no. 5 (2014): 348.

Z. Shi, C. Jin, W. Yang, L. Ju, J. Horng, X. Lu, H. A. Bechtel et al., "Gate-dependent pseudospin mixing in graphene/boron nitride moiré superlattices," *Nature Physics* 10, no. 10 (2014): 743-747.

J. Lee, W. Bao, L. Ju, P. J. Schuck, F. Wang, and A. Weber-Bargioni, "Switching individual quantum dot emission through electrically controlling resonant energy transfer to graphene," *Nano Letts.* 14, no. 12 (2014): 7115-7119.

S.-F. Shi, T.-T. Tang, B. Zeng, L. Ju, Q. Zhou, A. Zettl, and F. Wang, "Controlling graphene ultrafast hot carrier response from metal-like to semiconductor-like by electrostatic gating," *Nano Letts.* 14, no. 3 (2014): 1578-1582.

K. F. Mak, L. Ju, F. Wang, and T. F. Heinz, "Optical spectroscopy of graphene: From the far infrared to the ultraviolet," *Solid State Communications* 152, no. 15 (2012): 1341-1349.

L. Ju, B. Geng, J. Horng, C. Girit, M. Martin, Z. Hao, H. A. Bechtel et al., "Graphene plasmonics for tunable terahertz metamaterials," *Nature Nanotechnology* 6, no. 10 (2011): 630.

Jeehwan Kim

Associate Professor of Mechanical Engineering
Associate Professor of Materials Science and Engineering
Principal Investigator of Research Laboratory of Electronics

Remote epitaxy, Two-dimensional materials, 2D material-based layer transfer, III-V / III-N electronics, Complex oxides-based applications, Heterogeneous integration, Flexible electronics, Electronic skin, Sensor fusion, Neuromorphic computing.

Rm. 38-276 | 617-324-1948 | jeehwan @ mit . edu

POSTDOCTORAL ASSOCIATES

Celesta S. Chang, MechE
Chanyeol Choi, RLE
Junseok Jeong, RLE
Jihoon Kang, RLE
Hyunseok Kim, MechE
Ki Seok Kim, RLE
Sangho Lee, MechE
Jiho Shin, MechE
Min-Kyu Song, MechE
Jun Min Suh, MechE

GRADUATE STUDENTS

Ne Myo Han, MechE
Doyoon Lee, MechE
Yunpeng Liu, MechE
Kuangye Lu, MechE
Kuan Qiao, MechE
Xinyuan Zhang, MSE

VISITOR

Dusik Bae, Samsung

SUPPORT STAFF

John Mayo, Administrative Assistant

SELECTED PUBLICATIONS

S. Choi, S. Tan, Z. Li, Y. Kim, C. Choi, P.-Y. Chen, H. Yeon, S. Yu, and J. Kim, "SiGe epitaxial memory for neuromorphic computing with reproducible high performance based on engineered dislocations," *Nature Materials*, Vol. 17, 335–340 (2018).

W. Kong, H. Li, K. Qiao, Y. Kim, K. Lee, Y. Nie, D. Lee, T. Osadchy, R. J. Molnar, D. K. Gaskill, R. L. Myers-Ward, K. M. Daniels, Y. Zhang, S. Sundram, Y. Yu, S.-H. Bae, S. Rajan, Y. Shao-Horn, K. Cho, A. Ougazzaden, J. C. Grossman, and Jeehwan Kim, "Polarity governs atomic interaction through two-dimensional materials," *Nature Materials*, Vol. 17, 999–1004 (2018).

J. Shim, S.-H. Bae, W. Kong, D. Lee, K. Qiao, D. Nezich, Y. J. Park, R. Zhao, S. Sundaram, X. Li, H. Yeon, C. Choi, H. Kum, R. Yue, G. Zhou, Y. Ou, K. Lee, J. Moodera, X. Zhao, J.-H. Ahn, C. Hinkle, A. Ougazzaden, and J. Kim, "Controlled crack propagation for atomic precision handling of wafer-scale two-dimensional materials," *Science*, Vol. 362, Issue 6415, 665-670 (2018).

S.-H. Bae, H. Kum, W. Kong, Y. Kim, C. Choi, B. Lee, P. Lin, Y. Park, and J. Kim, "Integration of bulk materials with two-dimensional materials for physical coupling and applications," *Nature Materials*, Vol. 18, 550–560 (2019).

W. Kong, H. Kum, S.-H. Bae, J. Shim, H. Kim, L. Kong, Y. Meng, K. Wang, C. Kim, and J. Kim, "Path towards graphene commercialization from lab to market," *Nature Nanotechnology*, Vol. 14, 927–938 (2019).

H. Kum, D. Lee, W. Kong, H. Kim, Y. Park, Y. Kim, Y. Baek, S.-H. Bae, K. Lee, and J. Kim, "Epitaxial growth and layer-transfer techniques for heterogeneous integration of materials for electronic and photonic devices," *Nature Electronics*, Vol. 2, 439–450 (2019).

H. S. Kum, H. Lee, S. Kim, S. Lindemann, W. Kong, K. Qiao, P. Chen, J. Irwin, J. H. Lee, S.n Xie, S. Subramanian, J. Shim, S.-H. Bae, C. Choi, L. Ranno, S. Seo, S. Lee, J. Bauer, H. Li, K. Lee, J. A. Robinson, C. A. Ross, D. G. Schlom, M. S. Rzchowski, C.-B. Eom, and J. Kim, "Heterogeneous integration of single crystalline complex-oxide membranes," *Nature*, Vol. 578, 75-81 (2020).

S.-H. Bae, K. Lu, Y. Han, S. Kim, K. Qiao, C. Choi, Y. Nie, H. Kim, H. S. Kum, P. Chen, W. Kong, B.-S. Kang, C. Kim, J. Lee, Y. Baek, J. Shim, J. Park, M. Joo, D. A. Muller, K. Lee, and J. Kim, "Graphene-assisted spontaneous relaxation towards dislocation-free heteroepitaxy," *Nature Nanotechnology*, Vol. 15, 272-276 (2020).

H. Yeon, P. Lin, C. Choi, S. H. Tan, Y. Park, D. Lee, J. Lee, F. Xu, B. Gao, H. Wu, H. Qian, Y. Nie, S. Kim, and J. Kim, "Alloying conducting channels for reliable neuromorphic computing," *Nature Nanotechnology*, Vol. 15, 574–579 (2020).

H. Yeon, H. Lee, Y. Kim, D. Lee, Y. Lee, J.-S. Lee, J. Shin, C. Choi, J.-H. Kang, J. M. Suh, H. Kim, H. S. Kum, J. Lee, D. Kim, K. Ko, B. S. Ma, P. Lin, S. Han, S. Kim, S.-H. Bae, T.-S. Kim, M.-C. Park, Y.-C. Joo, E. Kim, J. Han, and J. Kim, "Long-term reliable physical health monitoring by sweat pore–inspired perforated electronic skins," *Science Advances*, Vol. 7, Issue 27 (2021).

Sang-Gook Kim

Professor

Department of Mechanical Engineering

AI for Design and Manufacturing, MEMS Knowledge Representation

Rm. 1-306 | 617-452-2472 | sangkim @ mit . edu

VISITING RESEARCH STAFF

Sang-Hyun Lee, Hyundai Motor Co.

GRADUATE STUDENTS

Haluk Akay, MechE

Jack Gammack, MechE

UNDERGRADUATE STUDENT

Ceylan Ceylan, MechE

SUPPORT STAFF

Tony Pulsone, Administrative Assistant

SELECTED PUBLICATIONS

K. W. D.Araujo, S. Kohles, S.-G. Kim, H. A. Sanchez, "Affordance-Based Surgical Design Methods Considering Biomechanical Artifacts," *Ecological Psychology*, V. 33.1, 2021.

H. Akay, and S.-G. Kim, "Extracting Functional Requirements from Design Documentation using Machine Learning," *27th CIRP Design Conference*, Procedia CIRP Volume 50, 2021.

H. Akay, and S.-G. Kim, «Reading functional requirements using machine learning-based language processing," *CIRP Annals - Manufacturing Technology*, v70.1, 2021.

J. Gammack, H. Akay, C. Ceylan, S.G. Kim, "Semantic knowledge management system for design documentation with heterogeneous data using machine learning," *28th CIRP Design Conference*, Procedia CIRP, 2022 (in press).

Jing Kong

MTL Associate Director
Professor of Electrical Engineering
Department of Electrical Engineering & Computer Science

Synthesis, characterization and applications of low-dimensional materials, including carbon nanotube, graphene and other two dimensional materials.

Rm. 13-3065 | 617-324-4068 | jingkong @ mit . edu

RESEARCH SCIENTISTS

Xiang Ji, RLE

POSTDOCTORAL ASSOCIATES

Yunfan Guo, RLE
Nannan Mao, RLE
Ji-Hoon Park, RLE
Jiangtao Wang, RLE
Tianyi Zhang, RLE
Peng Wu, RLE

GRADUATE STUDENTS

Luiz Gustavo Pimenta Martins, Physics
Angyu Lu, EECS
Zhantao Chen, MechE
Zhien Wang, DMSE
Xudong (Sheldon) Zheng, EECS

VISITING STUDENTS

Shin-Yi Tang, RLE

SUPPORT STAFF

Arlene Wint, Administrative Assistant

SELECTED PUBLICATIONS

Y. Guo, E. Shi, J. Zhu, P.-C. Shen, J. Wang, Y. Lin, Y. Mao, S. Deng, B. Li, J.-H. Park, A.-Y. Lu, S. Zhang, Q. Ji, Z. Li, C. Qiu, S. Qiu, Q. Li, L. Dou, Y. Wu, J. Zhang, T. Palacios, A. Cao, and J. Kong, "Soft-lock drawing of super-aligned carbon nanotube bundles for nanometre electrical contacts," *Nature Nanotechnology*, 17 278-284 (2022).

P.-C. Shen, Y. Lin, C. Su, C. McGahan, A.-Y. Lu, X. Ji, X. Wang, H. Wang, N. Mao, Y. Guo, J.-H. Park, Y. Wang, W. Tisdale, J. Li, X. Ling, K. E. Aidala, T. Palacios, and J. Kong, "Healing of donor defect states in monolayer molybdenum disulfide using oxygen-incorporated chemical vapour deposition," *Nature Electronics*, 5, 28-36, (2022).

H. Wang, Z. Yao, G. S. Jung, Q. Song, M. Hempel, T. Palacios, G. Chen, M. J. Buehler, A. Aspuru-Guzik, and J. Kong, "Frank-van der Merwe growth in bilayer graphene," *Matter*, 4(10), 3339-3353 (2021).

Qi. Ji, C. Su, N. Mao, X. Tian, J.-C. Idrobo, J. Miao, W. A. Tisdale, A. Zettl, J. Li, and J. Kong, "Revealing the Brønsted-Evans-Polanyi relation in halide-activated fast MoS2 growth toward millimeter-sized 2D crystals," *Science Advances*, 7 (44), eabj3274 (2021).

M. Sun, J. Li, Q. Ji, Y. Lin, J. Wang, C. Su, M.-H. Chiu, Y. Sun, H. Si, T. Palacios, J. Lu, D. Xie, and J. Kong, "Anomalous heavy doping in chemical-vapor-deposited titanium trisulfide nanostructures," *Physical Review Materials*, 5 (9), 094002 (2021).

X. Ji, J. Zhao, S. M. Jung, A. I. H. Hrdina, M. J. Wolf, X. Yang, G. Vaartstra, H. Xie, S.-X. L. Luo, A.-Y. Lu, R. E. Welsch, E. N. Wang, L.-J. Li, and J. Kong, "Bottom-Up Synthesized All-Thermal-Catalyst Aerogels for Heat-Regenerative Air Filtration," *Nano Letts.*, 21(19), 8160-8165 (2021).

Y. Guo, Y. Lin, K. Xie, B. Yuan, J. Zhu, P.-C. Shen, A.-Y. Lu, C. Su, E. Shi, K. Zhang, C. H. Fu, H. Xu, Z. Cai, J.-H. Park, Q. Ji, J. Wang, X. Dai, X. Tian, S. Huang, L. Dou, L. Jiao, J. Li, Y. Yu, J.-C. Idrobo, T. Cao, T. Palacios, and J. Kong, "Designing artificial two-dimensional landscapes via atomic-layer substitution," *PNAS*, 118(32), e2106124118 (2021).

J.-H. Park, A.-Y. Lu, P.-C. Shen, B. G. Shin, H. Wang, N. Mao, R. Xu, S. J. Jung, D. Ham, K. Kern, Y. Han, and J. Kong, "Synthesis of High-Performance Monolayer Molybdenum Disulfide at Low Temperature," *Small Methods*, 5 (6), 2000720, (2021).

P.-C. Shen, C. Su, Y. Lin, A.-S. Chou, C.-C. Cheng, J.-H. Park, M.-H. Chiu, A.-Y. Lu, H.-L. Tang, M. M. Tavakoli, G. Pitner, X. Ji, Z. Cai, N. Mao, J. Wang, V. Tung, J. Li, J. Bokor, A. Zettl, C.-I. Wu, T. Palacios, L.-J. Li, and J. Kong, "Ultralow contact resistance between semimetal and monolayer semiconductors," *Nature*, 593 (7858), 211-217 (2021).

Jeffrey H. Lang

Vitesse Professor of Electrical Engineering
Department of Electrical Engineering & Computer Science

Analysis, design, and control of electro-mechanical systems with application to traditional rotating machinery and variable-speed drives, micro/nano-scale (MEMS/NEMS) sensors and actuators, flexible structures, and the dual use of actuators as force and motion sensors.

Rm. 10-176 | 617-253-4687 | lang @ mit . edu

POSTDOCTORAL RESEARCHERS

Jinchi Han, RLE
Apoorva Murarka, RLE

GRADUATE STUDENTS

Quang Kieu, EECS
Hunjoo Kim, LGO
Sajjad Mohammadiyangijeh, EECS
Tareq Saqr, LGO
Aaron Yeiser, EECS
John Zhang, MechE

UNDERGRADUATE STUDENTS

William Nolan, EECS

SUPPORT STAFF

Donna Gale, Administrative Assistant
Arlene Wint, Administrative Assistant

SELECTED PUBLICATIONS

P. Garcha, V. Schaffer, S. Ramaswamy, B. Haroun, J. Wieser, J. H. Lang, and A. P. Chandrakasan, "A 770 kS/s integrated-fluxgate magnetometer with duty cycling for contactless current sensing," *Proceedings: International Solid-State Circuits Conference*, 80-81, San Francisco, CA, Feb. 14-18, 2021.

N. X. Wang, H. W. Wang, J. Mei, S. Mohammadi, J. Moon, J. H. Lang, and J. L. Kirtley, "Robust wireless power transfer system based on rotating fields for multi-user charging," *IEEE Transactions on Energy Conversion*, 36, 693-702, Jun. 2021.

U. Radhakrishna, Y. Yang, A. B. Shin and J. H. Lang, "Resource allocation in Vibration energy harvesters," *IEEE/ASME J. of Microelectromechanical Systems*, 30, 744-750, Oct. 2021.

E. Ng, J. D. Boles, J. H. Lang and D. J. Perreault, "Non-isolated DC-DC converter implementations based on piezoelectric transformers," *Proceedings: IEEE ECCE*, 1749-1756, Vancouver, CA, Oct 10-14, 2021.

B. G. Cary, J. Z. Zhang, C. I. McHugh, I. Kymisses, E. S. Olson, H. H. Nakajima and J. H. Lang, "An implantable umbo microphone for fully-implantable assistive hearing devices," *Proceedings: IEEE Sensors Conference*, 1-4, Virtual, Oct. 31 - Nov. 4, 2021.

S. Zhao, U. Radhakrishna, J. H. Lang, and D. Buss, "Low-voltage broadband piezoelectric vibration energy harvesting enabled by a highly-coupled harvester and tunable PSSHI circuit," *Smart Materials and Structures*, 30, 125030, Nov. 2021.

J. Bonavia, J. D. Boles, J. H. Lang, and D. J. Perreault, "Augmented piezoelectric resonators for power conversion," *Proceedings: IEEE COMPEL Workshop*, 1-8, Cartagena, Columbia, Nov. 2-5, 2021.

J. Piel, J. D. Boles, J. H. Lang, and D. J. Perreault, "Feedback control for a piezoelectric-resonator-based DC-DC power converter," *Proceedings: IEEE COMPEL Workshop*, 1-8, Cartagena, Columbia, Nov. 2-5, 2021.

M. M. Qasim, D. M. Otten, J. H. Lang, J. L. Kirtley, and D. J. Perreault, "Comparison of inverter topolgies for high-speed motor drive applications," *Proceedings: IEEE COMPEL Workshop*, 1-8, Cartagena, Columbia, Nov. 2-5, 2021.

J. D. Boles, E. Ng, J. H. Lang, and D. J. Perreault, "DC-DC converter implementations based on piezoelectric transformers," *IEEE J. of Emerging and Selected Topics in Power Electronics*, Nov. 16, 2021.

J. Han, Z. Nelson, M. R. Chua, T. M. Swager, F. Niroui, J. H. Lang, and V. Bulovic, "Molecular platform for fast low-voltage nanoelectromechanical switching," *Nano Letts.*, 21, 10244-10251, Dec. 7, 2021.

J. Han, J. H. Lang, and V. Bulovic, "A thin-film piezoelectric speaker based on an active microstructure array," *Proceedings: IEEE MEMS Workshop*, 852-855, Tokyo, Japan, Jan. 9-13, 2022.

J. Zhang, B. Cary, H. H. Nakajima, E. S. Olson, and J. H. Lang, "A PVDF-TrFE intracochlear hydrophone and amplifier for totally implantable cochlear implants," *Proceedings: IEEE MEMS Workshop*, 408-11, Tokyo, Japan, Jan. 9-13, 2022.

J. D. Boles, J. Bonavia, P. Acosta, Y. Ramadass, J. H. Lang, and D. J. Perreault, "Evaluating piezoelectric materials and vibration modes for power conversion," *IEEE Transactions on Power Electronics*, 37, 3374-3390, Mar. 2022.

Hae-Seung Lee

Director of Microsystems Technology Laboratories
Director of Center for Integrated Circuits and Systems
ATSC Professor of Electrical Engineering & Computer Science
Department of Electrical Engineering & Computer Science

Analog and Mixed-signal Integrated Circuits, with a Particular Emphasis in Data Conversion Circuits in scaled CMOS.

Rm. 39-521 | 617-253-5174 | hslee @ mtl . mit . edu

POSTDOCTORAL ASSOCIATE

Anand Chandrasekhar, EECS

GRADUATE STUDENTS

Ruicong Chen, EECS
Rebecca Ho, EECS
Mina Kim, EECS
Jaehwan Kim, EECS
Rishabh Mittal, EECS
Vipasha Mittal, EECS

SUPPORT STAFF

Elizabeth Green, Sr. Administrative Assistant
Elizabeth Kubicki, Administrative Assistant

PUBLICATIONS

J. Seo, H.-S. Lee, and C. Sodini, "Non-invasive Evaluation of a Carotid Arterial Pressure Waveform Using Motion-Tolerant Ultrsound Measurements During Valsalva Maneuver," *IEEE J. of Biomedical and Health Informatics,* vol. 25, pp. 163-174, Jan. 2021

T. Jeong, A. Chandrakasan, and H.-S. Lee, "S2ADC: A 12-bit, 1.25MS/s Secure SAR ADC with Power Side-Channel Attack Resistance," *IEEE J. Solid-State Circuits,* vol. SC-53, pp. 844-854 Mar. 2021.

M. Kim, C. Wang, L. Yi, H.-S. Lee, and R. Han, "A Sub-THz CMOS Molecular Clock with 20 ppt Stability at 10,000 s Based on A Dual-Loop Spectroscopic Detection and Digital Frequency Error Integration," to appear in *2022 IEEE RFIC*, Jun. 19-21, 2022, Denver, CO.

R. Chen, A. Chandrakasan, and H.-S. Lee, "RaM-SAR: A Low Energy and Area Overhead, 11.3fJ/conv.-step. 12b 25MS/s Secure Random-mapping SAR ADC with Power and EM Side-channel Attack Protection," to appear in *2022 IEEE Symposium on VLIS Circuits*, Jun. 12-17, 2022, Hawaii, HI.

H.-S. Lee and D. Daly, "Push-pull dynamic amplifier circuits," U.S. Patent 10,951,184, Mar. 16, 2021

H.-S. Lee, "Analog current memory with droop compensation," U.S. Patent 11,031,090, Jun. 8, 2021

H.-S. Lee, "Photo receiver circuits", U.S. Patent 11,067,439, Jul. 20, 2021

H.-S. Lee, "Constant level-shift buffer amplifier circuits," U.S. Patent 11,114,986, Sep. 7, 2021

Luqiao Liu

Associate Professor
Department of Electrical Engineering & Computer Science

Spintronics; spin based logic and memory device; nanoscale magnetic material for information storage and microwave application; fabrication technique of magnetic nanodevices; spin related phenomena in semiconductor, topological insulator, superconductors and low dimensional material; magnetic dynamics

Rm. 39-553a | 617-253-0019 | luqiao @ mit . edu

GRADUATE STUDENTS

Taqiyyah Safi, EECS
Justin Hou, EECS
Pengxiang Zhang, EECS
Josh Chou, Physics
Brooke C McGoldrick, EECS
Zhongqiang Hu, EECS
Qiuyuan Wang, EECS

SUPPORT STAFF

Elizabeth Green, Administrative Assistant

SELECTED PUBLICATIONS

D. D. Awschalom, C. H. R. Du, R. He, J. Heremans, A. Hoffmann, J. Hou, H. Kurebayashi, Y. Li, L. Liu, V. Novosad, J. Sklenar, S. Sullivan, D. Sun, H. Tang, V. Tyberkevych, C. Trevillian, A. W. Tsen, L. Weiss, W. Zhang, X. Zhang, L. Zhao, and C. W. Zollitsch, "Quantum engineering with hybrid magnonics systems and materials," *IEEE Transactions on Quantum Engineering*, 1-1, (2021).

Y. Fan, J. Finley, M. E. Holtz, P. Quarterman, A. J. Grutter, J. Han, P. Zhang, T. S. Safi, J. T. Hou, and L. Q. Liu, "Resonant spin transmission mediated by magnons in a magnetic insulator," *Advanced Materials*, 2008555 (2021).

Q. Shao, P. Li, L. Liu, H. Yang, S. Fukami, A. Razavi, H. Wu, K. Wang, F. Freimuth, Y. Mokrousov, M. D. Stiles, S. Emori, A. Hoffmann, J. Åkerman, K. Roy, J. P. Wang, S. H. Yang, K. Garello, and W. Zhang, "Roadmap of Spin–Orbit Torques," *IEEE Transactions on Magnetics* 57, 1 (2021).

J. Han, and L. Liu, "Topological insulators for efficient spin-orbit torques," *APL Materials* 9, 060901 (2021).

B. Khurana, J. J. Bauer, P. Zhang, T. Safi, C.-T. Chou, J. T. Hou, T. Fakhrul, Y. Fan, L. Liu, and C. A. Ross, "Magnetism and spin transport in platinum/scandium-substituted terbium iron garnet heterostructures" *Physical Review Materials* 5, 084408 (2021).

J. T. Hou, P. Zhang, and L. Liu, "Proposal for a Spin-Torque-Oscillator Maser Enabled by Microwave Photon-Spin Coupling," *Physical Review Applied* 16, 034034 (2021).

J. Han, Y. Fan, B. C. McGoldrick, J. Finley, J. T. Hou, P. Zhang, and L. Liu, "Nonreciprocal Transmission of Incoherent Magnons with Asymmetric Diffusion Length," *Nano Letts.* 21, 7037 (2021).

J. Han, B. C. McGoldrick, C.-T. Chou, T. S. Safi, J. T. Hou, and L. Liu, "Current-induced switching of a ferromagnetic Weyl semimetal Co_2MnGa," *Applied Physics Letts.* 119, 212409 (2021).

B. C. McGoldrick, J. Z. Sun, and L. Liu, "Ising Machine Based on Electrically Coupled Spin Hall Nano-Oscillators," *Physical Review Applied* 17, 014006 (2022).

Scott R. Manalis

David H. Koch Professor in Engineering
Departments of Biological and Mechanical Engineering

Development and application of novel single-cell measurement approaches with a primary focus on cancer research.

Rm. 76-261 | 617-253-5039 | srm @ mit . edu

POSTDOCTORAL ASSOCIATES

Chuyi Chen, KI
Georgios (Yorgos) Katsikis, KI
Teemu Miettinen, KI
Peter Winter, KI
Yanqi Wu, KI
Jiaquan (Jason) Yu, KI
Ye Zhang, KI

GRADUATE STUDENTS

Sarah Duquette, BE
Adam Langenbucher, SB
Alex Miller, HST
Felicia Rodriguez, BE
Weida (Richard) Wu, BE

UNDERGRADUATE STUDENTS

Sofia Flores, BE
Zak Zhang, BE

RESEARCH STAFF

Christina Bray, KI
Sarah Ishamuddin, KI
Lin Lin, KI
Jennifer Yoon, KI

SUPPORT STAFF

Mariann Murray, Administrative Assistant

SELECTED PUBLICATIONS

G. Katsikis, I. E. Hwang, W. Wang, V. S. Bhat, N. L. McIntosh, O. A. Karim, B. J. Blus, S. Sha, V. Agache, J. M. Wolfrum, S. L. Springs, A. J. Sinskey, P. W. Barone, R. D. Braatz, and S. R. Manalis, "Weighing the DNA content of Adeno-Associated Virus vectors with zeptogram precision using nanomechanical resonators," *Nano Letts.*, 22(4), 2022.

M. A. Stockslager, S. Malinowski, M. Touat, J.C. Yoon, J. Geduldig, M. Mirza, A. S. Kim, P. Y. Wen, K. H. Chow, K. L. Ligon, S. R. Manalis, "Functional drug susceptibility testing using single-cell mass predicts treatment outcome in patient-derived cancer spheroid models," *Cell Reports*, 37(1) 2021.

B. Hamza, A. B. Miller, L. Meier, M. Stockslager, S. R. Ng, E. M. King, L. Lin, K.L. DeGouveia, N. Mulugeta, N.L. Calistri, H. Strouf, C. Bray, F. Rodriguez, W. A. Freed-Pastor, C. R. Chin, G. C. Jaramillo, M. L. Burger, R. A. Weinberg, A. K. Shalek, T. Jacks, and S. R. Manalis, "Measuring kinetics and metastatic propensity of CTCs by blood exchange between mice," *Nature Communications* 12, 2021.

G. Katsikis, J. F. Collis, S. M. Knudsen, V. Agache, J. E. Sader, and S. R. Manalis, "Inertial and viscous flywheel sensing of nanoparticles," *Nature Communications*, 12, 2021.

J. H. Kang, G. Katsikis, M. A. Stockslager, D. Lim, M. B. Yaffe, S. R. Manalis, and T. P. Miettinen, "Monitoring and Modeling of Lymphocytic Leukemia Cell Bioenergetics Reveals Decreased ATP Synthesis During Cell Division," *Nature Communications*, 11(1), 2020.

L. Mu, J. H. Kang, S. Olcum, K. R. Payer, N. L. Calistri, R.J. Kimmerling, S. R. Manalis, and T. P. Miettinen, "Mass Measurements During Lymphocytic Leukemia Cell Polyploidization Decouple Cell Cycle and Cell Size-dependent Growth," *PNAS*, 117(27), 2020.

M. Urbanska, H. E. Muñoz, J. S. Bagnall, O. Otto, S. R. Manalis, D. D. Carlo, and J. Guck, "A Comparison of Microfluidic Methods for High-throughput Cell Deformability Measurements," *Nature Methods*, 17(6), 2020.

M. Gagino, G. Katsikis, S. Olcum, L. Virot, M. Cochet, A. Thuaire, S. R. Manalis, and V. Agache, "Suspended Nanochannel Resonators Arrays with Piezoresistive Sensors for High-throughput Weighing of Nanoparticles in Solution," *ACS Sensors*, 5(4), 2020.

M. A. Stockslager, S. Olcum, S. M. Knudsen, R. J. Kimmerling, N. Cermak, K. Payer, V. Agache, and S. R. Manalis, "Rapid and High-precision Sizing of Single Particles Using Parallel Suspended Microchanne Resonator Arrays and Deconvolution," *Review of Scientific Instruments*, 90(8), 2019.

J. H. Kang, T. P. Miettinen, L. Chen, S. Olcum, G. Katsikis, P. S. Doyle, and S. R. Manalis, "Noninvasive Monitoring of Single-cell Mechanics by Acoustic Scattering," *Nature Methods*, 16(3):263-269, 2019.

Farnaz Niroui

Assistant Professor

Department of Electrical Engineering & Computer Science

Nanofabrication technologies at the few-nanometer-scale and for the emerging nanomaterials. Surfaces, interfaces and forces at the nanoscale. Active nanoscale devices with applications in molecular electronics, nanoelectromechanical systems, reconfigurable nanosystems with embedded intelligence, and quantum technologies.

Rm. 13-3005B | 617-324-7415 | fniroui @ mit . edu

GRADUATE STUDENTS

Patricia Jastrzebska-Perfect, EECS, NSF Fellow
Peter Satterthwaite , EECS, NSF Fellow
Sarah Spector, EECS, NSF Fellow
Spencer (Weikun) Zhu, ChemE

UNDERGRADUATE STUDENTS

Shelly Ben-David, EECS
Will Jack, EECS
Lejla Skelic, EECS

SUPPORT STAFF

Catherine Bourgeois, Administrative Assistant

SELECTED PUBLICATIONS

W. Zhu, P. F. Satterthwaite, F. Niroui, "Scalable fabrication of active nanogaps with sub-nanometer tunability for nanoscale sensors and actuators," 2022. [Accepted]

Z. Ren, S. Kim, X. Ji, W. Zhu, F. Niroui, J. Kong, Y. Chen, "High lift micro-aerial-robot powered by low voltage and long endurance dielectric elastomer actuators," *Adv. Mater.*, vol. 34, 2106757, 2022.

J. Han, Z. Nelson, M. R. Chua, T. M. Swager, F. Niroui, J. H. Lang, V. Bulović, "On-site, deterministic, and salable growth of perovskite nanocrystals," *Nano Letts.*, vol. 21, pp. 10244-10251, 2021.

F. Niroui, M. Saravanapavanantham, J. Han, J. J. Patil, T.M. Swager, J. H. Lang, V. Bulović, "Hybrid approach to fabricate uniform and active molecular junctions,"*Nano Letts.*, vol. 21, pp. 1606-1612, 2021.

V. Jamali*, F. Niroui*, L. W. Taylor, O. S. Dewey, B. A. Koscher, M. Pasquali, A. P. Alivisatos, "Perovskite-carbon nanotube light-emitting fibers," *Nano Letts.*, vol. 20, pp.3178-3184, 2020. *Equal contribution.

S. Fathipour, S. F. Almeida, Z. A. Ye, B. Saha, F. Niroui, T. King Liu, J. Wu, "Reducing adhesion energy of nanoelectromechanical relay contacts by self-assembled perfluoro(2,3-dimethylbutan-2-ol) coating," *AIP Advances*, vol. 9, 055329, 2019.

Jelena Notaros

Robert J. Shillman (1974) Career Development Assistant Professor
Department of Electrical Engineering & Computer Science

Silicon photonics platforms, devices, and systems for applications including displays, sensing, communications, quantum, and biology.

Rm. 26-343 | **617-253-3073** | **notaros @ mit . edu**

GRADUATE STUDENTS

Sabrina Corsetti, EECS, MIT Locher Fellow & NSF Fellow
Daniel DeSantis, EECS, MIT McWhorter Fellow
Andres Garcia, EECS
Ashton Hattori, EECS, MIT Analog Devices Fellow, NDSEG Fellow, & NSF Fellow
Milica Notaros, EECS, MIT Jacobs Fellow & NSF Fellow
Tal Sneh, EECS, MIT Cronin Fellow & NSF Fellow

UNDERGRADUATE STUDENT

Carol Pan, EECS
Abigail Shull, EECS & Physics

SUPPORT STAFF

Dianne Lior, Administrative Assistant

SELECTED PUBLICATIONS

S. Corsetti, M. Notaros, T. Sneh, A. Stafford, Z. A. Page, and J. Notaros, "Visible-Light Integrated Optical Phased Arrays for Chip-Based 3D Printing," in *Proceedings of Integrated Photonics Research, Silicon, and Nanophotonics (IPR)* (OSA, 2022).

T. Sneh, S. Corsetti, M. Notaros, and J. Notaros, "Focusing Integrated Optical Phased Arrays for Chip-Based Optical Trapping," in *Proceedings of Conference on Lasers and Electro-Optics (CLEO)* (OSA, 2022), paper STh4G.4.

M. Notaros, T. Dyer, M. Raval, C. Baiocco, J. Notaros, and M. R. Watts, "Integrated Visible-Light Liquid-Crystal Phase Modulators," *Optics Express* 30(8), 13790 (2022).

J. Notaros, "Silicon Photonics for LiDAR, Augmented Reality, and Beyond," in *Proceedings of Computational Optical Sensing and Imaging (COSI)* (OSA, 2022). (Invited Talk)

J. Notaros, "Integrated Optical Phased Arrays for Augmented Reality, LiDAR, and Beyond," in *Proceedings of Optical Fiber Communication Conference (OFC)* (OSA, 2022), paper M2E.1. (Invited Talk)

J. Notaros, M. Notaros, M. Raval, C. V. Poulton, M. J. Byrd, N. Li, Z. Su, E. S. Magden, E. Timurdogan, T. Dyer, C. Baiocco, T. Kim, P. Bhargava, V. Stojanovic, and M. R. Watts, "Integrated Optical Phased Arrays for LiDAR, Augmented Reality, and Beyond," in *Proceedings of Applied Industrial Optics (AIO)* (OSA, 2021), paper M2A.3.

U. Chakraborty, J. Carolan, G. Clark, D. Bunandar, G. Gilbert, J. Notaros, M. R. Watts, and D. R. Englund, "Cryogenic Operation of DC Kerr Silicon Photonic Modulators," in *Proceedings of Conference on Lasers and Electro-Optics (CLEO)* (OSA, 2021), paper STh1Q.1.

William D. Oliver

Professor of Electrical Engineering and Computer Science, Physics
Laboratory Fellow of Lincoln Laboratory
Director of Center for Quantum Engineering
Associate Director of Research Laboratory of Electronics

The materials growth, fabrication, design, measurement of superconducting qubits. The development of cryogenic packaging and control William electronics involving cryogenic CMOS and single-flux quantum digital logic.

Rm. 13-3050 | 617-258-6018 | william . oliver @ mit . edu

RESEARCH SCIENTIST

Jeff Grover, RLE
Simon Gustavsson, RLE
Joel I. J. Wang, RLE

POSTDOCTORAL ASSOCIATES

Agustin Di Paolo, RLE
Patrick Harrington, RLE
Max Hays, RLE
Ilan Rosen, RLE
Miuko Tanaka, RLE
Roni Winik, RLE

GRADUATE STUDENTS

Aziza Almanakly, EECS, PD Soros/ CBL Fellow
Junyoung An, EECS, KFAS Fellow
Lamia Ateshian, EECS, EECS Alan L. McWhorter/ NSF Fellow
Will Banner, EECS
Shoumik Chowdhury, EECS, MIT Irwin Mark Jacobs and Joan Klein Jacobs Presidential / NSF Fellow
Leon Ding, Physics, IBM Fellow
Qi (Andy) Ding, EECS
Ami Greene, EECS, Google PhD Fellow
Shantanu Jha, EECS
Bharath Kannan, EECS
Amir Karamlou, EECS
Chris McNally, EECS, CQA/NSA Fellow
Sarah Muschinske, EECS, NASA Fellow
Yanjie (Jack) Qiu, EECS
David Rower, Physics, MIT SOS Fellow
Gabriel O. Samach, EECS, Lincoln Laboratory Fellow
Youngkyu Sung, EECS
Sameia Zaman, EECS, Lisa Su Fellow

UNDERGRADUATE STUDENTS

Sebastian N Alberdi, EECS
Franck N Belemkoabga, EECS
Thomas Bergamaschi, Physics
Lauren Li, Physics and Mathematics
Fischer J Moseley, EECS
Ilan Mitnikov, Physics
Helen O Propson, EECS
Elaine Pham, EECS
Julian Yocum, Physics
Daniela A Zaidenberg, Physics

VISITING STUDENTS

Tim Menke, Harvard University
Cora Barrett, Wellesley College

SUPPORT STAFF

Chihiro Watanabe, Administrative Assistant

SELECTED PUBLICATIONS

J. Braumüller, A. H. Karamlou, Y. Yanay, B. Kannan, D. Kim, M. Kjaergaard, A. Melville, B. M. Niedzielski, Y. Sung, A. Vepsäläinen, R. Winik, J. L. Yoder, T. P. Orlando, S. Gustavsson, C. Tahan, W. D. Oliver, "Probing quantum information propagation with out-of-time-ordered correlators," *Nature Physics* 18, 172-178, Feb. 2022.

J. Ruane, A. McAfee, W. D. Oliver, "Quantum computing for business leaders," *Harvard Business Review*, Jan. – Feb. 2022, 2022.

N. Holman, D. Rosenberg, D. Yost, J. L. Yoder, R. Das, W. D. Oliver, R. McDermott, M. A. Eriksson, "3D integration and measurement of a semiconductor double quantum dot with a high-impedance TiN resonator," *npj Quantum Inf* 7, 137, Sep. 2021.

Y. Sung, L. Ding, J. Braumüller, A. Vepsäläinen, B. Kannan, M. Kjaergaard, A. Greene, G. O. Samach, C. McNally, D. Kim, A. Melville, B. M. Niedzielski, M. E. Schwartz, J. L. Yoder, T. P. Orlando, S. Gustavsson, W. D. Oliver, "Realization of high-fidelity CZ and ZZ-free iSWAP gates with a tunable coupler," *Phys. Rev. X* 11, 021058, Jun. 2021.

S. Huang, B. Lienhard, G. Calusine, A. Vepsäläinen, J. Braumüller, D. K. Kim, A. J. Melville, B. M. Niedzielski, J. L. Yoder, B. Kannan, T. P. Orlando, S. Gustavsson, W. D. Oliver, "Microwave package design for superconducting quantum processors," *PRX Quantum* 2, 020306, Apr. 2021.

Y. Sung, A. Vepsäläinen, J. Braumüller, F. Yan, J. I-J. Wang, M. Kjaergaard, R. Winik, P. Krantz, A. Bengtsson, A. J. Melville, B. M. Niedzielski, M. E. Schwartz, D. K. Kim, J. L. Yoder, T. P. Orlando, S. Gustavsson, W. D. Oliver, "Multi-level quantum noise spectroscopy," *Nature Communications* 12, 967, Feb. 2021.

Tomás Palacios

Professor
Department of Electrical Engineering & Computer Science

Design, fabrication, and characterization of novel electronic devices and systems based on wide bandgap semiconductors & two-dimensional (2-D) materials, polarization & bandgap engineering, transistors for high voltage, sub-mm wave power & digital applications, sensors and heterogeneous integration.

Rm. 39-567A | 617-324-2395 | tpalacios @ mit . edu

GRADUATE STUDENTS

Jung-Han (Sharon) Hsia, EECS
Kevin Limanta, EECS
Christian Lopez Angeles, EECS
Yiyue Luo, EECS
Elaine McVay, EECS
John Niroula, EECS
Joshua Perozek, EECS
Pao-Chuan Shih, EECS
Qingyun Xie, EECS
Mantian Xue, EECS
Mengyang Yuan, EECS
Jiadi Zhu, EECS

UNDERGRADUATE STUDENTS

Adina Golden, UROP
Rolando Gonzalez, SuperUROP
Alisa Hathaway, UROP
Neelambar Mondal, UROP

VISITORS

Javier de Mena Pacheco, Universidad Politécnica de Madrid
Anthony Taylor, Edwards Vacuum

SUPPORT STAFF

Preetha Kingsview, Administrative Assistant

SELECTED PUBLICATIONS

P.-C. Shen, T. Palacios, et al, "Ultralow contact resistance between semimetal and monolayer semiconductors," *Nature*, 593, 211-217 (2021).

Y. Luo, T. Palacios, et al., "Learning human–environment interactions using conformal tactile textiles," *Nature Electronics*, 4, 193-201 (2021).

B. Han, T. Palacios, et al., "Deep-Learning-Enabled Fast Optical Identification and Characterization of 2D Materials," *Advanced Materials*, Vol. 32, Issue 29, pg. 2000953 (2020).

S. Warnock, T. Palacios, et al., "InAlN/GaN-on-Si HEMT with 4.5 W/mm in a 200-mm CMOS-Compatible MMIC Process for 3D Integration," *2020 IEEE/MTT-S International Microwave Symposium (IMS)*, pg. 289-292 (2020).

S. J. Bader, T. Palacios, et al., "Prospects for wide bandgap and ultrawide bandgap CMOS devices," *IEEE Transactions on Electron Devices*, Vol. 67, Issue 10, pg. 4010-4020 (2020).

X. Zhang, T. Palacios, et al, "Two-dimensional MoS2-enabled flexible rectenna for Wi-Fi-band wireless energy harvesting," *Nature*, 566, 7744, 368 (2019).

Y. Zhang, T. Palacios, et al, "Large Area 1.2 kV GaN Vertical Power FinFETs with a Record Switching Figure-of-Merit," *IEEE Electron Device Letts.*, 1, pp. 75-78 (2019).

H. Amano, T. Palacios et al, "The 2018 GaN Power Electronics Roadmap," *J. of Phys. D,* vol. 51, pp. 163001 (2018).

S. Joglekar, T. Palacios, et al, "Large signal linearity enhancement of AlGaN/GaN high electron mobility transistors by device-level Vt engineering for transconductance compensation," *2017 IEEE International Electron Devices Meeting (IEDM)*, 2017.

F. Gao, T. Palacios, et all, "Impact of Water-Assisted Electrochemical Reactions on the OFF-State Degradation of AlGaN/GaN HEMTs," *IEEE Trans. Electron Devices*, vol. 61, no. 2, pp. 437–444 (2014).

B. Lu, T. Palacios, et al, "Tri-Gate Normally-off GaN Power MISFET," *Electron Dev. Letts*. Vol. 33, pp. 360-362 (2012).

D. S. Lee, T. Palacios, et al, "300-GHz InAlN/GaN HEMTs With InGaN Back-Barrier," *IEEE Electron Device Letts.*, vol. 32(11), pp. 1525 (2011).

J. W. Chung, T. Palacios, et al, "Seamless On-Wafer Integration of Si (100) MOSFETs and GaN HEMTs," *Electron Dev. Letts.*, vol. 30, pp. 1015-1017 (2009).

Negar Reiskarimian

X-Window Consortium Career Development Assistant Professor
Department of Electrical Engineering & Computer Science

Integrated circuits and systems and applied electromagnetics with a focus on analog, RF, millimeter-Wave (mm-Wave) and optical integrated circuits, metamaterials and systems for a variety of applications.

Rm. 39-427a | 617-253-0726 | negarr @ mit . edu

GRADUATE STUDENTS

Soroush Araei, EECS
Shahabeddin Mohin, EECS

SUPPORT STAFF

Jami L. Mitchell, Administrative Assistant

SELECTED PUBLICATIONS

N. Reiskarimian, "A Review of Nonmagnetic Nonreciprocal Electronic Devices: Recent advances in nonmagnetic nonreciprocal components," *IEEE Solid-State Circuits Magazine* vol. 13, no. 4, pp. 112-121, Fall 2021.

N. Reiskarimian, M. Khorshidian, and H. Krishnaswamy, "Inductorless, Widely Tunable N-Path Shekel Circulators Based on Harmonic Engineering," *IEEE J. of Solid-State Circuits (JSSC)* (invited), vol. 56, no. 4, Apr. 2021.

A. Nagulu, N. Reiskarimian and H. Krishnaswamy, "Non-reciprocal Electronics Based on Temporal Modulation," *Nature Electronics*, May 2020.

N. Reiskarimian, M. Khorshidian and H. Krishnaswamy, "Inductorless, Widely-Tunable N-Path Shekel Circulators Based on Harmonic Engineering," in *IEEE Radio Frequency Integrated Circuits Symposium (RFIC)*, pp 39-42, Jun. 2020.

M. Khorshidian, N. Reiskarimian and H. Krishnaswamy, "A Compact Reconfigurable N-Path Low-Pass Filter Based on Negative Trans-Resistance with <1dB Loss and >21dB Out-of-Band Rejection," in *IEEE International Microwave Symposium (IMS)*, pp. 799-802, Jun. 2020.

M. Khorshidian, N. Reiskarimian and H. Krishnaswamy, "High-Performance Isolators and Notch Filters based on N-Path Negative Trans-Resistance," in *IEEE International Solid-State Circuits Conference (ISSCC)*, Feb. 2020.

M. Baraani Dastjerdi, S. Jain, N. Reiskarimian, A. Natarajan and H. Krishnaswamy, "Analysis and Design of Full-Duplex 2x2 MIMO Circulator-Receiver with High TX power handling Exploiting MIMO RF and Shared-delay Baseband Self-Interference Cancellation," *IEEE J. of Solid State Circuits (JSSC)* (invited), vol. 54, no. 12, pp. 3525-3540, Dec. 2019.

N. Reiskarimian, M. Tymchenko, A. Alu and H. Krishnaswamy, "Breaking Time-Reversal Symmetry Within Infinitesimal Dimensions Through Staggered Switched Networks," in *Metamaterials*, Sep. 2019.

N. Reiskarimian, A. Nagulu, T. Dinc and H. Krishnaswamy, "Non-Reciprocal Devices: A Hypothesis Turned into Reality," *IEEE Microwave Magazine* (invited), vol. 20, no. 4, pp. 94-111, Apr. 2019.

N. Reiskarimian, T. Dinc, J. Zhou, T. Chen, M. Baraani Dastjerdi, J. Diakonikolas, G. Zussman, and H. Krishnaswamy, "A One-Way Ramp to a Two-Way Highway: Integrated Magnetic-Free Non-Reciprocal Antenna Interfaces for Full Duplex Wireless," in *IEEE Microwave Magazine* (invited), vol. 20, no. 2, pp. 56-75, Feb. 2019.

M. B. Dastjerdi, S. Jain, N. Reiskarimian, A. Natarajan, and H. Krishnaswamy, "Full-Duplex 2x2 MIMO Circulator-Receiver with High TX Power Handling Exploiting MIMO RF and Shared-Delay Baseband Self-Interference Cancellation," *IEEE International Solid-State Circuits Conference (ISSCC),* Feb. 2019.

Charles G. Sodini

LeBel Professor
Department of Electrical Engineering & Computer Science

Electronics and integrated circuit design and technology. Specifically, his research involves technology intensive integrated circuit and systems design, with application toward medical electronic devices for personal monitoring of clinically relevant physiological signals.

Rm. 39-527b | 617-253-4938 | sodini @ mtl . mit . edu

COLLABORATORS

Sam Fuller, Analog Devices, Inc
Thomas O'Dwyer, MTL Research Affiliate
Joohyun Seo, Analog Devices, Inc.

POSTDOCTORAL ASSOCIATES

Anand Chandraksekhar, MTL

GRADUATE STUDENT

Jeanne Harabedian, MTL

SUPPORT STAFF

Kathleen Brody, Administrative Assistant

SELECTED PUBLICATIONS

S. M. Imaduddin, C. G. Sodini, and T. Heldt, "Deconvolution-based partial volume correction for volumetric blood flow measurement," *IEEE Transactions on Ultrasonics, Ferroelectrics, and Frequency Control,* Accepted for publication, Apr. 2022

J. Seo, H.-S. Lee, and C. G. Sodini, "Non-Invasive Evaluation of a Carotid Arterial Pressure Waveform Using Motion-Tolerant Ultrasound Measurements During the Valsalva Maneuver," *IEEE J. of Biomedical and Health Informatics*, vol. 25, no. 1, Jan. 2021.

H. Lai, G. Saavedra-Peña, C. G. Sodini, V. Sze and T. Heldt, "Measuring Saccade Latency Using Smartphone Cameras," *IEEE J. of Biomedical and Health Informatics*, vol. 24, no. 3, pp. 885-897, Mar. 2020.

J. Liu, C. G. Sodini, Y. Ou, B. Yan, Y. T. Zhang, N. Zhao, "Feasibility of Fingertip Oscillometric Blood Pressure Measurement: Model-based Analysis and Experimental Validation," *IEEE J. of Biomedical and Health Informatics (JBHI)*, May 2019.

M. Delano, and C. Sodini, "Evaluating Calf Bioimpedance Measurements for Fluid Overload Management in a Controlled Environment," *Physiological Measurement*, vol. 39, no. 12, p. 125009, 2018.

Vivienne Sze

Associate Professor of Electrical Engineering & Computer Science
Department of Electrical Engineering & Computer Science

Joint design of signal processing algorithms, architectures, VLSI and systems for energy-efficient implementations. Applications include computer vision, machine learning, autonomous navigation, image processing and video coding.

Rm. 38-260 | 617-324-7352 | sze @ mit . edu

GRADUATE STUDENTS

Tanner Andrulis (co-advised with Joel Emer)
Keshav Gupta (co-advised with Sertac Karaman)
Jamie Koerner, EECS (co-advised with Thomas Heldt)
Peter Li, EECS (co-advised with Sertac Karaman)
Soumya Sudhakar, AeroAstro (co-advised with Sertac Karaman)
Yannan Nellie Wu, EECS (co-advised with Joel Emer)

UNDERGRADUATE STUDENTS

Michael Gilbert, EECS
Ari Grayzel, AeroAstro

SUPPORT STAFF

Janice L. Balzer, Administrative Assistant

SELECTED PUBLICATIONS

P. Z. X. Li, S. Karaman, and V. Sze, "Memory-Efficient Gaussian Fitting for Depth Images in Real Time," *IEEE International Conference on Robotics and Automation (ICRA)*, May 2022.

S. Sudhakar, V. Sze, and S. Karaman, "Uncertainty from Motion for DNN Monocular Depth Estimation," *IEEE International Conference on Robotics and Automation (ICRA)*, May 2022.

H.-Y. Lai, G. Saavedra-Pena, C. G. Sodini, T. Heldt, and V. Sze, "App-based saccade latency and directional error determination across the adult age spectrum," *IEEE Transactions on Biomedical Engineering (TBME)*, Vol. 69, No. 2, pp. 1029 – 1039, Feb. 2022.

Y.-L. Liao, S. Karaman, V. Sze, "Searching for Efficient Multi-Stage Vision Transformers," *ICCV 2021 Workshop on Neural Architectures: Past, Present and Future*, Oct. 2021.

K. Gupta, P. Z. X. Li, S. Karaman, V. Sze, "Efficient Computation of Map-scale Continuous Mutual Information on Chip in Real Time," *IEEE/RSJ International Conference on Intelligent Robots and Systems (IROS)*, Sept. 2021.

T.-J. Yang, Y.-L. Liao, and V. Sze, "NetAdapt v2: Efficient Neural Architecture Search with Fast Super-Network Training and Architecture Optimization," *Conference on Computer Vision and Pattern Recognition (CVPR)*, Jun. 2021.

F. Wang, Y. Wu, M. Woicik, V. Sze, and J. S. Emer, "Architecture-Level Energy Estimation for Heterogeneous Computing Systems," *IEEE International Symposium on Performance Analysis of Systems and Software (ISPASS)*, Mar. 2021.

Y. Wu, P. Tsai, A. Parashar, V. Sze, and J. Emer, "Sparseloop: An Analytical, Energy-Focused Design Space Exploration Methodology for Sparse Tensor Accelerators," *IEEE International Symposium on Performance Analysis of Systems and Software (ISPASS),* Mar. 2021.

J. Ray, A. Brahmakshatriya, R. Wang, S. Kamil, A. Reuther, V. Sze, and S. Amarasinghe, "Domain-Specific Language Abstractions for Compression," *Data Compression Conference (DCC)*, Mar. 2021.

L. Bernstein, A. Sludds, R. Hamerly, V. Sze, J. Emer, and D. Englund, "Freely-scalable, reconfigurable optical hardware for deep learning," *Scientific Reports*, vol. 11, no. 3144, Feb. 2021.

V. Sze, Y.-H. Chen, T.-J. Yang, and J. S. Emer, "Efficient Processing of Deep Neural Networks," *Synthesis Lectures on Computer Architecture* - Morgan & Claypool Publishers, 2020.

Carl V. Thompson

Stavros Salapatas Professor of Materials Science and Engineering
Department of Materials Science & Engineering
Director, Materials Research Laboratory

Optimization of processing and properties of thin films and nanostructures for applications in electronic, microelectromechanical, and electrochemical devices and systems. Interconnect and device reliability.

Rm. 13-2098 | 617-253-7652 | cthomp @ mit. edu

POSTDOCTORAL ASSOCIATES

Pushpendra Kumar, SMART
Haemin Paik, DMSE
Hui Teng Tan, SMART
An Tao, SMART

GRADUATE STUDENTS

Misong Ju, DMSE
Maxwell L'Etoile, DMSE
Yoon Ah Shin, DMSE
Lin Xu, DMSE

UNDERGRADUATE STUDENTS

Udochukwu D. Eze, DMSE

SUPPORT STAFF

Sarah Ciriello, Administrative Assistant

SELECTED PUBLICATIONS

Y. A. Shin, and C.V. Thompson, "Templated Fingering During Solid State Dewetting," *Acta Materialia*, vol. 207, pp.16669, 2021.

L. Xu, and C. V. Thompson, "Electrochemically Controlled Reversible Formation of Organized Channel Arrays in Nanoscale-Thick RuO_2 Films: Implications for Mechanically Stable Thin Films and Microfluidic Devices," *ACS Appl. Nano Mater.*, vol. 4, pp. 13700–13707, 2021.

S. Curiotto, A. Chame, P. Müller, C. V. Thompson, and O. Pierre-Louis, "Hole Opening From Growing Interfacial Voids: A Possible Mechanism of Solid State Dewetting," *Appl. Phys. Letts.*, vol. 120, pp. 091603, 2022.

Kripa K. Varanasi

Professor of Mechanical Engineering
Associate Member, The Broad Institute
Department of Mechanical Engineering

Research lies at the intersection of Interfacial Engineering, Thermal-Fluids, and Materials & Manufacturing. Central theme is the design and manufacturing of nano-engineered surfaces and their applications to Energy, Water, Oil & Gas, Agriculture, Transportation, Electronics Cooling Systems for significant efficiency enhancements.

Rm. 35-209 | 617-324-5608 | varanasi @ mit.edu

POSTDOCTORAL ASSOCIATE

Baptiste Blanc, MechE

GRADUATE STUDENTS

Bert Joannes C. Vandereydt, MechE
Caroline Taylor McCue, MechE
Fabian Jau-Shiuen Dickhardt, MechE
Jack R Lake, MechE
Michael P Nitzsche, MechE
Sean Parks, MechE
Simon B. Rufer, MechE
Sreedath Panat, MechE
Tal Joseph, MechE
Victor Julio Leon, MechE

SUPPORT STAFF

Alexandra Trias, Administrative Assistant

PUBLICATIONS

V. Jayaprakash, M. Costalonga, S. Dhulipala, and K. K. Varanasi, "Enhancing the Injectability of High Concentration Drug Formulations Using Core Annular Flows," *Advanced Healthcare Materials*, vol.9(18), p.2001022, Aug. 2020.

S. A. McBride, R. Skye, and K. K. Varanasi, "Differences between Colloidal and Crystalline Evaporative Deposits," *Langmuir*, 36, 40, 11732–11741, Sep. 2020.

S. Khan, J. Hwang, Y. S. Horn, and K. K. Varanasi, "Catalyst-proximal plastrons enhance activity and selectivity of carbon dioxide electroreduction," *Cell Reports Physical Science*, vol. 2(2), 100318, Jan. 2021.

S. A. McBride, H. L. Girard, and K. K. Varanasi, "Crystal critters: Self-ejection of crystals from heated, superhydrophobic surfaces," *Science Advances*, vol. 7(18), 6960, Apr. 2021.

Luis Fernando Velásquez-García

Principal Research Scientist
Microsystems Technology Laboratories

Micro- and nano-enabled, multiplexed, scaled-down systems that exploit high electric field phenomena; powerMEMS; additively manufactured MEMS/NEMS. Actuators, cold cathodes, ionizers, microfluidics, microplasmas, CubeSat hardware, portable mass spectrometry, pumps, sensors, X-ray sources.

Rm. 39-415B | 617-253-0730 | lfvelasq @ mit . edu

POSTDOCTORAL ASSOCIATES

Han-Joo Lee, EECS
Nicholas Lubinsky, EECS

GRADUATE STUDENTS

Ashley L. Beckwith, MechE
Zoey Bigelow, EECS
Jorge Canada Perez-Sala, EECS
Liliosa Cole, MechE
Alejandro Diaz, EECS
Colin Eckhoff, EECS
Alex Kashkin, MechE
Hyeonseok Kim, MechE
Yosef S. Kornbluth, MechE
Isabelle Liu, EECS

UNDERGRADUATE STUDENTS

Maisha Pome, BioE

VISITOR

Javier Izquierdo Reyes, Tecnológico de Monterrey

SUPPORT STAFF

Jami L. Mitchell, Administrative Assistant

SELECTED PUBLICATIONS

Y. Kornbluth, R. H. Mathews, L. Parameswaran, L. Racz, and L. F. Velásquez-García, "Fully 3D-Printed, Ultrathin Capacitors via Multi-Material Microsputtering", In-press, *Advanced Materials Technologies*, 2022.

A. Beckwith, J. Borenstein, and L. F. Velásquez-García, "Physical, Mechanical, and Microstructural Characterization of Novel, 3D-Printable, Tunable, Lab-Grown Plant Materials Generated from Zinnia Elegans Cell Cultures," In-Press, *Materials Today*, 2022.

L. F. Velásquez-García, J. Izquierdo-Reyes, and H. Kim, "Review of In-Space Plasma Diagnostics for Studying the Earth's Ionosphere," *J. of Physics D – Applied Physics*, vol. 55, no. 26, 263001 (26pp), Jun. 2022.

A. Kachkine, and L. F. Velásquez-García, "Nanowire-Coated Emitter Electrospray Ionizer Coupled to Digital Microfluidics for Liquid Analysis," *Technical Digest 35th Conference on Micro Electro Mechanical Systems (MEMS 2022)*, Tokyo, Japan, pp. 95 – 98, Jan. 9 — 13, 2022.

L. F. Velásquez-García, and Y. Kornbluth, "Biomedical Applications of Metal 3D Printing," *Annual Review of Biomedical Engineering*, vol. 23, pp. 307 – 338, Jul. 2021.

Joel Voldman

Clarence J. Lebel Professor of Electrical Engineering
Faculty Head, Electrical Engineering
Department of Electrical Engineering & Computer Science

Microtechnology for basic cell biology, applied cell biology, Immunology, and human health.

Rm. 36-824 | 617-253-2094 | voldman @ mit . edu

POSTDOCTORAL ASSOCIATES

Sarvesh Varma, RLE

GRADUATE STUDENTS

Kru Kikkeri, EECS
Wei Liao, EECS
Dousabel May Yi Tay, ChemE

VISITING POSTDOCTORAL ASSOCIATES

Mahdi Aeinehvand, Tec de Monterrey

SUPPORT STAFF

Chadwick Collins, Administrative Assistant

SELECTED PUBLICATIONS

K. Kikkeri, D. Wu, and J. Voldman, "A sample-to-answer electrochemical biosensor system for biomarker detection," *Lab on a Chip*, vol. 22, pp. 100-107, 2022.

B. Jundi, D.-H. Lee, H. Jeon, M. G. Duvall, J. Nijmeh, R.-E. E. Abdulnour, M. Pinilla-Vera, R. M. Baron, J. Han, J. Voldman, B. D. Levy, "Inflammation resolution circuits are uncoupled in acute sepsis and correlate with clinical severity," *JCI Insight*, vol. 6, pp. e148866, 2021.

H. Jeon, D.-H. Lee, B. Jundi, M. Pinilla-Vera, R. M. Baron, B. D. Levy, J. Voldman, J. Han, "Fully automated, sample-to-answer leukocyte functional assessment platform for continuous sepsis monitoring via microliters of blood," *ACS Sensors*, vol. 6, pp. 2747-2756, 2021.

K. Kikkeri, D. Wu, and J. Voldman, "A sample-to-answer electrochemical biosensor system for biomarker detection," in *Micro Total Analysis Systems 2021*, Palm Springs, California, 2021

D.-H. Lee and J. Voldman, "Large-scale Single-cell Pairing and Fusion For Hybridoma Production," in *Micro Total Analysis Systems 2021*, Palm Springs, California, 2021.

D. Wu and J. Voldman, "An integrated model for bead-based immunoassays," *Biosens Bioelectron*, vol. 154, p. 112070, Apr. 15 2020.

D. Wu and J. Voldman, "An integrated and automated electronic system for point-of-care protein testing," in *41st Annual International Conference of the IEEE Engineering in Medicine and Biology Society*, Berlin, Germany, 2019.

C. P. Tostado, J. W. J. Heng, L. X. D. Ong, R. DasGupta, J. Voldman, and Y.-C. Toh, "Automation and integration of computer vision image analysis for cancer immunotherapy research with on-chip cell trapping," in *Micro Total Analysis Systems 2019*, Basel, Switzerland, 2019.

D.-H. Lee, B. Jundi, H. Ryu, R. M. Baron, J. Han, B. D. Levy, and J. Voldman, "Electrical profiling of septic neutrophils using microfluidics," in *Biomedical Engineering Society Annual Meeting*, Philadelphia, Pennsylvania, 2019.

D.-H. Lee, H. Jeon, B. Jundi, R. M. Baron, B. D. Levy, J. Han, and J. Voldman, "Rapid monitoring of sepsis by integration of spiral inertial microfluidics and isodielectric separation," in *Micro Total Analysis Systems 2019*, Basel, Switzerland, 2019.

B. Jundi, H. Ryu, D.-H. Lee, R.-E. E. Abdulnour, B. D. Engstrom, M. G. Duvall, A. Higuera, M. Pinilla-Vera, M. E. Benson, J. Lee, N. Krishnamoorthy, R. M. Baron, J. Han, J. Voldman, and B. D. Levy, "Leukocyte function assessed via serial microlitre sampling of peripheral blood from sepsis patients correlates with disease severity," *Nature Biomedical Engineering*, vol. 3, pp. 961-973, 2019.

R. Yuan, M. B. Nagarajan, J. Lee, J. Voldman, P. S. Doyle, and Y. Fink, "Designable 3d microshapes fabricated at the intersection of structured flow and optical fields," *Small*, vol. 14, p. e1803585, Dec. 2018.

R. Yuan, J. Lee, H.-W. Su, E. Levy, T. Khudiyev, J. Voldman, and Y. Fink, "Microfluidics in structured multimaterial fibers," *Proc Natl Acad Sci USA*, vol. 115, pp. E10830-E10838, 2018.

D. Wu, D. Rios-Aguirre, M. Chounlakone, S. Camacho-Leon, and J. Voldman, "Sequentially multiplexed amperometry for electrochemical biosensors," *Biosensors and Bioelectronics*, vol. 117, pp. 522-529, 2018.

S. Varma, G. Garcia-Cardena, and J. Voldman, "Unraveling endothelial cell phenotypic regulation by spatial hemodynamic flows with microfluidics," in *Micro Total Analysis Systems Kaohsiung*, Taiwan, 2018.

A. Jaffe and J. Voldman, "Multi-frequency dielectrophoretic characterization of single cells," *Microsystems & Nanoengineering*, vol. 4, p. 23, 2018.

Evelyn N. Wang

Department Head and Ford Professor of Engineering
Department of Mechanical Engineering

Heat and mass transport at the micro- and nano-scales, nanoengineered surfaces, and thermal microdevices for applications in thermal management, solar thermal energy conversion, and water desalination.

Rm. 3-174 | 617-253-3523 | enwang @ mit . edu

POSTDOCTORAL ASSOCIATES

Hyeongyun Cha, MechE
Bachir El Fil, MechE
Gustav Graeber, MechE
Xiangyu Li, MechE
Xinyue Liu, MechE

GRADUATE STUDENTS

Liliosa Cole, MechE
Samuel Cruz, MechE
Carlos Daniel Diaz Marin, MechE
Young Ko, MechE
Adela Li, MechE
Emily Lin, MechE
Geoffrey Vaartstra, MechE
Chad Wilson, MechE
Lenan Zhang, MechE
Yajing Zhao, MechE
Yang Zhong, MechE

UNDERGRADUATE STUDENT

Kemi Chung, MechE
Kezia Hector, MechE
Diane Li, MechE
Anna Simmons, MechE
Amir White, MechE

SUPPORT STAFF

Alexandra Cabral, Administrative Assistant

SELECTED PUBLICATIONS

K. L. Wilke, Z. Lu, Y. Song, and E. N. Wang, "Turning traditionally nonwetting surfaces wetting for eve ultra-high surface energy liquids," *Proceedings of the National Academy of Sciences of the United States of America (PNAS)*, 2022.

R. Iwata, L. Zhang, Z. Lu, S. Gong, J. Du, and E. N. Wang, "How Coalescing Bubbles Depart from a Wall," *Langmuir*, 2022.

L. Zhang, X. Li, Y. Zhong, A. Leroy, Z. Xu, L. Zhao, and E. N. Wang, "Highly efficient and salt rejecting solar evaporation via a wick-free confined water layer," *Nature Communications*, 2022.

Y. Song, C. Wang, D. J. Preston, G. Su, M. M. Rahman, H. Cha, J. H. Seong, P. Bren, M. Bucci, and E. N. Wang, "Enhancement of Boiling with Scalable Sandblasted Surfaces," *ACS Applied Materials & Interfaces*, 2022.

C. D. Díaz-Marín, L. Zhang, Z. Lu, M. Alshrah, J. C. Grossman, and E. N. Wang, "Kinetics of Sorption in Hygroscopic Hydrogels," *Nano Letts.*, 2022.

Z. Liu, Y. Song, A. Rajappan, E. N. Wang, and D. J. Preston, "Temporal evolution of surface contamination under ultra-high vacuum," *Langmuir*, 2022.

A. Leroy, B. Bhatia, J. Sircar, and E. N. Wang, "Thermal transport in solar-reflecting and infrared-transparent polyethylene aerogels," *International J. of Heat and Mass Transfer*, 2022.

Y. Song, H. Cha, Z. Liu, J. H. Seong, L. Zhang, D. J. Preston, and E. N. Wang, "Alteration of pool boiling heat transfer on metallic surfaces by in situ oxidation," *International J. of Heat and Mass Transfer*, 2021.

G. Vaartstra, Z. Lu, J. Grossman, and E. N. Wang, "Numerical validation of the dusty-gas model for binary diffusion In low aspect ratio capillaries," *Physics of Fluids*, 2021.

Y. Song, L. Zhang, C. D. Díaz-Marín, S. S. Cruz, and E. N. Wang, "Unified descriptor for enhanced critical heat flux during pool boiling of hemi-wicking surfaces," *International J. of Heat and Mass Transfer*, 2021.

C. D. Díaz-Marín, R. M. Shetty, S. Cheung, G. Vaartstra, A. Gopinath, and E. N. Wang, "Rational Fabrication of Nano-to-Microsphere Polycrystalline Opals Using Slope Self-Assembly," *Langmuir*, 2021.

S. Yang, E. Strobach, D. Bierman, L. Zhao, B. Bhatia, and E. N. Wang, "Effect of AI_2O_3 ALD coating on thermal stability of silica aerogel," *J. of Porous Materials*, 2021.

X. Ji, J. Zhao, S. M. Jung, A. I. H. Hrdina, M. J. Wolf, X. Yang, G. Vaartstra, H. S. Xie, L. Luo, A. Lu, R. E. Welsch, E. N. Wang, L. Li, and J. Kong, "Bottom-Up Synthesized All-Thermal-Catalyst Aerogels for Heat-Regenerative Air Filtration," *Nano Letts.*, 2021.

L. Zhang, Y. Zhong, X. Qian, Q. Song, J. Zhou, L. Li, L. Guo, G. Chen, and E. N. Wang, "Heterostructures via van der Waals Binding Effects," *ACS Applied Materials and Interfaces*, 2021.

L. Zhang, S. Gong, Z. Lu, P. Cheng, and E. N. Wang, "Boiling crisis due to bubble interactions," *International J.of Heat and Mass Transfer*, 2021.

Theses Awarded

S.M.

- **Christian Allinson** (D. BONING/ S. SPEAR)
  Enabling Proactive Quality in Commercial Airplanes using Natural Language Processing
- **Samuel Cruz** (J. KIM)
  Mechanism of Remote Epitaxy Using Two Dimensional Materials
- **Farri Gaba** (D. BONING/M. WINKENBACH)
  Solutions to the Generalized UAV Delivery Routing Problem for Last-Mile Delivery with Societal Constraints
- **Jack Gammack** (S.-G. KIM)
  Design Knowledge Base Using Natural Language Processing
- **Elizabeth Hau** (L. DANIEL)
  Digital Thread and Analytics Model to Improve Quality Controls in Surgical Stapler
- **Anjali Krishnamachar** (L. DANIEL)
  Ful llment Simula-tion and Inventory Location Optimization
- **Hunjoo Kim** (J. LANG)
  Development of Industrial Internet of Things Architecture and Business Strategy for Digital Substation Asset Management
- **Christopher Lui** (D. BONING/R. WELSCH)
  An Investigation of Multivariate Process Control for Biomanufacturing
- **Colin Poler** (D. BONING/N. REPENNING)
  Improving Operational Efficiency of a Small Manufacturing Maintenance Organization
- **Tareq Saqr** (J. LANG)
  Deep Unsupervised Anomaly Detection Applied to Motor-Driven Blowers
- **Andrew Tindall** (D. BONING/ R. WELSCH)
  Analytics to Make Hybrid Work, Work
- **John Zhang** (J. LANG)
  An Intracochlear Hydrophone and Amplifier

M. ENG

- **Jaeyoung Jung** (A. CHANDRAKASAN)
  Low-Power Communication Circuits for Net-Zero-Energy IoT Nodes
- **Joshua J. Piel** (D. PERREAULT)
  Closed-Loop Control for a Piezoelectric-Resonator-Based DC-DC Power Converter
- **Tanya Smith** (D. BONING)
  Data Driven Surrogate Models for Faster SPICE Simulation of Power Supply Circuits
- **Fan-Keng Sun** (D. BONING)
  Adjusting for Autocorrelated Errors in Neural Networks for Time Series
- **Peter Tran** (D. BONING)
  Automated Visual Inspection of Lyophilized Products via Deep Learning and Autoencoders
- **Babu Wanyeki** (D. PERREAULT)
  A Two-Stage Piezoelectric Resonator and Switched-Capacitor DC-DC Converter

S.B.

- **Ceylan Caylan** (S.-G. KIM)
  Application of Natural Language Processing to Unstructured Data: A Case Study of Climate Change

PH.D.

- **Haluk Akay** (S.-G. KIM)
  Representing Knowledge for Data-Driven Design
- **Marc-Joseph Antonini** (P. ANIKEEVA)
  Customizing Multifunctional Bidirectional Neural Interfaces Through Fiber Drawing
- **Ashley Beckwith** (L. VELASQUEZ-GARCIA)
  Rethinking Plant-Based Materials Production: Selective Growth of Tunable Materials Using Cell Culture Techniques
- **Chanyeol Choi** (J.KIM)
  Memristor-based AI Hardware for Reliable and Reconfigurable Neuromorphic Computing
- **Sally El-Henawy** (D.BONING)
  Statistical Modeling of the Effects of Process Variations on Silicon Photonics
- **Taylor Facen** (L. DANIEL)
  How Enhanced Data Availability Affects Multi-Channel Marketing Attribution
- **Henri-Louis Girard** (K. VARANASI)
  Interaction at Interfaces Across Scales: from Adsorption to Adhesion
- **Jiahao Han** (L. LIU)
  Harnessing Magnetic Switching and Dynamics Using Electron and Magnon Spin Currents
- **Jinchi Han** (V. BULOVIC)
  Active Micro-/Nano-Structures for Electromechanical Actuation
- **Vishnu Jayaprakash** (K. VARANASI)
  Engineering Physico-chemical Interactions Across Drug Delivery, Agriculture and Carbon Capture

PH.D. (CONTINUED)

- **Yunjo Kim** (J. KIM)
  Interface Engineering for Exfoliation and Integration of Heteroepitaxial III-V Films
- **Yosef S. Kornbluth** (L. VELASQUEZ-GARCIA)
  Microplasma-Enabled Sputtering of Nanostructured Materials for the Agile Manufacture of Electronic Components
- **Madeleine Reynolds Laitz** (V. BULOVIC)
  Light-Matter Interactions in High-Efficiency Photovoltaics, Light-Emitting Devices, and Strongly Coupled Microcavities
- **Christopher Lang** (D. BONING)
  Applications of Probabilistic Machine Learning Models to Semiconductor Fabrication
- **Sangho Lee** (J. KIM)
  Nanoscale Engineering for Mixed-Dimensional Heterostructure Growth and Integration
- **Youngbin Lee** (P. ANIKEEVA)
  Engineering Biomedical and Bioinspired Fiber Devices via Thermal Drawing
- **Xinhao Li** (N. FANG)
  Disordered Optics for Multidimensional Information Processing
- **Sajjad Mohammadiyangijeh** (J. LANG)
  Modeling, Design, Identification, Drive, and Controlof a Rotary Actuator with Magnetic Restoration
- **Jimin Park** (P. ANIKEEVA)
  Electrochemical and Magnetochemical Approaches for Neuronal Modulation
- **Melany Sponseller** (V. BULOVIC)
  Stability of PbS Quantum Dot Solar Cells
- **Richard Swartwout** (V. BULOVIC)
  Scalable Perovskite Thin-Film Photovoltaics
- **Georgios Varnavides** (P. ANIKEEVA/ P. NARANG)
  Electron Hydrodynamics in Crystalline Solids: Microscopic Origins, Mesoscopic Size Effects, and Macroscopic Observables

Glossary

TECHNICAL ACRONYMS

ADC	Analog-to-Digital Converters
CMOS	Complementary Metal–Oxide–Semiconductor
CNT	Carbon Nanotubes
ECP	Electro-chemical Plating
FET	Field-effect Transistor
HSQ	Hydrogen Silsesquioxane
InFO	Integrated Fan Out
MOSFET	Metal–Oxide–Semiconductor Field-effect Transistor
nTRON	Nanocryotron
RDL	Re-distribution Layers
RIE	Reactive ion etching
SNSPDs	Superconducting nanowire single photon detectors
SS	Subthreshold swing
TMAH	Tetramethylammonium Hydroxide
TREC	Thermally regenerative electrochemical cycle

MIT ACRONYMS & SHORTHAND

BE	Department of Biological Engineering
Biology	Department of Biology
ChemE	Department of Chemical Engineering
CICS	Center for Integrated Circuits and Systems
CMSE	Center for Materials Science and Engineering
IRG	Interdisciplinary Research Group
DMSE	Department of Materials Science & Engineering
EECS	Department of Electrical Engineering & Computer Science
ISN	Institute for Soldier Nanotechnologies
KI	David H. Koch Institute for Integrative Cancer Research
LL	Lincoln Laboratory
MAS	Program in Media Arts & Sciences
MechE	Department of Mechanical Engineering
MEDRC	Medical Electronic Device Realization Center
MIT-CG	MIT/MTL Center for Graphene Devices and 2D Systems
MITEI	MIT Energy Initiative
MIT-GaN	MIT/MTL Gallium Nitride (GaN) Energy Initiative

MISTI	MIT International Science and Technology Initiatives
MIT-SUTD	MIT-Singapore University of Technology and Design Collaboration Office
MIT Skoltech	MIT Skoltech Initiative
MTL	Microsystems Technology Laboratories
NSE	Department of Nuclear Science & Engineering
Physics	Department of Physics
Sloan	Sloan School of Management
SMA	Singapore-MIT Alliance
↳**SMART**	Singapore-MIT Alliance for Research and Technology Center
↳**SMART-LEES**	SMART Low Energy Electronic Systems Center
SUTD-MIT	MIT-Singapore University of Technology and Design Collaboration Office
UROP	Undergraduate Research Opportunities Program

U.S. GOVERNMENT ACRONYMS

AFOSR	U.S. Air Force Office of Scientific Research
↳**FATE-MURI**	Foldable and Adaptive Two-dimensional Electronics Multidisciplinary Research Program of the University Research Initiative
AFRL	U.S. Air Force Research Laboratory
ARL	U.S. Army Research Laboratory
↳**ARL-CDQI**	U.S. Army Research Laboratory Center for Distributed Quantum Information
ARO	Army Research Office
ARPA-E	Advanced Research Projects Agency - Energy (DOE)
DARPA	Defense Advanced Research Projects Agency
↳**DREaM**	Dynamic Range-enhanced Electronics and. Materials
DoD	Department of Defense
DoE	Department of Energy
↳**EFRC**	U.S. Department of Energy: Energy Frontier Research Center (Center for Excitonics)
DTRA	U.S. DoD Defense Threat Reduction Agency
IARPA	Intelligence Advanced Research Projects Activity
↳**RAVEN**	Rapid Analysis of Various Emerging Nanoelectronics
NASA	National Aeronautics and Space Administration
↳**GSRP**	NASA Graduate Student Researchers Project
NDSEG	National Defense Science and Engineering Graduate Fellowship
NIH	National Institutes of Health
↳**NCI**	National Cancer Institute
NNSA	National Nuclear Security Administration

NRO	National Reconnaissance Office
NSF	National Science Foundation
↿**CBMM**	NSF Center for Brains, Minds, and Machines
↿**CIQM**	Center for Integrated Quantum Materials
↿**CSNE**	NSF Center for Sensorimotor Neural Engineering
↿**E3S**	NSF Center for Energy Efficient Electronics Science
↿**GRFP**	Graduate Research Fellowship Program
↿**IGERT**	NSF The Integrative Graduate Education and Research Traineeship
↿**NEEDS**	NSF Nano-engineered Electronic Device Simulation Node
↿**SEES**	NSF Science, Engineering, and Education for Sustainability
↿**STC**	NSF Science-Technology Center
ONR	Office of Naval Research
↿**PECASE**	Presidential Early Career Awards for Scientists and Engineers

OTHER ACRONYMS

CNRS Paris	Centre National de la Recherche Scientifique
CONACyT	Consejo Nacional de Ciencia y Tecnología (Mexico)
IEEE	Institute of Electrical and Electronics Engineers
IHP Germany	Innovations for High Performance Microelectronics Germany
KIST	Korea Institute of Science and Technology
KFAS	Kuwait Foundation for the Advancement of Sciences
MASDAR	Masdar Institute of Science and Technology
NTU	Nanyang Technological University
NUS	National University of Singapore
NYSCF	The New York Stem Cell Foundation
SRC	Semiconductor Research Corporation
↿**NEEDS**	NSF/SRC Nano-Engineered Electronic Device Simulation Node
SUTD	Singapore University of Technology and Design
TEPCO	Tokyo Electric Power Company
TSMC	Taiwan Semiconductor Manufacturing Company

Principal Investigator Index

W

Y

IN APPRECIATION OF OUR MICROSYSTEMS INDUSTRIAL GROUP MEMBER COMPANIES:

Analog Devices, Inc.
Applied Materials
Draper
Edwards
HARTING
Hitachi High-Tech Corporation
IBM
Lam Research
NEC
TSMC
Texas Instruments

AND MIT.NANO CONSORTIUM MEMBER COMPANIES:

Agilent Technologies
Analog Devices, Inc.
Dow
Draper
DSM
Edwards
Fujikura
IBM
Lam Research
NCSOFT
NEC
Oxford Instruments Asylum Research
Raith
Waters